UNIVERSITÉ DU QUÉBEC À CHICOUTIMI

MÉMOIRE PRÉSENTÉ À
L'UNIVERSITÉ DU QUÉBEC À CHICOUTIMI
COMME EXIGENCE PARTIELLE
DE LA MAÎTRISE EN INGÉNIERIE

PAR
YUMEI HAN

PHÉNOMÈNE DE FUSION LOCALE DES PHASES DU CUIVRE DANS LES ALLIAGES Al-Si-Cu-Mg

DÉCEMBRE 2007

Bibliothèque
Paul-Émile-Boulet

UQAC
Université du Québec
à Chicoutimi

Mise en garde/Advice

Afin de rendre accessible au plus grand nombre le résultat des travaux de recherche menés par ses étudiants gradués et dans l'esprit des règles qui régissent le dépôt et la diffusion des mémoires et thèses produits dans cette Institution, **l'Université du Québec à Chicoutimi (UQAC)** est fière de rendre accessible une version complète et gratuite de cette œuvre.

Motivated by a desire to make the results of its graduate students' research accessible to all, and in accordance with the rules governing the acceptation and diffusion of dissertations and theses in this Institution, the **Université du Québec à Chicoutimi (UQAC)** is proud to make a complete version of this work available at no cost to the reader.

L'auteur conserve néanmoins la propriété du droit d'auteur qui protège ce mémoire ou cette thèse. Ni le mémoire ou la thèse ni des extraits substantiels de ceux-ci ne peuvent être imprimés ou autrement reproduits sans son autorisation.

The author retains ownership of the copyright of this dissertation or thesis. Neither the dissertation or thesis, nor substantial extracts from it, may be printed or otherwise reproduced without the author's permission.

UNIVERSITÉ DU QUÉBEC À CHICOUTIMI

MÉMOIRE PRÉSENTÉ À
L'UNIVERSITÉ DU QUÉBEC À CHICOUTIMI
COMME EXIGENCE PARTIELLE
DE LA MAÎTRISE EN INGÉNIERIE

BY
YUMEI HAN

OCCURRENCE OF INCIPIENT MELTING OF COPPER PHASES IN Al-Si-Cu-Mg ALLOYS

DECEMBER 2007

RÉSUMÉ

Les alliages aluminium-silicium-cuivre-magnésium de type 319 sont largement répandus dans la production des blocs de moteur grâce à leur résistance élevée à la fatigue. Ces alliages qui sont thermiquement traitables appartiennent à la classe des alliages d'aluminium dont les propriétés peuvent être améliorées en utilisant un traitement thermique spécifique comportant un traitement thermique de mise en solution, suivi d'une trempe et d'un vieillissement. Le but du traitement de mise en solution est de maximiser la quantité des corps dissous durcissants (Cu et Mg) dans la solution solide en matrice d'aluminium. Dans le cas des alliages 319, la température de solution doit être gardée la plus proche possible de la température eutectique du cuivre, à un niveau au-dessous du maximum pour éviter la surchauffe et fondre, par conséquent, partiellement la phase d'Al_2Cu (nommée fusion locale). Le traitement de mise en solution peut être effectué dans des étapes simples ou multiples. Puisque le traitement à une seule étape est habituellement limité à 495 °C, pour éviter la fusion locale, il ne peut être suffisant ni pour maximiser la dissolution des phases riches en cuivre, ni pour modifier la morphologie des particules de silicium, deux considérations importantes en ce qui concerne l'amélioration des propriétés d'alliage. On a donc proposé des traitements de mise en solution en deux étapes et en étapes multiples pour rectifier ce problème.

Ce travail de recherche a été réalisé sur les alliages Al-Si-Cu-Mg de type 319 pour étudier le rôle du traitement thermique de mise en solution sur la dissolution des phases contenant du cuivre ($CuAl_2$ et $Al_5Mg_8Cu_2Si_6$) dans les alliages 319 contenant des niveaux de magnésium différents, 0, 0.3 et 0.6 % en poids, pour déterminer le traitement thermique de mise solution optimum en ce qui concerne l'occurrence de la fusion locale par rapport aux propriétés d'alliage. Deux séries d'alliages ont été étudiées. Une série d'alliages expérimentaux Al-7%Si-3.5%Cu contenant des niveaux de magnésium de 0, 0.3, et 0.6 % en poids. Cette série a été préparée au laboratoire en utilisant des éléments purs. La deuxième série a été basée sur l'alliage industriel B319 (contenant 0.3% en Mg), où le niveau de magnésium a été augmenté jusqu'à 0.6% en poids en ajoutant du Mg pur au métal liquide. Afin d'étudier l'effet de la modification, le strontium a été ajouté par quantité de 150 ppm aux alliages expérimentaux et industriels, pour fournir un ensemble d'alliages modifiés par le strontium. Ainsi, un total de dix alliages a été étudié dans ce cas.

Pour chaque alliage, cent barreaux pour les essais de traction ont été préparés en utilisant un moule métallique permanent de type ASTM B-108. Chaque coulée a fourni deux barreaux pour l'essai. Les barreaux de traction ont été traités thermiquement par

divers traitements thermiques de mise en solution, c.-à-d. quatre étapes simples, huit étapes doubles, et quatre étapes triples de traitements de mise en solution. Les températures de mise en solution utilisés étaient 450°C, 490°C, 500°C et 520°C, pendant des temps de mise en solution de 4h et de 8h, dans diverses combinaisons de ces températures et périodes. Après le traitement thermique de mise en solution, toutes les barreaux ont été trempés dans l'eau chaude (60°C), suivi d'un vieillissement à 155°C pour une période de 5h. Les réactions se produisant pendant la solidification ont été surveillées en utilisant l'analyse thermique, alors que la dissolution des phases de cuivre était analysée en utilisant un système optique d'analyseur d'image. Une microsonde électronique (EPMA) couplé aux rayons X à énergie dispersive (EDX) et de la spectroscopie de longueur d'onde (WDS) ont été utilisés.

Les résultats montrent que dans la condition de tel que coulé, la ségrégation du cuivre se produit aux joints de grain, et la présence du strontium ou du magnésium peut empirer la ségrégation. Quand le magnésium et le strontium sont ajoutés en même temps, cependant, la ségrégation est affaiblie dans une certaine mesure comparée à leur addition individuelle. Après le traitement thermique de mise en solution, et particulièrement dans les alliages modifiés par le strontium, le cuivre commence à se distribuer à travers les dendrites aussi bien que dans la matrice, avec l'augmentation du temps de mise en solution et de la température. La quantité non dissoute d'Al_2Cu diminue et le cuivre augmente dans la matrice, atteignant un maximum après un traitement thermique de mise solution de 490° durant 8h. L'addition du Mg dans les alliages 319 (expérimentaux ou industriels) mène à un point de fusion bas et une phase complexe insoluble de type $Al_5Mg_8Cu_2Si_6$. L'augmentation d'addition de magnésium à 0.6 % en poids augmente la fraction volumique de cette phase et les précipitations pré-eutectique et post-eutectique $Al_5Mg_8Cu_2Si_6$ sont observées. Dans les traitements thermiques de mise en solution où la dernière température utilisée excède le point de fusion de la phase $Al_5Mg_8Cu_2Si_6$, la fusion locale de cette phase se produit, entraînant une détérioration grave des propriétés mécaniques d'alliage.

La présence du Sr a comme conséquence la modification de la morphologie des particules de silicium eutectique d'une forme aciculaire dans les alliages non modifiés à une forme fine et fibreuse dans les alliages modifiés par le strontium. On observe également une dépression correspondante à la température Al-Si eutectique. Cependant, le strontium mène également à la ségrégation de la phase de cuivre dans des secteurs loin des régions eutectiques de silicium, de sorte que la phase d'Al_2Cu a une tendance à précipiter dans une forme de blocs plus massifs plutôt que dans sa forme eutectique plus fine. Ce changement de la morphologie de la phase de cuivre ralentit son taux de dissolution pendant le traitement thermique de mise en solution de sorte que quand (a) le temps du traitement de mise en solution de la première étape n'est pas suffisamment long pour dissoudre les particules d'Al_2Cu, et (b) la température du traitement de la deuxième étape est plus haute que le point de fusion d'Al_2Cu, la fusion locale aura lieu, et en raison du rétrécissement de volume pendant la trempe, on observera la formation de porosité. L'addition du Sr peut occasionner également des augmentations du pourcentage surfacique

de porosité et de la longueur des pores, en particulier à la température de traitement de mise en solution de 520 °C.

Les propriétés de traction, c.-à-d, les valeurs de la limite ultime (L.U), de la limite élastique (L.É), de l'allongement à la rupture (A%) et de l'index de qualité (Q) obtenues montrent que l'addition du magnésium aux alliages expérimentaux 319 mène à une augmentation de la limite d'élasticité et de la limite ultime, mais une dégradation dans l'allongement à la rupture. Dans les alliages non modifiés, la perte d'élongation est balancée par l'augmentation de la résistance, ainsi les valeurs de Q sont augmentées. Dans les alliages expérimentaux modifiés, la dégradation de l'élongation n'est pas équilibrée par l'augmentation de la résistance, ainsi les valeurs de Q sont diminuées. Le magnésium augmente la limite élastique (L.É) davantage que la limite ultime (L.U). La combinaison optimum du Mg et du Sr est de 0.3% de Mg avec 150 ppm Sr. Les propriétés de traction correspondantes dans la condition de tel que coulé sont 260 MPa (L.É), 326 MPa (L.U), 1.50% (A%), 352 MPa (Q), montrant une augmentation de 79% et 40% pour L.É et L.U, respectivement, une diminution de l'élongation de 38%, et une augmentation de l'index de qualité de 21% comparé à l'alliage de base. Une augmentation ultérieure du contenu de magnésium mène à la dégradation des propriétés de traction.

Pour les alliages étudiés, en l'absence du magnésium, le traitement thermique de mise en solution recommandé est 450°C/4h + 500°C/4h + 520°C/4h, pour lequel les propriétés de traction et l'index de qualité correspondants sont 385 MPa (L.U), 240 MPa (L.É), 5.25% (A%), et 493 MPa (Q). Dans les alliages contenants du Mg, le traitement thermique de mise solution optimum est 490°C/8h + 520°C/4h; les propriétés de traction correspondantes sont 445 MPa (L.U), 334 MPa (L.É), 4.24% (A%), et 539 MPa (Q), respectivement. Dans le cas des alliages industriels, les éléments de trace tels que le Ni, le Fe et le C, tendent à former autres intermétalliques de cuivre qui, à leur tour, fournissent des propriétés mécaniques plus élevées que les alliages expérimentaux contenant le même niveau du magnésium.

ABSTRACT

Aluminum-silicon-copper-magnesium 319 type alloys are widely used in the production of engine blocks due to their high fatigue resistance. These alloys belong to the heat-treatable class of aluminum alloys whose properties may be improved using a specific heat treatment comprising solution heat treatment, quenching and aging. The purpose of the solution treatment is to maximize the amount of hardening solutes (Cu and Mg) in solid solution in the aluminum matrix. In the case of 319 alloys, the solution temperature must be kept as close as possible to the copper eutectic temperature, limited, however, to a safe level below the maximum to avoid overheating and partial melting of the Al_2Cu phase (termed "incipient melting"). The solution treatment may be carried out in single or multiple steps. While the single-step treatment is usually limited to 495°C, to avoid incipient melting, it may not be sufficient to maximize dissolution of the Cu-rich phases, nor modify the silicon particle morphology, two important considerations in respect to improving the alloy properties. Two-step and multi-step solution treatments have therefore been proposed to rectify this problem.

The study presented in this thesis was performed on Al-Si-Cu-Mg 319 type alloys to investigate the role of solution heat treatment on the dissolution of copper-containing phases ($CuAl_2$ and $Al_5Mg_8Cu_2Si_6$) in 319 type alloys containing 0, 0.3 and 0.6 wt% Mg levels, to determine the optimum solution heat treatment with respect to the occurrence of incipient melting, in relation to the alloy properties. Two series of alloys were investigated: a series of experimental Al-7 wt% Si-3.5 wt% Cu alloys containing 0, 0.3, and 0.6 wt% Mg levels. This series was prepared in the laboratory using pure elements. The second series was based on industrial B319 alloy (containing 0.3 wt% Mg), where the Mg level was increased to 0.6 wt% by adding pure Mg metal to the melt. In order to study the effect of modification, strontium was added in the amount of 150 ppm to both the experimental and the industrial alloys, to provide a set of Sr-modified alloys. Thus a total of ten alloys were investigated in the present case.

For each alloy, one hundred tensile test bars were prepared using an ASTM B-108 type permanent metallic mold. Each casting provided two test bars. The tensile bars were heat-treated using various solution heat treatments, *i.e.* four single-step, eight two-step, and four triple-step solution treatments. The solution temperatures and times used were 450°C, 490°C, 500°C and 520°C, for solution times of 4h and 8h, in various combinations of these temperatures and times. After solution heat treatment, all bars were quenched in warm water (60°C), followed by aging at 155°C for 5h. The reactions occurring during

solidification were monitored using thermal analysis, while the dissolution of the copper phases was analyzed using an optical microscope-image analyzer system, and an electron probe microanalyzer (EPMA) coupled with energy dispersive X-ray (EDX) and wavelength dispersive spectroscopy (WDS) facilities.

The results show that in the as-cast condition, Cu segregation occurs at grain boundaries, and the presence of Sr or Mg can worsen the segregation. When Mg and Sr are added at the same time, however, the segregation is weakened to some extent compared to when they are added individually. After heat treatment, especially in the Sr-modified alloys, the copper begins to distribute evenly across the dendrites as well as in the matrix, with increasing solution time and temperature; the amount of undissolved Al_2Cu decreases and Cu in the matrix increases, reaching a maximum after a solution heat-treatment of 490°C/8h. Addition of Mg to 319 alloys (experimental or industrial) leads to the formation of the low-melting-point, insoluble complex phase $Al_5Mg_8Cu_2Si_6$. Increasing the Mg addition to 0.6 wt% increases the volume fraction of this phase and both *pre-eutectic* and *post-eutectic* $Al_5Mg_8Cu_2Si_6$ precipitation is observed. In solution heat treatments where the last solution temperature used exceeds the melting point of the $Al_5Mg_8Cu_2Si_6$ phase, incipient melting of this phase occurs, causing severe deterioration of the alloy mechanical properties.

The presence of Sr results in the modification of the eutectic Si particle morphology from a coarse, flake-like form in the non-modified alloys to a fine, fibrous form in the Sr-modified alloys. A corresponding depression of the Al-Si eutectic temperature is also observed. However, strontium also leads to the segregation of the copper phase in areas away from the eutectic silicon regions, so that the Al_2Cu phase has a tendency to precipitate in the more massive block-like form rather than its finer eutectic-like form. This change in the Cu-phase morphology slows its dissolution rate during solution heat treatment so that when (a) the solution time of the first-step treatment is not sufficiently long to dissolve the Al_2Cu particles, and (b) the temperature of the second-step treatment is higher than the melting point of Al_2Cu, incipient melting will take place, and as a result of volume shrinkage during quenching, porosity formation will be observed. The addition of Sr is also found to lead to increases in area percent porosity and pore length, particularly at the 520°C solution treatment temperature.

The tensile properties, *i.e.* ultimate tensile strength (UTS), yield strength (YS), percentage elongation (%El), and quality index (Q) values obtained show that the addition of Mg to the experimental 319 alloys leads to an increase in the YS and UTS, but a degradation in the %El. In the non-modified alloys, the loss of elongation is overcome by the increase in strength, thus the Q values are increased. In the modified experimental alloys, the degradation of elongation is not balanced by the increase in strength, thus the Q values are decreased. Magnesium increases the yield strength more than the ultimate tensile strength. The optimum combination of Mg and Sr is that of 0.3wt% Mg with 150 ppm Sr. The corresponding tensile properties in the as-cast condition are 260 MPa (YS), 326 MPa

(UTS), 1.50% (El%), 352 MPa (Q), showing an increase of 79% and 40% for YS and UTS, respectively, a decrease in elongation of 38%, and an increase in the quality index of 21% compared with the base alloy. Further increasing the Mg content leads to degradation of the tensile properties.

For the alloys studied, in the absence of Mg, the recommended solution heat treatment is 450°C/4h + 500°C/4h + 520°C/4h, for which the corresponding tensile properties and quality index are 385 MPa (UTS), 240 MPa (YS), 5.25% (%El), and 493 MPa (Q). In the Mg-containing alloys, the optimum solution heat treatment is 490°C/8h + 520°C/4h; the corresponding tensile properties are 445 MPa (UTS), 334 MPa (YS), 4.24% (%El), and 539 MPa (Q), respectively. In the case of the industrial alloys, trace elements such as Ni, Fe and C tend to form other Cu-intermetallics which, in turn, provide higher mechanical properties than the experimental alloys containing the same level of magnesium.

ACKNOWLEDGMENTS

It is a great pleasure to have the chance to convey my thanks to all those who were involved, directly or indirectly, in making this project a success. I would like to express my sincere thanks to my supervisors, Professors F. H. Samuel and A.M. Samuel, for giving me the opportunity to undertake this research.

I would like to convey my appreciation to all members of the TAMLA group for their assistance during my two years of research, particularly to Alain Bérubé, Mathieu Paradis and Sabrina Tremblay for their help with the castings and sample preparation; also to Hany Ammar, Ahmed Nabawy and Junfeng Guo, who created a congenial environment conducive to study. Many thanks also go to Deyu Yang who recommended me to UQAC and provided me with much assistance when I came here.

I wish to express my grateful acknowledgement to the Natural Sciences and Engineering Research Council of Canada (NSERC), General Motors Powertrain Group (U.S.A.), Corporativo Nemak (Mexico), and the Fondation de l'Université du Québec à Chicoutimi (FUQAC) for financial assistance (in the form of scholarships) and in-kind support.

Finally, I would like to express my profound gratitude to the members of my family, especially my parents, without whose encouragement and support, I would not have been able to fulfill my goal of completing a Master's Degree successfully.

TABLE OF CONTENTS

RÉSUMÉ iii

ABSTRACT vi

ACKNOWLEDGMENTS ix

TABLE OF CONTENTS x

LIST OF FIGURES xiii

LIST OF TABLES xx

CHAPTER 1

DEFINITION OF THE PROBLEM 1

1.1 INTRODUCTION 2

1.2 OBJECTIVES 5

CHAPTER 2

REVIEW OF THE LITERATURE 7

2.1 ALUMINUM-SILICON ALLOYS 8

2.1.1 Al-Si-Cu-Mg Alloys 9

2.2 SOLIDIFICATION OF Al-Si-Cu-Mg ALLOYS 12

2.3 COPPER INTERMETALLIC PHASES 14

2.4 SILICON PARTICLE CHARACTERISTICS 19

2.5 ROLE OF STRONTIUM 24

2.6 ROLE OF MAGNESIUM 30

2.7 COMBINED EFFECTS OF MAGNESIUM AND STRONTIUM....33
2.8 HEAT TREATMENT OF Al-Si-Cu-Mg ALLOYS....35
2.8.1 Solution Heat-Treatment....36
2.8.2 Quenching....45
2.8.3 Aging Treatment....45
2.9 INCIPIENT MELTING....47
2.10 POROSITY....48
2.11 TENSILE PROPERTIES....52
2.12 QUALITY INDEX....55

CHAPTER 3

EXPERIMENTAL PROCEDURES....57

3.1 ALLOY PREPARATION....58
3.2 MELTING AND CASTING....59
3.3 THERMAL ANALYSIS....61
3.4 SOLUTION HEAT TREATMENT AND AGING....62
3.5 TENSILE TESTING....63
3.6 METALLOGRAPHY....64

CHAPTER 4

RESULTS AND DISCUSSION....66

4.1 CHARACTERIZATION OF MICROSTRUCTURE....68
4.1.1 Thermal Analysis....68
4.1.2. Dissolution of Al_2Cu phase....75
4.1.2.1 Non-modified alloys....76
4.1.2.2 Sr-modified alloys....82
4.1.3 Melting of $Al_5Mg_8Cu_2Si_6$ Complex Phase....92
4.1.4 Porosity Characteristics....96
4.1.5 Silicon Particle Characteristics....108
4.2 TENSILE PROPERTIES....123

4.2.1 As-Cast Condition....124
4.2.1.1 Effect of Mg....124
4.2.1.2 Effect of Sr....127
4.2.1.3 Combined effects of Sr and Mg....130
4.2.2 Effect of Solution Heat-Treatment....131
4.2.2.1 Experimental alloys....131
4.2.2.2 Industrial alloys....146

CHAPTER 5

CONCLUSIONS....158

RECOMMENDATIONS FOR FUTURE WORK....165

REFERENCES....166

LIST OF FIGURES

CHAPTER 2

Figure 2.1 Part of Al-Si phase diagram showing composition ranges of various alloy types. 9

Figure 2.2 Microstructure of 319.1 alloy showing morphologies of Al_2Cu: (a) eutectic-like Al-Al_2Cu, and (b) block-like Al_2Cu. 15

Figure 2.3 Backscattered image showing the dissolution process of Al_2Cu particles.[10] 16

Figure 2.4 Variation in the percentage of undissolved Al_2Cu as a function of solution time in the temperature range 480–540°C. (■) 480°C, (▲) 505°C, (●) 515°C, (*) 540°C.[13] 17

Figure 2.5 Measured concentration values of copper in the aluminum matrix as a function of solution time in the temperature range 480°C to 515°C.[9] 18

Figure 2.6 Variations in (a) YS and UTS, (b) ductility (pct elongation) as a function of copper concentration in the aluminum matrix.[13] 18

Figure 2.7 Microstructures of A356 alloy showing the morphology of eutectic Si as a function of time at a solution temperature of 540°C (500X). Unmodified: (a) As-cast, (b) 2 h, (c) 8 h; Modified: (d) As-cast, (e) 2 h, (f) 8 h. 20

Figure 2.8 Variation of average equivalent Si particle diameter in A356 alloy as a function of solution temperature. Solution time: 100 min (permanent mold).[18] 22

Figure 2.9 Microstructure showing the morphology of large Si particles in unmodified A356 alloy treated at 570°C for 100 min.[18] 22

Figure 2.10 Silicon particle aspect ratio in 357 alloys as a function of solution time, at two different cooling rates (noted in terms of the cell count).[19] 23

Figure 2.11 Arithmetic mean Si particle volume as a function of time at 540°C for Al-Si alloys. Three compositions are averaged at each time.[20] 23

Figure 2.12 The relationship between the strontium level and the characteristic temperatures of the copper-rich eutectic phases for a cooling rate of approximately 0.48°C/s.[1] 28

Figure 2.13 Al_2Cu phase dissolution in (a) experimental Al-7% Si-3.5% Cu base alloy (coded ASC), and (b) the Sr-modified base alloy (coded ASCS) during solution heat-treatment at 505°C as a function of solution treatment time.[10] 28

Figure 2.14 Depression of eutectic temperature as a function of Mg level for unmodified and Sr-modified Al-Si alloys.[39] 31

Figure 2.15 Hardness of AlSiCu and AlSiCuMg alloys as a function of the aging time at 160°C.[41] 33

Figure 2.16 Comparison of non-modified and Sr-modified microstructures from thermal analysis samples of Al-11%Si alloy containing various Mg levels: (a) 0.1 wt% Mg, 0 ppm Sr; (b) 0.1 wt% Mg, 200 ppm Sr; (c) 0.45 wt% Mg, 0 ppm Sr; (d) 0.45 wt% Mg, 200 ppm Sr; (e) 1.0 wt% Mg, 0 ppm Sr and (f) 1.0 wt% Mg, 200 ppm Sr.[39] 34

Figure 2.17 Effects of solution time on silicon particle morphology in (1) 354 and (2) 355 alloys solution heat-treated at 527°C.[52] 39

Figure 2.18 Optical micrographs showing (a) silicon particle morphology, (b) copper-rich phase in an as-cast automotive component; (c) silicon particle following single-step solution treatment; (d) copper-rich phase segregation following single-step solution treatment; (e) silicon particle morphology following two-step solution treatment; (f) remnants of copper-rich phases following two-step solution treatment.[1] 41

Figure 2.19 Dark spots observed on the fracture surfaces of test bars of 319+0.5 wt% Mg alloy, solutionized for (a) 12h/510°C, and (b) 12h/520°C. Arrows show the progress in the size of the dark spot with increase in solution temperature.[21] 43

Figure 2.20 Microstructure of 319 alloy showing the occurrence of incipient melting taking place at grain boundaries (arrowed).[13] 48

Figure 2.21 The growth process of porosity formation.[66] 50

Figure 2.22 Effect of quench rate on UTS and % Elongation.[73] 54

Figure 2.23 Plots of logUTS *vs.* log%El for alloys studied with different heat treatments (T5 and T6).[74] 54

CHAPTER 3

Figure 3.1 (a) Permanent mold used for preparing tensile test bars, and (b) Casting obtained from (a). 60

Figure 3.2 Schematic diagram of graphite mold and setup used for thermal analysis....61

Figure 3.3 Servohydraulic MTS 810 Material Test System....63

Figure 3.4 Optical microscope - Clemex image analyzer system. 64

Figure 3.5 The JEOL JXA-8900L electron probe microanalyzer....65

CHAPTER 4

Figure 4.1 Cooling curve (blue) and first derivative (pink) obtained from unmodified 319 alloys (a) Y1 (0 wt% Mg), and (b) Y6 (0.6 wt% Mg)....69

Figure 4.2 Cooling curve (blue) and first derivative (pink) obtained from Sr-modified 319 alloys (a) Y1S (0 wt% Mg), and (b) Y6S (0.6 wt% Mg). 70

Figure 4.3 Backscattered image obtained from the as-cast alloy Y6S showing the co-existence of Al_2Cu (solid arrow) and $Al_5Mg_8Cu_2Si_6$ (open arrow) phases....74

Figure 4.4 EDX spectra corresponding to the phases shown in Figure 4.3: (a) Al_2Cu phase, (b) $Al_5Mg_8Cu_2Si_6$ complex phase....74

Figure 4.5 Backscattered image obtained from Y1S alloy heat-treated at 450°C/4h, the thick dark line in the oval corresponds to the path across which the distribution of Cu in the matrix was analyzed and which is plotted in Figure 4.12. The solid arrows point to the cell boundaries, while the open arrow shows an undissolved Al_2Cu particle....76

Figure 4.6 Distribution of Cu (wt%) across the cell boundaries of α-Al dendrites in Y1 alloy, obtained from the as-cast and solution heat-treated samples....78

Figure 4.7 Distribution of Cu (wt%) across the cell boundaries of α-Al dendrites in Y4 alloy, obtained from the as-cast and heat-treated samples....79

Figure 4.8 Distribution of Cu (wt %) across the cell boundaries of α-Al dendrites in Y6 alloy, obtained from the as-cast and heat-treated samples....79

Figure 4.9 Variation in volume fraction of undissolved Al_2Cu as a function of solution heat-treatment in alloy Y1. 80

Figure 4.10 Distribution of Cu (wt%) across the cell boundaries of α-Al dendrites in Y7 alloy, obtained from the as-cast and solution heat-treated samples....81

Figure 4.11 Distribution of Cu (wt%) across the cell boundaries of α-Al dendrites in Y8 alloy, obtained from the as-cast and solution heat-treated samples....81

Figure 4.12 Distribution of Cu (wt%) across the cell boundaries of α-Al dendrites in Y1S alloy, obtained from the as-cast and solution heat-treated samples....83

Figure 4.13 Distribution of Cu (wt%) across the cell boundaries of α-Al dendrites in Y4S alloy, obtained from the as-cast and solution heat-treated samples....83

Figure 4.14 Distribution of Cu (wt%) across the cell boundaries of α-Al dendrites in Y6S alloy, obtained from the as-cast and solution heat-treated samples....84

Figure 4.15 Distribution of Cu (wt%) across the cell boundaries of α-Al dendrites in Y7S alloy, obtained from the as-cast and solution heat-treated samples....84

Figure 4.16 Distribution of Cu (wt%) across the cell boundaries of α-Al dendrites in Y8S alloy, obtained from the as-cast and solution heat-treated samples....85

Figure 4.17 Undissolved Al_2Cu in alloys (a) Y1 and Y1S; (b) Y4 and Y4S; (c) Y6 and Y6S; (d) Y7 and Y7S; and (e) Y8 and Y8S as a function of single-step solution heat-treatment....87

Figure 4.18 Backscattered images of alloys (a) Y1, 60X (b) Y6, 60X (c) Y1S, 100X (d) Y6S, 100X in the as-cast condition showing severe segregation of Al_2Cu in areas away from the eutectic Si regions in the modified alloys....89

Figure 4.19 Backscattered images showing undissolved Al_2Cu in alloy Y1 obtained from the four single-step solution treatments: (a) 450°C/4h, 60X (b) 450°C/8h, 60X (c) 490°C/4h, 60X (d) 490°C/8h, 60X....90

Figure 4.20 High magnification of microstructure of Al-Al_2Cu in the as-cast samples: (a) Y6 and (b) Y6S alloys. Note the eutectic Al_2Cu (open arrow) and block-like Al_2Cu (solid arrow)....91

Figure 4.21 Schematic diagram showing the dissolution process of (a) eutectic Al_2Cu and (b) block-like Al_2Cu....92

Figure 4.22 Microstructures of Y6S alloy after a solution heat treatment of 490°C/8h + 500°C/4h (treatment J) showing: (a) fragmentation and

dissolution of Al_2Cu (solid arrow), (b) persistence of $Al_5Mg_8Cu_2Si_6$ complex phase (open arrows). The white platelets in (b) are Al_5FeSi phase (black arrow).....94

Figure 4.23 DSC run for a powdered sample obtained from the experimental 319 alloy solidified at 10°C/s. The arrow in the enlarged circled area indicates the onset of the melting of the Al_2Cu phase.[9].....95

Figure 4.24 Temperature difference between the sample and reference plate thermocouples used as input for pure aluminum simulations.[79].....95

Figure 4.25 Plot showing area percent porosity and pore length in alloy Y1 after various solution heat-treatments.....98

Figure 4.26 Plot showing area percent porosity and pore length in alloy Y1S after various solution heat-treatments.....99

Figure 4.27 Plot showing area percent porosity and pore length in alloy Y6 after various solution heat-treatments.....100

Figure 4.28 Plot showing area percent porosity and pore length in alloy Y6S after various solution heat-treatments.....104

Figure 4.29 Pore lengths in alloy Y1, Y6, Y1S and Y6S as a function of solution heat-treatment.....105

Figure 4.30 Area percent porosity of alloy Y1, Y6, Y1S and Y6S as a function of solution heat-treatment.....106

Figure 4.31 Backscattered images showing: (a) porosity in alloy Y1 heat-treated at 490°C/8h+500°C/4h+520°C/4h; (b) porosity in alloy Y6S heat-treated at 490°C/8h+500°C/4h+520°C/4h; (c) high magnification of (b) showing unmelted Al_2Cu (marked A) and melted zone (marked B) in alloy; (d) high magnification of a region similar to that of A in (c), showing the cavities between the Al_2Cu and $Al_5Mg_8Cu_2Si_6$ phases (white arrows).....107

Figure 4.32 Schematic diagram showing modification of Si particles during solution heat-treatment in the case of: (a) non-modified and (b) modified Al-Si alloys.[82].....108

Figure 4.33 Si particle characteristics of alloy Y1 as a function of solution heat-treatment.....110

Figure 4.34 Si particle characteristics of alloy Y6 as a function of solution heat-treatment.....111

Figure 4.35 Si particle characteristics of alloy Y1S as a function of solution heat-treatment.....112

Figure 4.36 Si particle characteristics of alloy Y6S as a function of solution heat-treatment. 113

Figure 4.37 Average Si particle aspect ratio of alloys Y1, Y1S, Y6 and Y6S as a function of solution heat-treatment type. 116

Figure 4.38 Average Si particle area of alloys Y1, Y1S, Y6 and Y6S as a function of solution heat-treatment type. 117

Figure 4.39 Microstructures of samples obtained from the tensile-tested bars of (a) Y1, (b) Y1S, (c) Y6, and (d) Y6S alloys under the as-cast condition, showing the morphology of the eutectic Si particles. 119

Figure 4.40 Microstructures of samples obtained from the tensile-tested bars of (a) Y1, (b) Y1S, (c) Y6, and (d) Y6S after treatment 490°C/8h, showing the morphology of Si particles. 120

Figure 4.41 Microstructures of samples obtained from the tensile-tested bars of (a) Y1, (b) Y1S, (c) Y6 and (d) Y6S after treatment 490°C/8h+500°C/4h+520°C/4h, showing morphology of Si particles. 121

Figure 4.42 Microstructures showing Si particle morphology of alloy Y6 obtained from: (a) solution treatment K (490°C/4h + 520°C/4h); and (b) solution treatment P (490°C/8h + 500°C/4h + 520°C/4h). 122

Figure 4.43 High magnification backscattered image showing the Si particle morphology in alloy Y6S after 490°C/8h+500°C/4h+520°C/4h solution heat-treatment. 123

Figure 4.44 Tensile properties of (a) unmodified and (b) modified 319 alloys obtained in the as-cast condition as a function of Mg content 125

Figure 4.45 Variation of tensile properties as a function of Sr content for experimental alloys. 128

Figure 4.46 Variation of tensile properties as a function of Sr content for industrial alloys. 129

Figure 4.47 Combined effects of Sr and Mg on tensile properties of experimental alloys. 130

Figure 4.48 Tensile properties of alloy Y1 as a function of solution heat-treatment type 134

Figure 4.49 Tensile properties of alloy Y4 as a function of solution heat-treatment type 135

Figure 4.50 Tensile properties of alloy Y6 as a function of solution heat-treatment type 136

Figure 4.51 Tensile properties of alloy Y1S as a function of solution heat-treatment type 137

Figure 4.52 Tensile properties of alloy Y4S as a function of solution heat-treatment type.....138
Figure 4.53 Tensile properties of alloy Y6S as a function of solution heat-treatment type.....139
Figure 4.54 Quality index of alloy Y1 as a function of solution heat-treatment type....140
Figure 4.55 Quality index of alloy Y4 as a function of solution heat-treatment type....141
Figure 4.56 Quality index of alloy Y6 as a function of solution heat-treatment type....142
Figure 4.57 Quality index of alloy Y1S as a function of solution heat-treatment type.....143
Figure 4.58 Quality index of alloy Y4S as a function of solution heat-treatment type.....144
Figure 4.59 Quality index of alloy Y6S as a function of solution heat-treatment type.....145
Figure 4.60 Tensile properties of alloy Y7 as a function of solution heat-treatment type.....150
Figure 4.61 Tensile properties of alloy Y8 as a function of solution heat-treatment type.....151
Figure 4.62 Tensile properties of alloy Y7S as a function of solution heat-treatment type.....152
Figure 4.63 Tensile properties of alloy Y8S as a function of solution heat-treatment type.....153
Figure 4.64 Quality index of alloy Y7 as a function of solution heat-treatment type....154
Figure 4.65 Quality index of alloy Y8 as a function of solution heat-treatment type....155
Figure 4.66 Quality index of alloy Y7S as a function of solution heat-treatment type.....156
Figure 4.67 Quality index of alloy Y8S as a function of solution heat-treatment type.....157

LIST OF TABLES

CHAPTER 2

Table 2.1 Chemical Composition of 319 Alloys (wt %). 11

Table 2.2 Mechanical properties of 319 alloys produced by applying different techniques.[6] 12

CHAPTER 3

Table 3.1 Chemical composition of the industrial 319.2 alloy. 58

Table 3.2 Experimental and industrial alloys and their respective codes. 59

Table 3.3 Average chemical compositions (wt %) of the experimental and industrial alloys studied. 60

CHAPTER 4

Table 4.1 Expected reactions in non-modified 319 alloys.[51] 71

Table 4.2 Expected reactions in 150ppm Sr-modified 319 alloys (present study) 72

Table 4.3 Effect of various solution heat-treatment on the dissolution of the Al_2Cu phase in experimental alloys Y1, Y4 and Y6 as well as industrial alloys Y7 and Y8. 80

Table 4.4 Effects of solution heat-treatment on the dissolution of the Al_2Cu phase in modified experimental alloys Y1S, Y4S, Y6S as well as industrial alloys Y7S and Y8S. 85

Table 4.5 Volume fraction of $Al_5Mg_8Cu_2Si_6$ phase in alloy Y6 and Y6S (Sr-modified) obtained from the as-cast condition and after 490°C/8h + 500°C/4h solution treatment. 93

Table 4.6 Tensile properties of each alloy investigated in the present study as obtained in the as-cast condition. 126

Table 4.7 Optimum solution heat-treatment obtained for 319 alloys investigated in this study. 149

CHAPTER 1

DEFINITION OF THE PROBLEM

CHAPTER 1

DEFINITION OF THE PROBLEM

1.1 INTRODUCTION

Aluminum-silicon alloys containing copper (Cu) and magnesium (Mg) are classified as 3xx.x series type alloys. The alloy known as A319 (Al-6.5%Si-3.5%Cu) is a commercially popular alloy used in various applications. In the case of automotive components, Mg is usually added to the alloy to increase the strength of the cast part. The Mg-containing version is termed B319 alloy.

The percentage of Si in Al-Si alloys together with its shape and distribution play an important role in determining mechanical properties. Normally, eutectic silicon has an acicular or lamellar morphology. Strontium (Sr) is commonly employed in Al-Si casting alloys to modify the morphology of eutectic silicon from a coarse, flake-like form to a fine fibrous one so as to improve the mechanical properties of the alloy, particularly ductility. With the addition of Sr, the temperature T_{eut} of the Al-Si eutectic reaction is depressed and this depression is often used to estimate the degree of modification that has taken place in the Al-Si alloy. Other alloying elements such as Cu and Mg, together with varying amounts of iron, manganese and zinc as impurity elements, go into solid solution in the matrix and form intermetallic particles during solidification.

The addition of copper to Al-Si alloys leads to the formation of the copper intermetallic Al_2Cu phase, which increases the alloy strength at room and high temperatures. This phase is present in two forms: the eutectic-like (Al-Al_2Cu) phase and block-like Al_2Cu phase. The block-like Al_2Cu phase is much harder to dissolve in the aluminum matrix, and thus the benefits of having Cu as a strengthening agent during heat treatment are reduced.

The presence of Mg leads to an increase in the yield and tensile strength but tends to decrease the ductility noticeably. The presence of Mg also leads to a reduction in the eutectic temperature pertaining to Cu-containing phases as a result of the precipitation of the $Al_5Mg_8Cu_2Si_6$ intermetallic phase, which would indicate that the addition of Mg limits the maximum solutionizing temperature. When the Mg content is less than 0.6 wt%, Mg has a tendency to refine the eutectic Si particles. The addition of Mg also leads to segregation of the Cu phase in areas away from the eutectic Si regions, leading to the formation of the block-like Al_2Cu, as well as to that of the $Al_5Mg_8Cu_2Si_6$ phase which forms from the Al_2Cu phase along its edges during the last stage of solidification.

When combined with Sr, the presence of Mg negates the effect of Sr modification to such an extent, that a much higher level of Sr is required to achieve full modification of the eutectic Si structure. In the Sr-modified Mg-free alloy, the Al-Si eutectic is better modified than the one in the Mg-containing alloy modified with the same amount of Sr. Strontium modification, however, also results in a large volume fraction of the interdendritic block-like Al_2Cu structure in 319 alloys, which is much harder to dissolve during solution heat-treatment, thus increasing the possibility of incipient melting and the consequent formation

of porosity; this is significant in that the increased porosity can adversely affect mechanical properties.[1]

Heat-treatable aluminum alloys are those whose mechanical properties may be improved by using a specified heat treatment or temper. Heat treatment is an elevated temperature process designed to allow soluble elements such as Mg and Cu to become supersatured in solid solution, followed by cooling which is rapid enough to make the excess solute precipitate. The treatment includes three steps, solution heat-treatment, quenching and aging. The purpose of the solution heat-treatment is to put the maximum amount of hardening solutes such as Cu and Mg into solid solution in the aluminum matrix. Thus, the temperature of solution heat-treatment in the case of 319 alloys must be as close as possible to the Cu eutectic temperature, although, at the same time, this temperature should be limited to a safe level, below the maximum, so as to avoid overheating and partial melting of the Al_2Cu phase.

The solution heat-treatment process may be carried out either in a single step or in multiple steps. The single-step treatment for 319 aluminum alloys is normally limited to 495°C, because a higher temperature may lead to the incipient melting of the copper phase. On the other hand, heat treatment at temperatures of 495°C, or less, is not enough to maximize the dissolution of the copper-rich phases, nor to modify the morphology of silicon particles. In order to overcome this problem, a two-step solution heat-treatment was proposed by Sokolowski *et al.*,[2] where a two-stage solution heat-treatment, with the second-stage maintained at temperatures below 525°C, was found to be more powerful than the conventional single-stage solution heat-treatment of 8h at 495°C.

Quenching is the step following solution heat-treatment, and it is usually conducted in water, which freezes the structure for a brief period of time. The purpose of this process is to preserve the solid solution formed at the solution heat-treating temperature, by rapidly cooling to some lower temperature, which is usually near room temperature.

Aging treatment is the controlled process of allowing the hardening constituents to re-precipitate, either at room temperature (natural aging) or at an elevated temperature (artificial aging), and thus provide a hardening effect. By the proper combination of solution heat-treatment, quenching, and artificial aging, the highest strength values may be obtained.

1.2 OBJECTIVES

For this study, experimental and industrial 319 alloys containing different Mg levels of 0, 0.3 and 0.6 wt% were used, in both the non-modified and Sr-modified conditions. Single-step and multiple-step solution heat-treatments were also carried out on these alloys.

The main purpose of this study was to investigate the metallurgical parameters controlling the occurrence of incipient melting of the copper phases in Al-Si-Cu-Mg alloys, including their consequent effect on the tensile properties. These objectives were accomplished by examining the following factors.

(1) Effects of Sr and Mg addition on the dissolution rates of Al_2Cu and the occurrence of incipient melting in each alloy;

(2) Combined effects of magnesium and strontium on the tensile properties of the alloy;

(3) Optimization of the solution heat-treatment parameters in relation to the alloy properties through a study of single-step and multiple-step solution treatments.

CHAPTER 2

REVIEW OF THE LITERATURE

CHAPTER 2

REVIEW OF THE LITERATURE

2.1 ALUMINUM-SILICON ALLOYS

Al-Si casting alloys are considered to be among the most important aluminum casting alloys because of the high fluidity imparted to them by the presence of relatively large volumes of the Al-Si eutectic. Besides this asset, Al-Si alloys have many other advantages including high resistance to corrosion, good weldability, excellent castability and the fact that the silicon phase reduces both the shrinkage during solidification and the coefficient of thermal expansion of the cast products. Machining may present certain difficulties, however, because of the presence of hard silicon particles in the microstructure. Silicon also has a low density (2.34 $g.cm^{-3}$), which may be an advantage in reducing the overall weight of the cast component. The maximum amount of silicon in cast alloys is of the order of 22-24%, but in alloys fabricated using powder metallurgy routes, the silicon level may be as high as 40-50%. [3]

Depending on the silicon content, Al-Si alloys can be divided into hypoeutectic, eutectic and hypereutectic alloys, as shown in Figure 2.1. In hypoeutectic alloys, the silicon varies between 5.5 and 10.5%, and primary aluminum is the first phase to precipitate during solidification. The microstructure consists of primary aluminum dendrites surrounded by the Al-Si eutectic structure. Eutectic alloys contain 10.5 to 13.5% silicon and have

microstructures consisting mainly of the Al-Si eutectic. Hypereutectic alloys contain 16 to 23% silicon. In these alloys, the first phase to solidify, the primary phase, is silicon. These alloys tend to display a distribution of coarse silicon particles which provide excellent wear resistance.

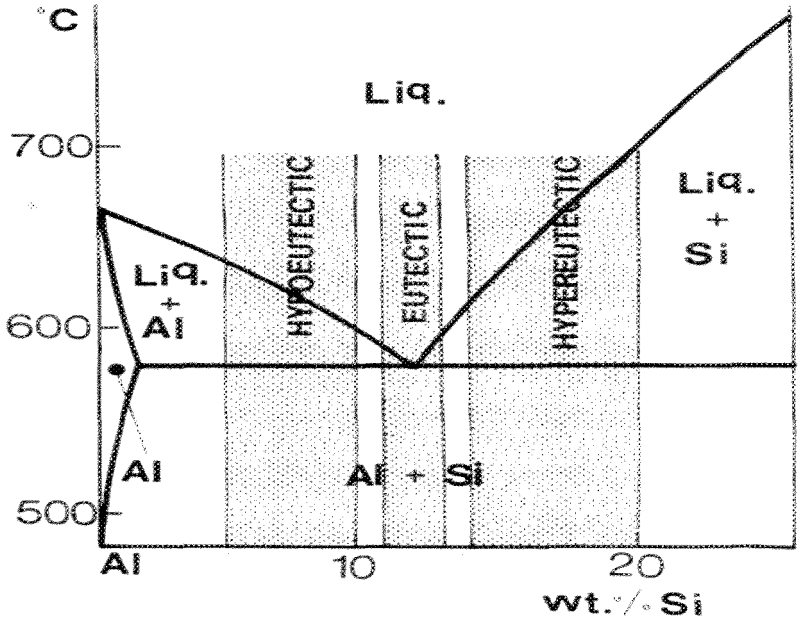

Figure 2.1 Part of Al-Si phase diagram showing composition ranges of various alloy types.[4]

2.1.1 Al-Si-Cu-Mg Alloys

Other alloying elements are often added to aluminum-silicon alloys to attain certain metallurgical objectives, such as permitting heat treatment, grain refinement, modification, and so forth. Among these elements, copper and magnesium are usually added to improve the strength and hardness through precipitation-hardening during aging. Copper substantially improves strength and hardness in both the as-cast and heat-treated alloy. Magnesium is the basis for hardness and strength development in heat-treated Al-Si alloys,

where the precipitation of Mg_2Si provides excellent obstacles for dislocation movement, thereby causing the hardening effect in the alloy.

Depending on their different chemical compositions, aluminum alloys are divided into several series. Each country has developed its own aluminum casting alloy nomenclature and designations, and so far, no internationally accepted system has yet been adopted for identification. In the U.S.A, the Aluminum Association has adopted a four-digit numerical system to identify aluminum casting alloys. The nine alloy series and their major alloying elements are shown below: [5]

1xx.x: unalloyed composition.

2xx.x: alloys containing copper as the main alloying element.

3xx.x: aluminum-silicon alloys also containing magnesium or copper.

4xx.x: binary aluminum-silicon alloys.

5xx.x: alloys containing magnesium as the main alloying element.

6xx.x: unused.

7xx.x: aluminum alloys containing zinc as the alloying element. It is common to find additions of copper, magnesium, chromium or manganese.

8xx.x: aluminum alloys containing tin as the main alloying element.

9xx.x: unused.

Among these digits, the first one indicates the main alloying element in the group. With respect to the 1xx.x group, the two digits to the left of the decimal denote the minimum of aluminum content. For example, for an alloy 190.x, the digit 90 indicates that the purity of this alloy is 99.90%. For the other groups, from 2xx.x to 9xx.x, these two

digits have no specific significance and serve only to identify the different alloys in the group. The last digit to the right of the decimal point is used to identify the product form. That is to say, digits 0, 1, or 2 denote castings, standard ingot, or ingot having composition ranges narrower than, but within, those of the standard ingot, respectively. In addition, owing to the percentage of impurities or small amounts of alloying elements, these alloys may be further identified by a prefix letter, A, B, and so forth. For instance, 319 alloys may be classified as A319.0, A319.1, B319.1, 319.1, 319.2, *etc.*, depending on their chemical composition, as shown in Table 2.1.

Table 2.1 Chemical Composition of 319 Alloys (wt %).[6]

AA	Si%	Fe%	Cu%	Mg%	Mn%	Zn%	Ti%	Ni%
319.0	5.5-6.5	1.0	3.0-4.0	0.1	0.5	1.0	0.25	0.35
319.1	5.5-6.5	0.8	3.0-4.0	0.1	0.5	1.0	0.25	0.35
319.2	5.5-6.5	0.6	3.0-4.0	0.1	0.1	1.0	0.25	0.10
A319.0	5.5-6.5	1.0	3.0-4.0	0.1	0.5	3.0	0.25	0.35
A319.1	5.5-6.5	0.8	3.0-4.0	0.1	0.5	3.0	0.25	0.35
B319.0	5.5-6.5	1.2	3.0-4.0	0.1-0.5	0.8	1.0	0.25	0.5
B319.1	5.5-6.5	0.9	3.0-4.0	0.1-0.5	0.8	1.0	0.25	0.5

Among Al-Si-Cu-Mg alloys, the Al-6.5% Si-3.5% Cu type 319 alloy is a commercially popular alloy used in various applications. In the case of automotive components, Mg is usually added to the alloy to increase the strength of the cast part. The Mg-containing version is termed B319 alloy. Table 2.2 lists the mechanical properties of 319 alloys cast by applying different techniques.[6]

Table 2.2 Mechanical properties of 319 alloys produced by applying different techniques.[6]

Technique	Condition	Yield Strength (MPa)	Ultimate Tensile Strength (MPa)	Elongation (%)
Sand Casting	As-Cast	125	185	2.0
	T6	165	250	2.0
Permanent Mold Casting	As-Cast	130	235	2.5
End Chill Casting	T6	185	280	3.0
	T5(180°C/8h) 100 mm from chill end	130.9	157.1±1.4	0.6 ± 0.2

2.2 SOLIDIFICATION OF Al-Si-Cu-Mg ALLOYS

All commercial solidification processes involve some non-equilibrium effects. True stable equilibrium conditions seldom exist during the solidification process of an alloy. The study of the equilibrium system is extremely valuable, however, because it constitutes a limiting condition from which the actual solidification conditions may be estimated.[7] In real casting processes, the extent of deviation from equilibrium conditions has a significant effect on the actual microstructure observed.

In the solidification process of 319 alloy (Al-6.23 wt% Si-3.8 wt% Cu-0.46 wt% Fe-0.14 wt% Mn-0.06 wt% Mg), Samuel *et al.*[8] have reported that the main sequence of phase precipitation is as follows:

(1) the formation of primary aluminum at about 608°C;

(2) the main silicon-forming eutectic reaction at about 563°C;

(3) an Al_2Cu-forming eutectic reaction at about 550°C ($L \rightarrow Al + Al_2Cu$);

(4) a complex eutectic reaction at about 525°C (L → Al + Al_2Cu + β-Al_5FeSi + Si).

Bäckerud *et al.*[4] reported the solidification sequence in 319 alloy (Al-5.7 wt% Si-3.4 wt% Cu-0.62 wt% Fe-0.36 wt% Mn-0.10 wt% Mg) as follows:

(1) development of α-aluminum network at ~ 609°C;

(2) formation of the β-Fe phase Al_5FeSi at ~ 590°C (Liq.→ Al + $Al_{15}Mn_3Si_2$ + Al_5FeSi);

(3) formation of Al-Si eutectic at ~ 575°C (Liq. → Al + Si + Al_5FeSi);

(4) formation of Al_2Cu phase at ~ 525°C (Liq. → Al_2Cu +Si + Al_5FeSi);

(5) formation of Al_2Cu + $Al_5Mg_8Cu_2Si_6$ at ~507°C (Liq. → (Al) + Al_2Cu + Si + $Al_5Mg_8Cu_2Si_6$)

From the description above, both solidification sequences differ only slightly. After primary deposition of the Al dendrites, Bäckerud *et al.* detected the precipitation of $Al_{15}Mn_3Si_2$ (possibly together with Al_5FeSi) which was not observed by Samuel *et al.*, presumably because of the smaller Mn content of the alloy used by these latter authors. The temperature for precipitation of the Al-Si eutectic differs significantly in these studies, 575°C for Bäckerud *et al.* and 563°C for Samuel *et al.*[8]

The solidification rate during casting is important in that it affects almost all the microstructural parameters, such as dendrite arm spacing (DAS), the degree of eutectic silicon modification, and the porosity and intermetallics which occur in the microstructure.

2.3 COPPER INTERMETALLIC PHASES

The addition of Cu to Al-Si alloys leads to a slight increase in the alloy fluidity, which enhances castability and weldability. Of even greater significance is the fact that the addition of Cu to Al-Si alloys leads to the formation of the copper intermetallic Al_2Cu phase, which increases room and high temperature strength values. This phase is present in two forms: the eutectic (Al-Al_2Cu) phase and block-like Al_2Cu phase. The block-like Al_2Cu phase is much harder to dissolve in the aluminum matrix, and thus the benefits of having Cu as a strengthening agent during heat-treatment are reduced. Figure 2.2 shows the morphology of the eutectic Al-Al_2Cu and block-like Al_2Cu phase particles. When Mg is present, the Cu-Mg intermetallic phase $Al_5Mg_8Cu_2Si_6$ precipitates during a complex eutectic reaction which takes place in the final stages of solidification, and results in the reduction of the eutectic temperature related to the copper-containing phases. The presence of Mg also leads to a significant increase in the volume fraction of copper-containing phases with a clear tendency for segregation in localized areas.

The form of the Al_2Cu precipitates depends to a great extent on the cooling rate. At high cooling rates, the Al_2Cu phase occurs in the form of a fine eutectic in the interdendritic regions, together with the Si particles. As the cooling rate decreases, there is the possibility for simultaneous precipitation of the Al_2Cu phase in the coarse block-like form as well as in the eutectic form.

The mechanism of Al_2Cu precipitation in Sr-modified 319 alloys was proposed by Samuel *et al.*[8] as follows: during the first stages of solidification, the formation of the α-Al dendritic network is associated with the segregation of the Si and Cu in the melt, in front of

the growing dendrites. When the solidification temperature reaches the Al-Si eutectic temperature, round/fibrous Si particles precipitate, leading to a local concentration of segregated Cu in the remaining area. The block-like Al_2Cu may precipitate directly from the liquid at Cu concentrations of ~ 53.5 wt%, while the eutectic Al-Al_2Cu forms at a lower Cu concentration of 33%, or in many cases, both forms precipitate together.[9]

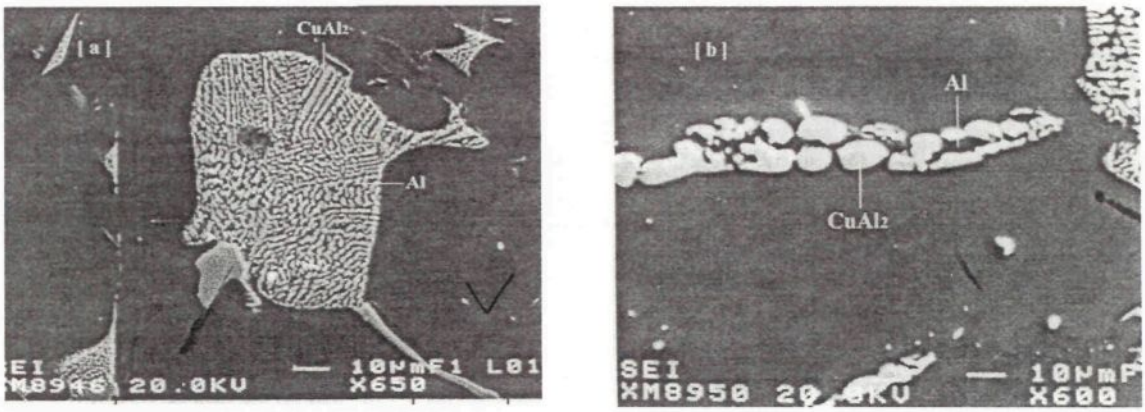

(a) (b)

Figure 2.2 Microstructure of 319.1 alloy showing morphologies of Al_2Cu: (a) eutectic-like Al-Al_2Cu, and (b) block-like Al_2Cu.[10]

Samuel *et al.*[11] made a detailed investigation of the dissolution of the Al_2Cu phase in 319.2 alloy. In their summary, they stated that dissolution of the eutectic copper phase occurs through its fragmentation into smaller segments which gradually dissolve in the surrounding Al matrix with an increase in solution treatment time. The location of the Al_2Cu eutectic phase (within the grain or at the grain boundary) does not alter the process of dissolution. Traces of the remaining eutectic phase were detected through the presence of the fine Si particles which co-precipitated along with the copper eutectic during its formation.

Li [10,12] reported the mechanism for the dissolution of the Al_2Cu phase in alloy 319 during solution heat-treatment as follows:

(1) separation of the Al_2Cu particles from the β-Al_5FeSi platelets;

(2) necking of the Al_2Cu particles followed by spheroidization;

(3) dissolution of the spheroidized particles by radial diffusion of Cu atoms in the surrounding aluminum matrix.

These stages are illustrated in Figure 2.3.

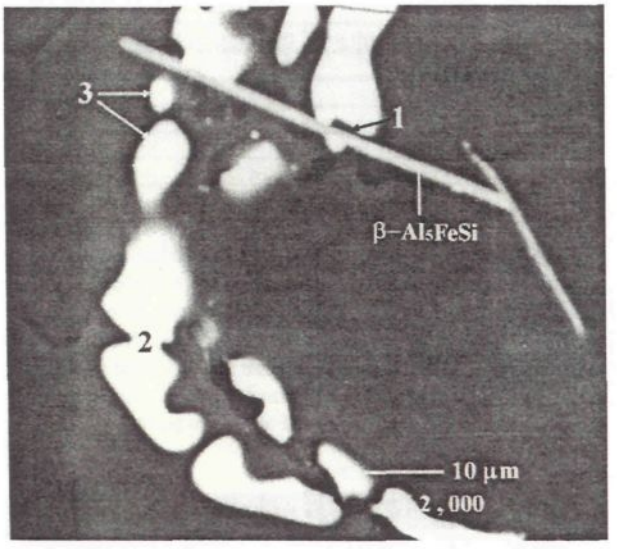

Figure 2.3 Backscattered image showing the dissolution process of Al_2Cu particles.[10]

The dissolution of the eutectic Al-Al_2Cu was found to take place at temperatures which were close to the final solidification temperature of the alloy (*i.e.* 480°C). From Figure 2.4, it is possible to observe that heating at 480°C results in a noticeably sluggish dissolution of the Al_2Cu phase. As soon as the solution temperature is increased to 505°C, the dissolution of Al_2Cu accelerates, and exhibits relatively linear behavior with solution treatment time. At 515°C, which is the temperature recommended for solution heat-

treatment; about 80% of the Al_2Cu is dissolved after 8 hours. Further heating at this temperature does not bring about much change in the amount of undissolved Al_2Cu phase, whereas solution treatment at 540°C apparently causes a marked change. This change, however, may be attributed to the melting of the Al_2Cu phase, rather than to its dissolution.[13]

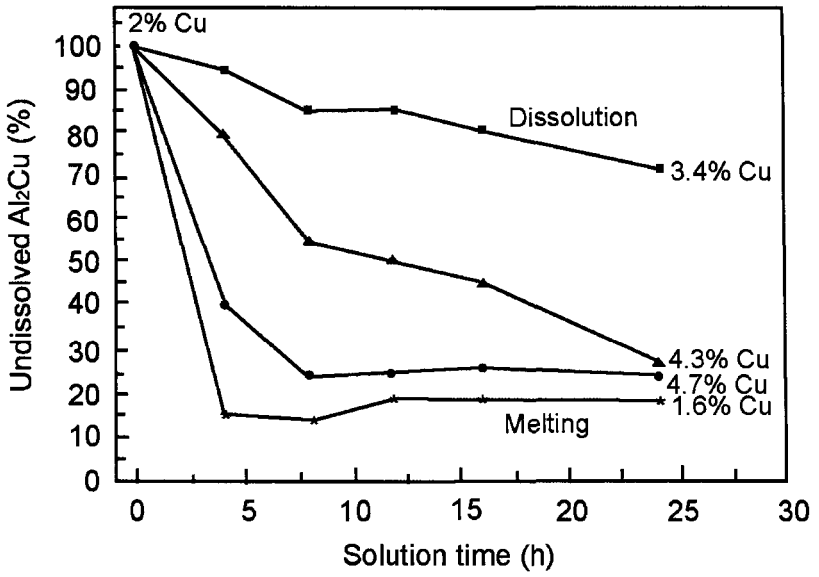

Figure 2.4 Variation in the percentage of undissolved Al_2Cu as a function of solution time in the temperature range 480–540°C. (■) 480°C, (▲) 505°C, (●) 515°C, (*) 540°C.[13]

Figure 2.5 reveals that reduction in the amount of undissolved Al_2Cu phase leads to enrichment of the surrounding matrix with copper,[9] which further reinforces the result that the tensile properties (YS, UTS and %El) show a linear relationship with the dissolved copper concentration in the temperature range studied (480°C-540°C),[13] as depicted in Figure 2.6, based on which the following corresponding equations were also proposed:

$$YS\ (MPa) = 81.1+24.9\times Cu\ (wt\%) \qquad (1)$$

$$\text{UTS (MPa)} = 154.5 + 36.6\times\text{Cu (wt\%)} \quad (2)$$

$$\text{El(\%)} = 0.023 + 1.01\times\text{Cu (wt\%)} \quad (3)$$

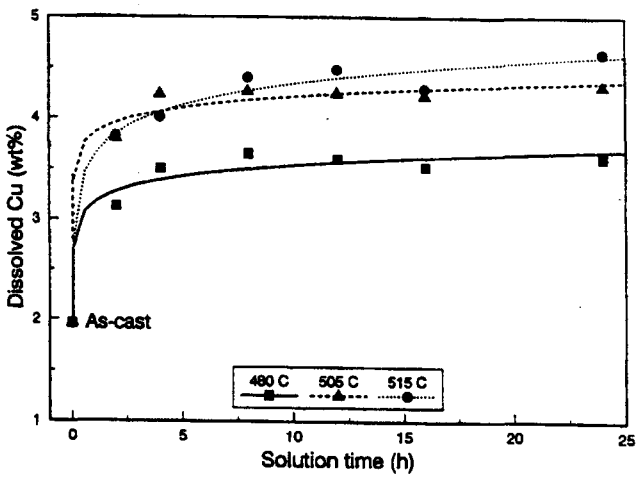

Figure 2.5 Measured concentration values of copper in the aluminum matrix as a function of solution time in the temperature range 480°C to 515°C.[9]

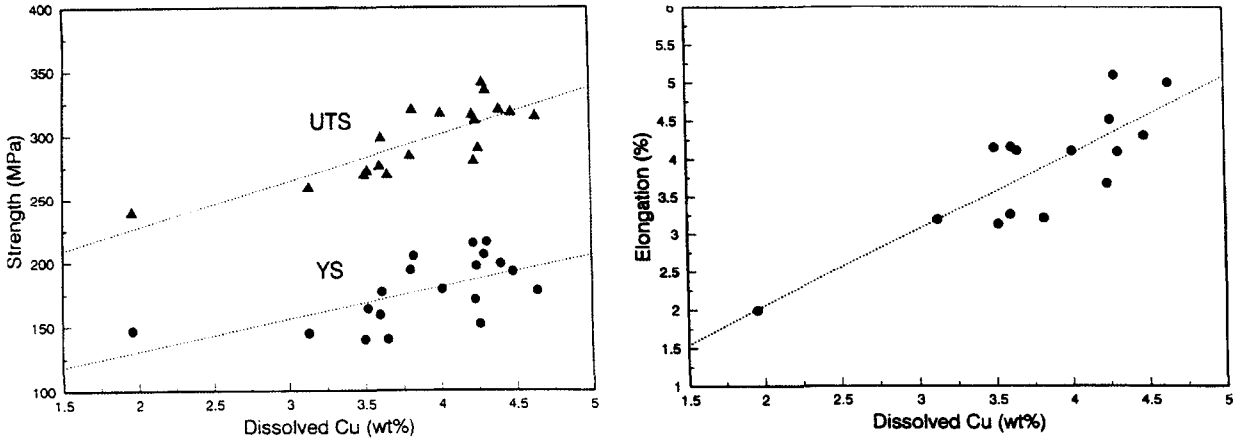

(a) (b)

Figure 2.6 Variations in (a) YS and UTS, (b) ductility (pct elongation) as a function of copper concentration in the aluminum matrix.[13]

2.4 SILICON PARTICLE CHARACTERISTICS

Eutectic silicon morphology, namely, particle size and shape, plays an important role in determining the mechanical properties of Al-Si alloy castings. Under normal cooling conditions, the eutectic silicon particles, present as coarse, acicular needles, act as crack initiators and lower the mechanical properties. The addition of small amounts of strontium (Sr) or sodium (Na) to the melt alters the morphology of the eutectic Si particles from acicular to fibrous, which is considered to enhance the mechanical properties significantly. Silicon particle characteristics can also be altered by subjecting the casting to a high temperature treatment for long periods. In recent years, chemical and thermal modifications have been used conjointly to produce the desired properties in a casting.

The changes in microstructure occurring during heat treatment of unmodified and Sr-modified A356 samples are shown in Figure 2.7.[14] Initially, Si particles break down into smaller fragments and spheroidize gradually (*cf.* Figs 2.7a and b). Prolonged solution treatment leads to coarsening of the particles, Figure 2.7(c). Both spheroidization and coarsening are driven by surface energy, *i.e.* the system tries to reduce excess surface area to the least possible. It will be observed clearly from Figure 2.7(d) that modification has a profound influence on spheroidization. In modified alloys, a higher degree of spheroidization is observed after only 2 hours of solution treatment, Figure 2.7(e), while in unmodified alloys, even after 2 hours, coarse needles of Si are visible, Figure 2.7(b). As solution time is increased, there is a progressive coarsening of the Si particles. In regions containing high concentrations of Si, eventual coalescence of adjacent particles takes place, see Figure 2.7(f).

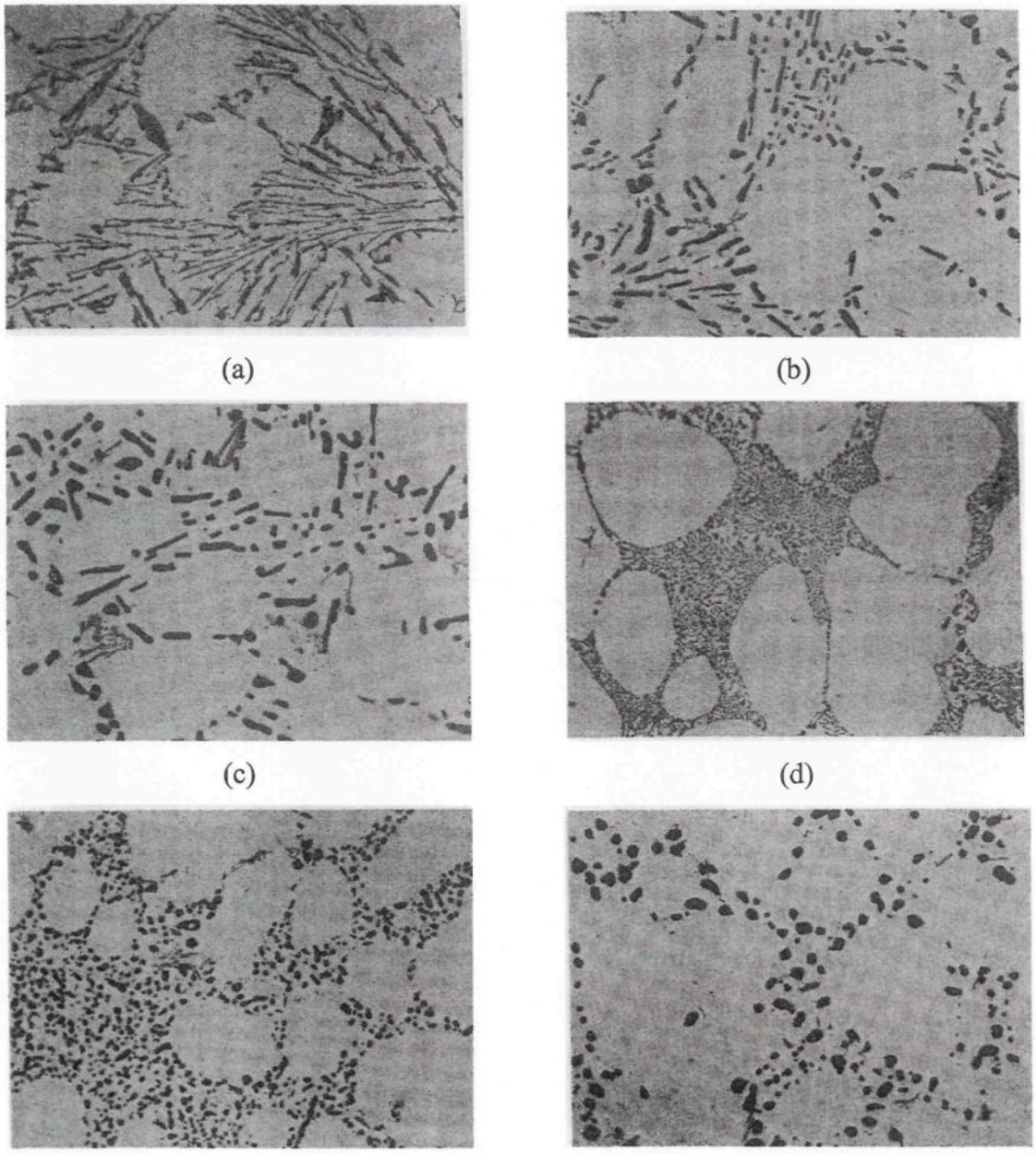

Figure 2.7 Microstructures of A356 alloy showing the morphology of eutectic Si as a function of time at a solution temperature of 540°C (500X). Unmodified: (a) As-cast, (b) 2 h, (c) 8 h; Modified: (d) As-cast, (e) 2 h, (f) 8 h. [14]

Zhu *et al.*[15] postulated that the change in Si morphology occurs in two stages: separation and spheroidization. In the first stage, the Si particles separate into segments at

corners or thin growth steps, but they retain their flake morphology. In the second stage, the broken segments spheroidize so that the Si particle aspect ratio decreases. These results agree with theoretical predictions that the initial breakdown of a eutectic structure during elevated temperature treatment arises from shape perturbations in the second phase constituent. The eutectic Si particles gradually break down into a series of nearly spherical crystals. The driving force for this process is a reduction in the total interfacial energy of the system.

The perturbation growth velocity is proportional to the solution treatment temperature. A higher perturbation growth velocity results in the formation of deep necks within the particles, so that the fragmentation and spheroidization processes occur rapidly. Consequently, the rate of spheroidization increases with temperature. Shape perturbations cannot readily occur in plate-like eutectics, and the structure is resistant to spheroidization. Thus, in unmodified alloys, complete spheroidization is not obtained, even after treating the alloy at 560°C for extended periods. By comparision, a spheroidized structure is observed in modified alloys within about 1 hour at 540°C.

The kinetics of spheroidization and coarsening of eutectic Si are determined primarily by the solution temperature. [16, 17] Shivkumar *et al.* [18] stated that solution heat treatment of alloy A356 at 520°C showed no significant change in Si particle diameter, even after about 800 min of heat treatment. As the temperature was increased, however, the Si particles underwent fragmentation, spheroidization and coarsening. At 560°C, even with a heat treatment of 100 min, the Si particle diameter increased abruptly, and extremely large silicon particles were observed. When the alloy was solutionized at a temperature of

570°C, faceting was observed at times as low as 25 min. By comparison, at 540°C, faceting was observed only after about 800 min. Figure 2.8 shows the variation of average Si particle diameter as a function of solution temperature (solution time 100 min). Figure 2.9 shows the morphology of faceted Si particles in A356 alloy treated at 570°C. Grain

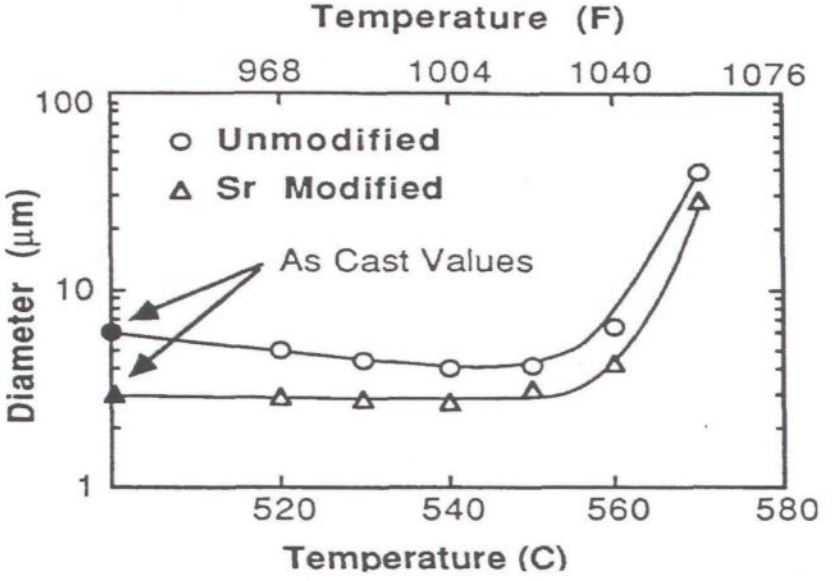

Figure 2.8 Variation of average equivalent Si particle diameter in A356 alloy as a function of solution temperature. Solution time: 100 min (permanent mold).[18]

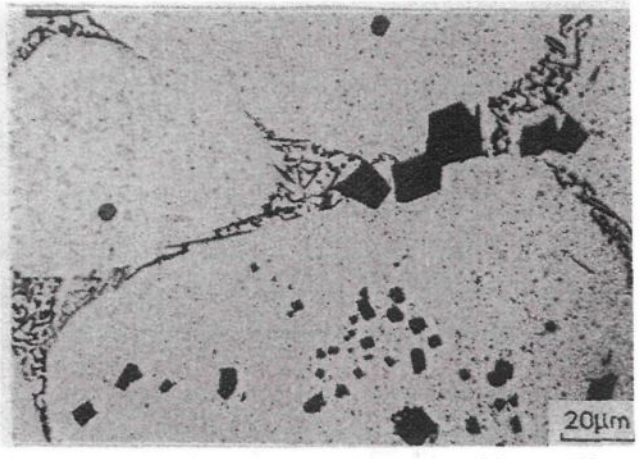

Figure 2.9 Microstructure showing the morphology of large Si particles in unmodified A356 alloy treated at 570°C for 100 min.[18]

boundary melting of ternary eutectics was also detected in samples solutionized at temperatures greater that 560°C and this melting had a strong detrimental effect on tensile properties. Rhines and Aballe[19] reported that the aspect ratio of Si particles in alloy 357 decreases with solution heat treatment time (see Figure 2.10). McLellan *et al.*[20] reported that the Si particle volume in Al-Si alloys increases linearly with time (Figure 2.11).

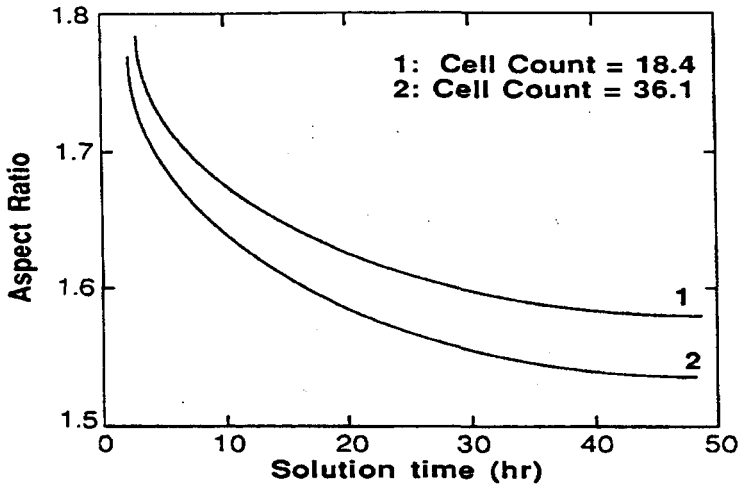

Figure 2.10 Silicon particle aspect ratio in 357 alloys as a function of solution time, at two different cooling rates (noted in terms of the cell count).[19]

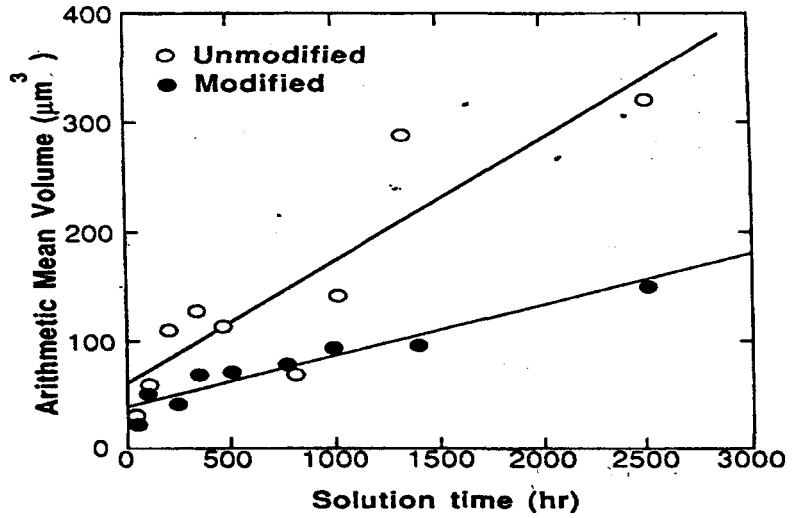

Figure 2.11 Arithmetic mean Si particle volume as a function of time at 540°C for Al-Si alloys. Three compositions are averaged at each time.[20]

De la Sablonnière and Samuel [21] found that the average particle size in the 319 alloy containing 0.5 wt% Mg is, in general, larger than the one with low Mg. For the 319 alloy containing a low Mg level, the roundness of the Si particles increases with increasing solution temperature, reflecting a continuous process of spheroidization, while for the alloy with 0.5 wt% Mg, spheroidization proceeds up to a certain stage (12h/510°C + 12h/525°C), then decreases at higher solution temperatures, as may be noted from the corresponding roundness values. Polygonal Si particles in the 319 alloy with 0.5wt% Mg may be observed when a two-step solution heat-treatment (12h/510°C + 12h/540°C) is applied. The authors explained that in the first instance, the Si particles undergo the normal fragmentation-spheroidization-coarsening process with progressing solution treatment. In the second case, however, it appears that a number of the Si particles undergo spheroidization directly, leading to the observation of coarser, primary-type Si particles for the same range of solution treatment conditions.

2.5 ROLE OF STRONTIUM

The mechanical properties of the 319 aluminum alloy (widely used for automobile components) are dependent to a high degree on the alloy structure, especially on the eutectic silicon which may assume an acicular form during solidification of unmodified melts, or may be fibrous in nature during solidification of modified melts. In unmodified alloy castings, the eutectic phase is brittle. Consequently, castings with lower strength and ductility are obtained. On the other hand, a properly modified melt produces castings with improved mechanical properties, particularly the percent elongation.[22]

Traditionally, in cast aluminum alloys, the modification of the silicon crystals has been carried out either through the enhancement of the solidification rate (*i.e.* quench modification) or through heat treatments for extended periods after solidification (*i.e.* thermal modification). In recent years, chemical modification through the addition of small quantities of elements such as Sr, Sb and Na to the melt has become an established industrial practice.[23] Strontium is commonly employed in Al-Si casting alloys to modify the morphology of the eutectic silicon from its coarse, flake-like form to a fine fibrous form so as to improve the mechanical properties of the alloy.

In their study on the effect of Sr addition on the microstructure of a rapidly solidified Al-12 wt% Si alloy, Wang *et al.*[24] observed that the Sr addition had a marked effect on the morphology, distribution and orientation of the eutectic silicon in the melt-spun Al-12 wt% Si alloy. They also found that under conventional casting conditions, Sr addition played a dominant role in the formation of fibrous Si in the Al-12 wt% Si alloy. Under rapid solidification conditions, however, the cooling rate played a dominant role in the formation of the microstructure of the Al-12 wt% Si alloy.

Djurdjevic *et al.* [25] studied the effects of strontium on the degree of eutectic silicon modification in 319 alloys and on the area fraction of copper phases formed. They found that the morphology of the silicon structure was coarse for 8 ppm Sr, lamellar for 38 ppm Sr, and partially modified for 56 ppm Sr additions, respectively. When the Sr added reached a level of 70 ppm, a modified-fibrous eutectic structure was produced, following which a finer fibrous silicon eutectic structure was obtained at levels of ~ 96 ppm Sr.

Modification with Sr lowers the Si eutectic reaction temperature to a considerable degree.[26] The decrease in the eutectic temperature after a modification treatment is called "depression", and can be taken as a measure of the degree or quality of the modification because it correlates well with the microstructural parameters of the eutectic silicon evaluated from image analysis.[27] The greater the depression observed in the eutectic temperature, the greater are the modification effects.

Li [10, 12] reported that the Al-Si eutectic reaction temperature in Al-Si-Cu alloy (Al-7% Si-3.5% Cu) with 60 ppm Sr decreased from 566°C to 558°C. De la Sablonnière and Samuel[28] found that modifying 319 alloy with 250 ppm Sr leads to a significant decrease in the eutectic silicon temperature from 560°C to 550°C. The combination of Mg and Sr results in the lowest eutectic temperature (545.4°C against 560.7°C). Beumler *et al.*,[22] however, found that the eutectic temperature decreased until ~ 0.016 wt% Sr was reached, and then it increased again with a further increase in Sr concentration.

Sr was also found to lead to an increase in the Al-Al_2Cu eutectic temperature. An additional benefit of Sr modification is that it considerably lowers the solution treatment time necessary to attain the desired property level.[29] Sokolowski *et al.*[1] found that an increase of strontium in 319 alloy, from 8 to 96 ppm, leads to an increase in the Al-Al_2Cu eutectic temperature ($\Delta T_{eut}^{Al\text{-}Si}$) from 505°C to 513°C and a considerable increase also in the final solidification temperatures for the copper phases from 485°C to 498°C. By using the depression in the Al-Si eutectic temperature $\Delta T_{eut}^{Al\text{-}Si}$ as a criterion, it will be observed that a Sr content between 75 and 85 ppm is sufficient to modify the eutectic Si particles. The fading effect of Sr decreases the degree of $\Delta T_{eut}^{Al\text{-}Si}$ by approximately 20%, indicating

a lower degree of silicon modification. It is likely that the alloy castings obtained from high strontium melts required to be subjected to higher-temperature solution treatments.

According to Samuel *et al.*,[13] Sr addition does not seem to have a significant effect on the precipitation of the copper-containing phase. From a study on seven alloys containing in common Al-6.5 wt% Si-3.5 wt% Cu with strontium additions in the range of 0-300 ppm, they were able to observe that the copper phase reactions were not affected in any way by the addition of up to 300 ppm Sr, in that the temperatures and the energies of the reactions remained the same.

Sr modification, however, results in the segregation of the copper phase in regions away from the eutectic Si areas, which in turn, leads to the formation of a large volume fraction of the interdendritic block-like Al_2Cu structure. Sokolowski *et al.*[1] reported that as the Sr content increased from 8 ppm to 96 ppm, the ratio of the block-like versus the eutectic-like copper phase changed from 1:3 to 9:1. On the one hand, as the block-like phase has a higher nucleation temperature, the characteristic temperatures pertaining to the copper–rich eutectic reactions ($T_{eut}^{Al\text{-}Al2Cu}$ and $T_{eut}^{Al5Mg8Cu2Si6}$) are raised by the addition of strontium (as seen in Figure 2.12); these temperatures determine the maximum temperature that 319 alloy castings can be exposed to during heat-treatment without incurring incipient melting. On the other hand, since the block-like form is more difficult to dissolve in the aluminum matrix, addition of Sr will slow down the rate of Al_2Cu dissolution during solution heat-treatment, as was observed by Li *et al.*,[10] as shown in Figure 2.13. In the case of the modified alloy, most of the Al_2Cu (~ 2.7%) is dissolved after 12 hours. The dissolution of remaining Al_2Cu is found to be sluggish. Compared with the unmodified

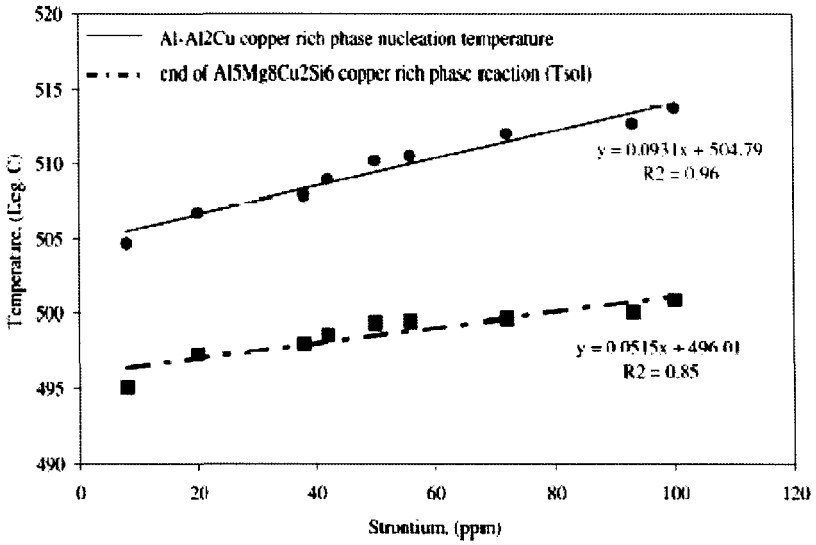

Figure 2.12 The relationship between the strontium level and the characteristic temperatures of the copper-rich eutectic phases for a cooling rate of approximately 0.48°C/s.[1]

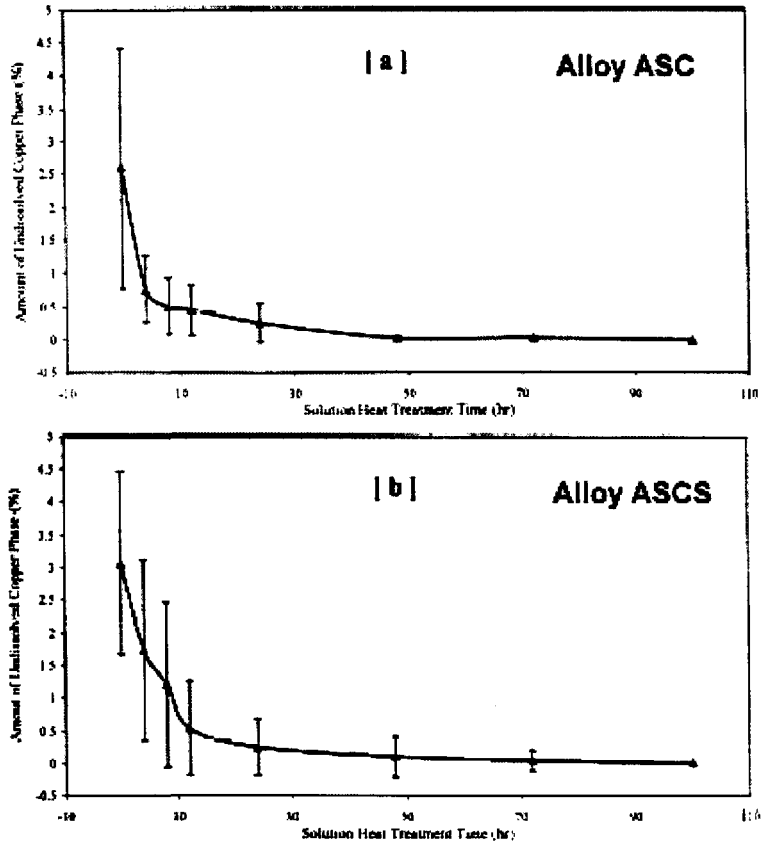

Figure 2.13 Al_2Cu phase dissolution in (a) experimental Al-7% Si-3.5% Cu base alloy (coded ASC), and (b) the Sr-modified base alloy (coded ASCS) during solution heat-treatment at 505°C as a function of solution treatment time.[10]

alloy (ASC), the amount of undissolved Al_2Cu in the Sr-modified alloy (ASCS) is about 20% higher in the as-cast condition.

Strontium was also found to increase the amount and size of defects in castings, particularly in the form of porosity.[30,31] Byczynski *et al.*[32] measured the porosity in Al-Si-Cu-Mg alloy samples obtained from cylinder head deck bolt boss and the main bearing saddle area sections, and found that the addition of Sr increased the average porosity from 0.05% to 0.20% in the bolt boss section and from 0.17 to 0.56% in the saddle area section; and the average maximum pore size from 125 μm to 697 μm, and from 206 μm to 1151 μm in the two sections, respectively. Thus, at slow rates of solidification the damaging effects of porosity surpass any positive influence that strontium may have on eutectic silicon modification and, hence, on the subsequent tensile and fatigue properties of the castings.

Traditionally, Sr is added in the form of waffle type Al-10%Sr master alloy, but Van Wiggen[33] stated that on average more than 50% of the strontium added disappeared, since reactions can occur between the strontium and the lining of the furnace or of the ladle, the slag, as well as the flux. Therefore, they recommended replacing the Al-Sr master alloy with the Al-Sr rod.

Although the presence of strontium (> 0.05 wt%) changes the morphology of the eutectic silicon particles in Al-Si alloys and thereby enhances the mechanical properties, the formation of undesirable Sr-compounds such as Al_4SrSi_2 can, at the same time, contribute to a decrease in properties.[34]

Addition of Mg, Cu, Ag, Ni and Zn to Sr-modified Al-Si base alloys, individually or in combination, reduces the modification effect of strontium, as a result of the interaction of these elements with the Sr to form complex intermetallic compounds.[35]

2.6 ROLE OF MAGNESIUM

The Mg content of the regular 319 aluminum alloy is specified at 0.1 wt% maximum. The need to keep the Mg at such a low level has always been questioned. In recent years, magnesium has been used extensively in Al-Si alloys to improve the mechanical properties. The addition of Mg increases the strength during aging as a result of the precipitation of submicroscopic and metastable phases containing Mg and Si which provide excellent obstacles for dislocation movement. [36, 37]

The presence of Mg in Al-Si-Cu-Mg alloys leads to precipitation of the intermetallic phase $Al_5Mg_8Cu_2Si_6$ during a complex eutectic reaction which takes place in the final stages of solidification. Samuel *et al.*[8] reported that when Mg is present in 319 alloys in quantities of up to ~ 0.5 wt%, the melting temperature of $Al_5Mg_8Cu_2Si_6$ is about 508°C, 10°C below that reported for low-Mg 319 alloys. This phase splits the copper phase formation temperature range into two explicit peaks representing the precipitation of Al_2Cu and $Al_5Mg_8Cu_2Si_6$ phases. Moustafa *et al.*[35] found that addition of Mg up to ~ 0.4% to the unmodified Al-11.7%Si eutectic alloy leads to the formation of Mg_2Si and partial transformation of the β-Al_5FeSi phase to π-$Al_8Mg_3FeSi_6$.

Samuel *et al.* [38] found that when the Mg content was less than 0.6 wt%, Mg had a tendency to refine the eutectic Si particles, whereas at a Mg content of ~ 1.0-1.2 wt%, the

formation of Mg_2Si replaced modification of the eutectic Si. A further increase in the Mg level produced both modification and increasing amounts of the Mg_2Si phase in script-like form.

Mg is also found to lower the eutectic temperature, as shown in Figure 2.14. That is to say, Mg acts as a modifier. Increasing the content of Mg to ~ 0.5 wt% leads to a significant decrease in the eutectic silicon temperature (1.5°C per 0.1 wt% Mg). Addition of Mg, however, is seen to result in an increase in the volume fraction of Cu-containing phases, with a clear tendency for segregation in areas away from the eutectic Si regions, leading to the formation of the block-like rather than the fine eutectic-like Al_2Cu phase.[21, 38] This makes it more difficult to dissolve the Al_2Cu phase during solution heat-treatment.

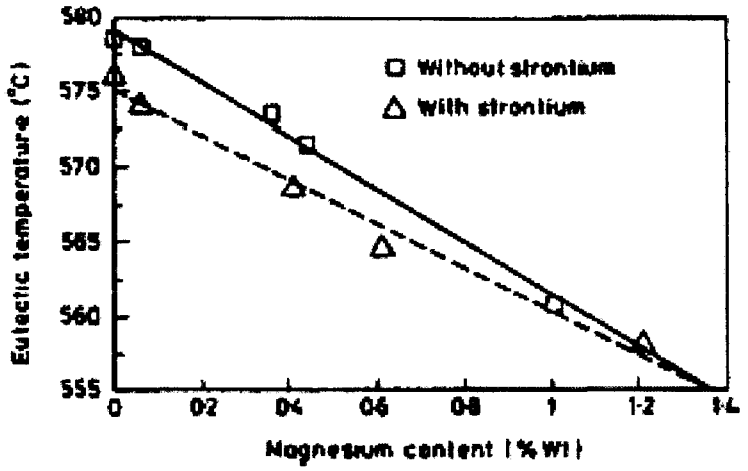

Figure 2.14 Depression of eutectic temperature as a function of Mg level for unmodified and Sr-modified Al-Si alloys.[39]

Addition of Mg is reported to improve mechanical characteristics of Al–Si alloys. Samuel *et al.* [28] reported that magnesium up to ~ 0.5 wt% in 319 alloys contributed to both strength parameters, *i.e.* YS and UTS by about 75%, and ductility by about 15%.

Ouellet *et al.*[40] studied the effects of increasing the Mg content to 0.5 wt% in B319.2 alloy on improving alloy properties after heat treatment, as well as the possibility of further improving the alloy strength through modification with Sr. The authors observed that when the Mg content was increased to 0.5 wt%, there was a noticeable decrease in the ductility, and when the solution heat-treatment temperature was raised to 500°C, the yield and tensile strengths increased from 330 MPa and 340 MPa to 410 MPa and 420 MPa, respectively. Increasing the solution temperature to 505°C lead to incipient melting of the $Al_5Mg_8Cu_2Si_6$ and Al_2Cu particles located at the grain boundaries. The researchers also recommended that a treatment at 500°C for 8-10h is the best solution heat-treatment for high Mg-containing 319 alloys.

Reif *et al.*[41] studied the hardness changes in an Al-9.0%Si-3.5%Cu alloy with and without the addition of 0.5 wt% Mg. It was found that with the addition of Mg, the maximum hardness achieved increased from 140 HV to 170 HV after aging at 160°C for 30 hours, as shown in Figure 2.15. This shows the beneficial effect of Mg additions in increasing the hardness and strength of the alloy.

Dunn and Dickert[42] compared the effect of Mg up to 0.55 wt% on the tensile properties and hardness of A380 alloy (Al-9.15%Si-3.25%Cu-0.1%Fe-0.035%Mg-0.43%Mn-1.81%Zn). The alloy was examined at three Mg levels, *i.e.* 0.1, 0.35 and 0.55 wt%. The presence of Mg was seen to increase the tensile strength, yield strength and hardness at all temperatures. Elongation, however, was observed to be reduced.

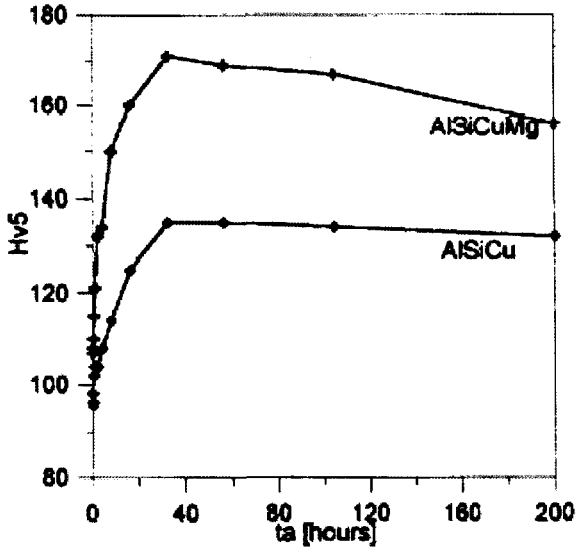

Figure 2.15 Hardness of AlSiCu and AlSiCuMg alloys as a function of the aging time at 160°C.[41]

2.7 COMBINED EFFECTS OF MAGNESIUM AND STRONTIUM

Joenoes *et al.*[43] reported that about 1% Mg refines the Si phase slightly in unmodified Al-Si alloys, but when combined with Sr, Mg has a negative effect on Sr modification, that is, it changes the microstructure from a well-modified to a partially modified one, as a result of the precipitation of the intermetallic phase, $Mg_2SrAl_4Si_3$, formed prior to the eutectic reaction. It is likely that a much higher level of Sr is required to achieve a full modification of the Si structure when Mg is present. Heusler and Schneider[39] reported that in an Al-11%Si alloy containing 100 ppm Sr, a depression of 4K was achieved, and that a further increase in the Sr content did not further depress the eutectic temperature. In the presence of Mg, a depression of 4K was attained at 50 ppm Sr, and a maximum of 7-8K with 100-150 ppm Sr. Nevertheless, in the Mg-free sample modified with 100 ppm Sr, the Al-Si eutectic was observed to be better modified than that in the Mg-containing alloy

which had been modified with the same amount of Sr. This would indicate that the possible interaction between Sr and Mg would leave less Sr available for modification of the Al-Si eutectic in the Mg-containing alloy.

Figure 2.16 shows a comparison of the non-modified and Sr-modified microstructures of Al-11%Si alloy containing various Mg levels.[39] A Mg content of 0.1wt%

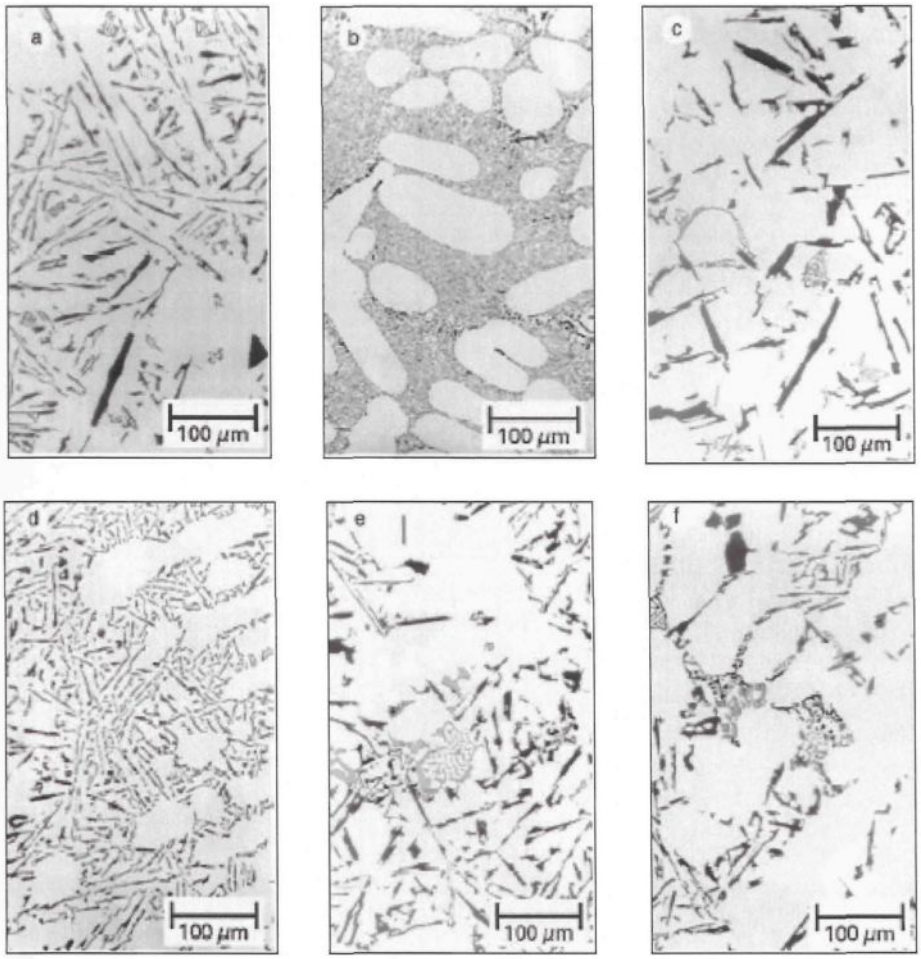

Figure 2.16 Comparison of non-modified and Sr-modified microstructures from thermal analysis samples of Al-11%Si alloy containing various Mg levels: (a) 0.1 wt% Mg, 0 ppm Sr; (b) 0.1 wt% Mg, 200 ppm Sr; (c) 0.45 wt% Mg, 0 ppm Sr; (d) 0.45 wt% Mg, 200 ppm Sr; (e) 1.0 wt% Mg, 0 ppm Sr and (f) 1.0 wt% Mg, 200 ppm Sr.[39]

in the unmodified Al-11%Si alloy results in a coarse lamellar eutectic structure (Figure 2.16a), which can be transformed into a modified morphology by the addition of 200 ppm Sr (Figure 2.16b). Increasing the Mg concentration to 0.45 wt% without Sr creates an acicular Al-Si eutectic (Figure 2.16c), while the addition of Sr has only a slight effect and leads to a partially modified and lamellar eutectic structure (Figure 2.16d). Addition of 1 wt% Mg leads to very similar eutectic microstructures for the non-modified and modified alloys, showing acicular eutectic Si with some modified areas (Figure 2.16e and f).

Roy *et al.*[44] reported the effect of Sr-Mg interaction in reducing the porosity volume fraction in Al-Si-Cu alloys. According to their results, the base alloy (containing no Sr or Mg, with a melt hydrogen level of ~ 0.3 ml/100g Al) exhibits about 2 vol% porosity. Addition of 300 ppm Sr and 0.5 wt% Mg provides a sounder casting (for the same level of hydrogen content), with a porosity level of about 0.8%.

Samuel *et al.*[38] reported that addition of both Mg and Sr can lead to severe segregation of the Al_2Cu phase in 319.2 alloy, resulting in the formation of massive amounts of the coarse block-like form of the phase compared to the finer eutectic-like form.

2.8 HEAT TREATMENT OF Al-Si-Cu-Mg ALLOYS

The initial strength of Al-Si alloy may be enhanced by the addition of alloying elements such as copper, magnesium, zinc and silicon. Since these elements, whether singly or in various combinations, show increasing solid solubility in aluminum with increasing temperatures, it is possible to subject them to thermal treatments which improve the alloy

strength and ductility. The heat treatment consists of solution heat-treatment, quenching, and a combination of natural and artificial aging processes. For Al-Si-Cu alloys, the improvement in properties is mainly due to the precipitation of Al_2Cu within the alloy matrix during the aging process. Changes in the morphology of silicon during the solution treatment also contribute to the improvement in the properties. [45]

2.8.1 Solution Heat-Treatment

Solution heat-treatment is an elevated temperature process designed to allow the soluble elements to become supersaturated in solid solution, followed by sufficiently rapid cooling so as to preserve the solid solution formed at the solution heat-treating temperature. The purpose of the solution heat-treatment is to put the maximum amount of hardening solutes such as Cu and Mg into solid solution in the aluminum matrix. The temperature of solution heat-treatment must, therefore, be as close as possible to the eutectic temperature, while at the same time, remaining limited to a safe level, below the maximum, to avoid overheating and partial melting of the copper phases. The safe level is maintained on the assumption that the formation of small amounts of liquid phase during solution treatment at a temperature slightly higher than the specified limit is detrimental to mechanical properties; this would imply that the grain boundary melting and other local melting are undesirable and should be avoided as far as possible. [46]

Solution temperature and solution time are the two important factors in solution heat-treatment. The dissolution rate of intermetallic compounds formed during

solidification is temperature sensitive and even a 10°C increase in temperature has an appreciable effect on optimum solution times and on mechanical properties. [47, 48]

When the solution temperature applied to 319 alloys is higher than the melting point of the copper phase, there will be localized incipient melting of that phase at the grain boundaries; this melting will result in the formation of shrinkage cavities when the alloy samples are quenched after solution heat-treatment, leading to a reduction in mechanical properties.

The results obtained by Gauthier *et al.* [49, 50] showed that the best combination of tensile strength and ductility for 319.2 alloy was obtained when the as-cast material was solution-heat-treated at 515°C for 8 to 16 hours, followed by quenching in warm water at 60°C; peak-aging was attained after 24 h at 155°C or 5 h at 180°C; and the associated tensile properties were 253 MPa (YS), 403 MPa (UTS) and 1.2% elongation.

Yang [51] recommended the solution temperature for experimental and industrial 319 alloys to avoid or minimize the occurrence of incipient melting, and also suggested that the solution heat treatment temperatures in each case should never exceed the following:

Experimental 319 Alloy with 0 wt% Mg	535°C
Experimental 319 Alloy with 0.3 wt% Mg	525°C
Experimental 319 Alloy with 0.6 wt% Mg	510°C
Industrial 319 Alloy with 0.3 wt% Mg	520°C
Industrial 319 Alloy with 0.6 wt% Mg	520°C

In his study, Li [52] reported that at 527°C solution treatment temperature, a 10-12 hour solution treatment time is most suitable for obtaining the right silicon structure for

both 354 and 355 alloys. Figure 2.17 illustrates the effect of solution time on silicon particle morphology for the two alloys solution heat-treated at 527°C.

The solution heat-treatment process can be carried out either in a single step or in multiple steps. The single-step treatment of 319 aluminum alloys is normally limited to 495°C, because a higher temperature leads to the incipient melting of the copper phase. On the other hand, heat treatment at temperatures of 495°C or less is not sufficient to maximize the dissolution of the copper-rich phases, nor is it adequate to modify the silicon particle morphology. In order to overcome this problem, a two-step solution heat-treatment was proposed by Sokolowski *et al.*,[1, 2] where a two-stage solution heat-treatment, with the second-stage kept at a temperature below 525°C, was found to be more powerful than the conventional single-stage solution heat-treatment of 8 h at 495°C in that the alloy strength improved from 200 to 240 MPa and the elongation increased from 0.6 to 1.6%.

The two-step solution heat-treatment comprises the single-step treatment, followed by a higher temperature solution treatment. That is to say, first, the solution temperature is held near the final solidification temperature in order to allow the phases with a low melting point to dissolve completely; several hours of holding time is needed at this temperature, after which the solution temperature is increased, and again maintained for several hours to cause the remainder of the copper intermetallics to dissolve completely in the matrix. After the two-stage solution heat-treatment, the amount of the undissolved copper-rich phase in 319 alloys is observed to be greatly reduced, and improved homogenization prior to aging is generated, all of which results in the general upgrading of mechanical properties.

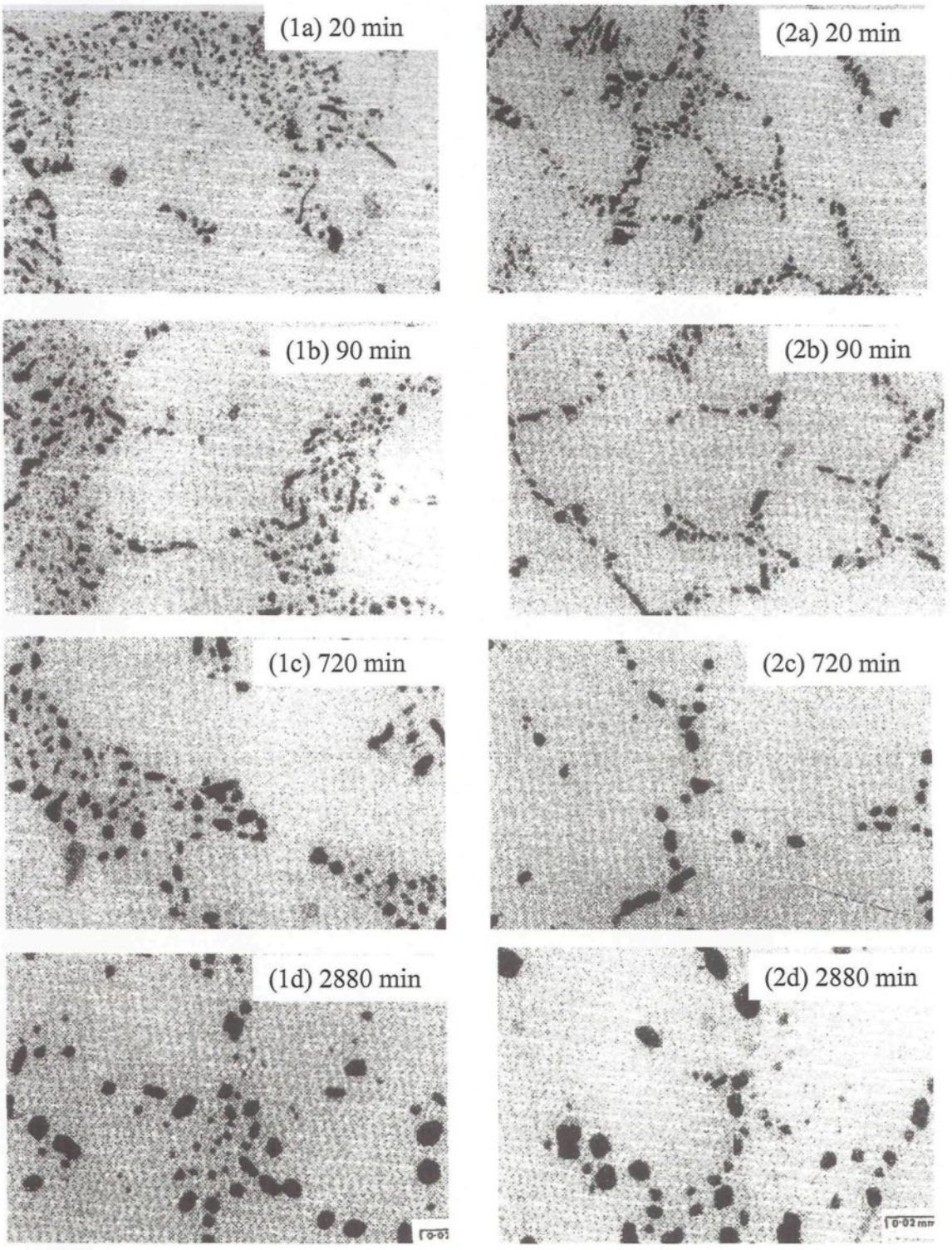

Figure 2.17 Effects of solution time on silicon particle morphology in (1) 354 and (2) 355 alloys solution heat-treated at 527°C. [52]

The holding time of the first stage and the solution temperature of the second stage are significant parameters in this context. The second-stage solution temperature must not be higher than 520°C since this may cause the incipient melting of the copper-rich phase. Sokolowski *et al.* [1] investigated the effect of one- and two-stage solution treatments on the mechanical properties of 319 aluminum alloy, for an alloy containing 18 ppm Sr. It was found that the traditional single-step solution treatment (495°C/8h) did not produce optimum mechanical properties because it did not maximize the dissolution of the copper-rich phases, nor was it able to modify the silicon particle morphology sufficiently. A two-step solution treatment, however, was capable of accomplishing these goals and was therefore recommended. They proposed an optimal two-step solution treatment for the alloy investigated, comprising a first step at 495°C for 2 h followed by a second step at 515°C for 4 h. This solution treatment was followed by water quenching to 74°C and artificial aging at a temperature of 250°C for 3 h. The optical micrographs shown in Figure 2.18 (a) and (b) revealed that there was significant copper segregation in the as-cast alloy. While conventional single-step solution treatment at 495°C improved the homogeneity considerably, some of the copper-rich phase remained in the matrix, as shown in Figure 2.18 (c) and (d); a two-step solution treatment resulted in a greatly improved homogeneity and only a small amount of the copper-rich phase remained, as shown in Figure 2.18 (f).

Gauthier *et al.* [50] recommended an optimum solution treatment of 12 h at 510°C for high Mg-containing 319 aluminum alloy to dissolve low-melting-point Cu phases, followed by a further 12 h at 520°C or 525°C to dissolve a maximum of the rest of these phases without causing incipient melting which would deteriorate mechanical properties of the

alloy. This treatment is insufficient, however, to dissolve the iron intermetallic phases such as β-Al_5FeSi or $Al_8Mg_3FeSi_6$ present in the alloy.

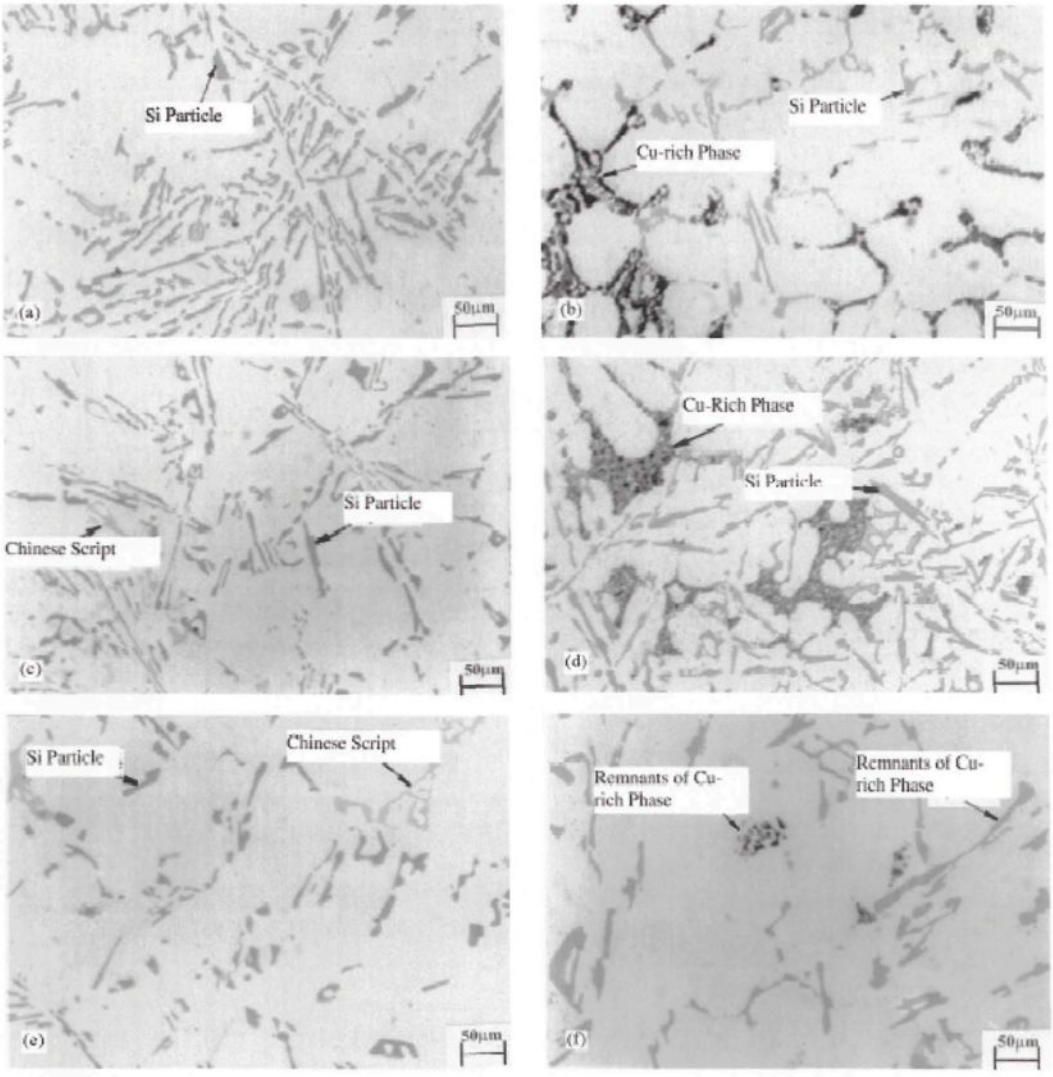

Figure 2.18 Optical micrographs showing (a) silicon particle morphology, (b) copper-rich phase in an as-cast automotive component; (c) silicon particle morphology after single-step solution treatment; (d) copper-rich phase segregation following single-step solution treatment; (e) silicon particle morphology following two-step solution treatment; (f) remnants of copper-rich phases following two-step solution treatment.[1]

De la Sablonnière and Samuel [28] observed that a two-stage solution heat-treatment consisting of 12h at 510°C (to dissolve all the copper-containing phases), followed by 12h at 540°C (to dissolve Al_5FeSi needles and so increase the area of the Al matrix) was a powerful heat-treatment for low Mg-containing and low intermetallic-containing 319 alloys. The two-stage solution heat-treatment process has a twofold purpose in that it aims at (a) dissolution of copper-containing phases, mainly Al_2Cu and $Al_5Mg_8Cu_2Si_6$ at 510°C, and (b) spheroidization of the eutectic silicon particles and dissolution of β-Al_5FeSi at higher temperatures. [49]

Two types of defects, nevertheless, were detected during solution heat-treatment of 319 alloy test bars as reported by de la Sablonnière and Samuel.[21] The salient points regarding these defects may be summarized as follows:

(1) The occurrence of dark spots, characterized by their irregular shape and no distinct boundary with the surrounding matrix, having no appreciable thickness and no significant difference in element concentration; they were observed independently of the Mg level of the alloy. The size of the dark spots and percentage of defective test bars obtained were proportional to the solution temperature (see Figure 2.19). The dark spots and the matrix had more or less similar concentrations of alloying elements. The authors, therefore, proposed that the presence of these dark spots might be attributed to hydrogen gas evolution during partial melting of the copper-containing phases. The dark spots were always observed near the periphery of the test bars, acting as a source for crack initiation. Their size increased with increasing solution temperature.

(2) The occurrence of burn spots which result from the burning of the molten phases in the alloy test bars containing high Mg levels, *i.e.* 0.5 wt%, when the solution temperature was maintained above 520°C. Such burn spots resulted in the distortion of all test bars solutionized under these conditions. The burn spots, contrary to what are termed dark spots, were not restricted to the fracture surface.

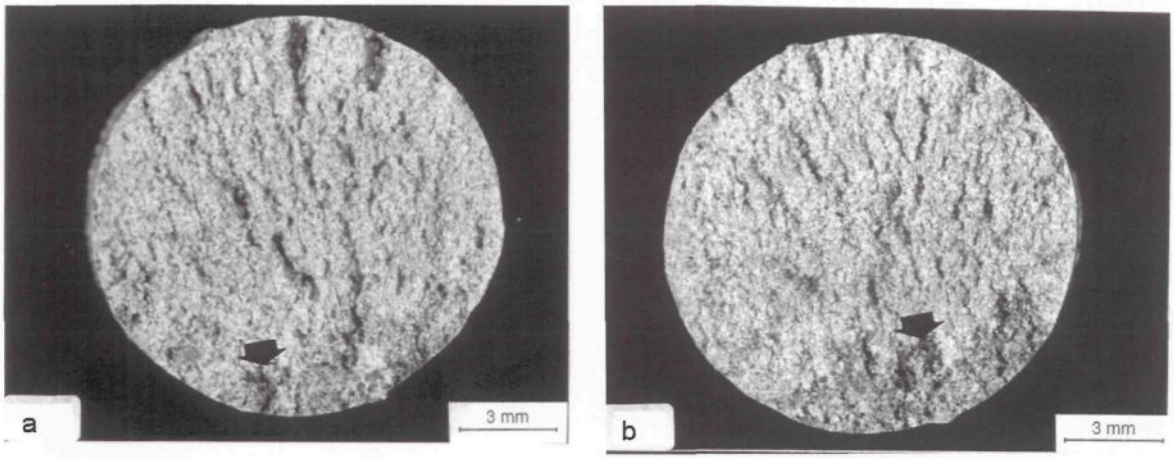

Figure 2.19 Dark spots observed on the fracture surfaces of test bars of 319+0.5 wt% Mg alloy, solutionized for (a) 12h/510°C, and (b) 12h/520°C. Arrows show the progress in the size of the dark spot with increase in solution temperature. [21]

Wang *et al.* [53] studied the influence of Cu content on solution treatment of Al-Si-Cu-Mg cast alloys using Differential Scanning Calorimetry (DSC) analyses. It was found that for Al-11%Si-0.3%Mg alloy with 1.0% Cu addition, the solution temperature for avoiding grain boundary melting should be restricted to 535°C, while for alloys with more than 2.0% Cu, it should be limited to 500°C. When the alloy is modified with Sr, the restrictive solution temperature to avoid incipient melting of intermetallic phases can be increased by 5°C. It was also found that for non-modified Al-11%Si-4%Cu-0.3%Mg alloy, solution heat treatment at 500°C for 10 h and then increasing solution temperature to 520°C is optimum;

while for the Sr-modified Al-11%Si-4%Cu-0.3%Mg alloy, solution treatment at 500°C for 12 h and then increasing the solution temperature to 525°C is optimum.

Cerri *et al.* [54] studied the effects of T5 and T6 heat treatments on the mechanical properties of 319 thixocast alloy, and observed that the hardness results showed no substantial differences in peak values in the T5 condition compared with the T6 condition. The T5 aging treatment also provides satisfactory results for elongation, while the UTS values are slightly lower than those obtained after T6 treatment. Thus, the researchers concluded that the T5 treatment is preferable to T6 because of its cost-effectiveness.

When Cavaliere *et al.* [55] studied the effect of T5 and T6 heat treatments on the mechanical properties of A356 and A319 thixocast alloys, they found that the hardness obtained under the T6 condition was at a higher level than that obtained under T5 conditions. They also found that at 200°C, overaging started after 2 hours while at 160°C, hardness increases continuously to reach a maximum after 24 hours under both T5 and T6 conditions.

Lasa *et al.* [56] studied the effect of the processing route on the solution treatment of four Al-Si-Cu-Mg alloys: H3 (Al-12.85%Si-1.3%Mg-1.37%Cu, permanent mold), H4 (Al-12.29% Si-1.3% Mg-4.40% Cu-0.12% Fe-0.11% Ti, permanent mold), E (Al-12.64% Si-1.09% Mg-4.39% Cu-0.19% Fe-0.13% Ti, lost-foam) and Thixo 477 (Al-15.30% Si-0.58% Mg-4.38% Cu-0.21% Fe-0.16% Ti, thixoforming). The researchers recommended that in permanent mold cast alloy H3, the optimum solution treatment should be carried out in two stages, 1.5 h at 500°C, followed by 2.5 h at 535°C; whereas they determined that in permanent mold cast alloy H4, between 2 h and 3 h at 500°C was sufficient to obtain

equilibrium dissolution of the θ phase, and only 2 h were needed to dissolve the π phase completely. For lost foam cast alloy E, the optimum solution treatment was 7 h at 500°C, while only 0.5 to 1 hour was needed for Thixo 477 alloy to reach equilibrium.

2.8.2 Quenching

Quenching is the step following solution heat-treatment, and it is usually conducted in water, which momentarily freezes the structure, rendering the alloy highly workable for a short period of time. The purpose of this process is to preserve the solid solution formed at the solution heat-treating temperature, by rapidly cooling to some lower temperature, which is usually close to room temperature. In general, the highest attainable and the best combination of strength and toughness values are those associated with the most rapid quenching rates.

2.8.3 Aging Treatment

At room or elevated temperatures, the alloy is not stable after quenching, and precipitation of the constituents from the supersaturated solution begins. However, after a period of several days at room temperature, termed natural aging or room temperature precipitation, the alloy strength increases, and the alloy is said to have undergone age- or precipitation-hardening. Many alloys approach a stable condition at room temperature, but a number of them, particularly those containing copper and silicon, or magnesium and zinc, continue to age-harden for long periods of time at room temperature.

Aging treatment is the controlled process of allowing the hardening constituents to reprecipitate either at room temperature (natural aging) or at an elevated temperature

(artificial aging) to provide a hardening effect. Through the proper combination of solution heat-treatment, quenching, cold working and artificial aging, the highest strengths may be obtained.

García-Celis and Colás [57] investigated the aging behavior of A319 alloys in the manufacture of automotive cylinder heads and engine blocks. They found that the aging behavior of a heat-treatable aluminum alloy depends on the cooling rate following the solution heat treatment, resulting in softer material when the cooling rate decreases. They also observed that the peak hardness did not increase beyond a certain value once a critical cooling rate (around 10°C/s) was attained.

Apelian *et al.* [58] studied the aging behavior of Al-Si-Mg alloys. They observed that the precipitation of fine β' (Mg_2Si) phase particles during aging treatment leads to a pronounced improvement in strength properties. Both aging time and temperature determine the final properties. It has been estimated that increasing the aging temperature by 10°C is equivalent to increasing the aging time by a factor of two. [59]

Beumler *et al.* [22] recommended a different T6 treatment consisting of 12 h at 537°C, quenching in water at 60°C, and then aging for 4 h at 155°C; the tensile properties obtained were 195 MPa (UTS) and 1.8% elongation in the as-cast condition, and 249 MPa (UTS) and 7.8% elongation after the T6 treatment.

The mechanical properties are found to depend solely on aging time and temperature. Newkirk *et al.* [60] found that aging time and aging temperature had the greatest effect on the hardness of A356-T6 after a slow quench in the range of aging times (5 h, 8 h) and temperatures (160°C-204°C) studied. Higher aging temperatures and longer times

promoted greater hardness after slow quenching in the range of 2 to 8 hours at 138-172°C. Gloria *et al.* [61] found that lower aging temperatures and shorter aging times generated higher hardness values, and that solution time did not play a significant role in the determination of hardness, whereas the solution temperature did have a certain effect on this parameter.

Wang *et al.*[62] investigated the effect of adding 0.4 wt% Mg on the precipitation and age hardening behavior of Al-8% Si-3% Cu alloy through hardness measurement by means of DSC and Transmission Electron Microscopy (TEM) analyses. They found that the age-hardening response of the Al-8% Si-3% Cu-0.4% Mg alloy was about 2.6 times that of the Al-8% Si-3% Cu alloy during aging at 220°C. The excellent age-hardening response of the Al-8% Si-3% Cu-0.4% Mg alloy was provided by the precipitation of a coherent Q'' phase besides precipitation of the θ' phase, while for Al-8% Si-3% Cu alloy, the age-hardening response was produced only by precipitation of the θ' phase.

2.9 INCIPIENT MELTING

During solution heat-treatment, when the 319 alloy composition exceeds the critical composition and the alloy is heat-treated at a higher temperature than the copper eutectic temperature, localized partial melting of the Al_2Cu phase will occur at the grain boundaries. This melting is called incipient melting, and results in the formation of shrinkage cavities when the alloy samples are quenched after solution heat-treatment, thereby lowering the alloy soundness and mechanical properties. In Al-Si-Cu alloys, with the segregation of the

alloying elements, the composition may exceed the critical composition locally, in which case, incipient melting will occur.

Figure 2.20 shows an example of incipient melting taking place at the grain boundaries in a 319 alloy sample (see arrowed sites). Samuel [13] noted that incipient melting of $Al_5Mg_8Cu_2Si_6$ and Al_2Cu phases of 319-type alloys took place when the high-Mg version of 319 was solution-treated at temperatures above 505°C for sufficiently long periods. This melting resulted in distortion of the test bars and deterioration of the mechanical properties of the alloy.

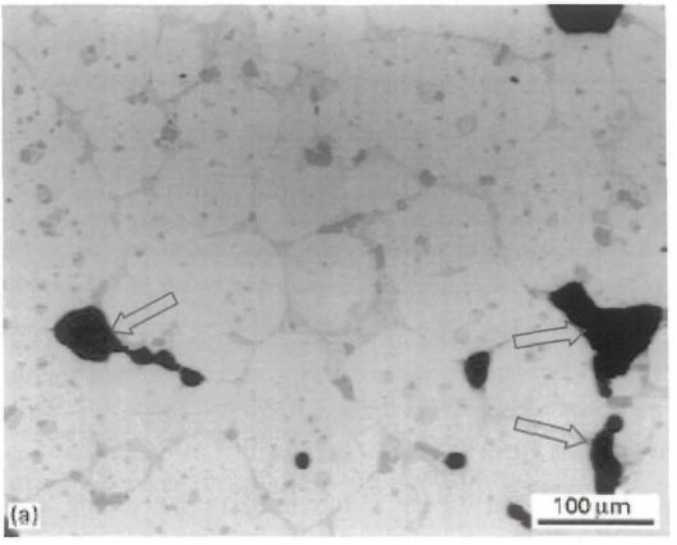

Figure 2.20 Microstructure of 319 alloy showing the occurrence of incipient melting taking place at grain boundaries (arrowed).[13]

2.10 POROSITY

Porosity in a casting can be regarded as one of the major factors which is critical to its quality. The presence of porosity, inevitable to a certain extent in any casting, can be detrimental, not only in terms of surface quality after machining, but also, more significantly, in terms of its effect on mechanical properties and corrosion resistance.

Porosity consists of voids or cavities which form within a casting during solidification. It occurs in castings because of the rejection of gas from the solution during solidification and/or the inability of the liquid metal to feed through the interdendritic regions to compensate for the volume shrinkage associated with the solidification. Hydrogen is the only gas capable of dissolving to a significant extent in molten aluminum. A poor casting design that prevents proper feeding causes "macroshrinkage", which includes large-scale defects such as cold shuts and misruns. "Gas porosity" is created when gas (mainly hydrogen in the case of aluminum melts) becomes entrapped in the molten metal. This type of porosity usually exhibits round pores, and can be avoided through proper degassing of the molten metal and good pouring techniques. "Microshrinkage" is a result of the natural volume contraction which accompanies transformation of the molten aluminum into the solid state.[63]

A number of researchers[64, 65] have reported results showing the deleterious effects of gas content in aluminum alloys. Besides the hydrogen concentration, the formation of porosity is also controlled by other factors such as grain-refining and inclusion content of the melt. Modification of aluminum melts is usually carried out to modify the eutectic Si morphology from acicular to fibrous, and thereby improve the mechanical properties of the casting. This advantage, however, is offset by the fact that modified castings generally exhibit an increased amount of porosity when compared to non-modified castings, due to the resulting enhancement in the susceptibility of these alloys to hydrogen absorption with the addition of strontium (used to carry out the modification).

A schematic diagram of the growth process of pores as depicted by Pehlke and Kubo[66] is shown in Figure 2.21. In (a), the gas pore nucleates at the base of the dendrite arms. The synergy between the shrinkage and gas pores overcomes the negative free energy required to form a gas-metal surface, facilitating nucleation. As solidification proceeds, the pore grows as a result of the increase in gas evolution with the decrease in temperature. The radius of the pore becomes large enough to diminish the contribution of interfacial energies, and the pore detaches from the dendrites, as shown in (b). At a still further stage of solidification, neighboring dendrites collide, making interdendritic feeding difficult. At this stage, the pore is thought to grow so as to compensate for solidification shrinkage, as shown in (c).

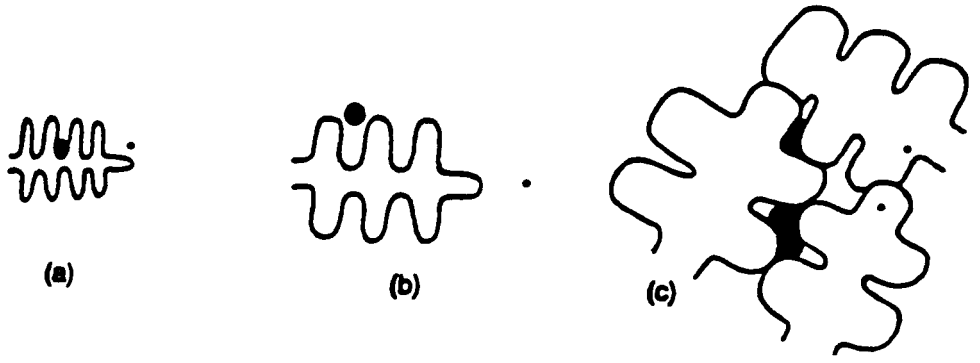

Figure 2.21 The growth process of porosity formation.[66]

According to Campbell[67], the conditions for the formation of a pore are best expressed by the relation

$$P_g + P_s > P_{atm} + P_h + P_{s\text{-}t} \quad (4)$$

where P_g = equilibrium presence of dissolved gases in the melt;

P_s = pressure drop as a result of shrinkage;

P_{atm} = pressure of the atmosphere over the system;

P_h = pressure as a result of the metallostatic head;

and P_{s-t} = pressure as a result of surface tension at the pore/ liquid interface.

It is generally observed that P_g and P_s are the major driving forces and act synergistically to form pores within the interdendritic regions which are neither solely due to gas evolution nor due to shrinkage. For a particular casting design, P_{atm} and P_h are constant, and addition of modifiers like sodium decreases P_{s-t} and leads to an increased probability of pore formation.

McDonald and his co-workers[68] studied the role of strontium in porosity formation, and found that the addition of Sr changes the porosity from localized connected regions to dispersed isolated pores, and that this effect may not necessarily be reflected in changes in the volume percentage porosity. As mentioned previously, Sr causes segregation of the Cu-phase particles in 319 alloys, which makes it difficult for them to dissolve during solution heat-treatment, thus increasing the possibility of incipient melting and consequent formation of porosity.

Bian *et al.*[69] used the HYSCAN II apparatus to measure the hydrogen content in unmodified and modified hypoeutectic Al-10wt%Si alloy melts. The results showed that Sr-addition markedly increased the hydrogen content and accelerated the gassing rate of the Al-Si melts. Moreover, without modification, the pores were found to be present in the form of long, fissured, irregular shapes in the microstructure. In modified samples, however, the pores were broad, rounded and regular.

Edwards *et al.*[70] studied the influence of Si, Cu, Mg and Fe content, and the cooling rate during solidification, on the amount of microporosity observed in plate castings of Al-Si-Cu-Mg alloys. The researchers found that adding Cu to the alloy significantly increased the amount of microporosity; the increase was attributed to the effect of Cu on the solidification shrinkage and the hydrogen gas pressure. Increasing the Si content from 4.5 wt% to 9 wt% led to a decrease in the amount of microporosity, while Mg and Fe appeared to have a negligible effect on porosity distribution at levels of less than about 0.5 wt%.

2.11 TENSILE PROPERTIES

The tensile properties of an alloy are evaluated in terms of the yield strength (YS), ultimate tensile strength (UTS), and percentage elongation (% El). The tensile properties of 319 aluminum alloy depend to a great extent on the alloy microstructure which, in turn, depends on the casting process used, the chemical additions made to control the eutectic silicon structure (termed modification), and the solution heat-treatment used to obtain the maximum dissolution of strengthening elements in the matrix.

The percentage of Si, and its shape and distribution, play an important role in determining the mechanical properties. Without any modification, the eutectic silicon has an acicular or lamellar morphology with limited properties. With the addition of a modifying agent, a fine and fibrous silicon network may be obtained, resulting in a noticeable increase in ductility as well as an increase in the tensile strength. Copper and magnesium, together with varying amounts of iron, manganese and zinc present as impurity elements in the alloy, go into solid solution in the matrix and also form intermetallic phases

during solidification. The presence of iron increases the hardness but drastically reduces elongation at all Fe concentrations.

Optimization of the heat-treatment process parameters may lead to the best combination of ductility, strength and hardness for a given cast component. One of the most common tempers used in the metal-casting industry for Al-Si-Cu alloys is the T6 heat treatment. It is generally accepted that this treatment allows for full enhancement of the mechanical properties in terms of higher strength and hardness values. This is due to a large amount of precipitation strengthening which occurs during the aging process. Meyer *et al.*[71] indicated that the best combination of material properties for 319 alloy was obtained after a T64 temper (495°C/5h, cold water quench, aging at 160°C for 5 hours). The T7 temper, a solution and overaging treatment, is also quite common, and results in somewhat reduced strength levels, with increased ductility, but it also produces better dimensional stability in the casting than does the T6 temper. [72]

The results of modified T7 experiments for the 319 alloy as presented by Byczynski *et al.*[73] showed that percentage elongation *vs.* log (quenching rate) exhibited a linear relationship. The percent elongation decreased by approximately 37%, while the UTS increased with the quench rate by approximately 23%, reaching a constant value of 186 MPa after a quench rate of 4°C/s, as shown in Figure 2.22.

Li *et al.*[74] found that the correlation between YS and the cooling rate was more complex under the T6 conditions than it was under T5 conditions, since it was also a function of the homogeneity of the alloy composition and Al_2Cu dissolution. Compared to the T5 conditions, the UTS, YS and %El increased significantly under T6 conditions, as

shown in Figure 2.23, in view of the fact that the T6 heat treatment assisted in homogenizing the alloy.

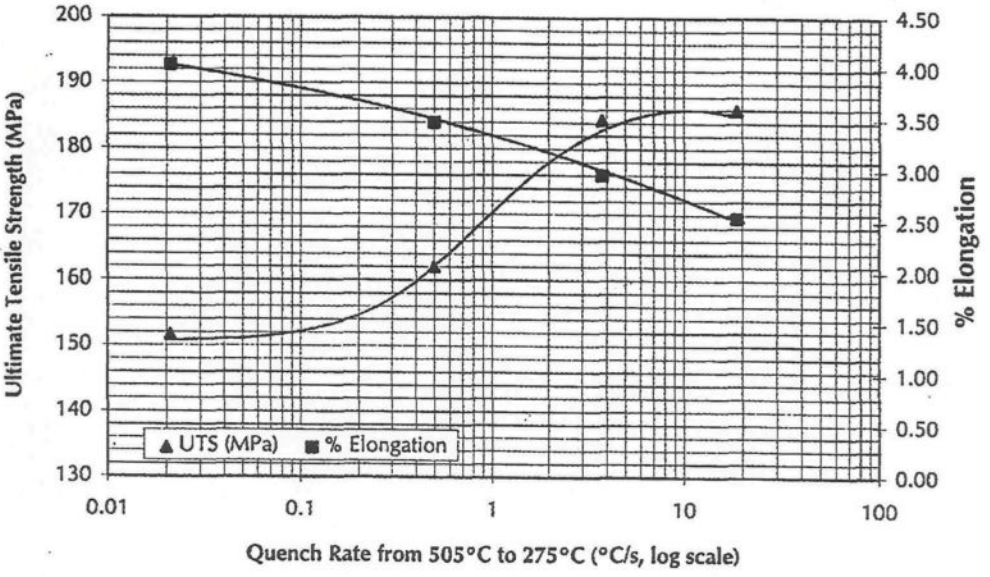

Figure 2.22 Effect of quench rate on UTS and % Elongation.[73]

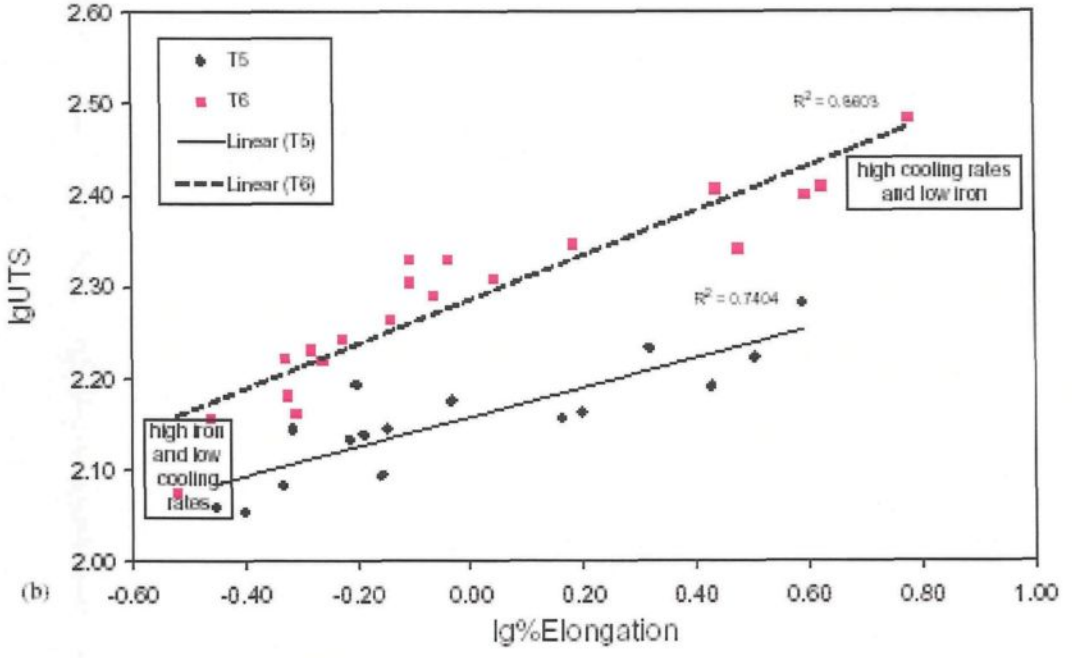

Figure 2.23 Plots of logUTS *vs.* log%El for alloys studied with different heat treatments (T5 and T6).[74]

The standard tensile properties of 319.2 alloy under T6 conditions (8h at 505°C, hot water quenching at 60°C followed by artificial aging for 5 h at 155°C) are 280 MPa (UTS), 185 MPa (YS) and 3% Elongation. The tensile properties of B319 alloy in the as-cast condition are 130 MPa (YS), 235 MPa (UTS), and 2.5% elongation.[75] The results provided by Gauthier *et al.* [49] reveal that the mechanical properties of 319.2 alloy are 125 MPa (YS), 220 MPa (UTS) and 2.63% elongation.

With Sr modification, an improvement in the ultimate tensile strength and a substantial increase in elongation may be achieved. DasGupta *et al.*[76] studied the effect of increased Sr content on the mechanical properties and microstructure of 319 alloys. Their results showed that the tensile strength of as-cast test bars increased by ~ 13% in the range 10-500 ppm Sr. A strontium content in excess of 500 ppm but less than 600 ppm contributed to a ~ 2% decrease in tensile strength. However, when the Sr content in the melt exceeded 0.06 wt%, a noticeable decrease in the tensile strength was observed.

2.12 QUALITY INDEX

The quality index Q is a concept that was introduced to describe the relationship of ultimate tensile strength (UTS) elongation (El) and yield strength (YS) of Al-7% Si-Mg alloys. [77, 78] It is defined as:

$$Q = UTS + K \log El \qquad \text{(K is a coefficient)} \qquad (5)$$

The UTS values are plotted against log El in order to correlate the quality index values with the tensile properties, the accuracy of linear regression is quantified by the parameters R^2 or the standard deviation. A perfect fitting corresponds to $R^2 = 1$, whereas a

coefficient of less than 0.7 indicates an unsatisfactory regression. The formula developed empirically by Drouzy *et al.*[77] to calculate the quality index is as follows:

$$Q = UTS + 150 \log\%El \quad (6)$$

Gauthier *et al.* [49] proposed a general form of quality index for 319 type alloys for each solution time for the temperature range 480-515 °C:

$$Q\ (MPa) = UTS\ (MPa) + 124 \log El \quad (7)$$

while after aging, the average quality index is expressed as:

$$Q\ (MPa) = UTS\ (MPa) + 108 \log El \quad (8)$$

Two equations describing the dependence of Q on $t^{1/3}$ with respect to aging temperature are obtained: for aging temperature in the range 155-180°C:

$$Q = 385 + 8.3\ t^{1/3} \quad (9)$$

and for aging temperatures in the range 200-220°C:

$$Q = 375\text{-}15.5\ t^{1/3} \quad (10)$$

CHAPTER 3

EXPERIMENTAL PROCEDURES

CHAPTER 3

EXPERIMENTAL PROCEDURES

3.1 ALLOY PREPARATION

Both experimental and industrial 319 alloys were used for the purposes of this study. The chemical composition of the as-received industrial 319 alloy (B319.2 alloy), supplied in the form of 12.5-kg ingots, is shown in Table 3.1.

Table 3.1 Chemical composition of the industrial 319.2 alloy.

Alloy	Element (wt%)							
	Si	**Cu**	**Mg**	**Fe**	**Mn**	**Zn**	**Ni**	**Al**
B319.2	6.75	3.082	0.2945	0.3003	0.2471	0.1126	0.0386	bal.

The Mg content of the B319.2 alloy was increased from 0.3 to 0.6 wt% by adding pure Mg to the alloy melt before casting. These two industrial alloys containing 0.3 and 0.6 wt % Mg were coded Y7 and Y8, respectively.

Measured quantities of pure aluminum, silicon, copper and magnesium were used to prepare the experimental 319 alloy (A1-7%Si-3.5%Cu-Mg); this experimental base alloy was coded Y1. Two other experimental alloys were prepared from this base alloy, with Mg levels of 0.3 and 0.6 wt %, coded as Y4 and Y6, respectively. Modified versions of the Y1, Y4 and Y6 experimental alloys, and the Y7 and Y8 industrial alloys were prepared using

Al-10% Sr master alloy to obtain Sr levels of 150 ppm in each case. Table 3.2 shows the ten different alloy compositions which were prepared and used in this study.

Table 3.2 Experimental and industrial alloys and their respective codes.

Alloy Type	Alloy Code		Composition
	Non-modified	Sr-modified	
Experimental 319 Alloy	Y1	Y1S	A1-7% Si-3.5%Cu (Base Alloy)
	Y4	Y4S	Base Alloy + 0.3 wt% Mg
	Y6	Y6S	Base Alloy + 0.6 wt% Mg
Industrial Alloy B319.2	Y7	Y7S	B319.2 Alloy (containing 0.3 wt % Mg)
	Y8	Y8S	B319.2 Alloy +0.3 wt% Mg

3.2 MELTING AND CASTING

The alloy ingots were melted in a 40 kg-capacity SiC crucible using an electrical resistance furnace. The melting temperature was maintained at 750±5 °C. At this temperature, measured Mg and Sr additions were made to the melt using a perforated graphite bell. Strontium was added in the form of Al-10% Sr master alloy to obtain 150 ppm Sr levels, whereas Mg was added in the form of pure metal.

Prior to casting, the molten metal was degassed for 15 min using pure, dry argon. The degassing speed/time was kept constant at 150 rpm/15 min. In addition, two samplings for chemical analysis were taken from each melt before the start of casting and at the end of casting, after the required number of castings had been obtained. The actual chemical composition of each of these alloys is shown in Table 3.3.

Table 3.3 Average chemical compositions (wt %) of the experimental and industrial alloys studied.

Alloy Code	Element Concentration (wt %)								
	Si	Fe	Cu	Mn	Mg	Sr	Ni	Zn	Al
Y1	6.91	0.1610	3.314	0.0008	0.0017		0.0529	<0.0017	Bal.
Y4	6.61	0.1409	3.248	<0.0005	0.2675		0.0042	<0.0017	Bal.
Y6	7.66	0.1635	3.703	0.0018	0.5880		0.0028	<0.0017	Bal.
Y7	6.75	0.3003	3.082	0.2471	0.2945		0.0386	0.1126	Bal.
Y8	6.81	0.2953	3.357	0.2411	0.6000		0.0388	0.1132	Bal.
Y1S	7.22	0.1450	3.843	0.0022	0.0049	0.0136	0.0063	0.0039	Bal.
Y4S	6.97	0.1721	3.597	0.0018	0.3178	0.0132	0.0074	0.0071	Bal.
Y6S	6.69	0.1691	3.711	0.0023	0.6332	0.0183	0.0063	<0.0017	Bal.
Y7S	7.76	0.2861	3.397	0.2836	0.3337	0.0142	0.0432	0.1268	Bal.
Y8S	7.55	0.2830	3.435	0.2768	0.6103	0.0211	0.0421	0.1270	Bal.

Chemical compositions were obtained from a study by Yang.[51]

The molten metal was poured into an ASTM B-108 type permanent mold preheated to 450°C, and each casting provided two test bars, as shown in Figure 3.1.

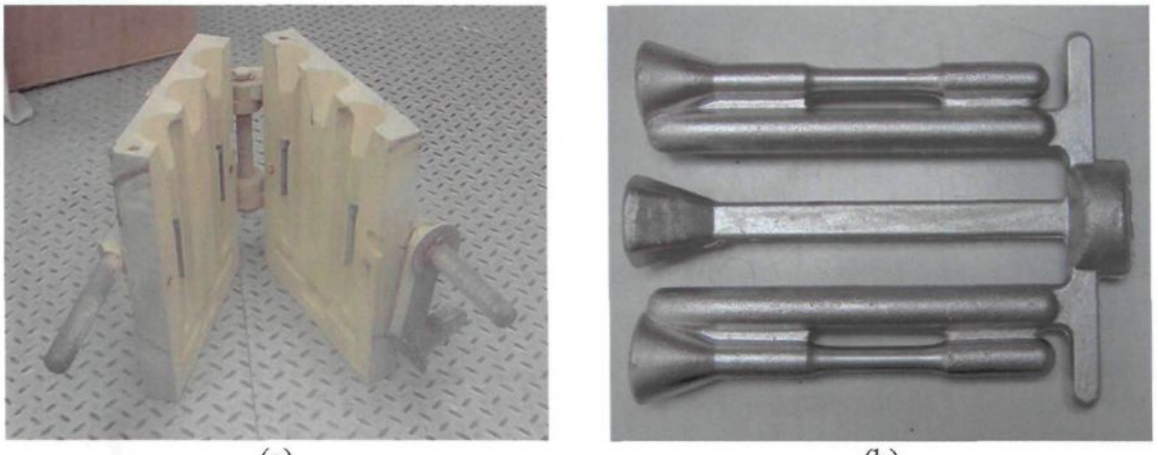

(a) (b)

Figure 3.1 (a) Permanent mold used for preparing tensile test bars, and (b) Casting obtained from (a).

3.3 THERMAL ANALYSIS

Thermal analysis tests were carried out for the five modified alloys Y1S, Y4S, Y6S, Y7S and Y8S. The data pertaining to the thermal analyses of unmodified alloys were obtained from the research investigations of Yang.[51] About 1 kg of the alloy was melted in a 2-kg capacity SiC crucible, using a small electrical resistance furnace; the melting temperature was maintained at 750°C±5°C. The melt was poured into a cylindrical graphite mold which was preheated to ~ 600°C to obtain close-to-equilibrium cooling conditions. A K-type thermocouple was inserted vertically in the hole at the bottom of the mold, reaching a height of about 30mm within the mold cavity. The setup used in this study is shown in Figure 3.2. The temperature-time data was collected by a high-speed acquisition system linked to the computer, with an acquisition rate of 10 readings/sec. The cooling curves and their first derivatives were plotted using Microsoft Excel software.

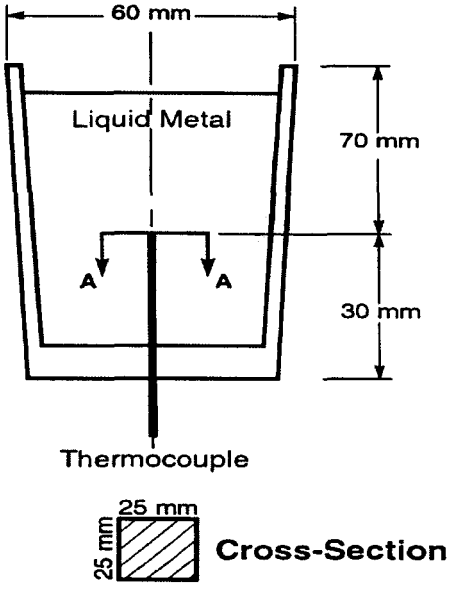

Figure 3.2 Schematic diagram of graphite mold and setup used for thermal analysis.

3.4 SOLUTION HEAT-TREATMENT AND AGING

The test bars obtained were solution heat-treated in a forced air Blue M furnace with a temperature control of ± 1°C, at a rate of ~ 3.5°C/min to reach the required solution temperatures of 450°C, 490°C, 500°C, and 520°C. In this study, three types of solution treatment were carried out using different temperatures and times in each case.

(1) Single-step solution heat-treatment

Four treatments (labeled A through D) were carried out as follows:

A = 450°C/4h C = 490°C/4h

B = 450°C/8h D = 490°C/8h

(2) Two-step solution heat-treatment

Eight treatments (labeled E through L) were carried out as follows:

E = 450°C/4h+500°C/4h I = 490°C/4h+500°C/4h

F = 450°C/8h+500°C/4h J = 490°C/8h+500°C/4h

G = 450°C/4h+520°C/4h K = 490°C/4h+520°C/4h

H = 450°C/8h+520°C/4h L = 490°C/8h+520°C/4h

(3) Triple-step solution heat-treatment

Four treatments (labeled M through P) were carried out as follows:

M = 450°C/4h+500°C/4h+520°C/4h O = 490°C/4h+500°C/4h+520°C/4h

N = 450°C/8h+500°C/4h+520°C/4h P = 490°C/8h+500°C/4h+520°C/4h

For each individual heat-treatment, five test bars were used. Once the solution heat-treatments were completed, the test bars were quenched in hot water at 60°C and then aged at 155°C for 5 hours.

3.5 TENSILE TESTING

The as-cast and solutionized test bars were pulled to fracture at room temperature using a Servohydraulic MTS 810 Material Testing Machine, as shown in Figure 3.3. Tensile testing was carried out at a strain rate of 2×10^{-4} s^{-1}. A 2 in/5.08 cm strain-gage extensometer was attached to the test bar and used for measuring the ductility of the alloy. Tensile properties, namely, ultimate tensile strength (UTS), yield strength (YS) at 0.2 percent offset strain, and fracture elongation (%El), were derived from the data acquisition and data treatment systems linked to the MTS machine. The purpose of the tensile tests was to determine how the Mg and Sr additions and the heat treatments applied would affect the incipient melting of the Al_2Cu phase, and hence the alloy properties.

Figure 3.3 Servohydraulic MTS 810 Material Test System.

3.6 METALLOGRAPHY

Samples for metallography were sectioned from the tensile-tested bars of all alloys studied, about 10 mm below the fracture surface, individually mounted in bakelite, and then polished to a fine finish (1μm diamond suspension). The percentage porosity and eutectic Si-particle characteristics were measured and quantified using an optical microscope linked to a Clemex image analysis system, as shown in Figure 3.4.

For porosity measurements, the sample surfaces were examined at a magnification of 100X, where the measurements were carried out over 20 fields, such that the sample surface was covered in a regular, systematic manner. The average values of area percent porosity and pore characteristics (length, area, and aspect ratio) were determined in each case in order to determine their contribution to the mechanical properties. The eutectic silicon particle characteristics (area and aspect ratio) were also measured. In this case, the sample surfaces were examined at a magnification of 500X, over 30 fields, again, making sure that the sample surface was traversed in a regular, systematic fashion.

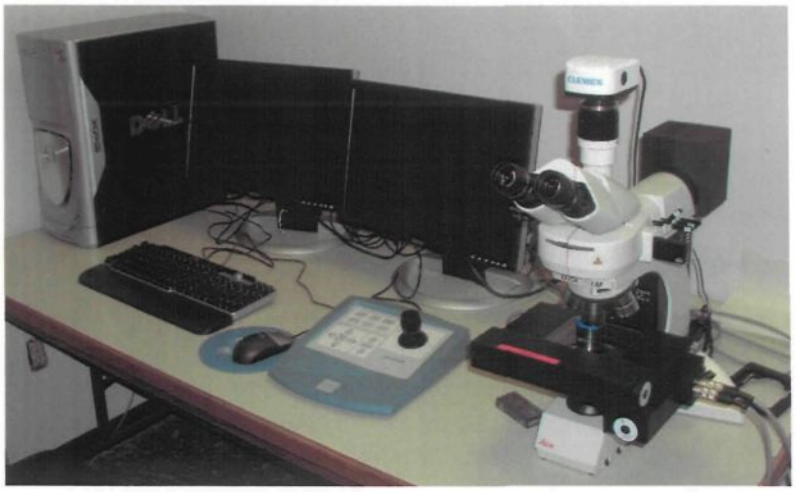

Figure 3.4 Optical microscope - Clemex image analyzer system.

The volume fraction of undissolved Al_2Cu phase and the copper distribution in the matrix were examined using electron probe microanalysis (EPMA), in conjunction with energy dispersive X-ray (EDX) analyses. For this purpose, a JEOL JXA-8900L WD/RD combined microanalyzer operating at 20 kV and 30 nA was employed, using an electron beam ~ 1μm in diameter. In each case, 10 fields were measured over the entire sample surface to determine the volume fraction of the undissolved Al_2Cu phase.

Line scans were then carried out for various alloy samples in order to determine the efficiency of a specific solution heat-treatment in dissolving the copper phases in the matrix. Each line scan path traversed across an α-Al dendrite, passing from the matrix into the dendrite, and out into the matrix again on the other side of the dendrite. Care was taken to ascertain that these line scans were taken from areas free of other phase particles, in particular, the Cu-intermetallic phases. Readings of the Cu concentration (wt %) were taken at 3 μm intervals, firstly, to avoid overlapping of the analyzed zones, and secondly, to obtain a continuous scan along the path selected.

Figure 3.5 The JEOL JXA-8900L electron probe microanalyzer

CHAPTER 4

RESULTS AND DISCUSSION

4.1 CHARACTERIZATION OF MICROSTRUCTURE

4.1.1 Thermal Analysis

Thermal analyses of all experimental and industrial alloys, including their Sr-modified versions, were carried out to determine the reactions which took place during solidification. The effects of Mg and Sr additions on the eutectic Al-Si temperature as well as on the eutectic Al_2Cu temperature were also investigated.

From thermal analysis data, the cooling curve and the first derivative curve were plotted for alloys Y1, Y6, Y1S and Y6S, as shown in Figures 4.1 and 4.2, while Tables 4.1 and 4.2 show the main reactions observed in non-modified and Sr-modified 319 alloys (marked A through D). The four main reactions observed correspond to the formation of the α-Al dendrite network (peak A), followed by the precipitation of the Al-Si eutectic (peak B), the precipitation of the Al-Al_2Cu eutectic (peak C) and the precipitation of the complex Cu-Mg phase $Al_5Mg_8Cu_2Si_6$ (peaks D' and D). This complex phase precipitates both before and after the precipitation of the Al_2Cu phase leading to two explicit peaks D' and D which correspond to pre-eutectic and post-eutectic reactions. The post-eutectic $Al_5Mg_8Cu_2Si_6$ precipitates at 491.3°C in alloy Y6, which is 10°C lower than the precipitation temperature of the Al_2Cu phase, namely 501.4°C. The $Al_5Mg_8Cu_2Si_6$ phase is an insoluble compound as a result of its complex nature, and when the solution heat-treatment temperature is higher than its melting point, it melts and porosity is formed at the local melting site when the sample is quenched following solution treatment.

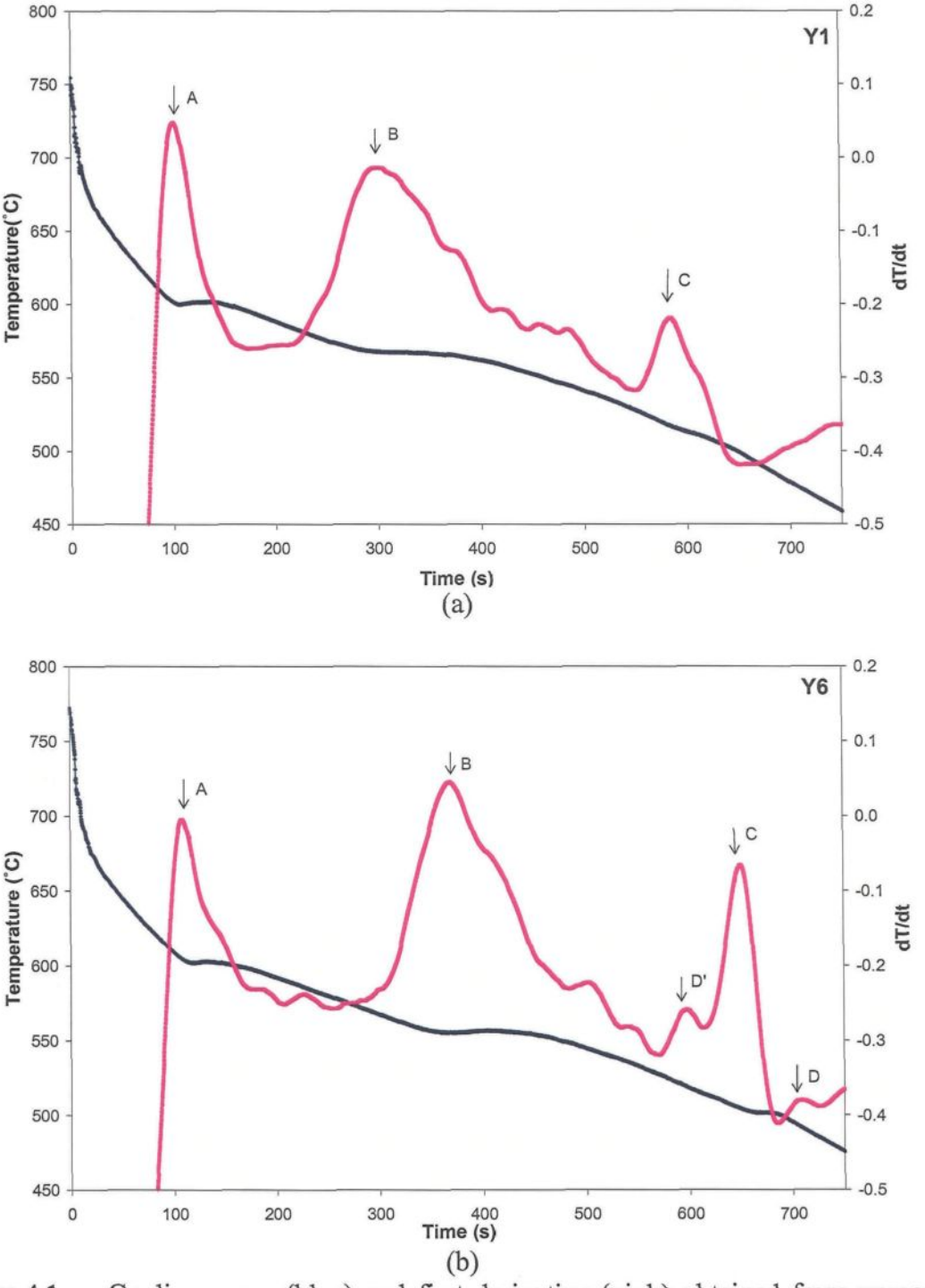

Figure 4.1 Cooling curve (blue) and first derivative (pink) obtained from unmodified 319 alloys (a) Y1 (0 wt% Mg), and (b) Y6 (0.6 wt% Mg).

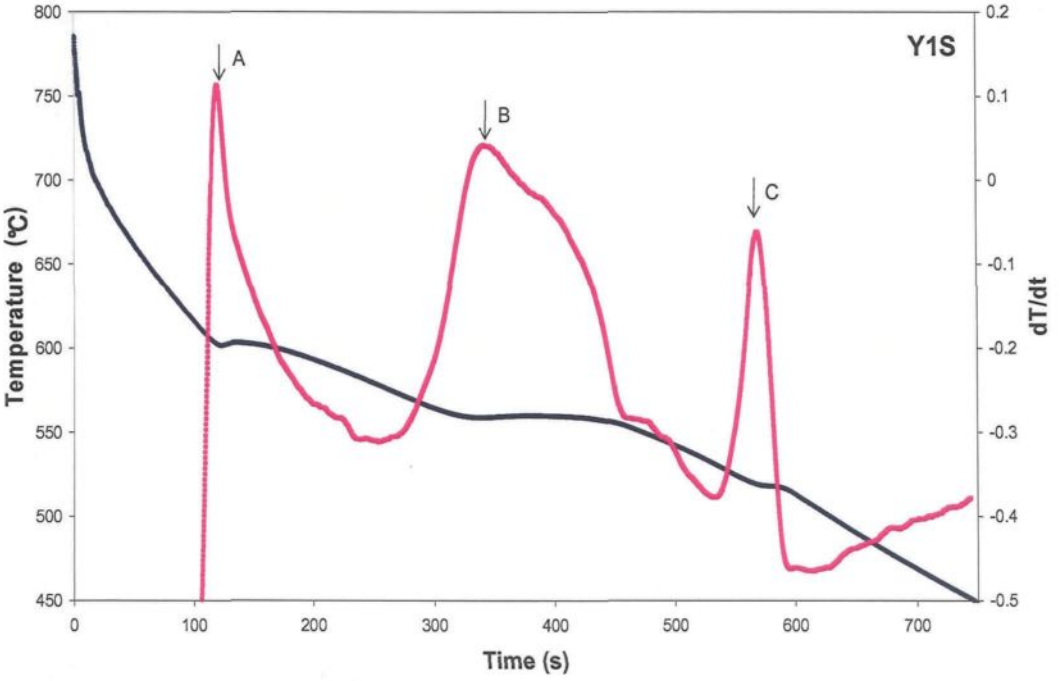

(a)

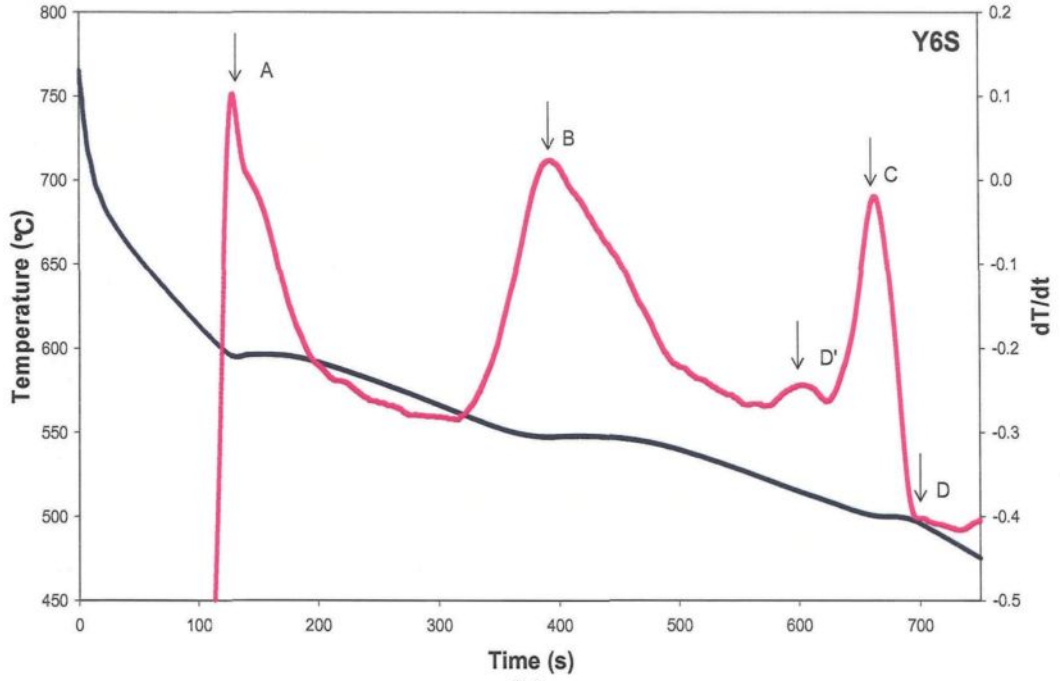

(b)

Figure 4.2 Cooling curve (blue) and first derivative (pink) obtained from Sr-modified 319 alloys (a) Y1S (0 wt% Mg), and (b) Y6S (0.6 wt% Mg).

Table 4.1 Expected reactions in non-modified 319 alloys.[51]

Alloy	Peak	Temperatures (°C)	Reactions
Y1 (0 wt% Mg)	A	601.3	Precipitation of α-Al dendrite network
	B	567.6	Al-Si eutectic network
	C	516.7	Al-Al_2Cu eutectic reaction
Y4 (0.3 wt% Mg)	A	602.1	Precipitation of α-Al dendrite network
	B	561.2	Al-Si eutectic network
	C	504.2	Al-Al_2Cu eutectic reaction
	D	498.1	Precipitation of $Al_5Mg_8Cu_2Si_6$
Y6 (0.6 wt% Mg)	A	604.2	Precipitation of α-Al dendrite network
	B	555.4	Al-Si eutectic network
	D'	518.1	Pre-eutectic $Al_5Mg_8Cu_2Si_6$
	C	501.4	Al-Al_2Cu eutectic reaction
	D	491.3	Post-eutectic $Al_5Mg_8Cu_2Si_6$
Y7 (0.3 wt% Mg)	A	598.4	Precipitation of α-Al dendrite network
	B	564.4	Al-Si eutectic network
	C	506.4	Al-Al_2Cu eutectic reaction
	D	495.4	Precipitation of $Al_5Mg_8Cu_2Si_6$
Y8 (0.6 wt% Mg)	A	599.4	Precipitation of α-Al dendrite network
	B	559.4	Al-Si eutectic network
	D'	516.2	Pre-eutectic $Al_5Mg_8Cu_2Si_6$
	C	501.7	Al-Al_2Cu eutectic reaction
	D	486.4	Post-eutectic $Al_5Mg_8Cu_2Si_6$

Precipitation of Mg_2Si was also observed prior to Al-Al_2Cu eutectic reaction in alloys Y4 and Y7.

Table 4.2 Expected reactions in 150ppm Sr-modified 319 alloys (present study)

Alloy	Peak	Temperatures (°C)	Reactions
Y1S (0 wt% Mg)	A	603.1	Precipitation of α-Al dendrite network
	B	558.5	Al-Si eutectic network
	C	518.1	Al-Al_2Cu eutectic reaction
Y4S (0.3 wt% Mg)	A	597.5	Precipitation of α-Al dendrite network
	B	552.8	Al-Si eutectic network
	C	513.7	Al-Al_2Cu eutectic reaction
	D	507.1	Precipitation of $Al_5Mg_8Cu_2Si_6$
Y6S (0.6 wt% Mg)	A	594.8	Precipitation of α-Al dendrite network
	B	547.6	Al-Si eutectic network
	D'	513.3	Pre-eutectic $Al_5Mg_8Cu_2Si_6$
	C	499.8	Al-Al_2Cu eutectic reaction
	D	493.3	Post-eutectic $Al_5Mg_8Cu_2Si_6$
Y7S (0.3 wt% Mg)	A	596.9	Precipitation of α-Al dendrite network
	B	551.1	Al-Si eutectic network
	C	496.5	Al-Al_2Cu eutectic reaction
	D	486.5	Precipitation of $Al_5Mg_8Cu_2Si_6$
Y8S (0.6 wt% Mg)	A	592.9	Precipitation of α-Al dendrite network
	B	540.9	Al-Si eutectic network
	D'	515.3	Pre-eutectic $Al_5Mg_8Cu_2Si_6$
	C	497.3	Al-Al_2Cu eutectic reaction
	D	491.4	Post-eutectic $Al_5Mg_8Cu_2Si_6$

Precipitation of Mg_2Si was also observed prior to Al-Al_2Cu eutectic reaction in alloys Y4S and Y7S.

Figure 4.3 shows the co-existence of the two copper-containing phases: Al_2Cu and $Al_5Mg_8Cu_2Si_6$, while Figure 4.4 shows the corresponding EDX spectra.

From the two preceding tables, it will be observed that the Al-Si eutectic temperatures of experimental alloys, whether they contain Mg or are Mg-free, decrease when modified with 150 ppm Sr. In the base alloy Y1, the Al-Si eutectic temperature is 567.6°C, and it drops to 558.2°C after modification, indicating that 150 ppm Sr contributes to a 10°C depression in the temperature of the Al-Si eutectic of 319 experimental alloys. This depression is considered to be an indicator of the degree of modification, where the greater the depression, the more the Si particles are expected to be modified.

The Al-Si eutectic temperature is also found to decrease with an increase in Mg content. When the Mg level is increased from 0 to 0.6 wt%, the eutectic temperature decreases from 567.6°C to 555.4°C, which is 12.2°C lower than it is in the Mg-free alloy, indicating that Mg can also act as a modifier. When Mg and Sr combine, the eutectic Al-Si temperature is further depressed, *i.e.* 547.6°C in alloy Y6S, which is 20°C lower than it is in the base alloy. These results are in accordance with those obtained by de la Sablonnière *et al.*,[31] who reported that the combination of Mg and Sr resulted in the lowest eutectic temperature in base 319 alloy. Similar observations may be made in the case of industrial alloys, where the Al-Si eutectic temperature in alloy Y8S may go as low as 540°C.

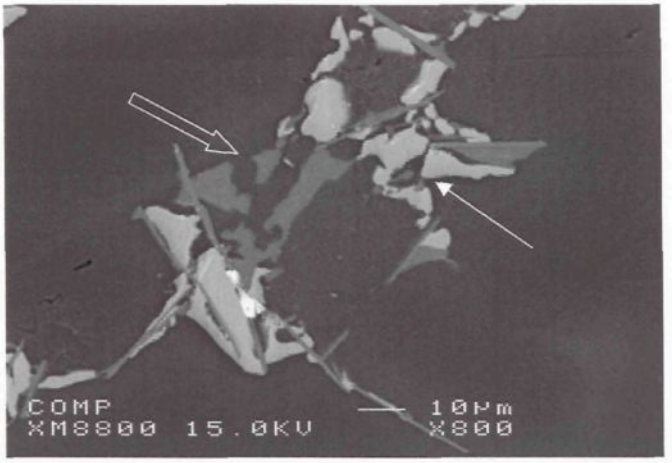

Figure 4.3 Backscattered image obtained from the as-cast alloy Y6S showing the co-existence of Al_2Cu (solid arrow) and $Al_5Mg_8Cu_2Si_6$ (open arrow) phases.

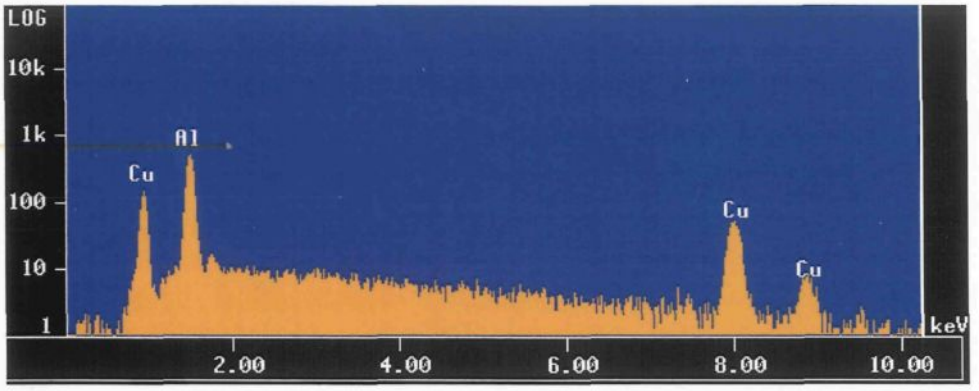

(a)

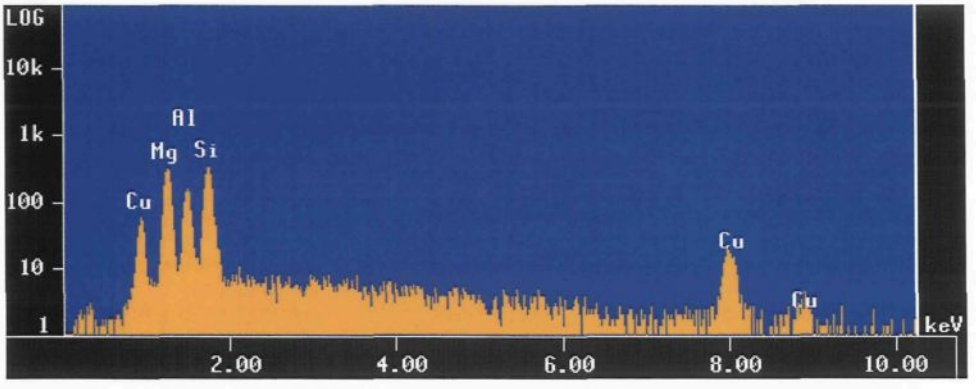

(b)

Figure 4.4 EDX spectra corresponding to the phases shown in Figure 4.3: (a) Al_2Cu phase, (b) $Al_5Mg_8Cu_2Si_6$ complex phase.

Modification with Sr leads to the depression of the Al-Si eutectic temperature, as was observed for all the alloys studied. The precipitation temperature of the eutectic Al-Al_2Cu phase was also observed to decrease with increasing Mg. When the quantity of added Mg was increased from 0 to 0.6 wt% in the experimental and industrial alloys, this temperature decreased from 516.7°C to 501.4°C, and to 501.7°C in the Y6 and Y8 alloys. It was also found that the precipitation temperatures of the eutectic Al-Al_2Cu in the modified alloys Y1S and Y4S were higher than those recorded for the non-modified experimental alloysY1 and Y4, but decreased in the case of the high Mg-containing alloys Y6S and Y8S.

4.1.2. Dissolution of Al_2Cu Phase

During solution heat-treatment, the Al_2Cu phase dissolves, thus the Cu content in the matrix increases and the hardening effect of Cu is obtained. Here, the distribution of Cu in the matrix was quantitatively and qualitatively measured by means of line scans using an electron probe microanalyzer (EPMA). The measurements were carried out across α-Al dendrites in the matrix, in areas free of Cu intermetallic phases. Figure 4.5 shows an example of the path across which the distribution of Cu was analyzed in the case of a solution heat-treated Y1S alloy sample. The readings of the Cu concentration were taken at intervals of 3 μm to obtain a continuous scan along the path selected, as well as to avoid overlap of the zones analyzed in consecutive measurements. In Figure 4.5, the line scan path corresponds to the dark broad line in the centre of the ellipse along its long axis.

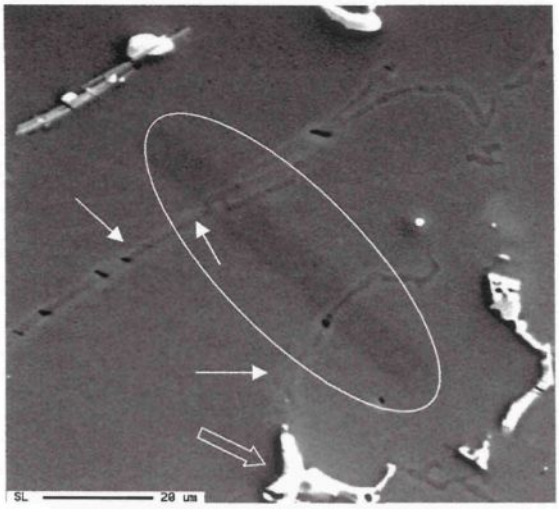

Figure 4.5 Backscattered image obtained from Y1S alloy heat-treated at 450°C/4h, the thick dark line in the oval corresponds to the path across which the distribution of Cu in the matrix was analyzed and which is plotted in Figure 4.12. The solid arrows point to the cell boundaries, while the open arrow shows an undissolved Al_2Cu particle.

4.1.2.1 Non-modified alloys

Figures 4.6 through 4.8 show the results of line scans carried out for samples of the experimental alloys Y1, Y4 and Y6 in the as-cast and the four single-step solution heat-treated conditions, namely 450°C/4h, 450°C/8h and 490°C/4h, 490°C/8h.

As may be seen from each figure, Cu segregates at the dendrite boundaries in the as-cast condition. After heat treatment, the copper begins to be distributed evenly across the dendrites as well as in the matrix. With increasing solution time and temperature, the amount of Cu dissolved in the matrix increases, reaching its maximum for the 490°C/8h solution heat-treatment.

In the case of Y4 alloy, the controlling factor appears to be the solution temperature rather than the solution time, whereas for alloys Y1 and Y6, solution time also makes a difference in the amount of Cu which dissolves in the matrix.

It is interesting to note from the line scan curves shown in Figure 4.8 for Y6 alloy (0.6 wt% Mg) that the 490°C/4h solution heat-treatment shows the highest amount of Cu dissolution in the matrix. It is thus reasonable to expect that increasing the solution time to 8 hours at this temperature would further improve the dissolution of copper phases, whereas, as Figure 4.8 reveals, the Cu level drops to 2.5% after the 490°C/8h solution heat-treatment.

This drop may be explained by taking into consideration the amount of undissolved Al_2Cu phase after each heat treatment. It may be observed from Table 4.3, however, that the amount of undissolved Al_2Cu phase in this alloy also drops noticeably (0.14%) compared to those for the Y1 and Y4 alloys (at 0.34% each). This fact indicates clearly that incipient melting occurs in the Y6 alloy if the solution treatment period at 490°C is extended. The occurrence of incipient melting would explain both these observations.

The amounts of the undissolved Al_2Cu phase in the Y1 and Y4 decrease in value progressively upon going from the as-cast condition through the four solution heat-treatment conditions (treatments A, B, C and D). Figure 4.9 shows the amount of undissolved Al_2Cu phase obtained from Y1 alloy for all the solution heat-treatments investigated for this thesis. It is clear that treatments reaching 520°C show complete dissolution of the Al_2Cu phase, while those reaching 500°C, or less, cannot attain its complete dissolution. It should be mentioned here that the term "complete dissolution" is taken to mean that the Al_2Cu particles cannot be detected in the matrix by an optical

microscope at a magnification of 60X. After single-step treatment D, the quantity of the Al_2Cu phase decreases to 0.34%, indicating that about 88% of the Al_2Cu phase dissolves in the matrix. This decrease may also indicate that a 490°C/8h treatment is sufficient for Mg-free 319 alloys to produce mechanical properties which are reasonably high.

In the case of industrial alloys Y7 (0.3 wt% Mg) and Y8 (0.6 wt% Mg), the results obtained are similar overall, as shown in Figures 4.10 and 4.11, respectively. At 450°C, a longer solution time leads to a greater quantity of Al_2Cu dissolving in the matrix, although when the temperature is raised to 490°C, the time factor seems to have no noticeable effect. The amounts of undissolved Al_2Cu phase in these alloys in the as-cast condition are relatively lower than those in the experimental alloys Y4 and Y6.

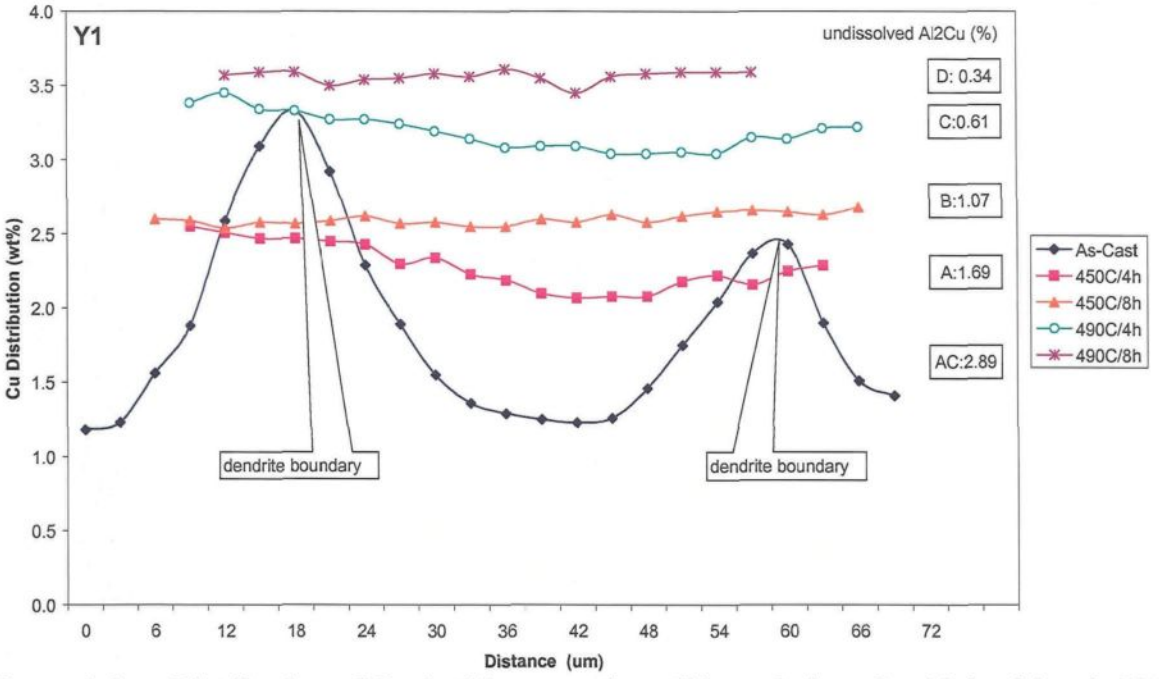

Figure 4.6 Distribution of Cu (wt%) across the cell boundaries of α-Al dendrites in Y1 alloy, obtained from the as-cast and solution heat-treated samples.

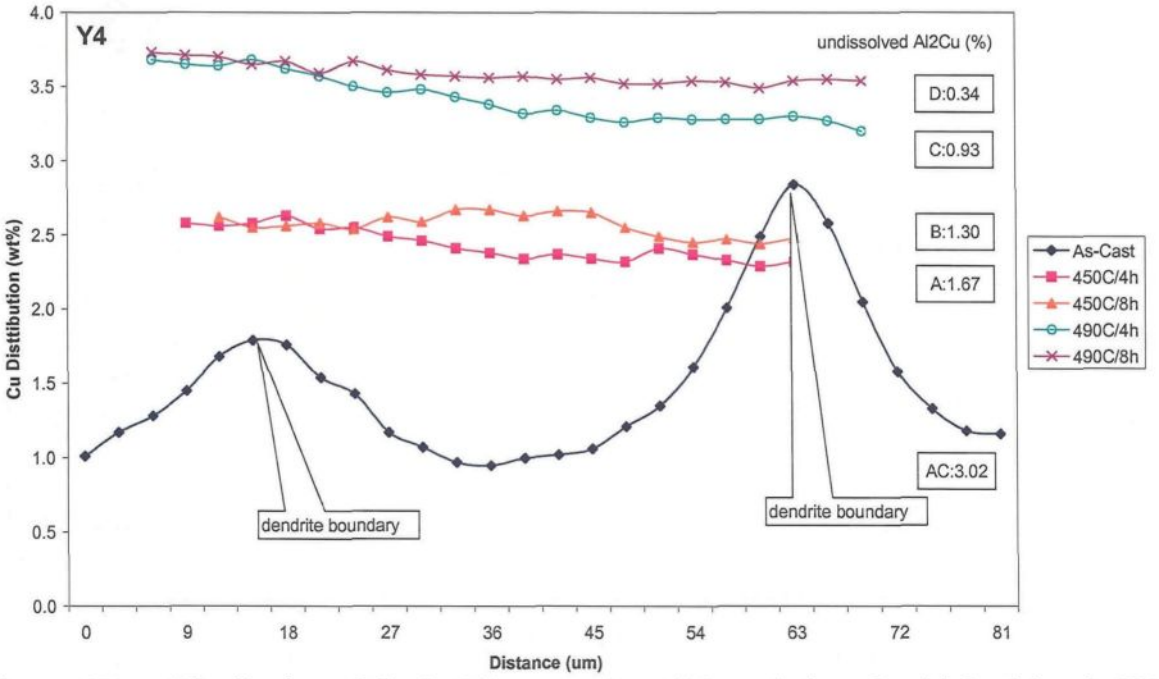

Figure 4.7 Distribution of Cu (wt%) across the cell boundaries of α-Al dendrites in Y4 alloy, obtained from the as-cast and heat-treated samples.

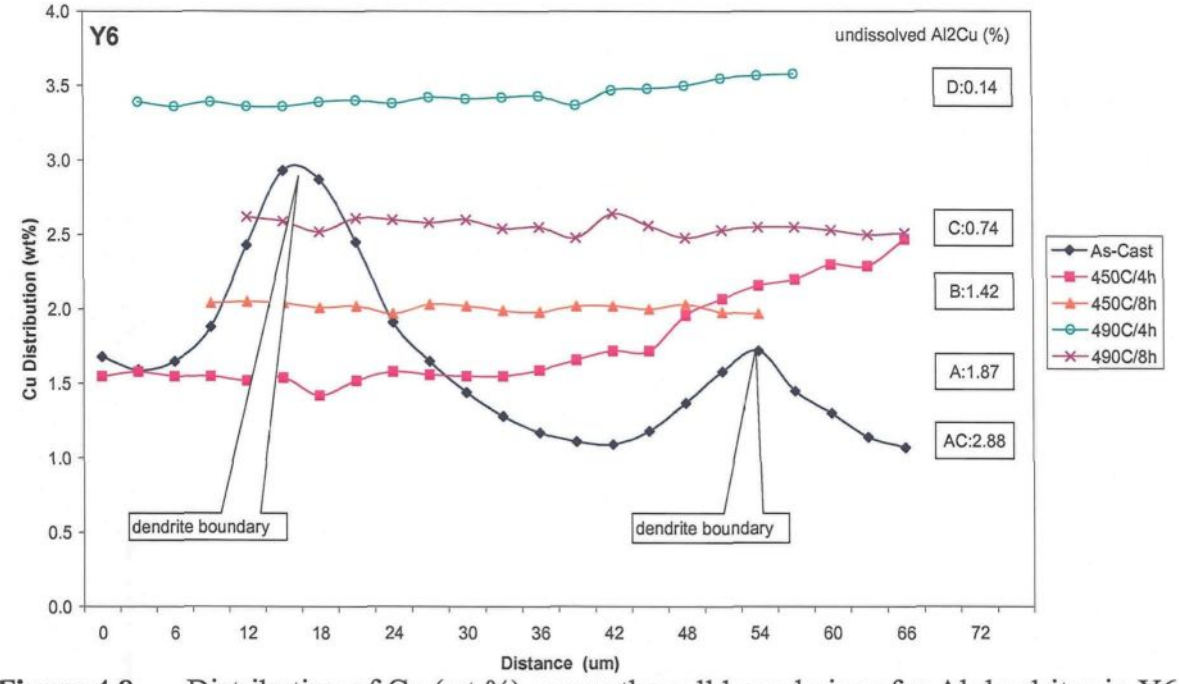

Figure 4.8 Distribution of Cu (wt %) across the cell boundaries of α-Al dendrites in Y6 alloy, obtained from the as-cast and heat-treated samples.

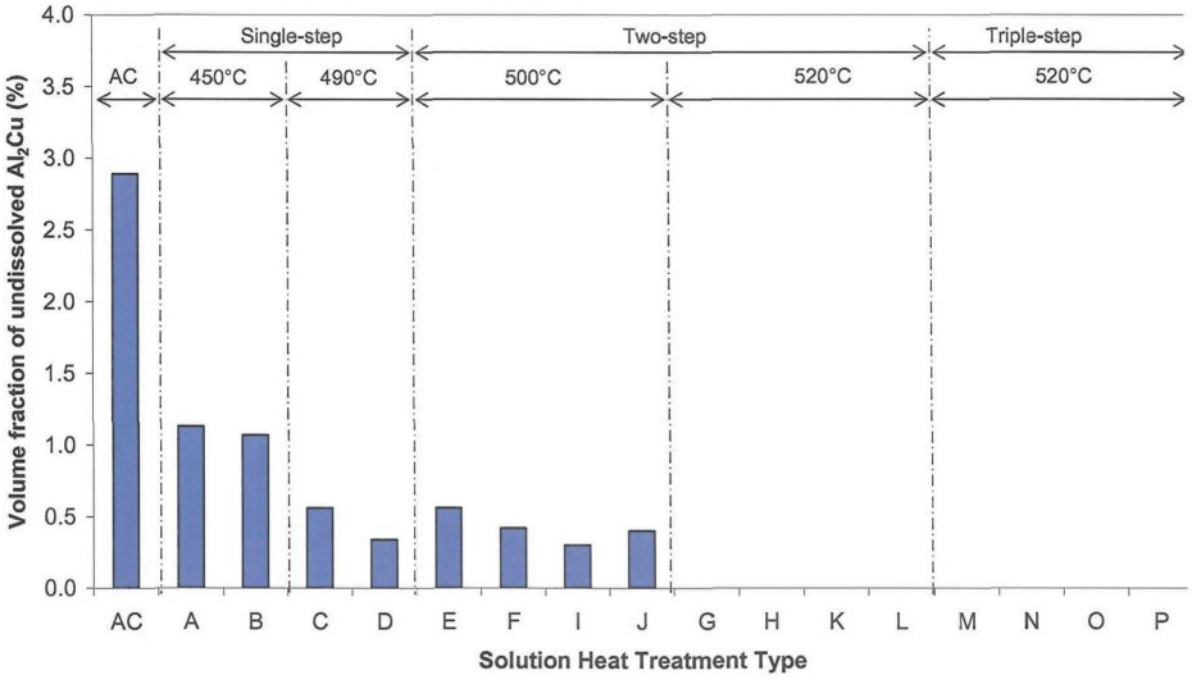

Figure 4.9 Variation in volume fraction of undissolved Al_2Cu as a function of solution heat-treatment in alloy Y1.

Table 4.3 Effect of various solution heat-treatment on the dissolution of the Al_2Cu phase in experimental alloys Y1, Y4 and Y6 as well as industrial alloys Y7 and Y8.

Heat Treatment	Volume fraction of undissolved Al_2Cu (%)				
	Y1	Y4	Y6	Y7	Y8
As-Cast	2.89	3.02	2.88	1.92	1.50
450°C/4h	1.69	1.67	1.87	1.07	1.23
450°C/8h	1.07	1.30	1.42	0.80	0.78
490°C/4h	0.61	0.93	0.74	0.51	0.39
490°C/8h	0.34	0.34	0.14	0.20	0.20

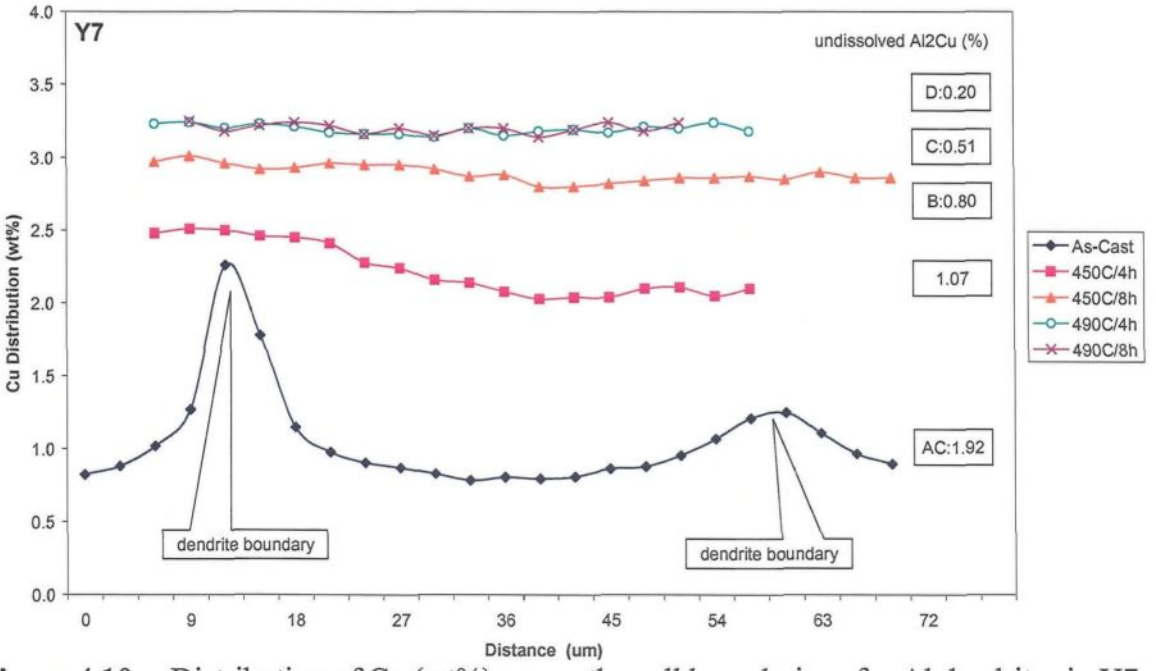

Figure 4.10 Distribution of Cu (wt%) across the cell boundaries of α-Al dendrites in Y7 alloy, obtained from the as-cast and solution heat-treated samples.

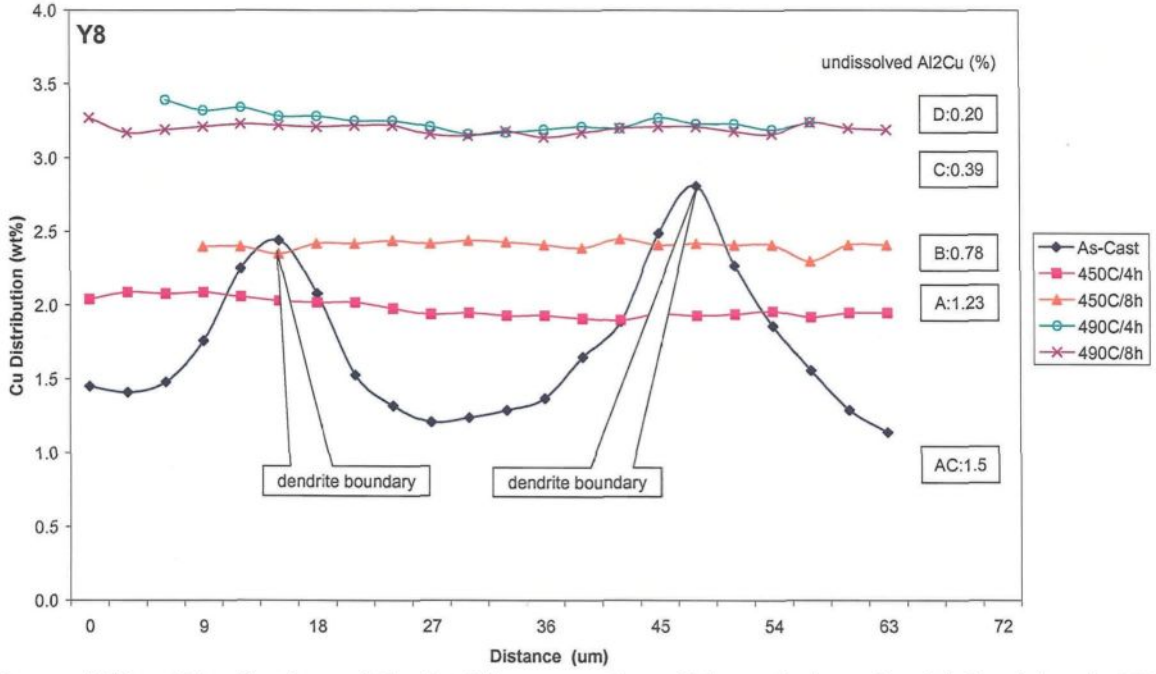

Figure 4.11 Distribution of Cu (wt%) across the cell boundaries of α-Al dendrites in Y8 alloy, obtained from the as-cast and solution heat-treated samples.

4.1.2.2 Sr-modified alloys

When the alloys are modified with 150 ppm Sr, some interesting results may be observed. From Figures 4.12 through 4.16, it will be seen that, after the solution treatments, the distribution of copper in the matrix is more even than it is in non-modified alloys. The most striking point is the high amount of undissolved Al_2Cu in the as-cast condition (4.58%), as may be seen clearly from Figure 4.17 (a). The same may be said for the solution-treated conditions also, when compared to the non-modified alloys. These high amounts result from the effect of Sr on the segregation of the Al_2Cu phase. Strontium is known to cause segregation of the copper phase in areas away from the eutectic silicon regions, thereby causing the copper phase to precipitate in a block-like form which is hard to dissolve.[2, 9-12] The Al_2Cu phase, thus, persists in the matrix even after 490°C/8h solution heat-treatment (treatment D), revealing that while 490°C/8h is the optimum solution heat-treatment for alloy Y1, it is not sufficient for alloy Y1S. It is likely that higher strontium melts need to be subjected to higher solution treatment temperatures.

The presence of Mg in alloys Y4S and Y6S negates this segregation effect of Sr to some extent, so that lower volume fractions of undissolved Al_2Cu are observed in Y4S and Y6S alloys. From Table 4.4, however, it will be observed that in Y4S alloy, 1.64% Al_2Cu persists after treatment at 490°C/8h, indicating that almost half (45 pct) Al_2Cu phase remains undissolved when compared to the as-cast condition. In the case of Y6S alloy, after the same treatment, only 0.67% of the Al_2Cu phase persists, which is much lower than that in Y1S alloy (1.61%), i.e. 24 pct and 35 pct of Al_2Cu remain in the two cases when compared to the respective amounts in the as-cast condition.

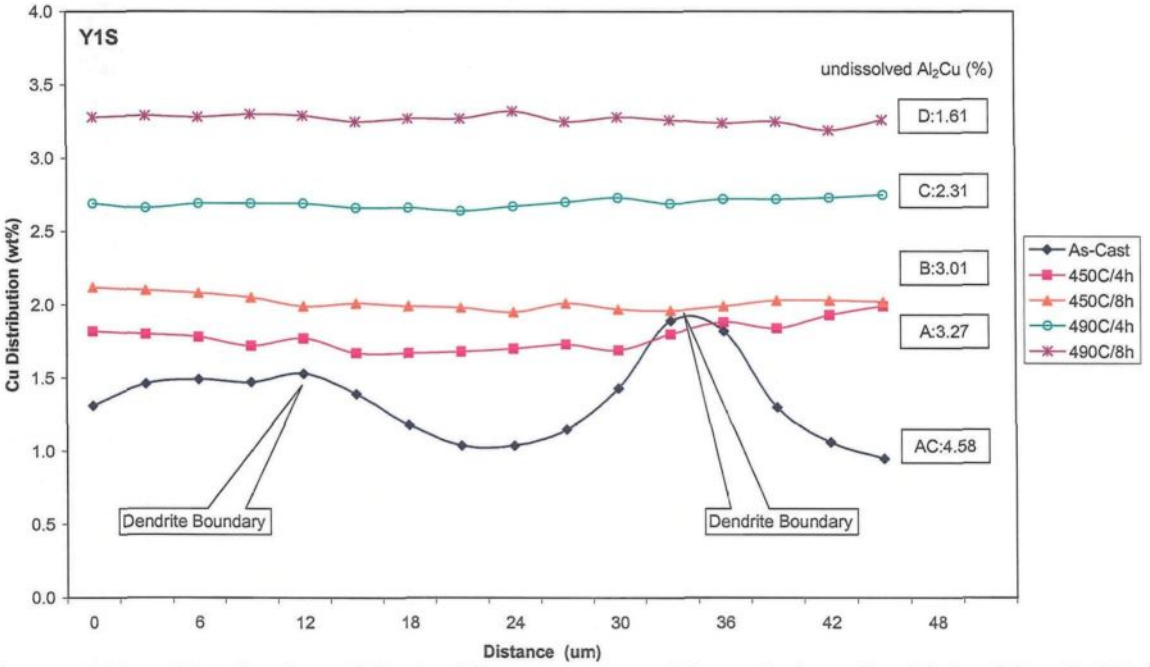

Figure 4.12 Distribution of Cu (wt%) across the cell boundaries of α-Al dendrites in Y1S alloy, obtained from the as-cast and solution heat-treated samples.

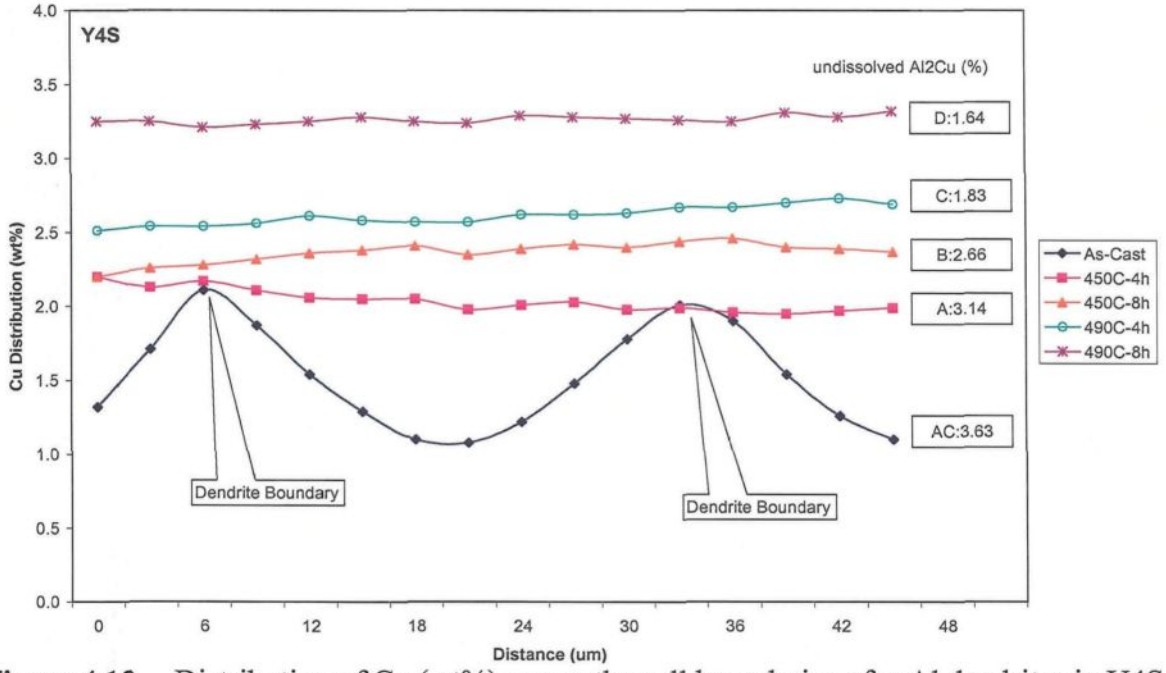

Figure 4.13 Distribution of Cu (wt%) across the cell boundaries of α-Al dendrites in Y4S alloy, obtained from the as-cast and solution heat-treated samples.

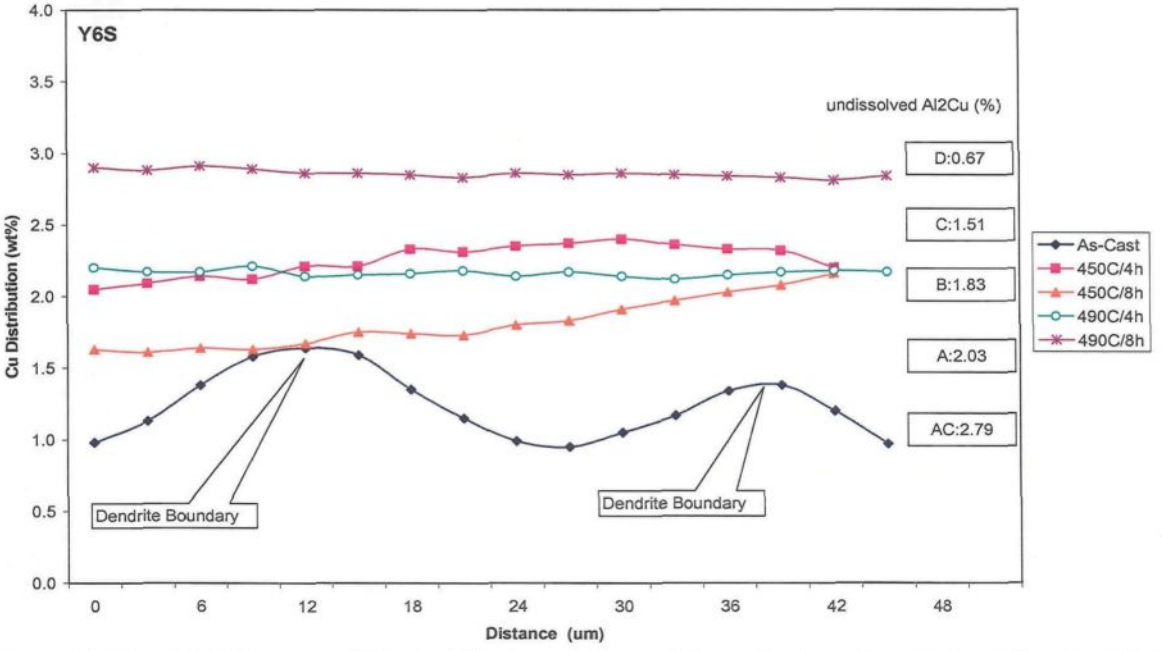

Figure 4.14 Distribution of Cu (wt%) across the cell boundaries of α-Al dendrites in Y6S alloy, obtained from the as-cast and solution heat-treated samples.

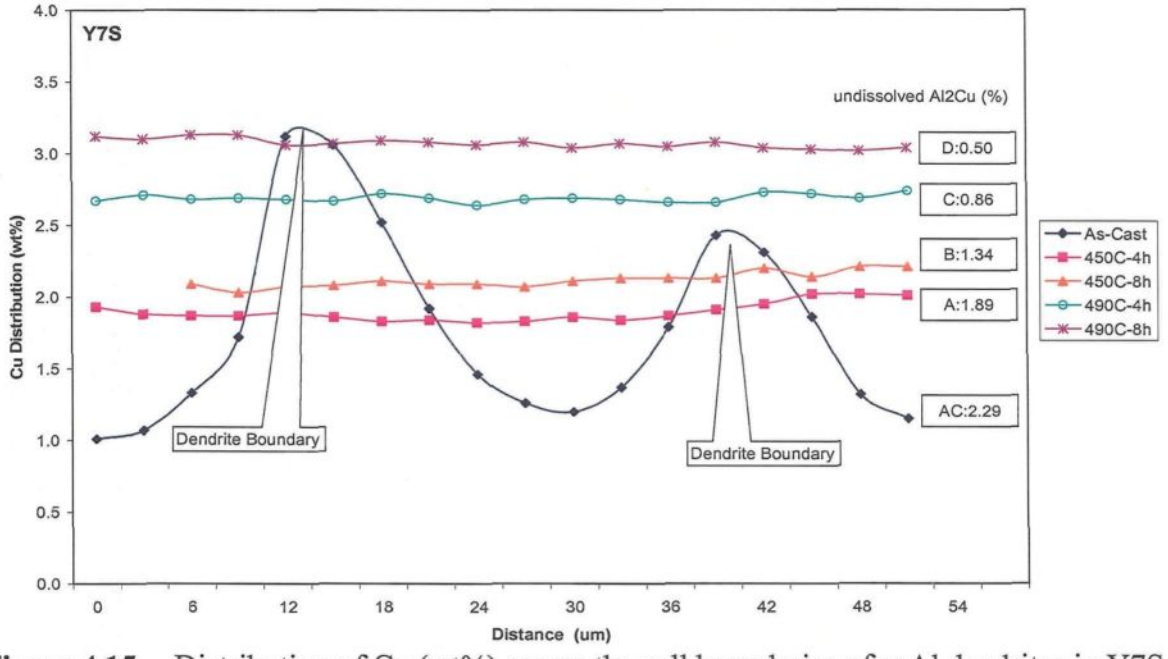

Figure 4.15 Distribution of Cu (wt%) across the cell boundaries of α-Al dendrites in Y7S alloy, obtained from the as-cast and solution heat-treated samples.

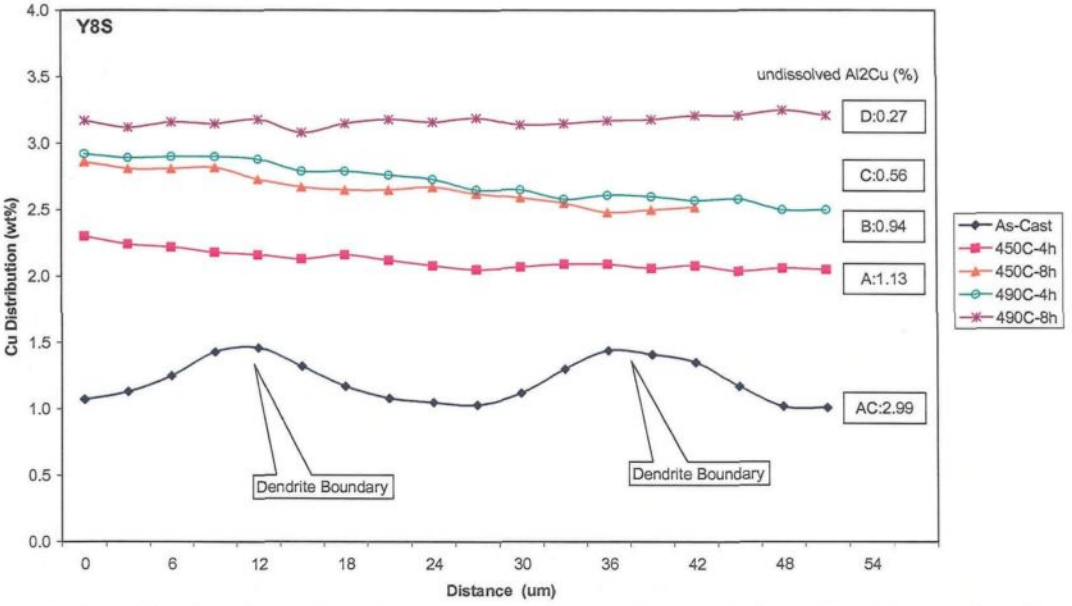

Figure 4.16 Distribution of Cu (wt%) across the cell boundaries of α-Al dendrites in Y8S alloy, obtained from the as-cast and solution heat-treated samples.

Table 4.4 Effects of solution heat-treatment on the dissolution of the Al_2Cu phase in modified experimental alloys Y1S, Y4S, Y6S as well as industrial alloys Y7S and Y8S.

Heat Treatment	Volume fraction of undissolved Al_2Cu (%)				
	Y1S	Y4S	Y6S	Y7S	Y8S
As-Cast	4.58	3.63	2.79	2.29	2.99
450°C/4h	3.27	3.14	2.03	1.89	1.13
450°C/8h	3.01	2.66	1.83	1.34	0.94
490°C/4h	2.31	1.83	1.51	0.86	0.56
490°C/8h	1.61	1.64	0.67	0.50	0.27

The unexpected decrease occurring in the Cu concentration in the matrix (from 2.25% to 1.9%) in alloy Y6S when changing from solution heat-treatment A to B would indicate that a certain amount of incipient melting occurs at 450°C/8h. Also, due to the higher Mg content of the alloy, greater amounts of the Cu-Mg intermetallic phase are

formed, reducing the Cu available to form the Al_2Cu phase that would then be able to dissolve in the matrix. The same results may be obtained from the corresponding industrial alloys Y7S and Y8S, as shown in Figures 4.15 and 4.16, respectively.

Figure 4.17 shows a comparison of undissolved Al_2Cu in non-modified and Sr-modified alloys. It is clear that the undissolved Al_2Cu in the Sr-modified alloys is higher than it is in non-modified alloys, and with the increase in Mg content, the difference in the undissolved Al_2Cu phase between non-modified and Sr-modified alloys diminishes, indicating that Mg negates the effect of Sr on the segregation of Al_2Cu. It will also be observed that when single-step solution treatment time and temperatures increase, undissolved Al_2Cu in all the alloys decreases as well.

Examples of backscattered images taken from the as-cast samples of alloys Y1 and Y6 as well as from alloys Y1S and Y6S (Figure 4.18), show the effect of Sr on the segregation of the copper phase in the Sr-modified alloys. The gradual dissolution of the Al_2Cu phase, with increasing solution time and temperature, may be seen clearly by comparing the backscattered images in Figure 4.19 obtained from heat-treated samples of alloy Y1.

(a)

(b)

(c)

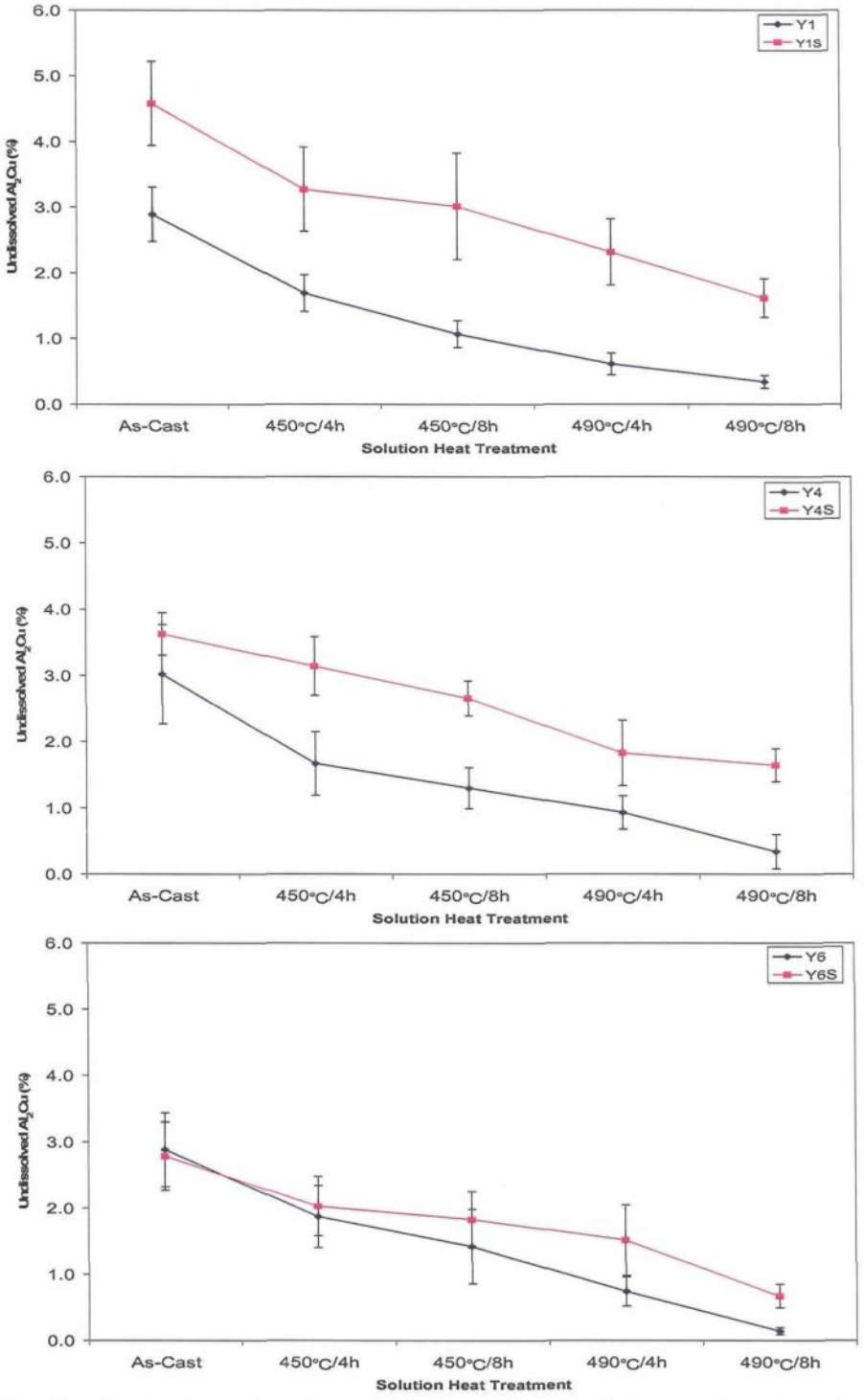

Figure 4.17 Undissolved Al_2Cu in alloys (a) Y1 and Y1S; (b) Y4 and Y4S; (c) Y6 and Y6S; (d) Y7 and Y7S; and (e) Y8 and Y8S as a function of single-step solution heat-treatment.

(d)

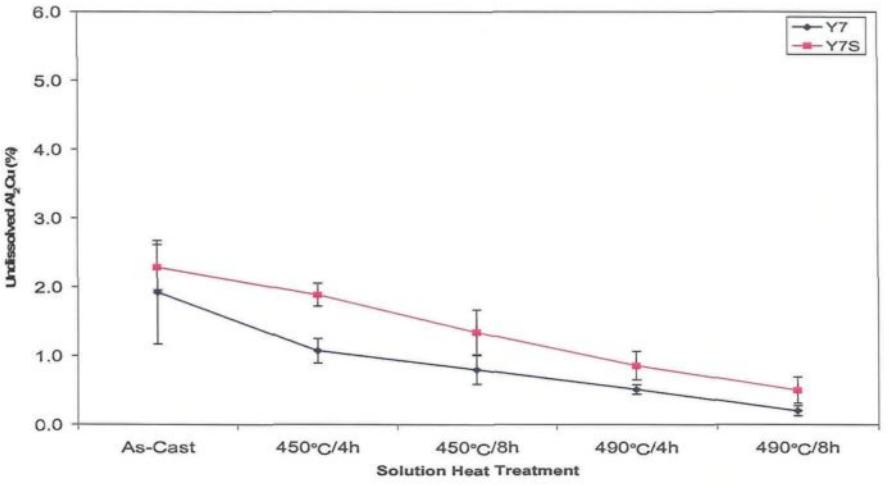

(e)

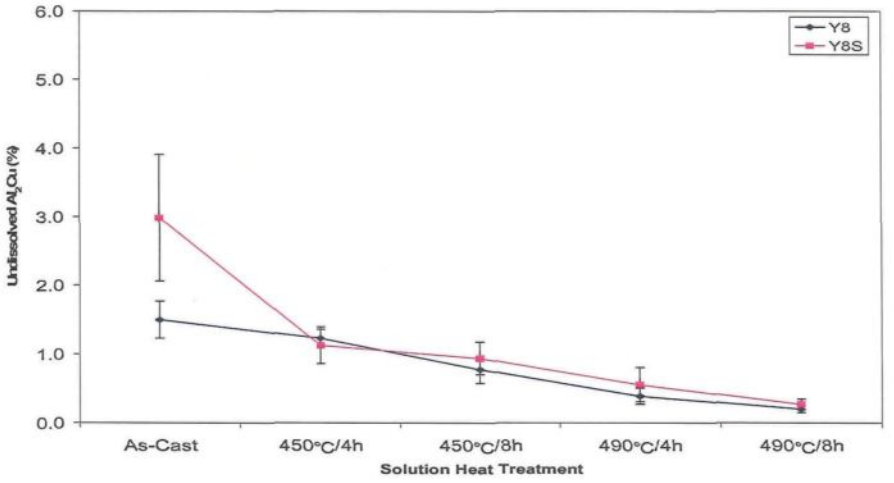

Figure 4.17 Undissolved Al_2Cu in alloys (a) Y1 and Y1S; (b) Y4 and Y4S; (c) Y6 and Y6S; (d) Y7 and Y7S; and (d) Y8 and Y8S as a function of single-step solution heat-treatment.

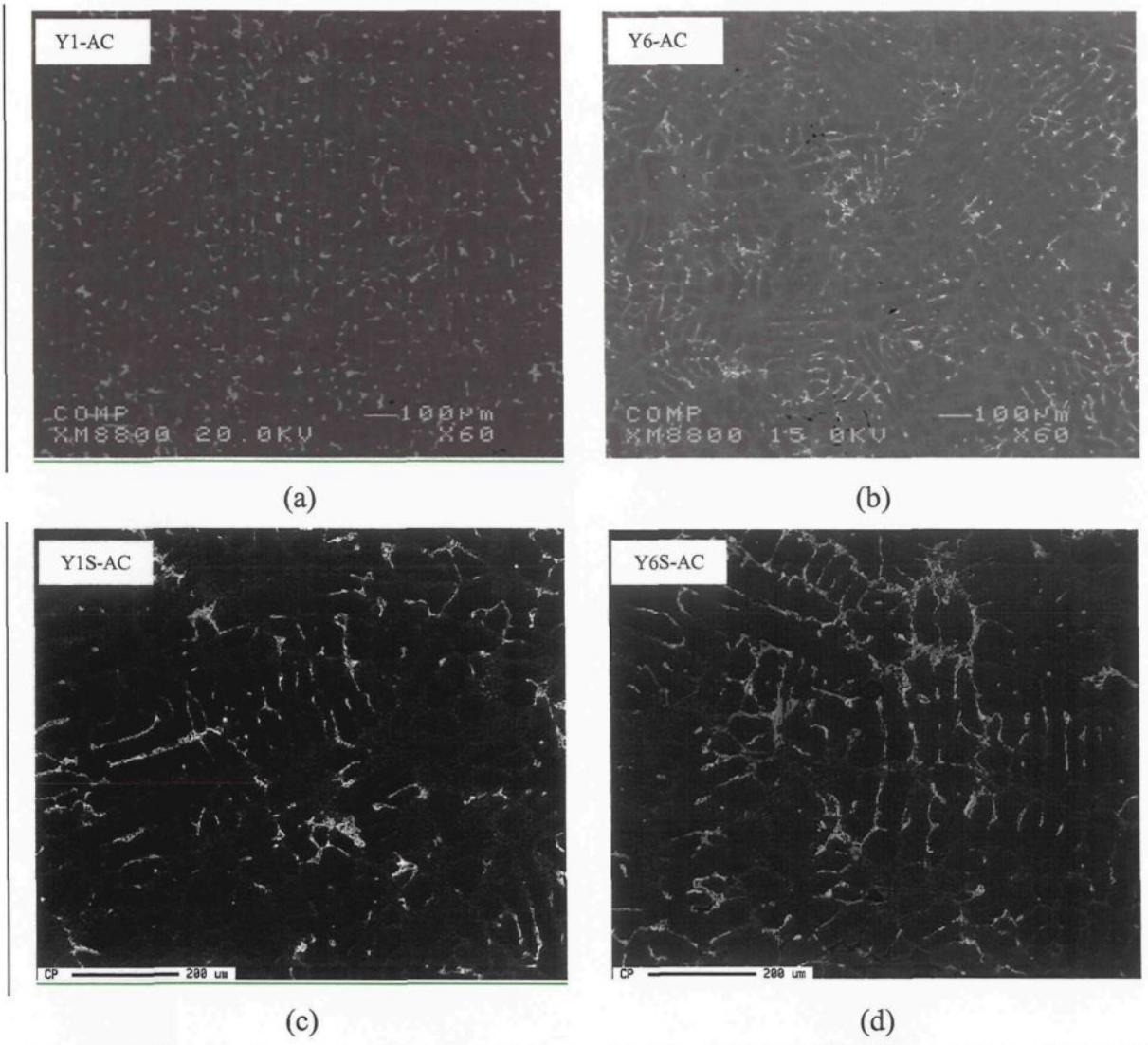

Figure 4.18 Backscattered images of alloys (a) Y1, 60X (b) Y6, 60X (c) Y1S, 100X (d) Y6S, 100X in the as-cast condition showing severe segregation of Al_2Cu in areas away from the eutectic Si regions in the modified alloys.

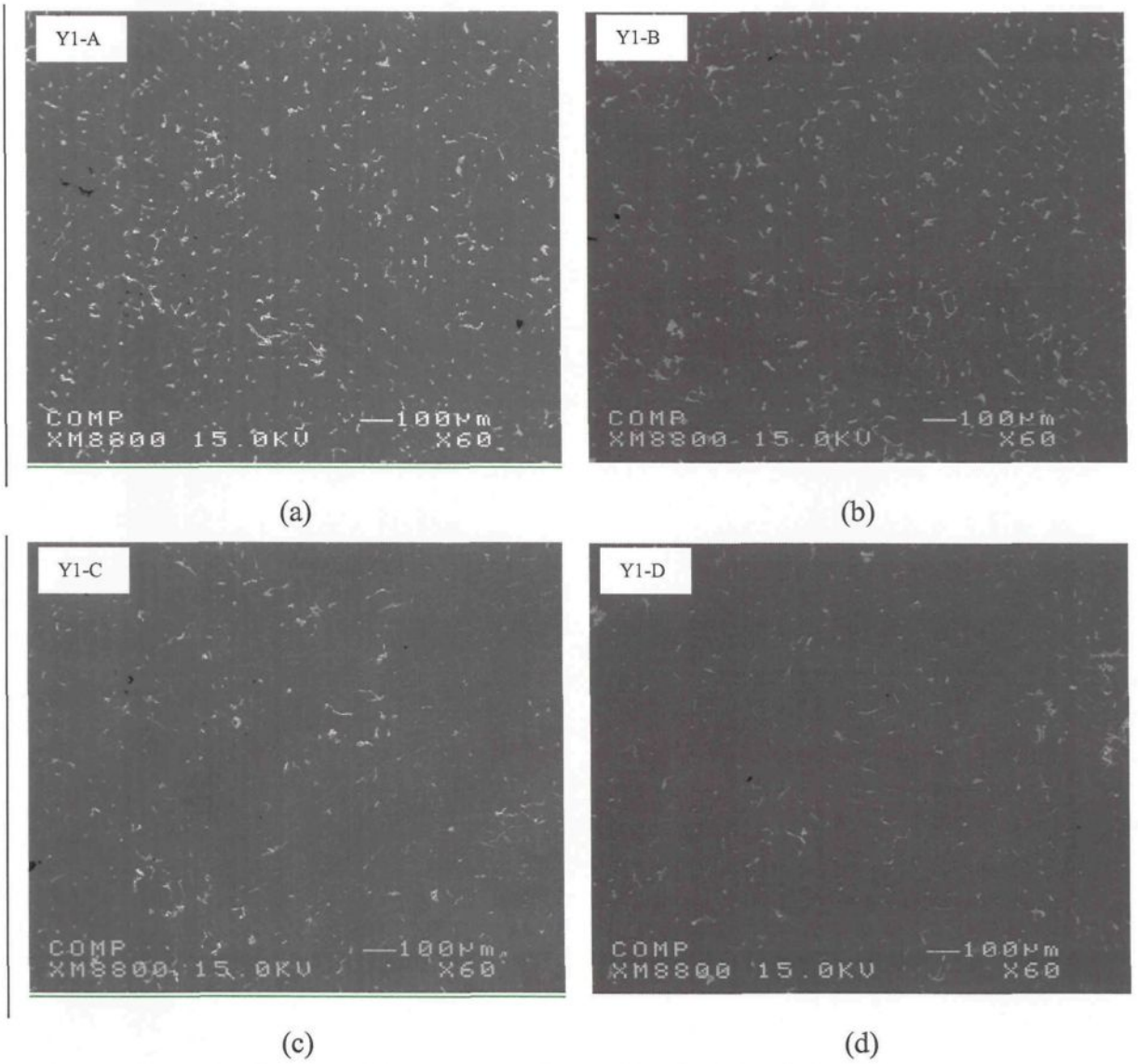

Figure 4.19 Backscattered images showing undissolved Al_2Cu in alloy Y1 obtained from the four single-step solution treatments: (a) 450°C/4h, 60X (b) 450°C/8h, 60X (c) 490°C/4h, 60X (d) 490°C/8h, 60X.

High magnification micrographs of the eutectic and block-like Al_2Cu phase particles are shown in Figure 4.20, where the open arrows indicate the eutectic-like Al_2Cu, and the white arrows point to the block-like Al_2Cu particles. A schematic representation of the dissolution process of the eutectic Al-Al_2Cu and block-like Al_2Cu particles during

solution heat-treatment is presented in Figure 4.21. The eutectic Al_2Cu particles undergo necking which takes place at several points along the length of the particles, leading to their breaking into smaller fragments; gradual spheroidization and dissolution of these smaller particles then occurs, followed by diffusion of the Cu atoms into the surrounding aluminum matrix.

In the case of the block-like Al_2Cu particles, spheroidization and diffusion are expected to take place directly (Figure 4.20b). As a result of their block-like morphology, however, the dissolution is much slower than it is in the case of the finer eutectic-like Al_2Cu particles. Thus, a much longer solution time and a higher solution temperature are required for these block-like particles to become smaller and reach complete dissolution. It is for this reason that the block-like Al_2Cu phase is harder to dissolve.

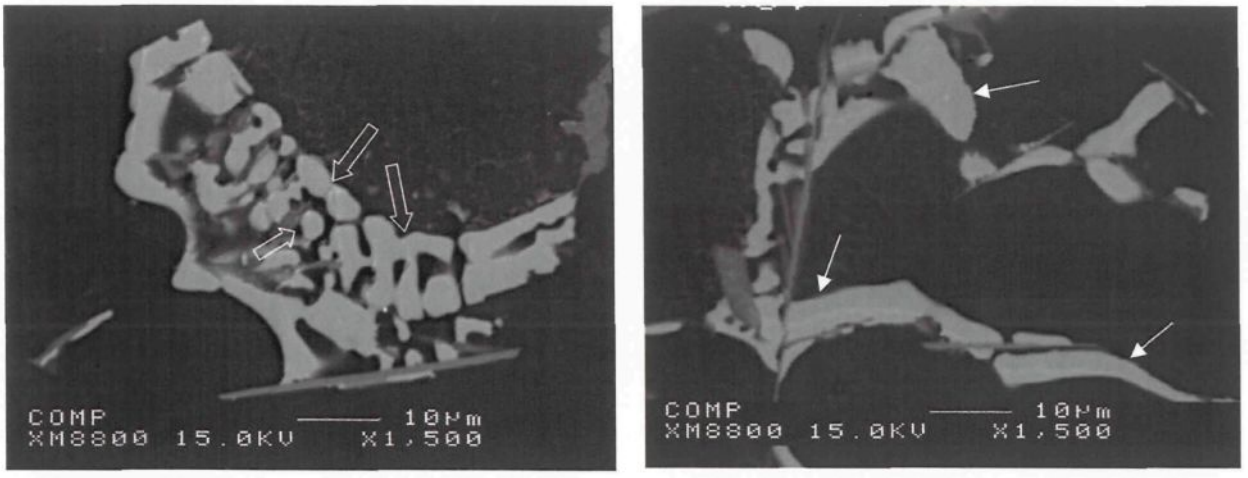

(a) (b)

Figure 4.20 High magnification of microstructure of Al-Al_2Cu in the as-cast samples: (a) Y6 and (b) Y6S alloys. Note the eutectic Al_2Cu (open arrow) and block-like Al_2Cu (solid arrow).

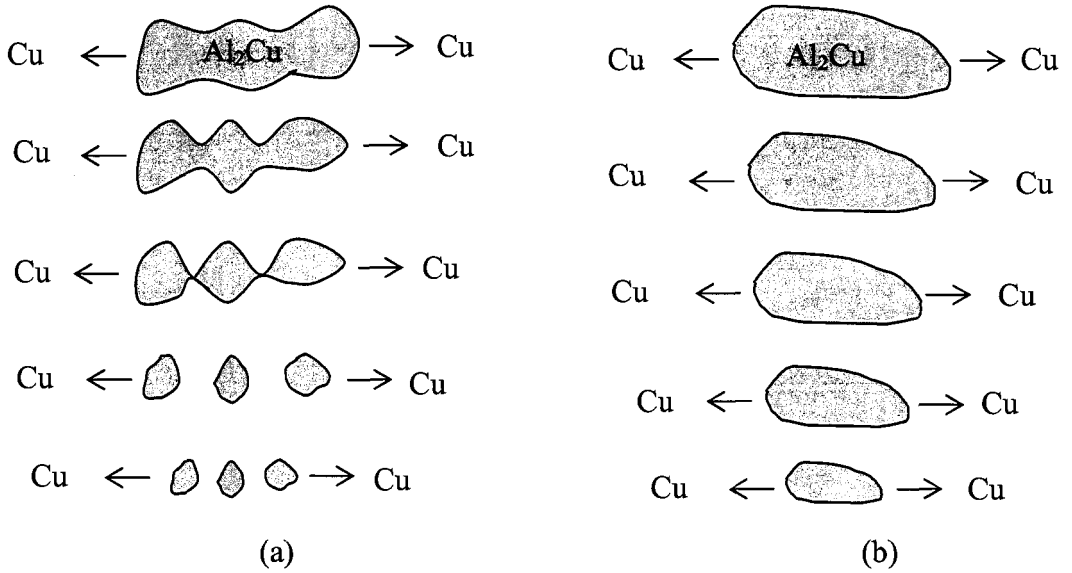

Figure 4.21 Schematic diagram showing the dissolution process of (a) eutectic Al_2Cu and (b) block-like Al_2Cu.

4.1.3 Melting of $Al_5Mg_8Cu_2Si_6$ Complex Phase

The presence of Mg in Al-Si-Cu-Mg alloys leads to the formation of $Al_5Mg_8Cu_2Si_6$ phase, which forms from the Al_2Cu phase along its edges during the last stage of solidification. Bäckerud *et al.*[4] reported that this phase precipitates at 507°C, and that the Al_2Cu started to precipitate at 525°C. In this study, as mentioned previously, the complex phase $Al_5Mg_8Cu_2Si_6$ precipitates both before and after the precipitation of the Al_2Cu phase, which leads to two explicit peaks D' (pre-eutectic) and D (post-eutectic). The post-eutectic $Al_5Mg_8Cu_2Si_6$ precipitates at 491.3°C in experimental alloy Y6 with 0.6 wt% Mg and at 486.4°C in the corresponding industrial alloy Y8. It was observed that this phase precipitates at a temperature which is 10°C lower than the precipitation temperature of Al_2Cu, *i.e.* 501.4°C, whereas, due to its complex nature, the $Al_5Mg_8Cu_2Si_6$ phase is insoluble. When the solution heat-treatment temperature is higher than its precipitation

temperature, this phase melts and porosity is formed at the local melting point when the sample is quenched following solution treatment. That is to say, the $Al_5Mg_8Cu_2Si_6$ phase determines the maximum temperature to which 319 alloy castings may be exposed during heat treatment without incurring incipient melting. Clearly, the maximum solution heat-treatment temperature is limited to a low value. At the same time, a low solutionizing temperature is not enough to dissolve Al_2Cu, thus the strengthening effect of Cu cannot be exploited to the fullest extent possible.

Table 4.3 shows the volume fraction of the $Al_5Mg_8Cu_2Si_6$ phase in the 0.6 wt% Mg-containing Y6 alloy and the Y6S (Sr-modified) alloy obtained from the as-cast condition and after undergoing 490°C/8h + 500°C/4h solution treatment. From this table, it is possible to observe that the volume fraction of the $Al_5Mg_8Cu_2Si_6$ phase in Y6 alloy, about 2.1%, is more or less the same under the as-cast condition and after 490°C/8h + 500°C/4h treatment. This fact proves that the $Al_5Mg_8Cu_2Si_6$ phase is insoluble. A similar observation may be noted for alloy Y6S, the volume fraction for which is a little higher than that of alloy Y6, around 2.35%, which may be attributed to the effect of Sr.

Table 4.5 Volume fraction of $Al_5Mg_8Cu_2Si_6$ phase in alloy Y6 and Y6S (Sr-modified) obtained from the as-cast condition and after 490°C/8h + 500°C/4h solution treatment.

Alloy Condition/ Heat Treatment	Volume fraction of $Al_5Mg_8Cu_2Si_6$ (%)	
	Y6	Y6S
As-Cast	2.11	2.32
490°C/8h + 500°C/4h	2.19	2.41

Figure 4.22 depicts the dissolution of the Al_2Cu phase and the persistence of the $Al_5Mg_8Cu_2Si_6$ phase even after 490°C/8h + 500°C/4h (treatment J). Here, it should be kept in mind that the solidifying temperature of the Cu phase on the cooling curve is always lower than that of the melting temperature on the heating curve.

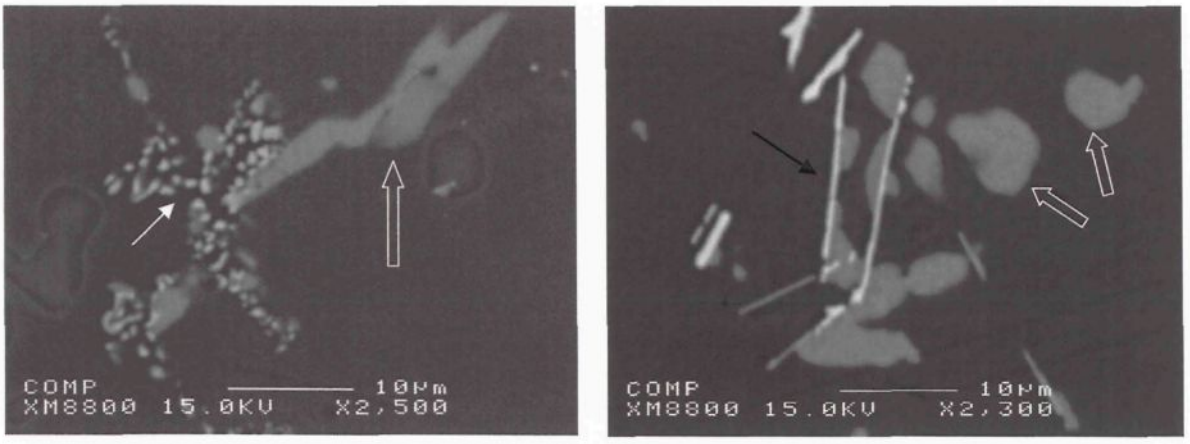

(a) (b)

Figure 4.22 Microstructures of Y6S alloy after a solution heat treatment of 490°C/8h + 500°C/4h (treatment J) showing: (a) fragmentation and dissolution of Al_2Cu (solid arrow), (b) persistence of $Al_5Mg_8Cu_2Si_6$ complex phase (open arrows). The white platelets in (b) are Al_5FeSi phase (black arrow).

Figure 4.23 shows the results of a DSC run carried out on a powdered sample of the experimental 319 alloy (containing 0.003 wt% Mg and 0.15 wt% Fe), where the fusion temperature of the Al_2Cu phase on the heating curve is observed to be 18°C higher than that observed for the cooling curve.[10]

Another good example is shown in Figure 4.24. In this study, DSC measurements were used to estimate the fractional latent heat release during phase changes in commercial A356 aluminum alloy. The temperature domain was found to be approximately 20 K and 100 K before the onset of melting and solidification, respectively.

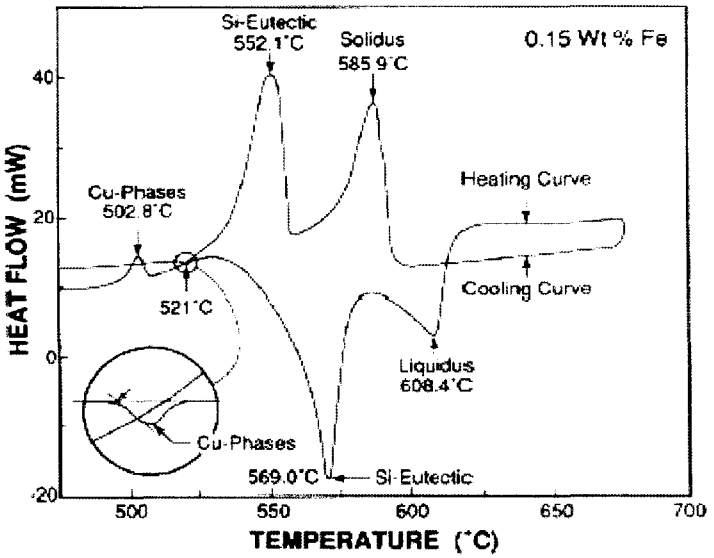

Figure 4.23 DSC run for a powdered sample obtained from the experimental 319 alloy solidified at 10°C/s. The arrow in the enlarged circled area indicates the onset of the melting of the Al_2Cu phase.[9]

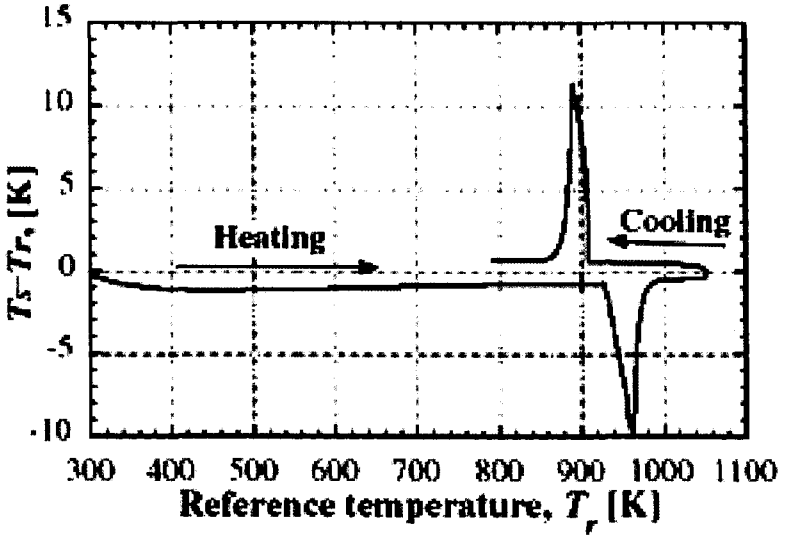

Figure 4.24 Temperature difference between the sample and reference plate thermocouples used as input for pure aluminum simulations.[79]

4.1.4 Porosity Characteristics

Porosity is one of the defects normally present in Al-Si cast alloys. The presence of porosity in a casting has a deleterious effect on its mechanical properties, namely, ductility, fracture toughness, and fatigue life; it also affects the surface finish of the casting.[80]

There may be two origins for the porosity observed in these samples: (i) porosity arising from casting defects, and (ii) porosity related to the effect of the incipient melting of the copper-containing phases during solution heat treatment. At times, both types of porosity emerge together and it is difficult to distinguish between them. Therefore, in this study, porosity measurement was carried out for both kinds, while avoiding apparent pore defects. The average area percent porosity (percentage porosity over a constant sample surface area) and average pore length for experimental alloys Y1, Y6 and their modified versions Y1S and Y6S, as a function of solution treatment, are shown in Figures 4.25 through 4.29. Each figure is divided into four regions:

(I) As-cast region (AC);

(II) Single-step treatment region, including treatments ending at 450°C (treatments A and B), and at 490°C (treatments C and D);

(III) Two-step treatment region, including treatments ending at 500°C (treatments E, F, I and J), and at 520°C (treatments G, H, K and L);

(IV) Triple-step treatment region, including treatments ending at 520°C (treatments M, N O and P).

In Figure 4.25, hardly any porosity is observed and the average pore length noted is about 10 μm. Even when the temperature goes as high as 520°C, the area percent porosity

is fairly low, which means that for alloy Y1, 520°C is still a safe temperature since no incipient melting is found to occur in the alloy structure.

When alloy Y1 is modified with 150 ppm Sr, the average pore length in alloy Y1S increases with treatment time and temperature. Single-step and two-step treatments ending at 500°C do not cause any great changes in area percent porosity, but when treatment temperature reaches 520°C, especially after triple-step heat-treatments, the area percent porosity increases, and this gives a clear indication that incipient melting of Al_2Cu has occurred subsequent to these treatments, as shown in Figure 4.27.

When 0.6 wt% Mg is present in alloy Y6, the overall average area percent porosity and pore length are found to increase, as shown in Figure 4.26. Of all the single-step heat treatments, treatment D exhibits the highest area percent porosity and largest pore size, namely, 0.39% and 15.8 μm; this observation attests to the conclusion reached in subsection 4.1.2 that incipient melting occurs after heat-treatment at 490°C/8h.

When samples are submitted to two-step heat treatments ending at 500°C, the values of both parameters increase. On the one hand, the addition of Mg leads to the precipitation of the low-melting-point yet insoluble $Al_5Mg_8Cu_2Si_6$ phase which occurs at 491.3°C in alloy Y6, as listed in Table 4.1. When samples are heat-treated to 500°C, this phase starts to melt and porosity is initiated in the local area, leading to an increase in the area percent porosity and pore length. On the other hand, the addition of Mg can also lead to the segregation of Al_2Cu, resulting in the block-like rather than the fine eutectic Al_2Cu, compared to which, the block-like Al_2Cu phase is much harder to dissolve during solution heat-treatment.

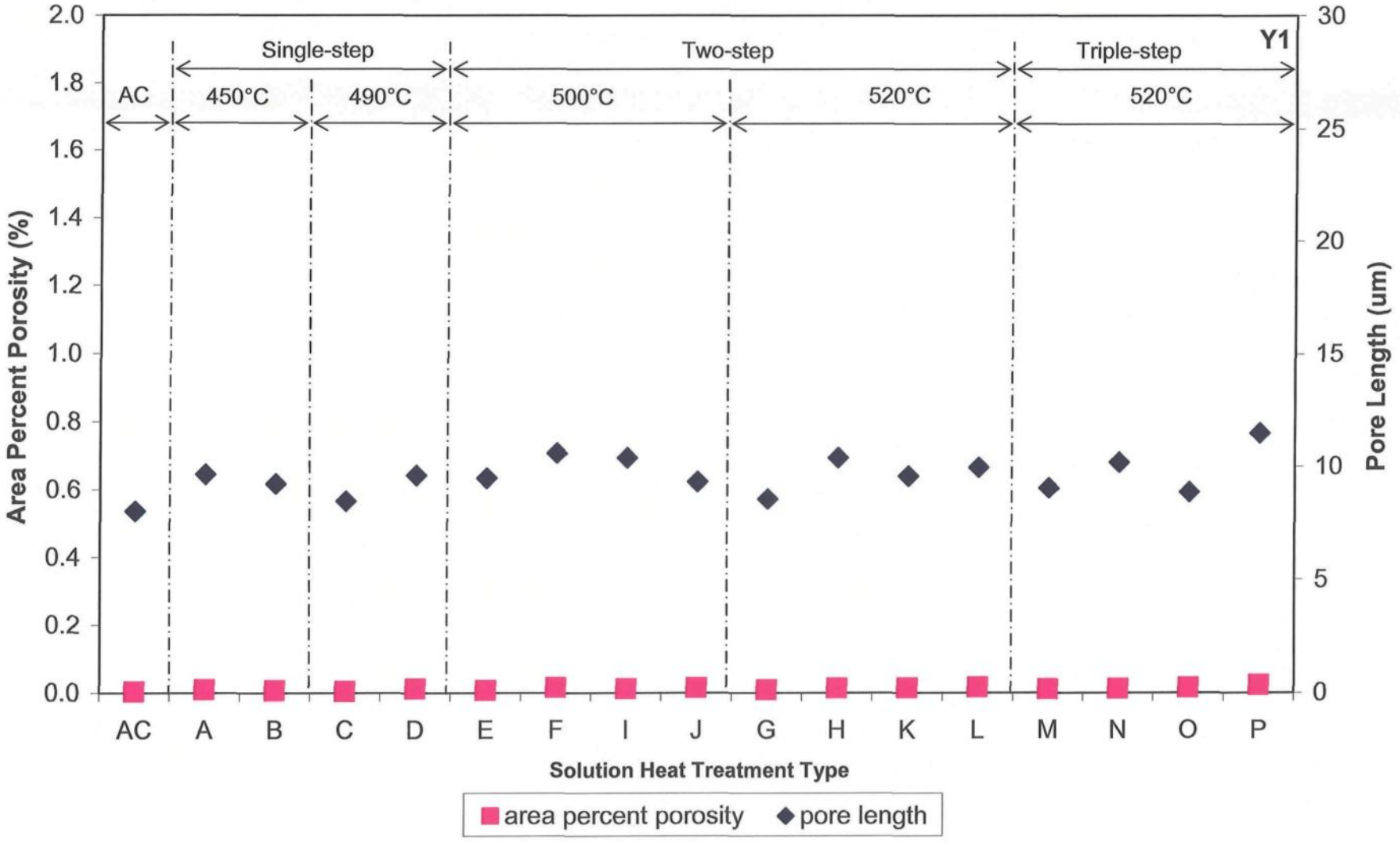

Figure 4.25 Plot showing area percent porosity and pore length in alloy Y1 after various solution heat-treatments.

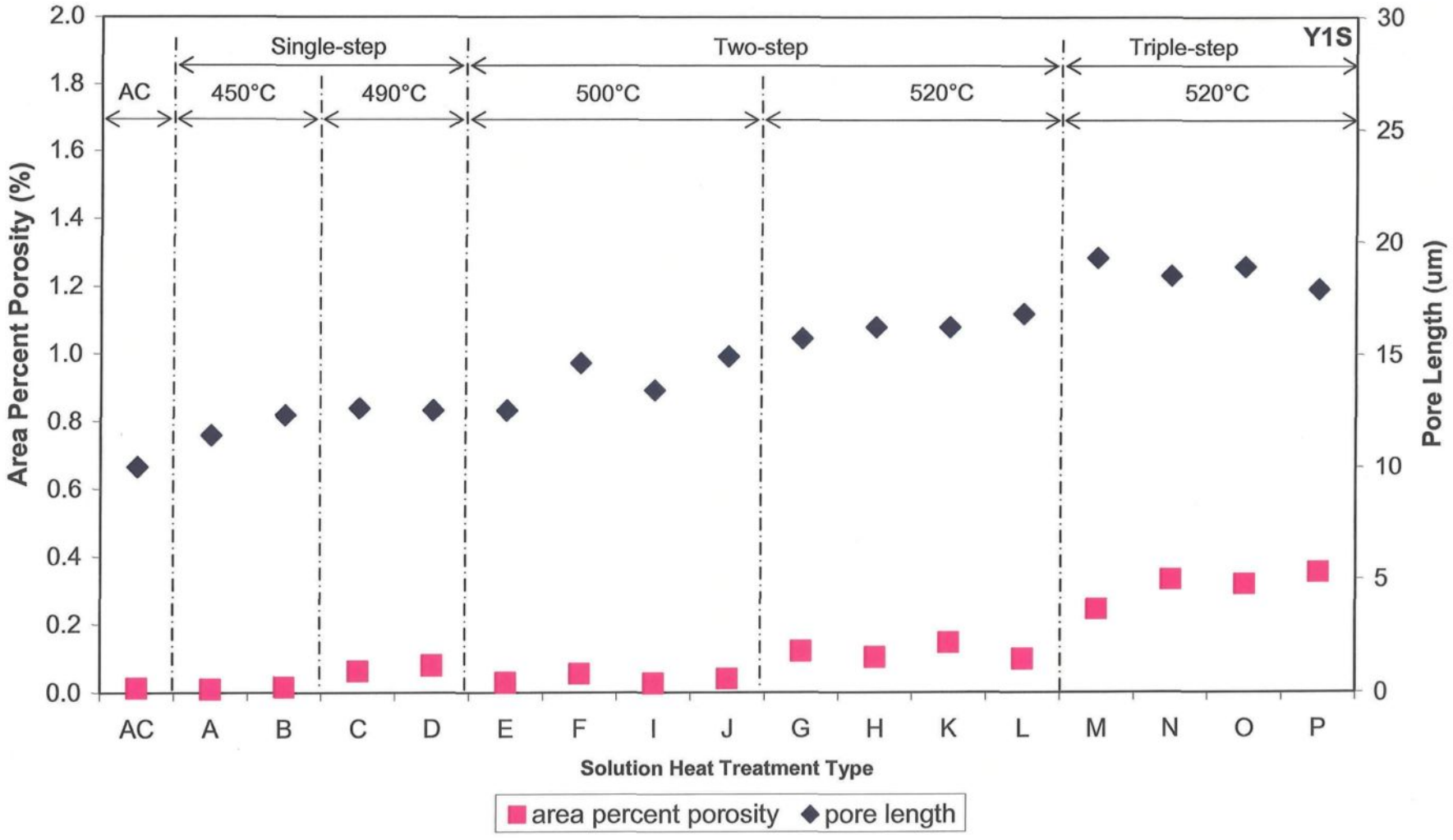

Figure 4.26 Plot showing area percent porosity and pore length in alloy Y1S after various solution heat-treatments.

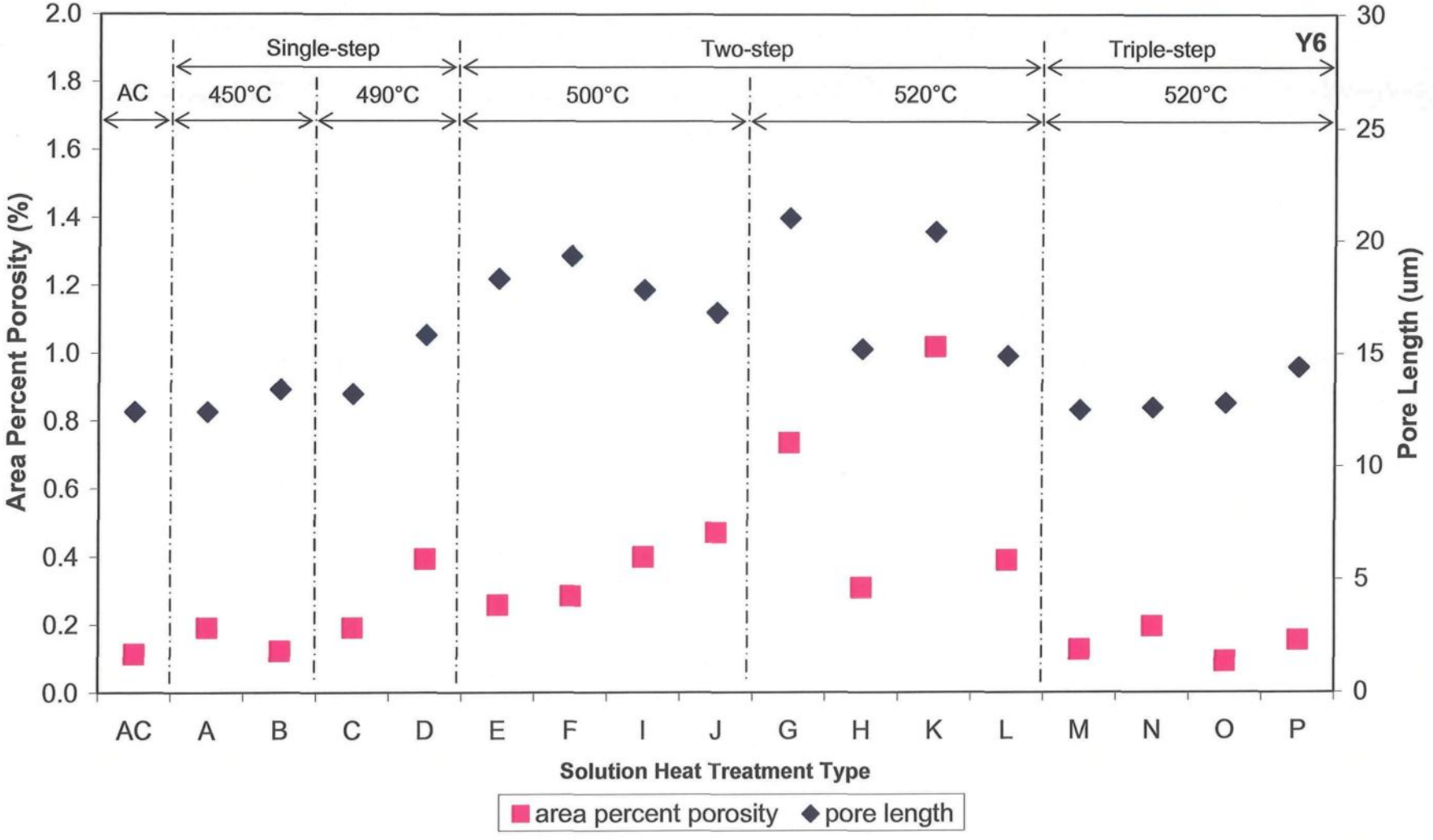

Figure 4.27 Plot showing area percent porosity and pore length in alloy Y6 after various solution heat-treatments.

Therefore, when a two-step treatment is carried out, if the heat-treatment time of the first step is not long enough to allow the Al_2Cu to dissolve and the second-step treatment temperature is higher than its melting-point, incipient melting of this phase will occur. This sequence may explain why samples after treatments G (450°C/4h+520°C/4h) and K (490°C/4h+520°C/4h) show higher area percent porosity than they do after treatments H (450°C/8h+520°C/4h) and L (490°C/8h+520°C/4h). The first-step treatment temperatures of 450°C and 490°C are lower than the melting point of the Al_2Cu phase; thus, at the first step, Al_2Cu undergoes dissolution, where the longer the solution heat-treatment time, the more the Al_2Cu dissolves, and less of the Al_2Cu phase remains. When the heat treatment temperature is raised suddenly to 520°C in the second step, the undissolved Al_2Cu melts. The drop in percent porosity and pore length after the alloy samples undergo triple-step treatments may also be explained in a similar fashion: the Al_2Cu phase dissolves completely after the triple-step treatment, and any incipient melting observed may be attributed to the melting of the $Al_5Mg_8Cu_2Si_6$ phase alone.

When 0.6 wt% Mg and 150 ppm Sr are added to the base alloy Y1 simultaneously, the values of both parameters increase, as shown in Figure 4.29. Also, as listed in Table 4.2, the $Al_5Mg_8Cu_2Si_6$ phase precipitates at 493.3°C, and thus single-step treatments show hardly any porosity, as was expected. When the samples are submitted to a two-step heat treatment with a final temperature of 500°C, the $Al_5Mg_8Cu_2Si_6$ phase starts to melt resulting in a slight increase in the percentage porosity and pore length. Higher temperatures and longer time lead to further incipient melting of the $Al_5Mg_8Cu_2Si_6$ phase

and hence to more porosity formation. In view of the fact that the melting point of the Al_2Cu phase in alloy Y6S is 500°C, the phase also melts and contributes further to the porosity observed in the sample when the temperature is raised to 520°C.

Figure 4.29 compares the pore lengths observed in alloys Y1, Y6, Y1S and Y6S as a function of solution heat-treatment. Figure 4.30 compares the area percent porosity observed in these alloys as a function of solution heat-treatment. It will be observed that base alloy Y1 exhibits the lowest area percent porosity and pore length. When modified with Sr, both average area percent porosity and pore length increase slightly; various explanations have been proposed for this observation. The addition of Sr may lead to a depression in the silicon eutectic temperature, thereby extending the alloy freezing range (*i.e.* the length of the mushy zone), resulting in a longer solidification time and a consequent larger pore size. Emadi *et al.*[81] concluded that Sr decreased the surface tension of the liquid and increased the volumetric shrinkage, facilitating porosity formation and increasing the pore size and amount of porosity. It was also reported that Sr may enhance the hydrogen solubility in the melts.[69] It is interesting to note that, in general, the pore length in alloy Y6S is higher than it is in Y1S when the temperature is below 500°C. When the temperature reaches 520°C, however, the reverse is observed.

Figure 4.31(a) shows the porosity present in alloy Y1. As may be observed, a certain amount of material exists within the pore. The undissolved Al_2Cu melts during solution heat-treatment at 520°C, *i.e.* at a temperature which is higher than its melting point. During quenching, and as a result of the rapid solidification of the molten region, shrinkage occurs, thus separating the material from the pore boundaries (see white arrows). Figure

4.31(b) shows relatively larger pores almost connected together (see solid arrows). The pores themselves are characterized by their round shape (open arrows). Figure 4.31(c) shows a spherical unmelted Al_2Cu phase region (marked A) near the molten zones (marked B). Within the circle in Figure 4.31(c), small particles of Al_2Cu may still be seen. A high magnification of region A in Figure 4.31(c) is shown in Figure 4.31(d). The white arrows point to the cavities between the Al_2Cu and $Al_5Mg_8Cu_2Si_6$ phases. Also, the shape of the Al_2Cu particles changes significantly from its fine eutectic form and coarsens, becoming massive. The circled area in Figure 4.31(d) reveals the onset of the melting of the $Al_5Mg_8Cu_2Si_6$ phase before that of the Al_2Cu phase.

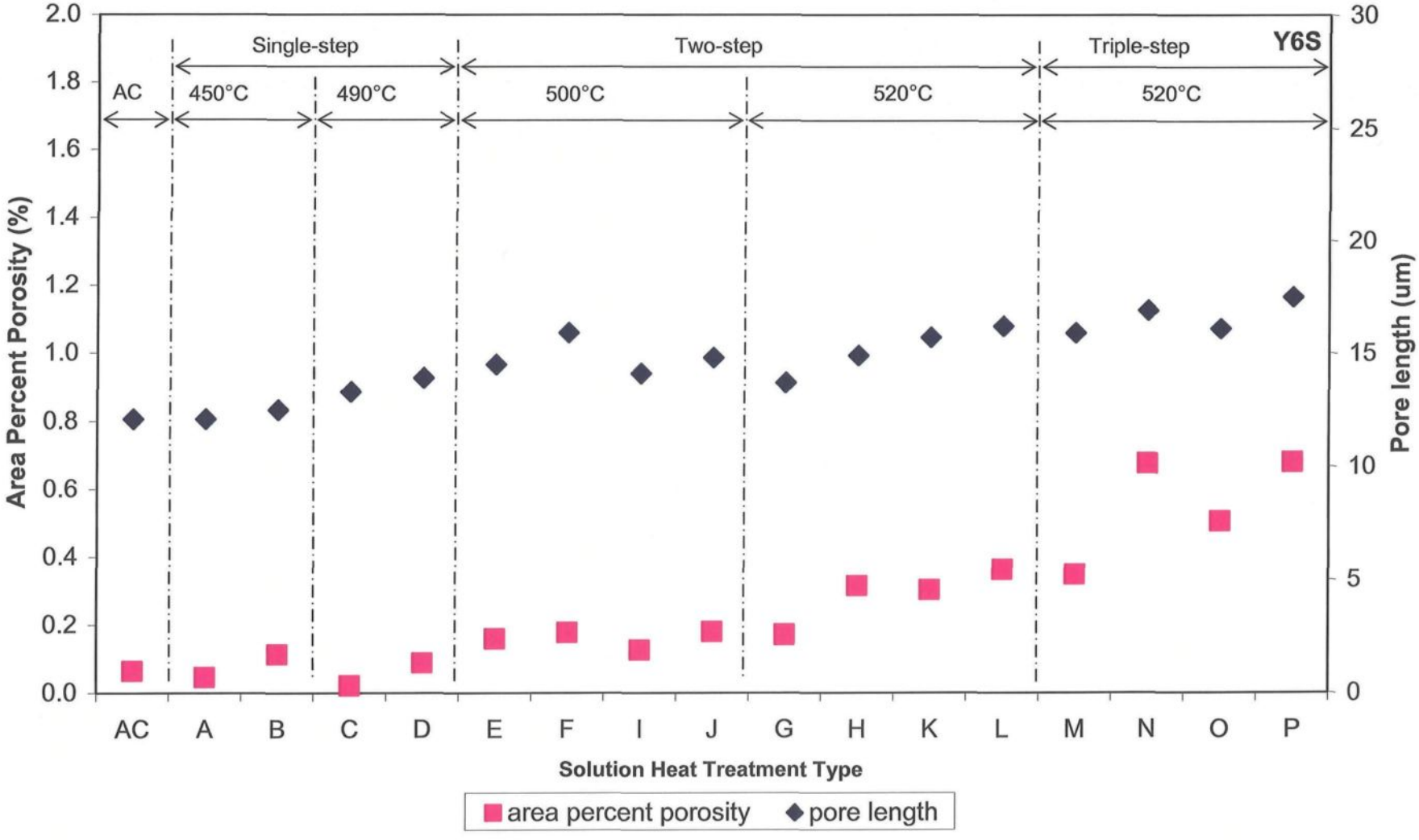

Figure 4.28 Plot showing area percent porosity and pore length in alloy Y6S after various solution heat-treatments.

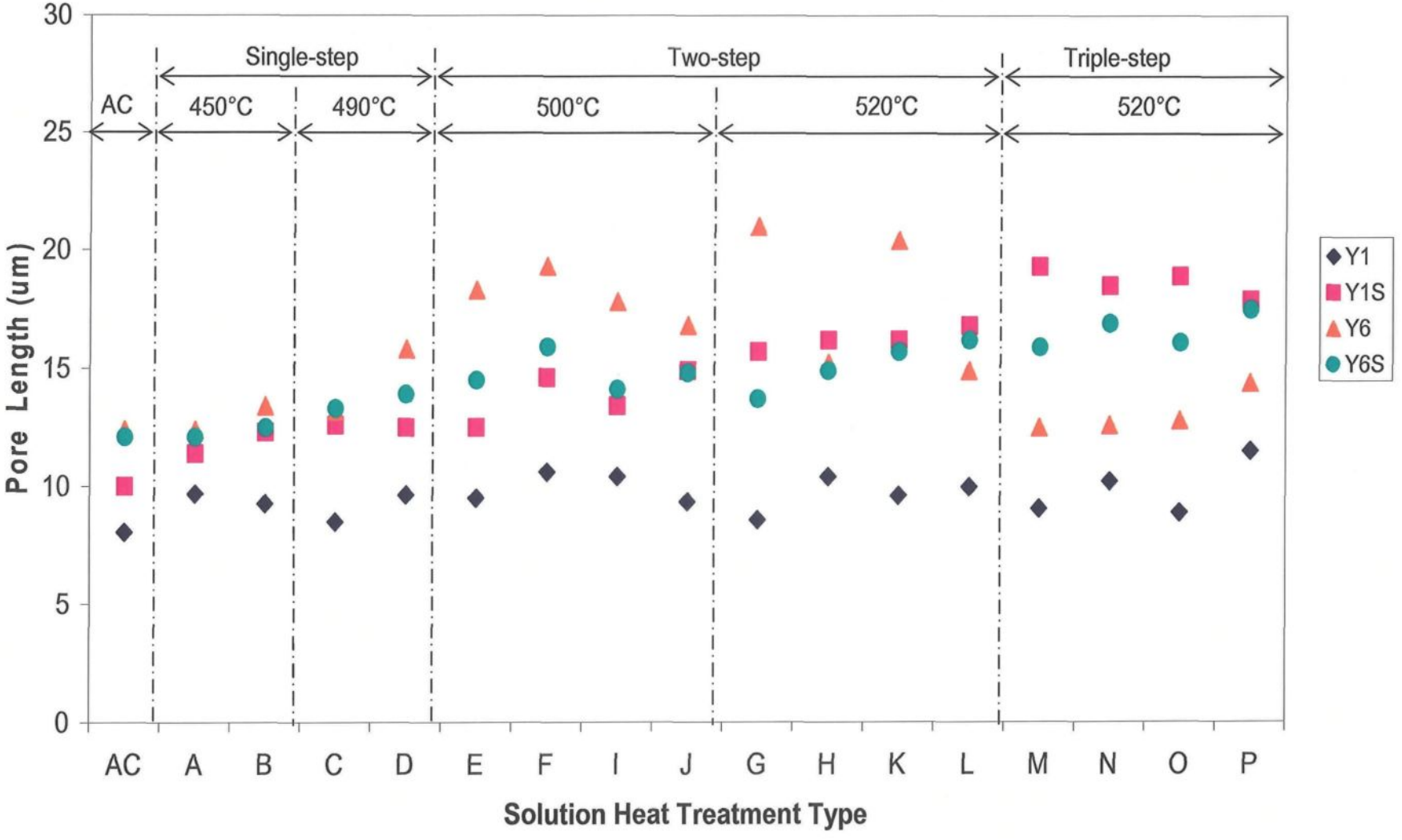

Figure 4.29 Pore lengths in alloy Y1, Y6, Y1S and Y6S as a function of solution heat-treatment.

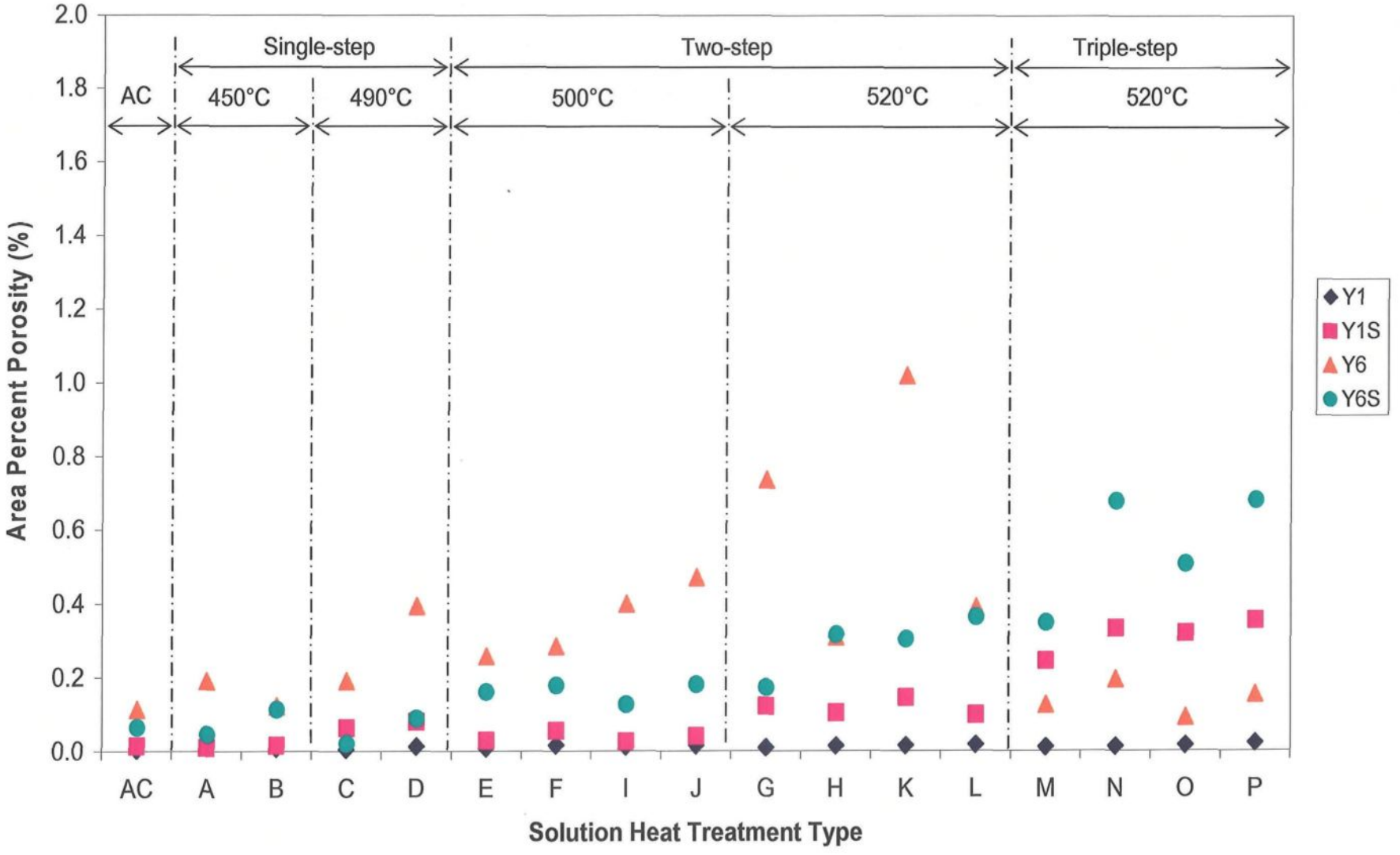

Figure 4.30 Area percent porosity of alloy Y1, Y6, Y1S and Y6S as a function of solution heat-treatment.

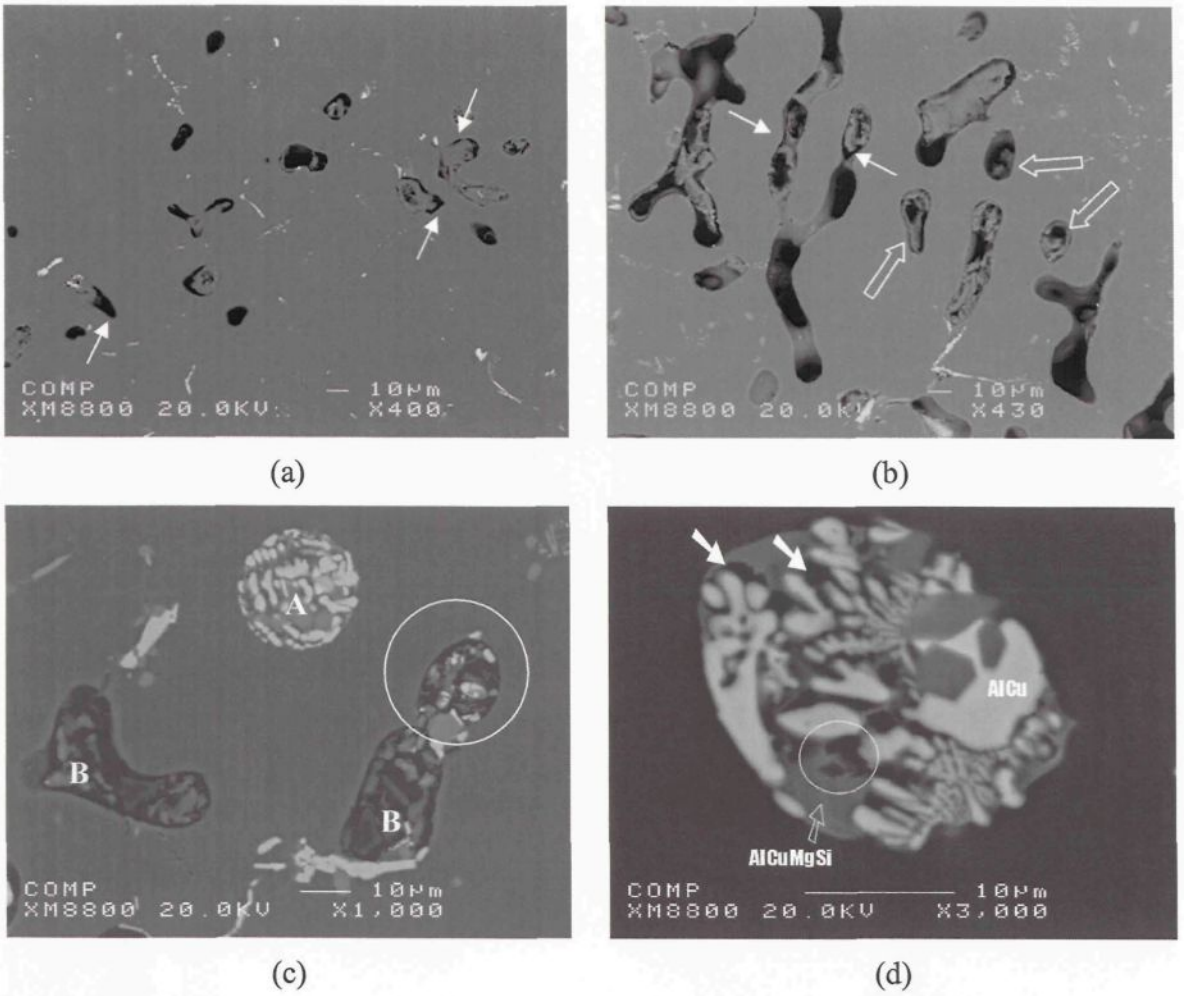

Figure 4.31 Backscattered images showing: (a) porosity in alloy Y1 heat-treated at 490°C/8h+500°C/4h+520°C/4h; (b) porosity in alloy Y6S heat-treated at 490°C/8h+500°C/4h+520°C/4h; (c) high magnification of (b) showing unmelted Al_2Cu (marked A) and melted zone (marked B) in alloy; (d) high magnification of a region similar to that of A in (c), showing the cavities between the Al_2Cu and $Al_5Mg_8Cu_2Si_6$ phases (white arrows).

4.1.5 Silicon Particle Characteristics

Figure 4.32 depicts the behavior of the Si particles in non-modified and modified alloys when they are subjected to solution heat-treatment.[82] In the case of non-modified alloys, the Si particles are large plates and display necking and fragmentation in the early stages of solution treatment. As the solution time and temperatures increase, the particles begin to spheroidize and coarsen, as shown in Figure 4.32 (a). In the modified alloys, the Si particles spheroidize rapidly in the early stages of solution treatment and a shorter heating time is required to reach a fully spheroidized eutectic Si structure. With further heat treatment, the Si particles begin to coarsen.

As-cast Breaking up Spheroidization & Coarsening

(a) Non-modified Silicon

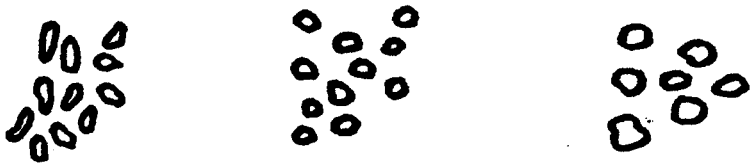

As-cast Spheroidization Coarsening

(b) Modified Silicon

Figure 4.32 Schematic diagram showing modification of Si particles during solution heat-treatment in the case of: (a) non-modified and (b) modified Al-Si alloys.[82]

Measurements were made of the silicon particle characteristics of alloys Y1 and Y6 together with those of Y1S and Y6S for samples obtained from the as-cast condition and after solution heat-treatment in each case; the results are shown in Figures 4.33 through 4.36. As these figures show, the aspect ratio of eutectic Si particles in all the four alloys decreases with increasing solution temperatures and time. Unmodified alloys Y1 and Y6 show a more rapid decrease than modified alloys Y1S and Y6S. Of all four alloys, base alloy Y1 shows the highest aspect ratio after the same solution heat-treatment. Nevertheless, when 150 ppm Sr is added to Y1, the aspect ratio decreases to a relatively low level. Taking the as-cast condition as an example, this value decreases from 2.60 in alloy Y1 to 1.91 in alloy Y1S. The presence of Mg in alloy Y6 is also found to result in a slight decrease in the aspect ratio to about 2.54. When Mg is combined with Sr, the aspect ratio is further decreased to 2.05, although this value is still higher than that of alloy Y1S.

Thus it may be concluded that the addition of 150 ppm Sr leads to a well-modified eutectic structure; the addition of 0.6 wt% Mg results in partially-modified Si particles; and the combined effect of Mg and Sr is much stronger than Mg alone but slightly weaker than Sr alone in modifying the Si particles. In other words, the addition of Mg decreases or weakens the effect of Sr as a modifier. Heusler and Schneider[39] attributed this to the interaction of Mg and Sr, which forms the complex intermetallic compound $Mg_2SrAl_4Si_3$; this agrees well with the observations made by Samuel *et al.*[9] who reported that less than 0.6 wt% of Mg is capable of refining the Si particles to some extent. Gruzleski *et al.*[34] reported that about 1% Mg refines the Si phase slightly and has a negative effect on Sr

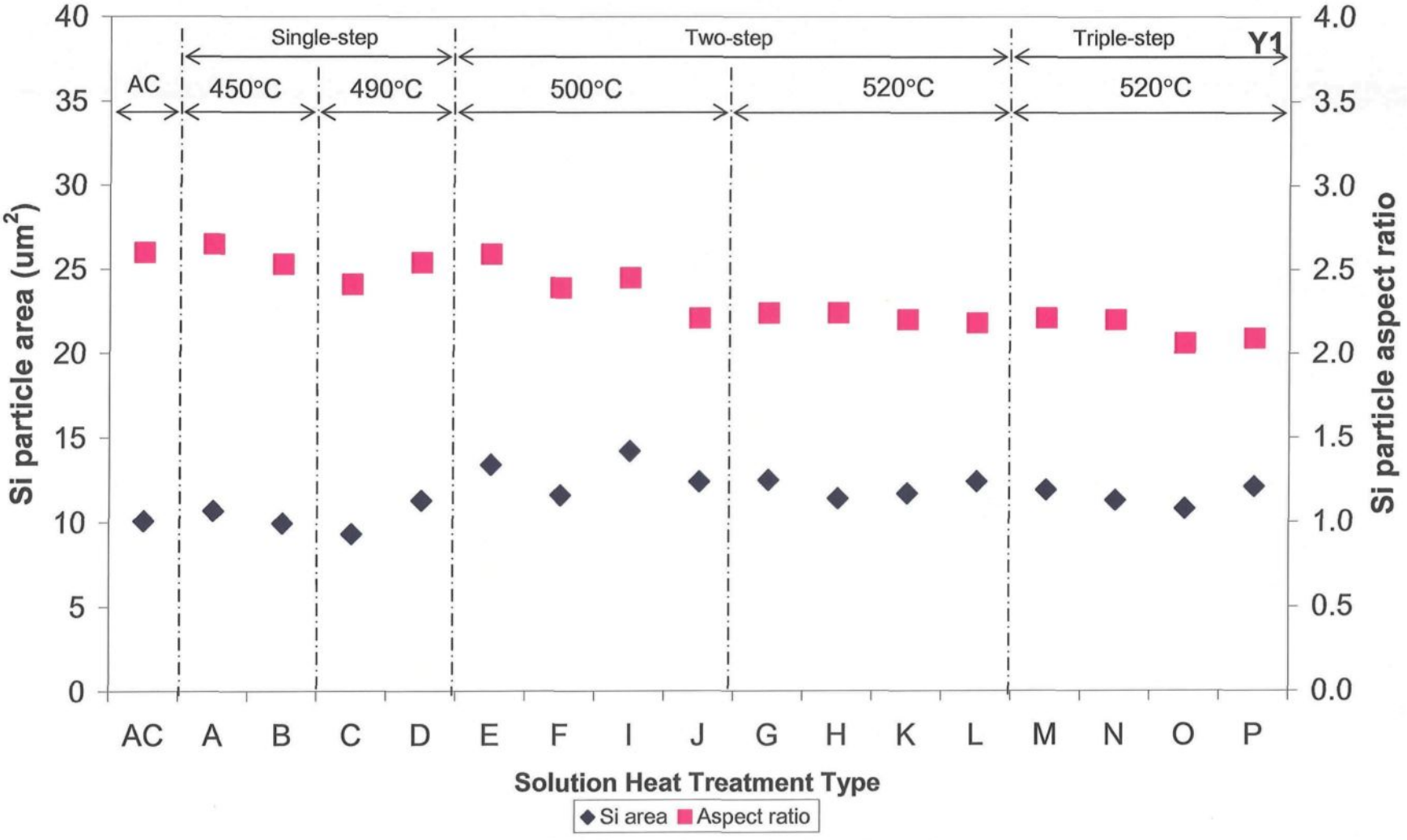

Figure 4.33 Si particle characteristics of alloy Y1 as a function of solution heat-treatment.

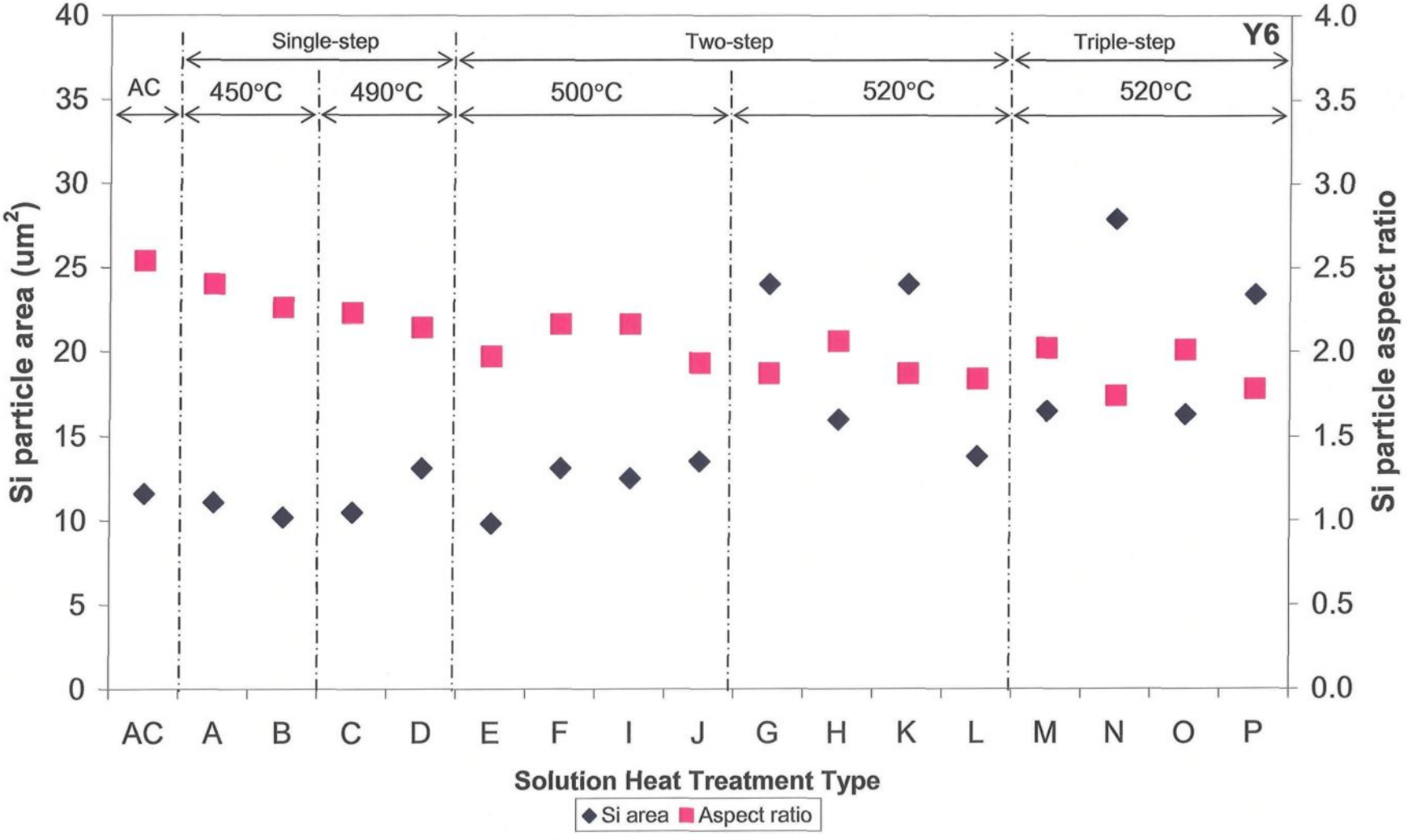

Figure 4.34 Si particle characteristics of alloy Y6 as a function of solution heat-treatment.

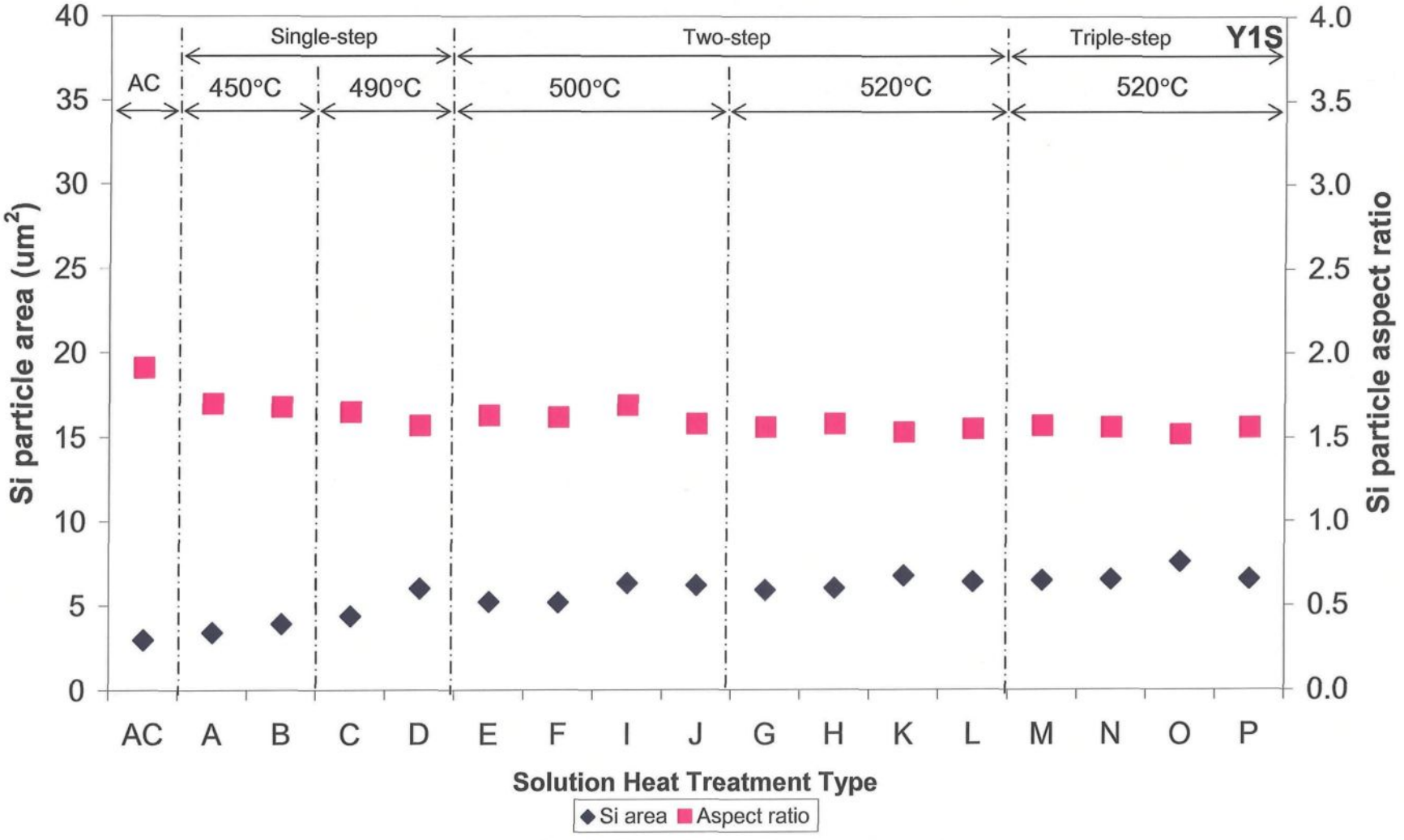

Figure 4.35 Si particle characteristics of alloy Y1S as a function of solution heat-treatment.

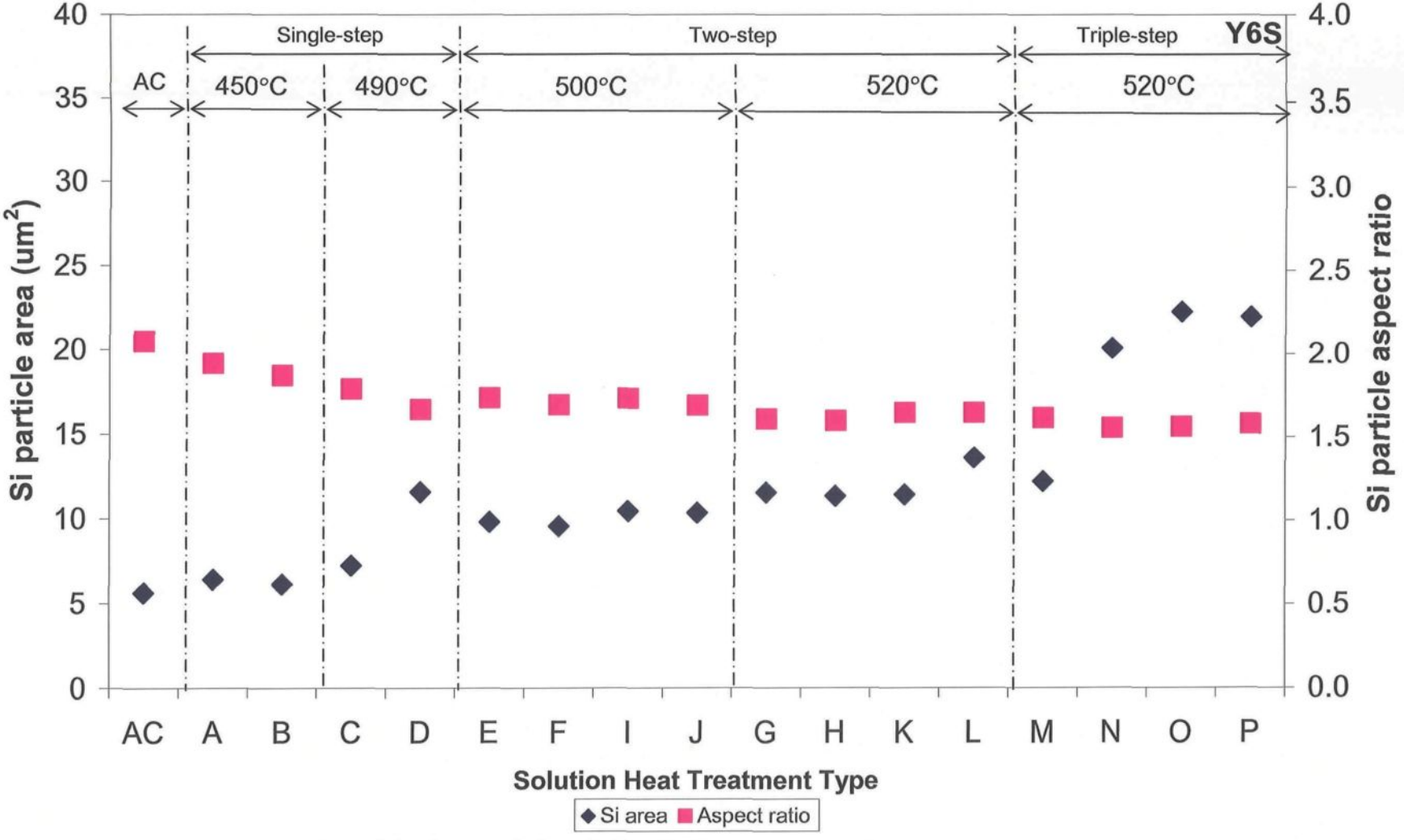

Figure 4.36 Si particle characteristics of alloy Y6S as a function of solution heat-treatment.

modification, that is, it changes the microstructure from a well-modified to a partially-modified one.

Comparisons of the Si particle aspect ratio and the Si particle area of these four alloys are provided in Figures 4.37 and 4.38, respectively. From Figure 4.38, it is possible to observe that the average Si particle size (area) in base alloy Y1 is 11.4 μm^2. It may thus be concluded that the Si particles spheroidize in the Mg-free base alloy Y1 when the treatment temperature is below 520°C. For the modified Mg-free alloy Y1S, the Si particles coarsen slightly and the average Si particle size shows a sluggish increase with an increase in solution heat-treatment time and temperatures. The Si particle size in alloy Y1S is always the lowest of all the four alloys after the same heat-treatment.

When 0.6 wt% Mg is present in alloy Y6, however, the Si particle size increases, and when the heat-treatment temperature reaches 520°C, the Si particles coarsen significantly. Here, it should be noted that two-step treatment at 450°C/4h + 520°C/4h (treatment G) and 490°C/4h + 520°C/4h (treatment K), triple-step treatment 450°C/8h + 500°C/4h + 520°C/4h (treatment N), 490°C/4h + 500°C/4h + 520°C/4h (treatment O) and 490°C/8h + 500°C/4h + 520°C/4h (treatment P) all show noticeably high values for Si particle size and are assumed to be responsible for the reduction of ductility in this alloy. These results agree well with those obtained by de la Sablonnière and Samuel [21] who found that the average particle size in 319 alloys with 0.5 wt% Mg is larger than it is in the low-Mg alloys.

In summing up the effect of Mg on the eutectic Si particles, it is possible to state that Mg modifies the eutectic Si morphology and increases the Si particle size. In alloy Y6S

(0.6 wt% Mg + 150 ppm Sr), the Si particles are also found to increase in size with solution time and temperature. High Si particle size values are obtained from triple-step treatments N, O and P. The large size of the Si particles may be the source of the low ductility observed in alloy Y6S following these three treatments.

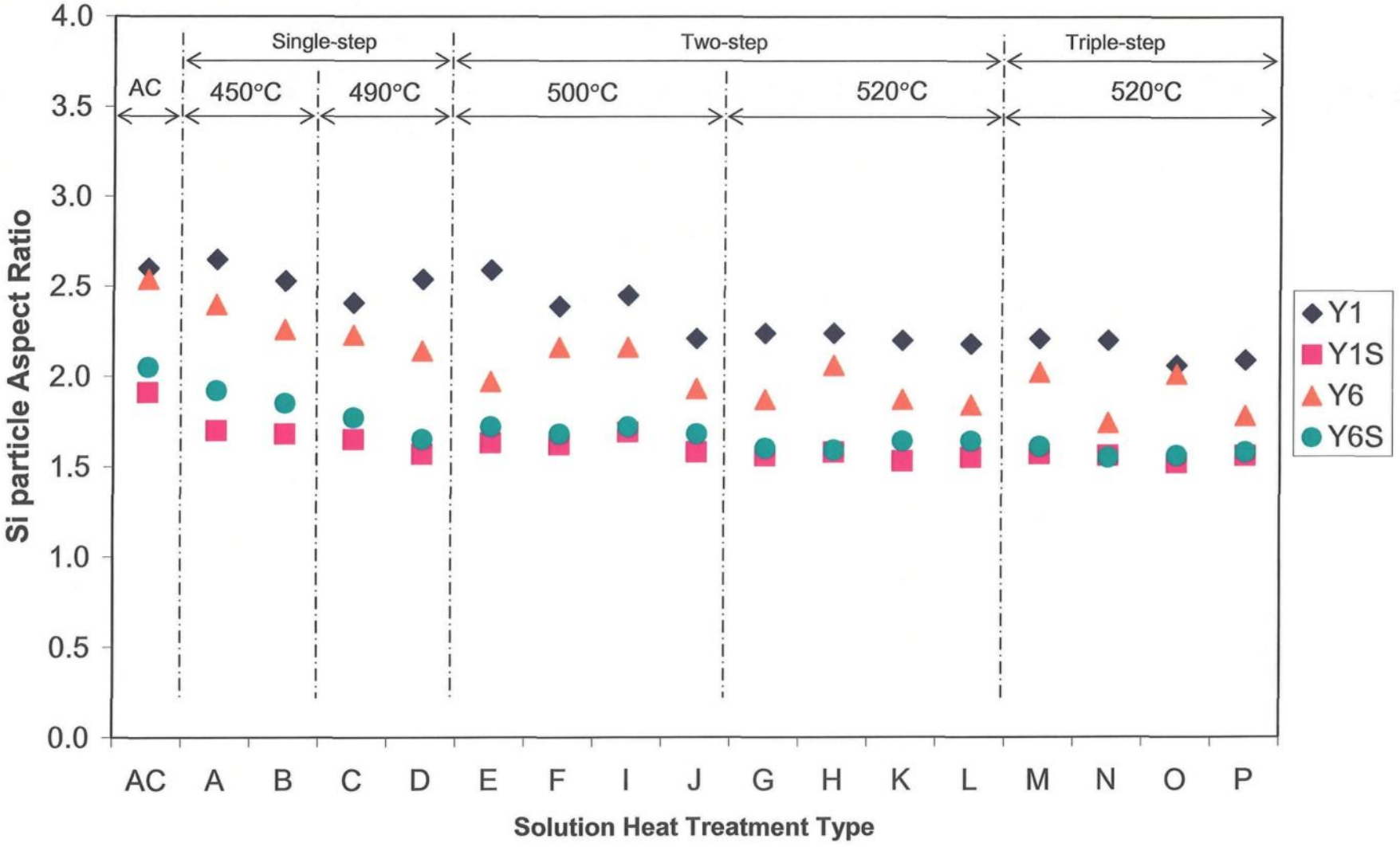

Figure 4.37 Average Si particle aspect ratio of alloys Y1, Y1S, Y6 and Y6S as a function of solution heat-treatment type.

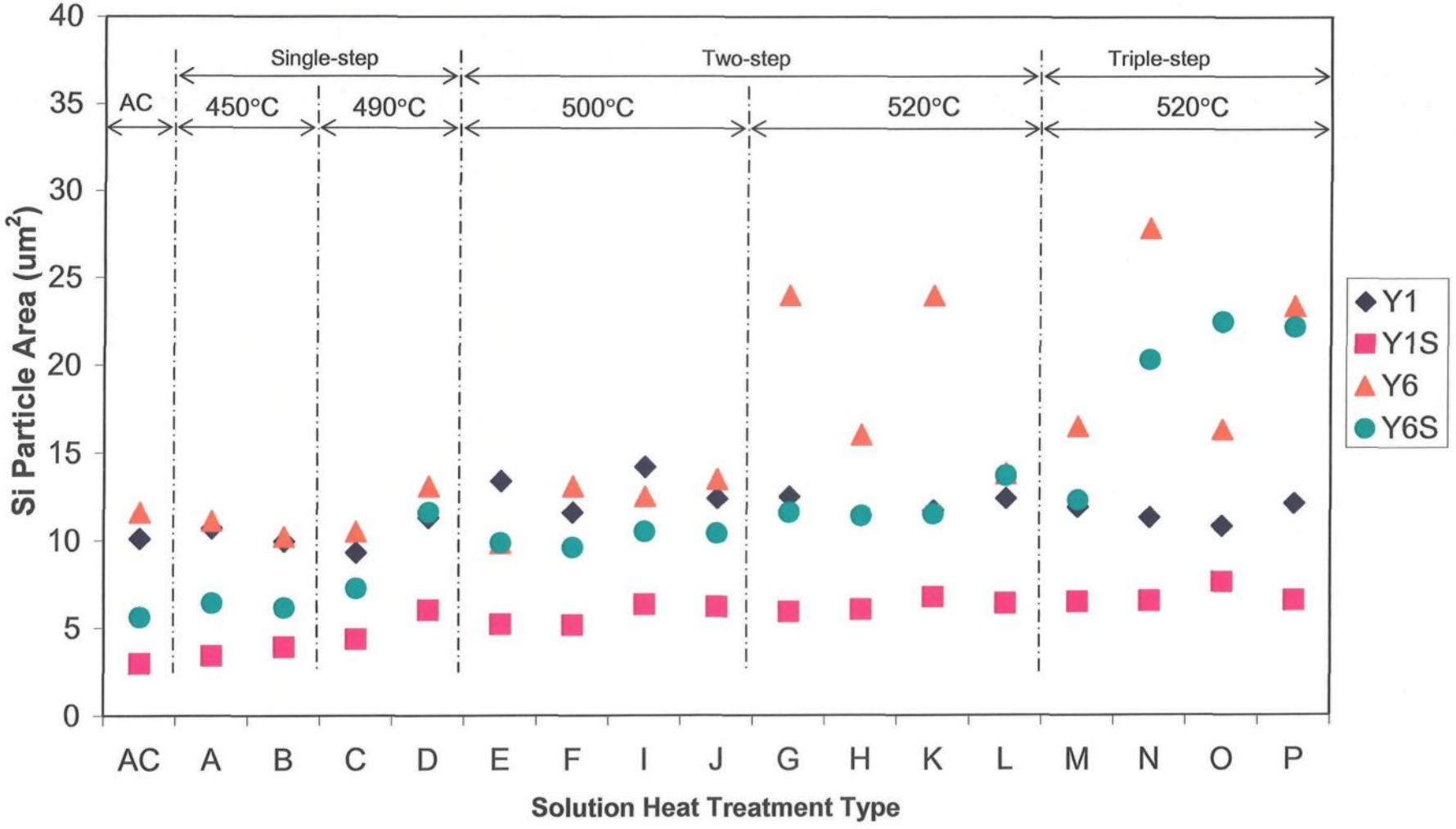

Figure 4.38 Average Si particle area of alloys Y1, Y1S, Y6 and Y6S as a function of solution heat-treatment type.

Figure 4.39 shows the Si particle morphology in the as-cast condition as obtained for alloys Y1, Y6, Y1S and Y6S. Silicon particles in alloy Y1 display an acicular shape, whereas when modified with Sr, the eutectic structure becomes finer and the Si particles become round, thereby contributing to higher ultimate tensile strength and ductility. In comparison with the structure of alloy Y1 in Figure 4.39(a), alloy Y6, with its high level of Mg (0.6 wt%), shows a partially-modified eutectic structure, as expected.

After a solution treatment of 490°C/8h, the Si particles become spheroidized in all the alloys under discussion, a fact which may be ascertained from Figure 4.40. After being heat-treated at 490°C/8h + 500°C/4h + 520°C/4h, however, the Si particles in alloys Y6 and Y6S coarsen and become faceted as shown in Figure 4.41. The same observations also apply in the case of other solution treatments involving the Y6 and Y6S alloys, as shown below, and they coordinate well with the case of the incipient melting of the $Al_5Mg_8Cu_2Si_6$ phase, as shown in Figure 4.41 and more clearly in Figure 4.42.

Y6 alloy:

450°C/4h + 520°C/4h; 490°C/4h + 520°C/4h;

450°C/8h + 500°C/4h + 520°C/4h;

Y6S alloy:

450°C/4h + 520°C/4h; 490°C/4h + 520°C/4h;

450°C/8h + 500°C/4h + 520°C/4h; 490°C/4h + 500°C/4h + 520°C/4h.

It is interesting to observe that these large-size Si particles are present in the vicinity of mixed $Al_5Mg_8Cu_2Si_6$ and Al_2Cu phases at the dendrite cell boundaries, and that they are frequently accompanied by the incipient melting of both phases; thus, it may reasonably be suggested that when the $Al_5Mg_8Cu_2Si_6$ phase melts, the Si in the phase is released and coalesces with the Si in the matrix, and hence large Si particles emerge.

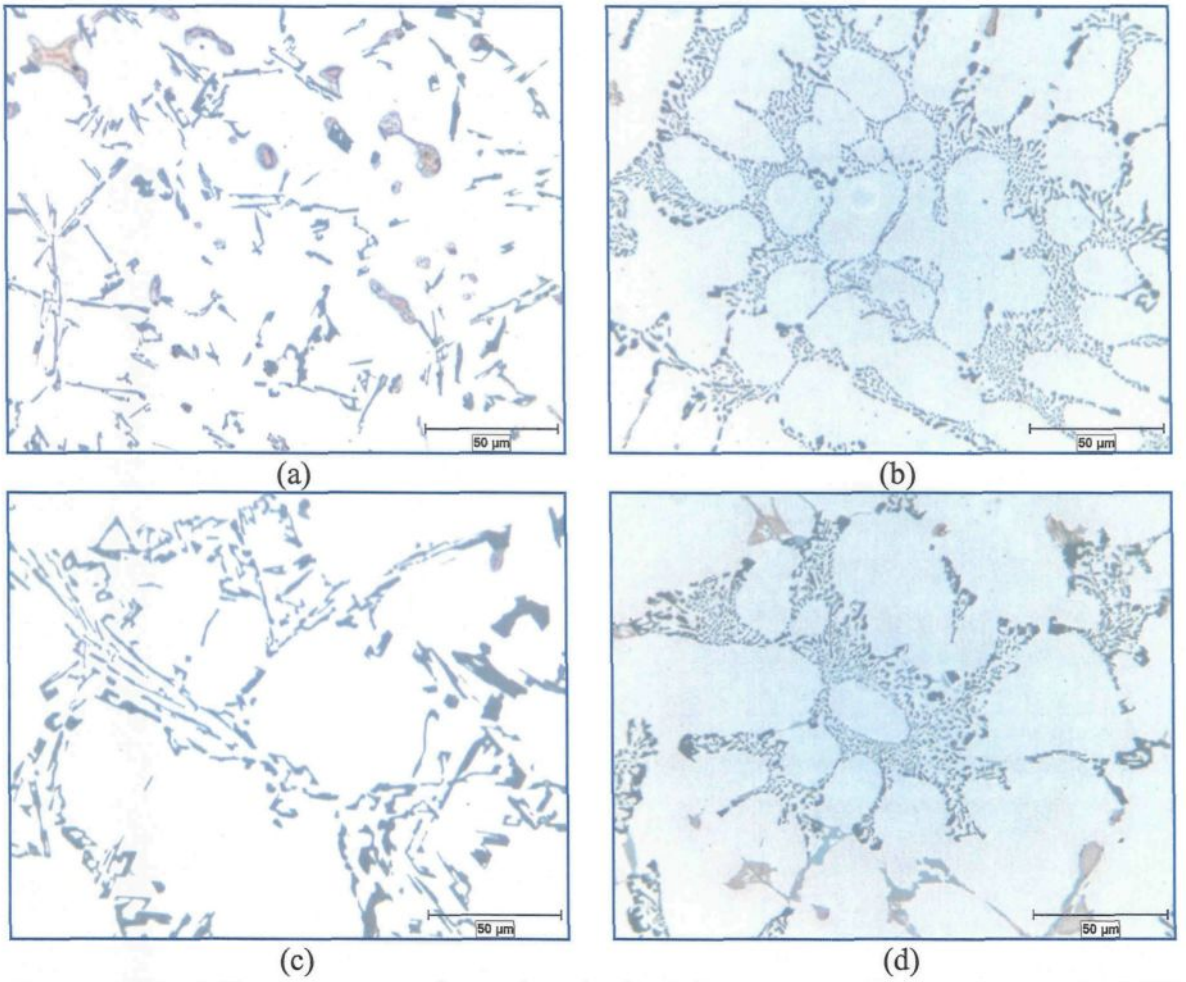

(a) (b)

(c) (d)

Figure 4.39 Microstructures of samples obtained from the tensile-tested bars of (a) Y1, (b) Y1S, (c) Y6, and (d) Y6S alloys under the as-cast condition, showing the morphology of the eutectic Si particles.

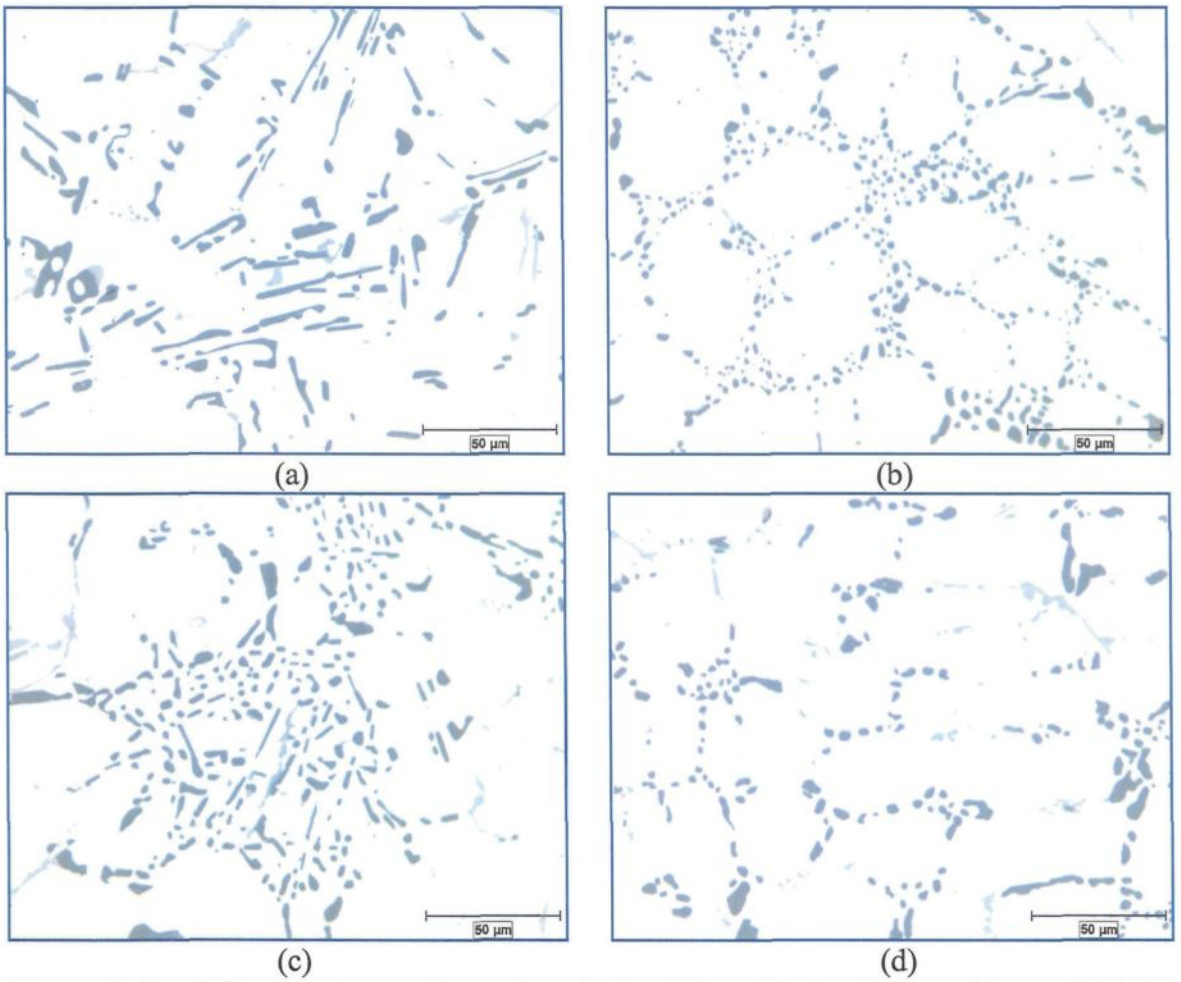

Figure 4.40 Microstructures of samples obtained from the tensile-tested bars of (a) Y1, (b) Y1S, (c) Y6, and (d) Y6S after treatment 490°C/8h, showing the morphology of Si particles.

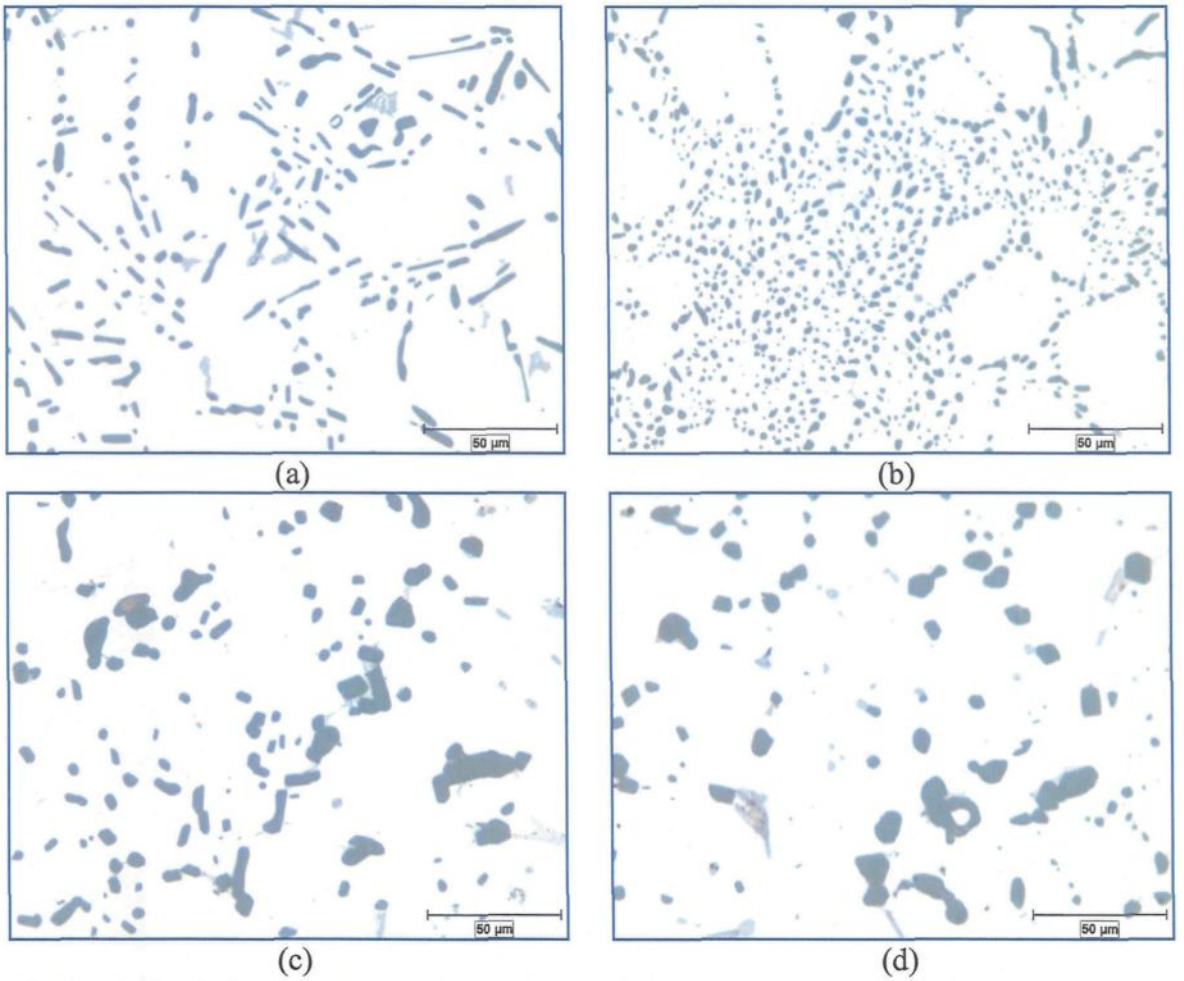

Figure 4.41 Microstructures of samples obtained from the tensile-tested bars of (a) Y1, (b) Y1S, (c) Y6 and (d) Y6S after treatment 490°C/8h+500°C/4h+520°C/4h, showing morphology of Si particles.

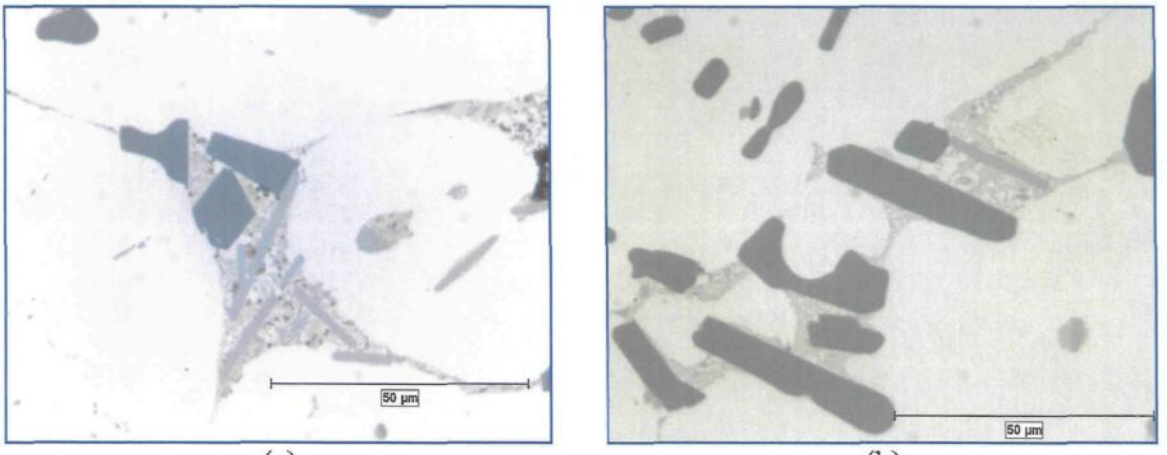

(a) (b)

Figure 4.42 Microstructures showing Si particle morphology of alloy Y6 obtained from: (a) solution treatment K (490°C/4h + 520°C/4h); and (b) solution treatment P (490°C/8h + 500°C/4h + 520°C/4h).

Figure 4.43 illustrates a Si particle within a pore showing an example of its morphology which is typical of that observed in Al-Si alloys after high-temperature solution heat-treatment. From Table 4.1, it will be observed that the Al-Si eutectic temperature for alloy Y6 is 555°C, and the final temperature of the solution treatment P (490°C/8h+500°C/4h+520°C/4h) is 520°C, which is 35°C lower than the Al-Si eutectic temperature. At such a high temperature and for Sr-modified alloys, rapid coarsening of Si particles is expected to be similar to that obtained from the solution treatment of 356 alloy at 540°C (the Al-Si eutectic temperature being 573°C in this case), leading to a large volume fraction of soft Al matrix which would enhance alloy ductility. With Mg as high as 0.6 wt% causing a serious problem of incipient melting, however, the beneficial effect of the soft Al matrix is countered by the relatively large porosity volume fraction created due

to the incipient melting. Thus, the balance between these two parameters would control or decide the overall mechanical properties of the alloy.

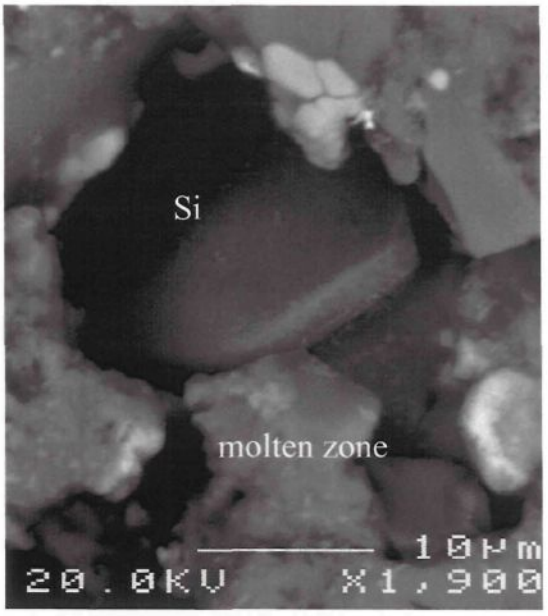

Figure 4.43 High magnification backscattered image showing the Si particle morphology in alloy Y6S after 490°C/8h+500°C/4h+520°C/4h solution heat-treatment.

4.2 TENSILE PROPERTIES

The tensile properties of 319 alloys are controlled mainly by their microstructures which depend to a large degree on the Si particle characteristics, the intermetallic phases formed, and the presence of casting defects such as porosity and inclusions. All of these factors may be modified by using certain melt and heat-treatment processes. Alloying elements such as Cu and Mg are often added to Al-Si base alloys to increase the alloy strength; these elements go into solid solution in the matrix and also form intermetallic compounds during solidification. Modifiers like Sr may be used to change the morphology of the Si particles from acicular, coarse, and flake-like to one that is fine and fibrous,

thereby enhancing ductility and strength. Solution heat-treatment is often used to obtain the maximum dissolution of the strengthening elements in the matrix, as well as spheroidize the Si particles. When the solution heat-treatment temperature exceeds the melting points of the Al_2Cu and $Al_5Mg_8Cu_2Si_6$ phases, however, incipient melting may occur at the grain boundaries, resulting in the formation of porosity upon quenching and a consequent deterioration of the tensile properties.

The average tensile properties, namely, yield strength (YS), ultimate tensile strength (UTS) and percentage elongation (%El) were investigated for all the alloys and heat-treatment conditions used in this study, and the quality index Q was calculated using the following formula, suggested by Drouzy *et al.*[77] who first proposed the concept of quality index to better represent the tensile properties of Al-Si-Mg alloys:

$$Q = UTS + 150 \log (\%El) \qquad (11)$$

4.2.1 As-Cast Condition

4.2.1.1 Effect of Mg

Figure 4.44 shows the tensile properties and quality index of (a) non-modified and (b) Sr-modified experimental and industrial alloys in the as-cast condition, as a function of Mg-content; Table 4.6 lists these values. In Mg-free experimental alloy Y1, the tensile properties are 145 MPa (YS), 232 MPa (UTS) and 2.44% (%El), respectively. When 0.3 wt% Mg is added, the values increase to 198 MPa (YS), 282 MPa (UTS) and 1.94% (%El), respectively, implying that 0.3 wt% Mg contributes to the YS and UTS by 37% and 22%,

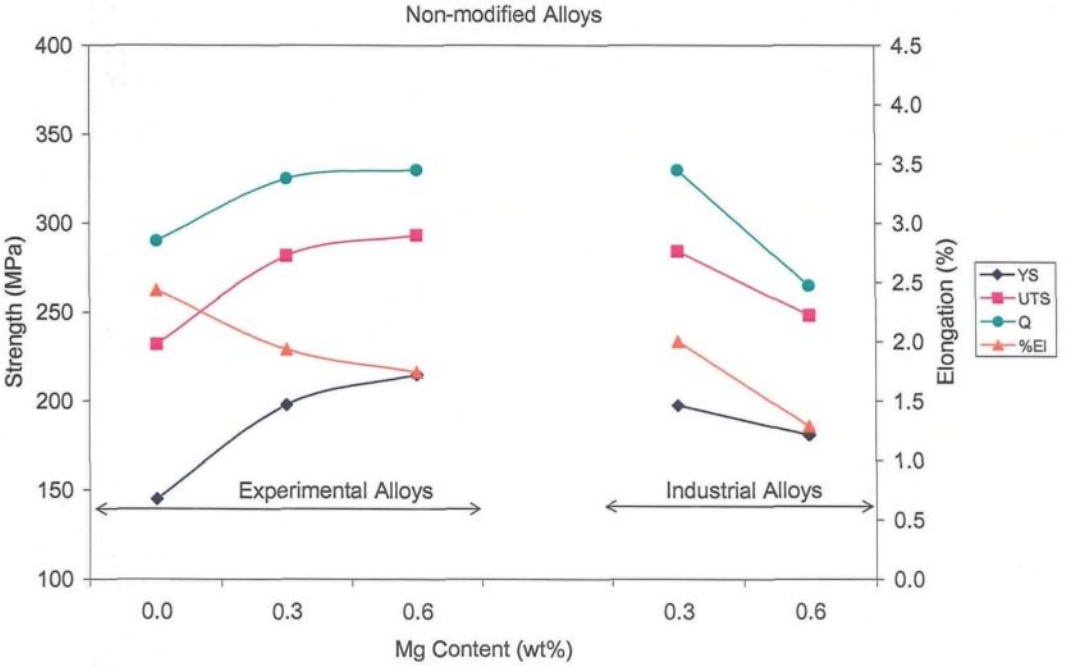

(a)

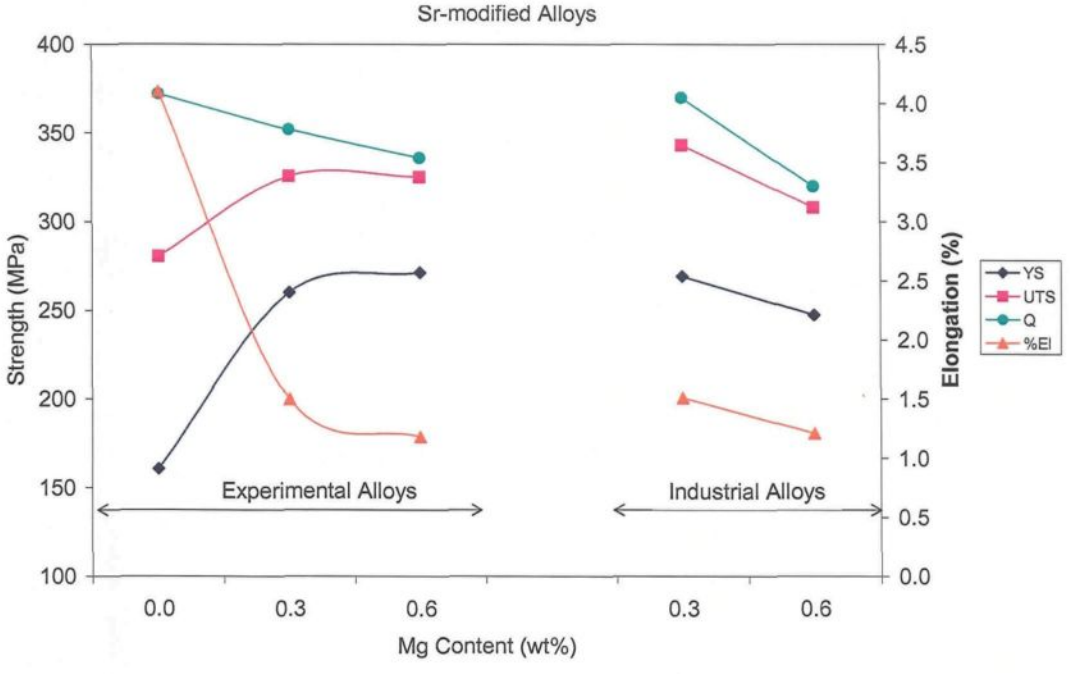

(b)

Figure 4.44 Tensile properties of (a) unmodified and (b) modified 319 alloys obtained in the as-cast condition as a function of Mg content.

Table 4.6 Tensile properties of each alloy investigated in the present study as obtained in the as-cast condition.

Alloy	YS (MPa)	UTS (MPa)	Elongation (%)	Q (MPa)
Y1	145	232	2.44	290
Y4	198	282	1.94	325
Y6	215	293	1.74	330
Y7	198	284	2.00	330
Y8	181	248	1.29	265
Y1S	161	280	4.10	372
Y4S	260	326	1.50	352
Y6S	271	325	1.18	336
Y7S	269	343	1.51	370
Y8S	248	308	1.21	320

but decreases the elongation by 21%. The value of Q increases from 290 MPa to 325 MPa. In the case of the Y6 alloy (with Mg up to 0.6 wt%), the YS, UTS, Q and %El exhibit values of 215 MPa, 293 MPa, 330 MPa and 2.0%, indicating that addition of 0.6 wt% Mg leads to an increase in YS, UTS and Q by about 48%, 26% and 14%, however, at the expense of a reduction in %El of about 29%. It was also found that Mg is more effective in increasing yield strength than in increasing ultimate tensile strength. Shivkumar *et al.*[83] reported that yield strength in A356.2 alloy was essentially determined by the Mg content and aging condition. Wang *et al.*[84] found that an increase in Mg content of up to 0.7 wt% in 356 alloys results in higher yield strength.

From Figure 4.44, it is possible to observe that even though the elongation is decreased in Mg-containing alloys, the quality index increases, which implies that Mg is

capable of increasing the alloy strength much more than the corresponding loss of elongation in the experimental alloys, so that an overall improvement in alloy quality is still obtained. These findings are in line with the results obtained by Sigworth.[85]

In the industrial alloys, however, the four tensile property parameters are found to decrease with the increase in Mg content from 0.3 to 0.6 wt%. It may also be observed that the tensile properties of industrial alloy Y7 with 0.3 wt% Mg are the same as those of experimental alloy Y4. With the addition of Mg up to 0.6 wt%, however, the tensile properties of industrial alloy Y8 are found to be much lower than those of alloy Y6.

The same observations may be made for the Sr-modified alloys. In the Sr-modified experimental alloys, however, the loss in ductility surpasses the benefits of the increase in strength with Mg addition, so that the Q value decreases with increasing Mg content in these alloys.

4.2.1.2 Effect of Sr

Figure 4.45 shows the tensile properties of the experimental alloys obtained in the as-cast condition, before and after Sr modification. It will be observed that the modified alloys exhibit higher YS and UTS values than the non-modified alloys, regardless of whether they are Mg-free or contain Mg. After modification, the YS and UTS of the Mg-free base alloy Y1 increase by 11% and 21%, respectively, while the elongation increases by as much as 68%. These facts indicate that in the Mg-free alloys, Sr contributes mainly to improving the elongation.

(a)

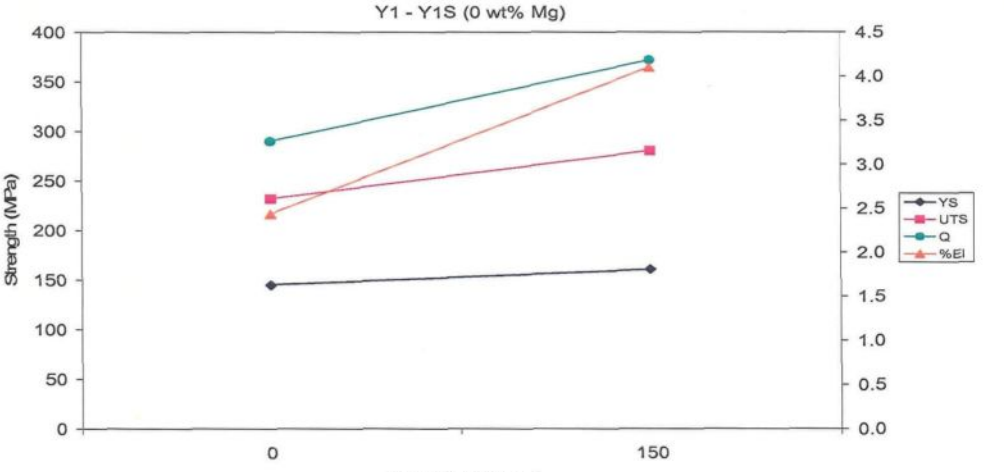

(b)

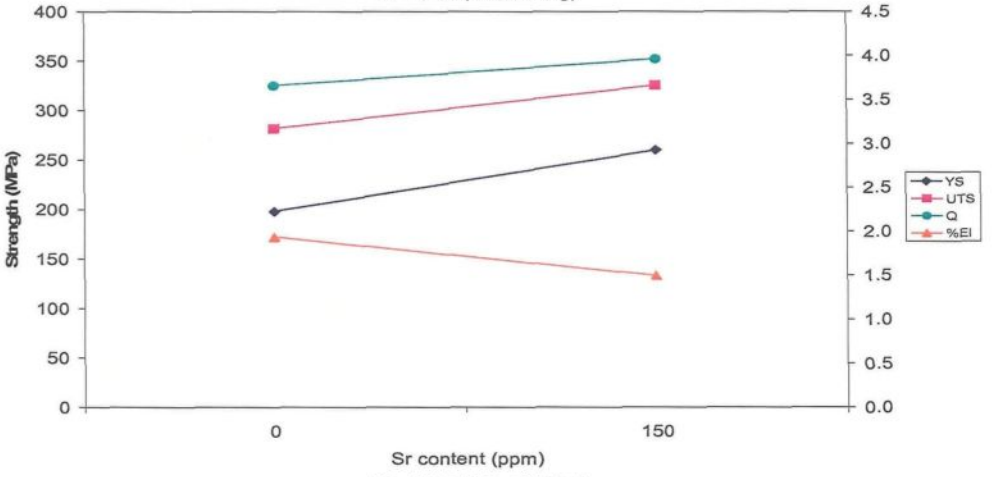

(c)

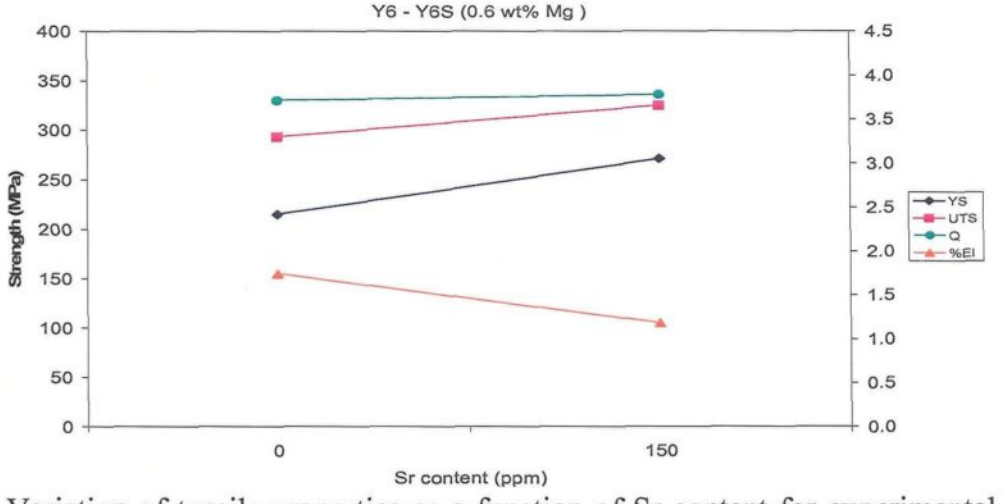

Figure 4.45 Variation of tensile properties as a function of Sr content for experimental alloys.

(a)

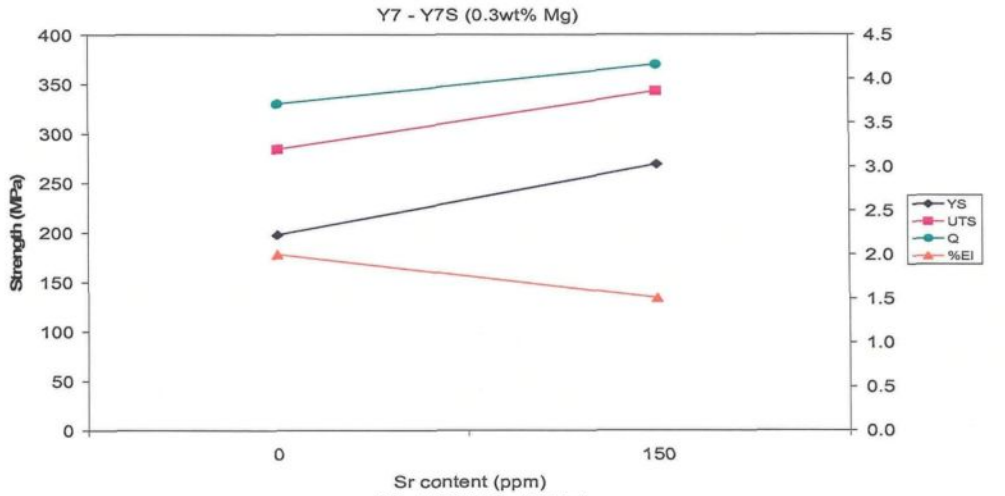

(b)

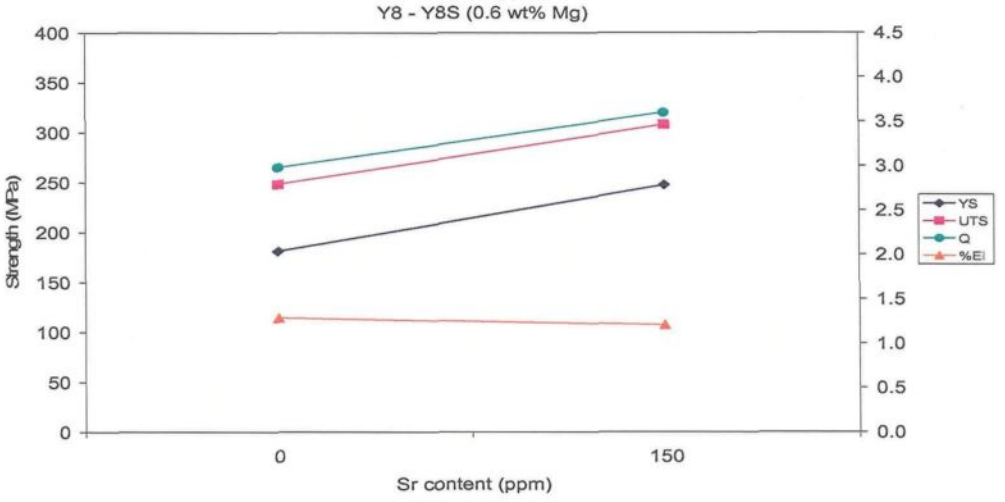

Figure 4.46 Variation of tensile properties as a function of Sr content for industrial alloys.

When Mg is present in the experimental alloys, however, the elongation of the modified alloys is found to be lower than that of unmodified alloys, and the higher the Mg content, the greater the decrease in elongation obtained, implying that the effect of Mg in decreasing the elongation is much stronger that the effect of Sr in improving it. From the overall results gathered for the industrial alloys (see Figure 4.46), it was found that a higher Mg content, surprisingly, leads to a weaker decrease in elongation, which is contrary to

expectations. This observation may be attributed to the presence of such trace elements as Ni, Fe, Mn and Zn in the industrial alloys.

4.2.1.3 Combined effects of Sr and Mg

Figure 4.47 compares tensile properties of base alloy Y1 and alloys Y4S and Y6S with both Mg and Sr additions: Y4S (0.3 wt% Mg + 150 ppm Sr) and Y6S (0.6 wt% Mg + 150 ppm Sr). It may be observed that when 0.3 wt% Mg and 150 ppm Sr are added to the base alloy simultaneously, YS and UTS increase from 145 MPa and 232 MPa to 260 MPa and 326 MPa, respectively, while the elongation decreases from 2.44% to 1.50%.

The value of Q is also found to increase from 290 MPa to 352 MPa. A further increase in Mg content leads to a slight increase in the YS value but to a further decrease in

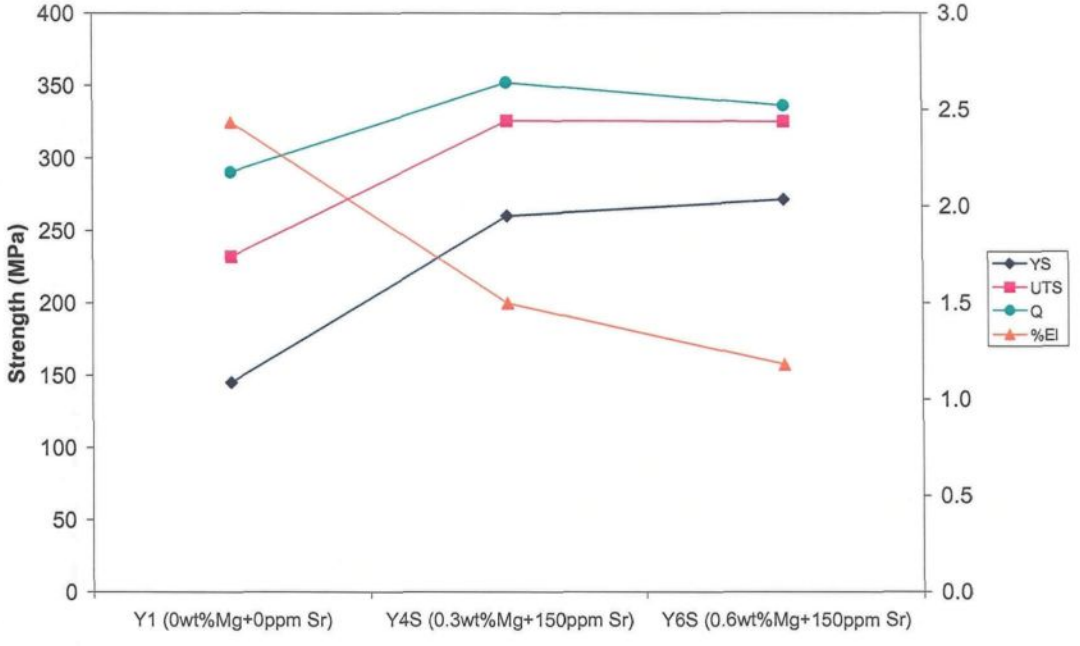

Figure 4.47 Combined effects of Sr and Mg on tensile properties of experimental alloys.

elongation, thus the quality index decreases. Therefore, it is reasonable to conclude that the optimum combination of Mg and Sr for this study is 0.3 wt% Mg with 150 ppm Sr. Further increases in Mg content lead to a degradation of tensile properties.

4.2.2 Effect of Solution Heat-Treatment

4.2.2.1 Experimental alloys

The average tensile properties of the experimental 319 alloys, as obtained after various heat treatments, are shown in Figures 4.48 through 4.53. The corresponding Q values for these alloys are shown in Figures 4.54 through 4.59.

Figure 4.48 summarizes the average tensile properties of alloy Y1 obtained from the as-cast and heat-treated conditions, using the single-step, two-step and triple-step solution heat-treatments. It may be observed that all three tensile property parameters and the Q value increase with solution time and temperature in the single-step treatments, the alloy properties believed to benefit from the dissolution of Al_2Cu and the change in the Si particle morphology with the solution treatment. Two-step and triple-step heat-treatments result in further slight increases in strength and a significant increase in elongation and Q values. From Figures 4.51 and 4.57, it will be observed that at the same temperature, longer solution time shows higher elongation and Q values in modified alloy Y1S, attributable to the dissolution of hard-to-dissolve block-like Al_2Cu particles. Upon comparing the tensile properties of non-modified and Sr-modified alloys, it will be observed that after the same heat treatment, the tensile properties of Y1S, especially percentage elongation, are always higher than those of Y1. The optimum solution heat-treatment for Y1 is treatment N

(450°C/8h+500°C/4h+520°C/4h). In modified alloy Y1S, although triple-step treatments O and P lead to spheroidized and finer Si particles, incipient melting of the block-like Al_2Cu also occurs, resulting in a large amount of porosity, so that the advantages of having a fine, modified eutectic Si structure are nullified and the optimum solution heat-treatment is then treatment N (450°C/8h+500°C/4h+520°C/4h) for which the corresponding tensile properties are 274 MPa (YS), 434 MPa (UTS), 8.5% (%El) and 574 MPa (Q), respectively.

The tensile properties of alloy Y4 and Y6, as well as of their modified versions, alloys Y4S and Y6S, are illustrated in Figures 4.49 and 4.50, and Figures 4.52 and 4.53, respectively. In alloys Y4 (0.3wt% Mg) and Y4S, both strength and elongation increase with solution time and temperature after single-step and two-step treatments ending at 500°C. All treatments with a final temperature of 520°C lead only to an insignificant increase in YS and UTS, implying that before the temperature reaches 520°C, most of the Al_2Cu and other strengthening phases, such as Mg_2Si, have dissolved in the matrix in both alloys.

It should be noted that when samples of Y4 alloy are subjected to treatment K (490°C/4h+520°C/4h), the elongation drops to a low value, assumed to be caused by the presence of a high degree of porosity. The highest Q value of alloy Y4 is obtained from treatment M (450°C/4h+500°C/4h+520°C/4h). Longer treatment times and higher temperatures lead to severe incipient melting of Al_2Cu, which will override the advantages of finer, rounder Si particles and lead to reduced tensile properties. It is interesting to observe that alloy Y4S shows higher tensile properties after all heat treatments up to F (including treatments A, B, C, D, E and F), whereas beyond treatment F (including

treatments I, J, G, H, K, L, M, N, O and P), it is alloy Y4 which shows higher tensile properties.

When Mg is up to 0.6 wt% in experimental alloy Y6, two-step treatments G and K exhibit noticeably poor tensile properties, as is clearly shown in Figure 4.50, and this may be attributed to the presence of a high degree of porosity caused by the incipient melting of block-like Al_2Cu and the complex $Al_5Mg_8Cu_2Si_6$ phase, as well as the coarsening of silicon particles as mentioned previously. It was also found that triple-step treatments M, N, O and P show low tensile properties, believed to be due to the coarsening of the Si particles and incipient melting of the complex $Al_5Mg_8Cu_2Si_6$ phase. When 150 ppm Sr and 0.6 wt% Mg combine, it will be observed that Y6S exhibits more stable tensile properties than Y6 after single-step and two-step treatments. When heat-treated using triple-step treatments N, O, and P, however, the tensile properties are observed to drop to noticeably low values, particularly in the case of elongation. This fact may be attributed to the incipient melting of the Al_2Cu and $Al_5Mg_8Cu_2Si_6$ phases and the coarsening of Si particles.

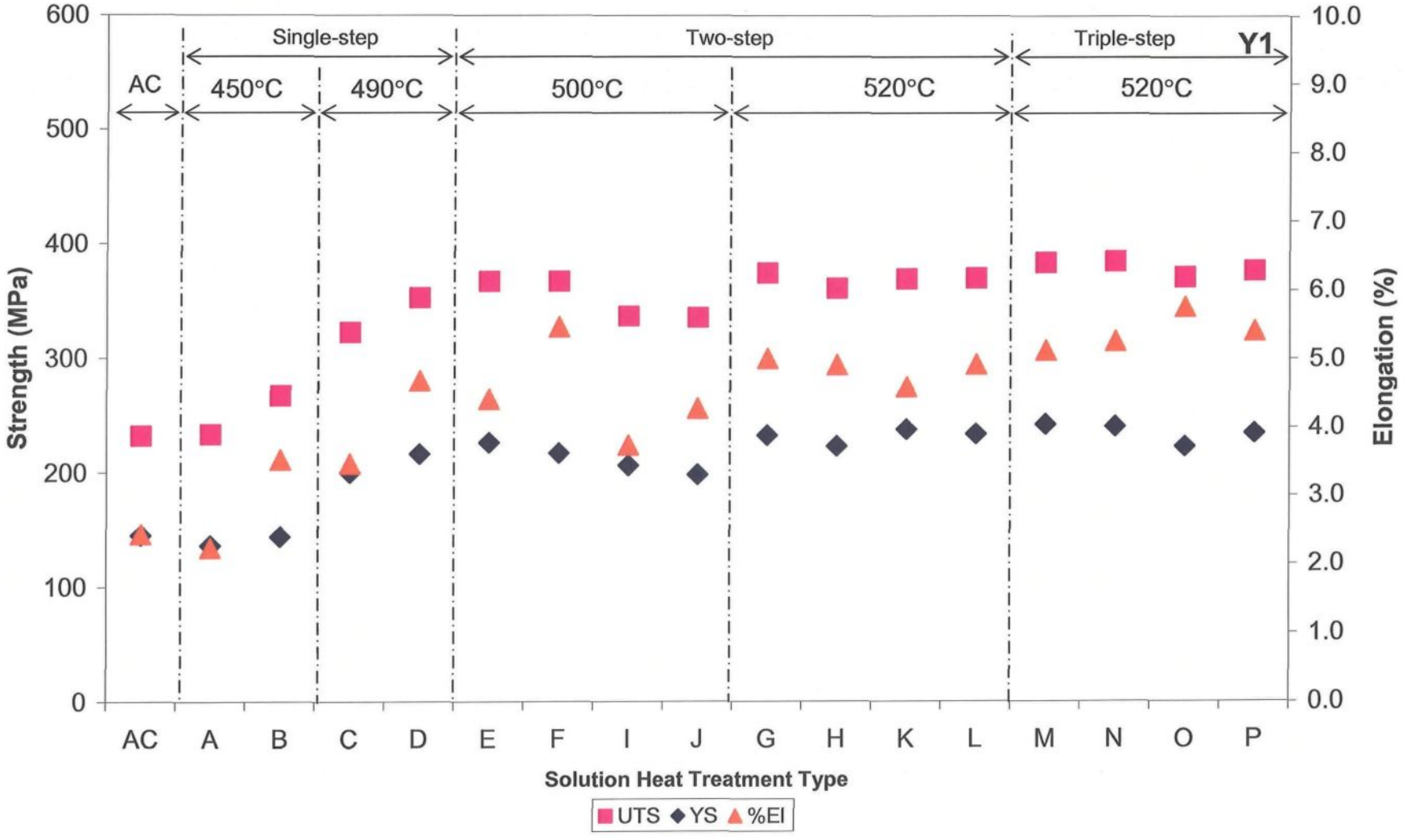

Figure 4.48 Tensile properties of alloy Y1 as a function of solution heat-treatment type.

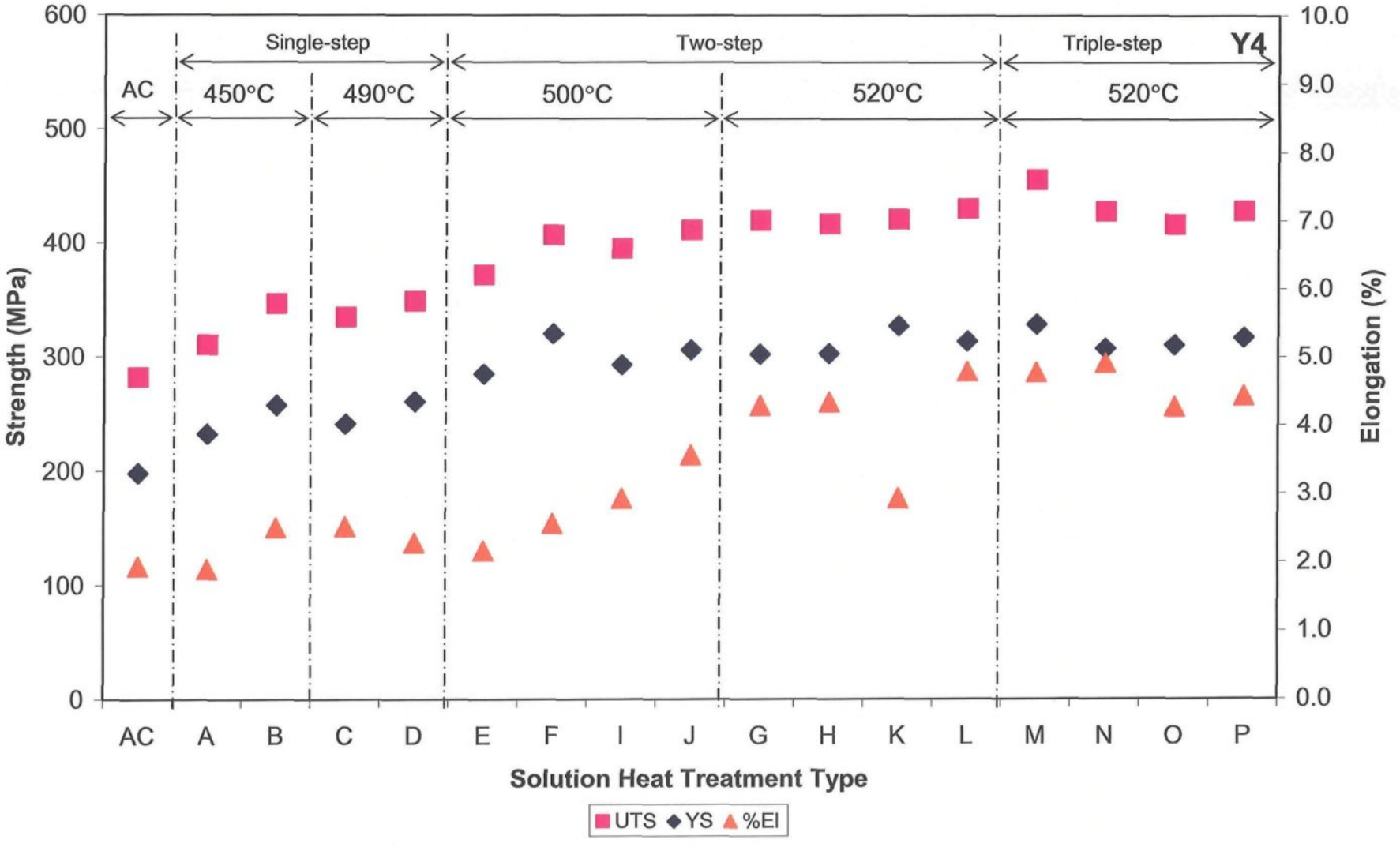

Figure 4.49 Tensile properties of alloy Y4 as a function of solution heat-treatment type.

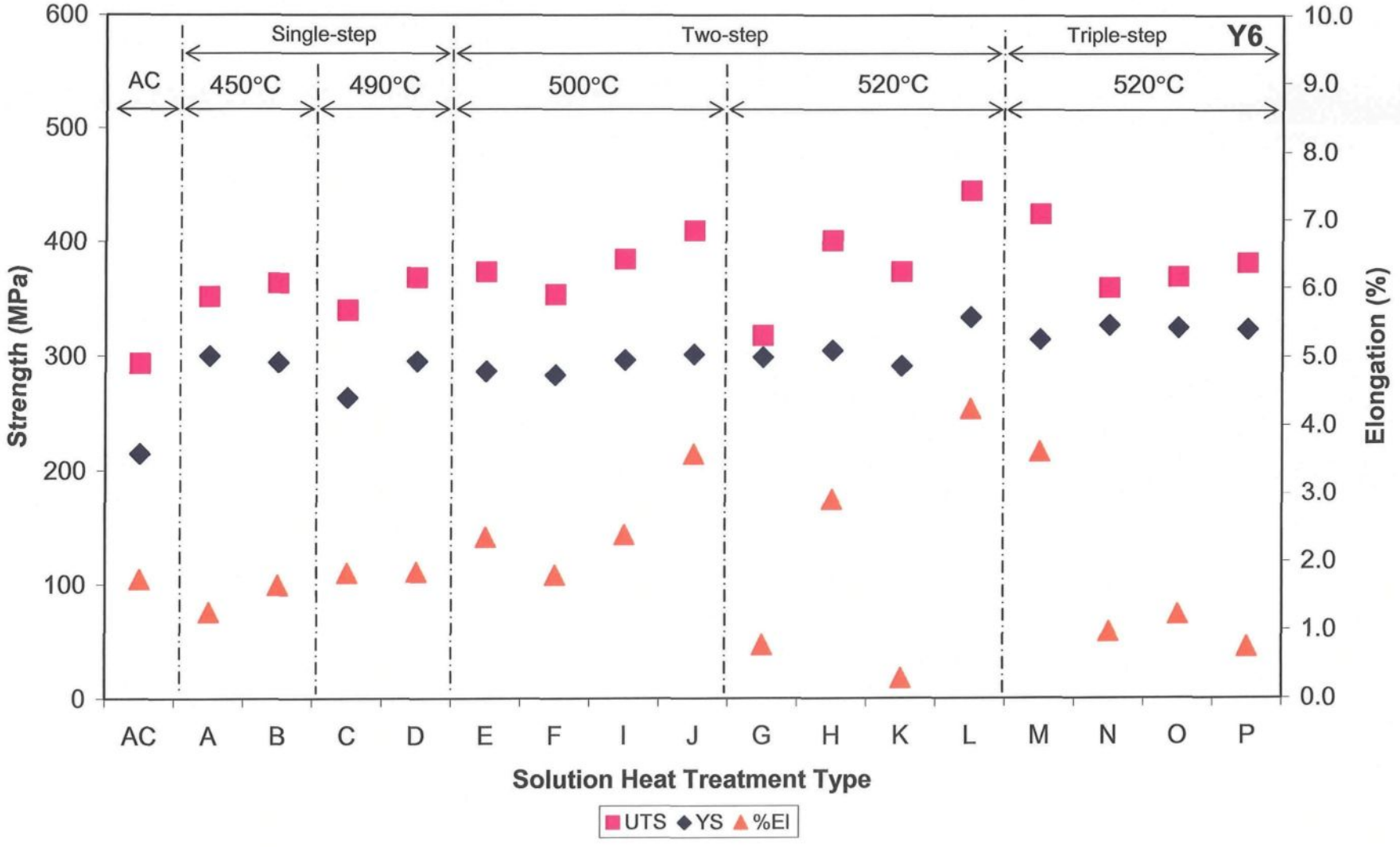

Figure 4.50 Tensile properties of alloy Y6 as a function of solution heat-treatment type.

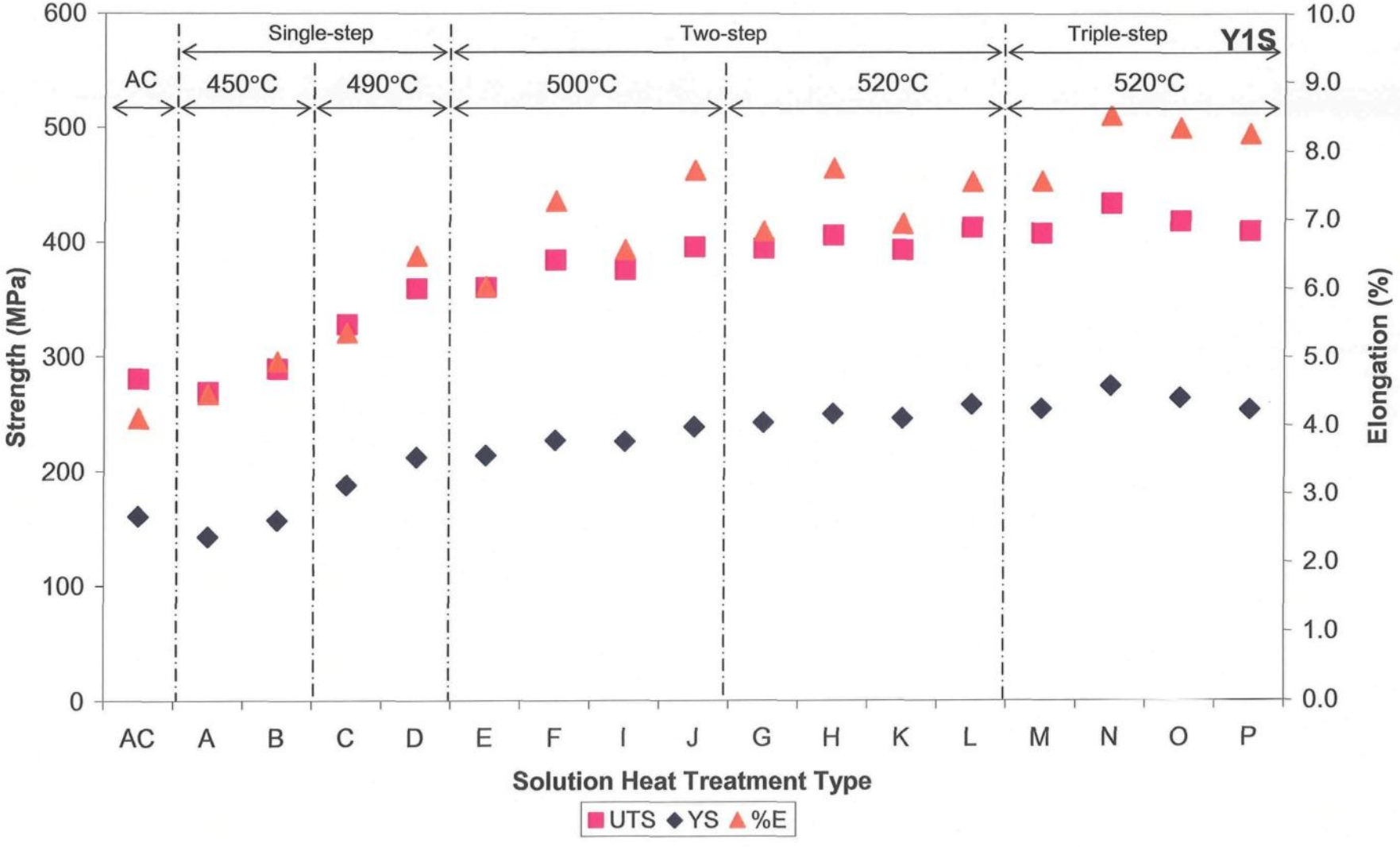

Figure 4.51 Tensile properties of alloy Y1S as a function of solution heat-treatment type.

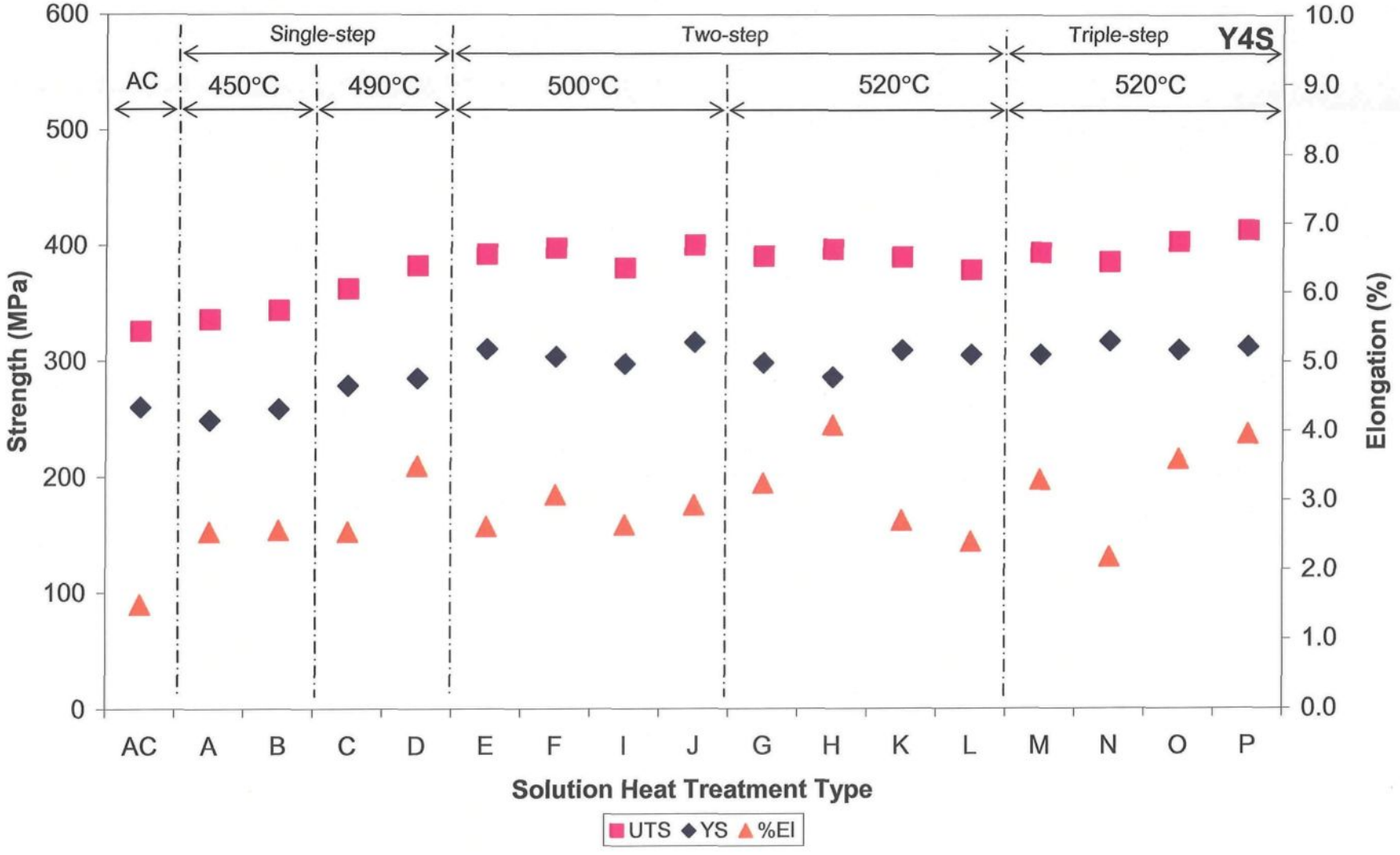

Figure 4.52 Tensile properties of alloy Y4S as a function of solution heat-treatment type.

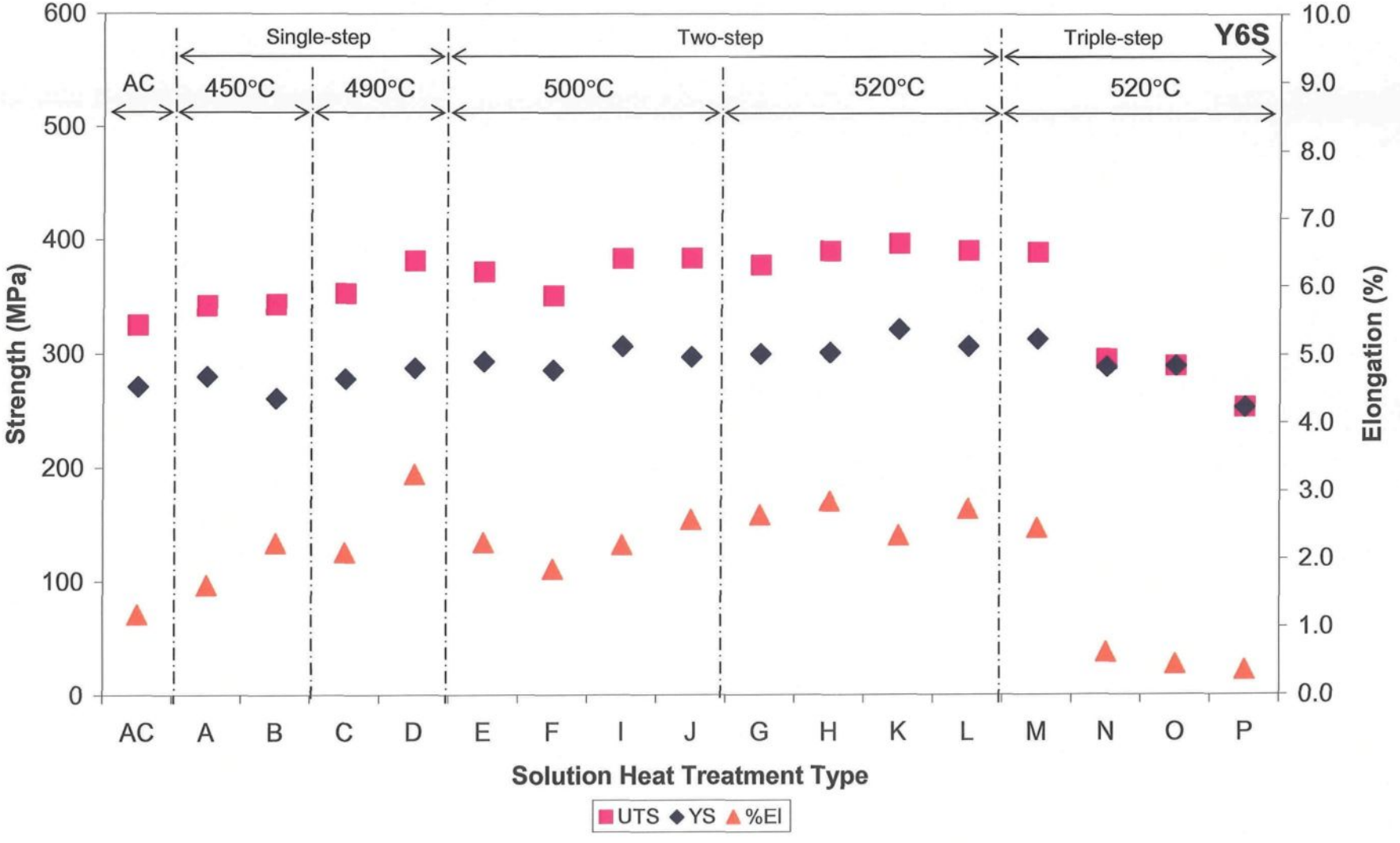

Figure 4.53 Tensile properties of alloy Y6S as a function of solution heat-treatment type.

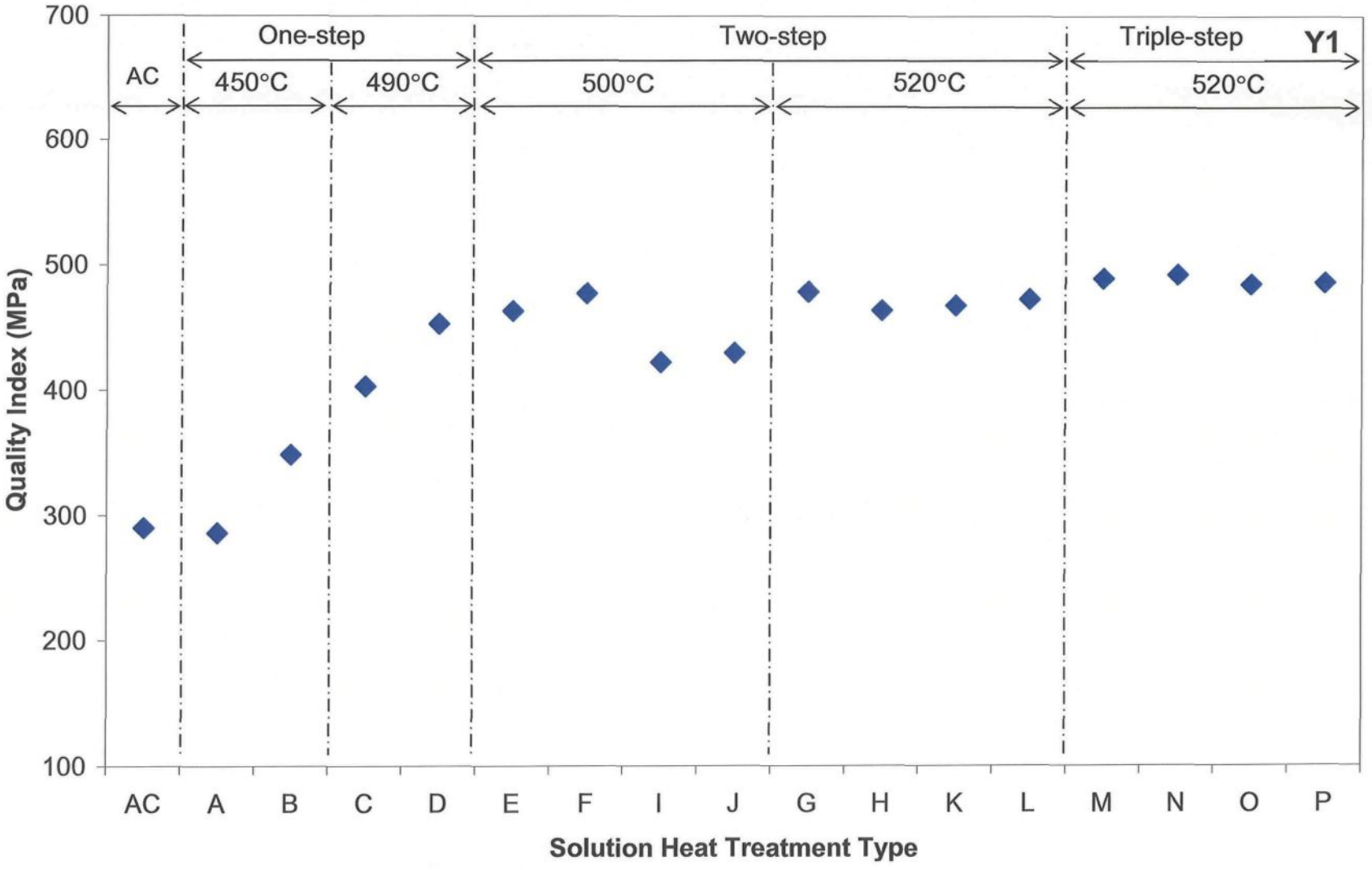

Figure 4.54 Quality index of alloy Y1 as a function of solution heat-treatment type.

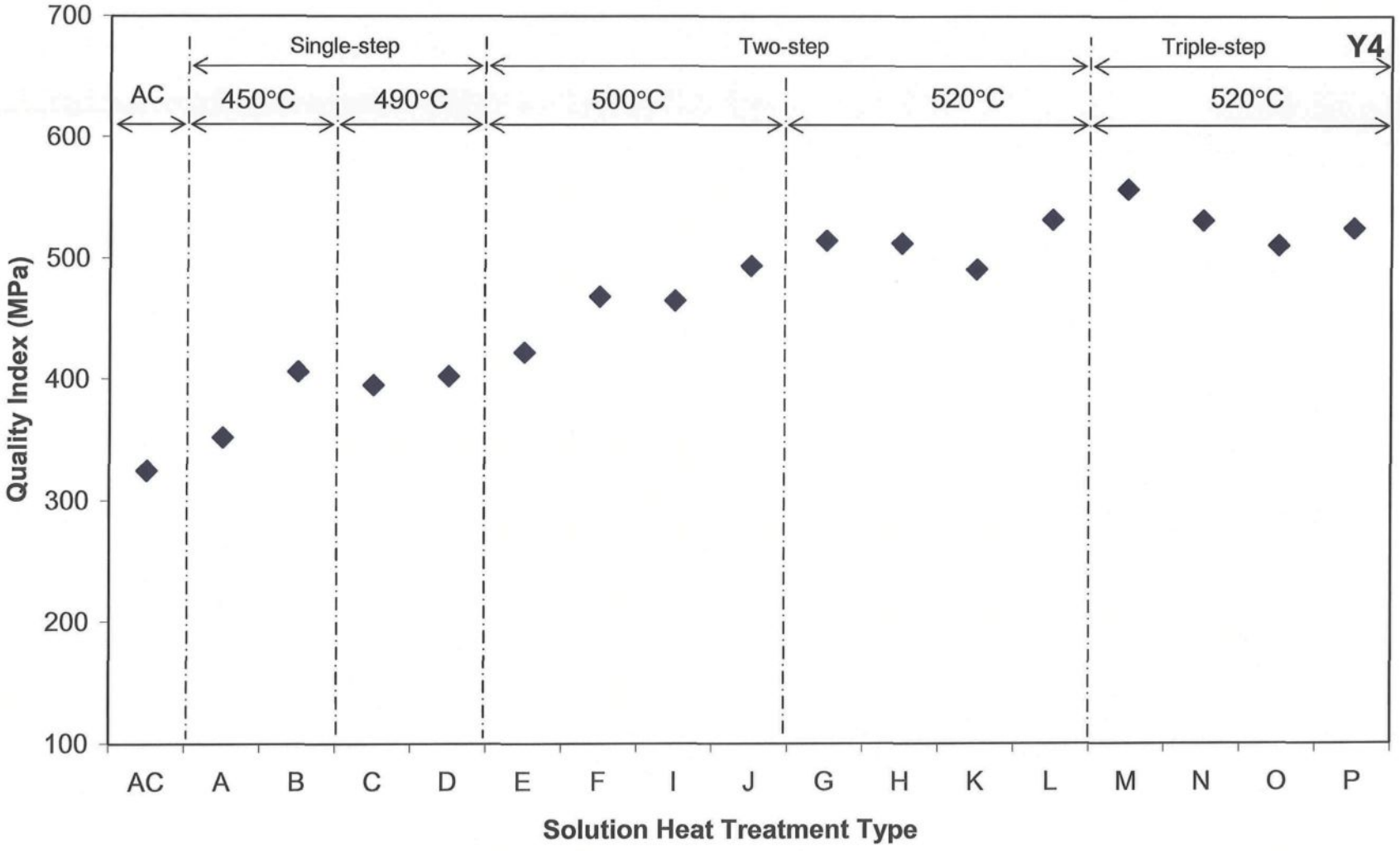

Figure 4.55 Quality index of alloy Y4 as a function of solution heat-treatment type.

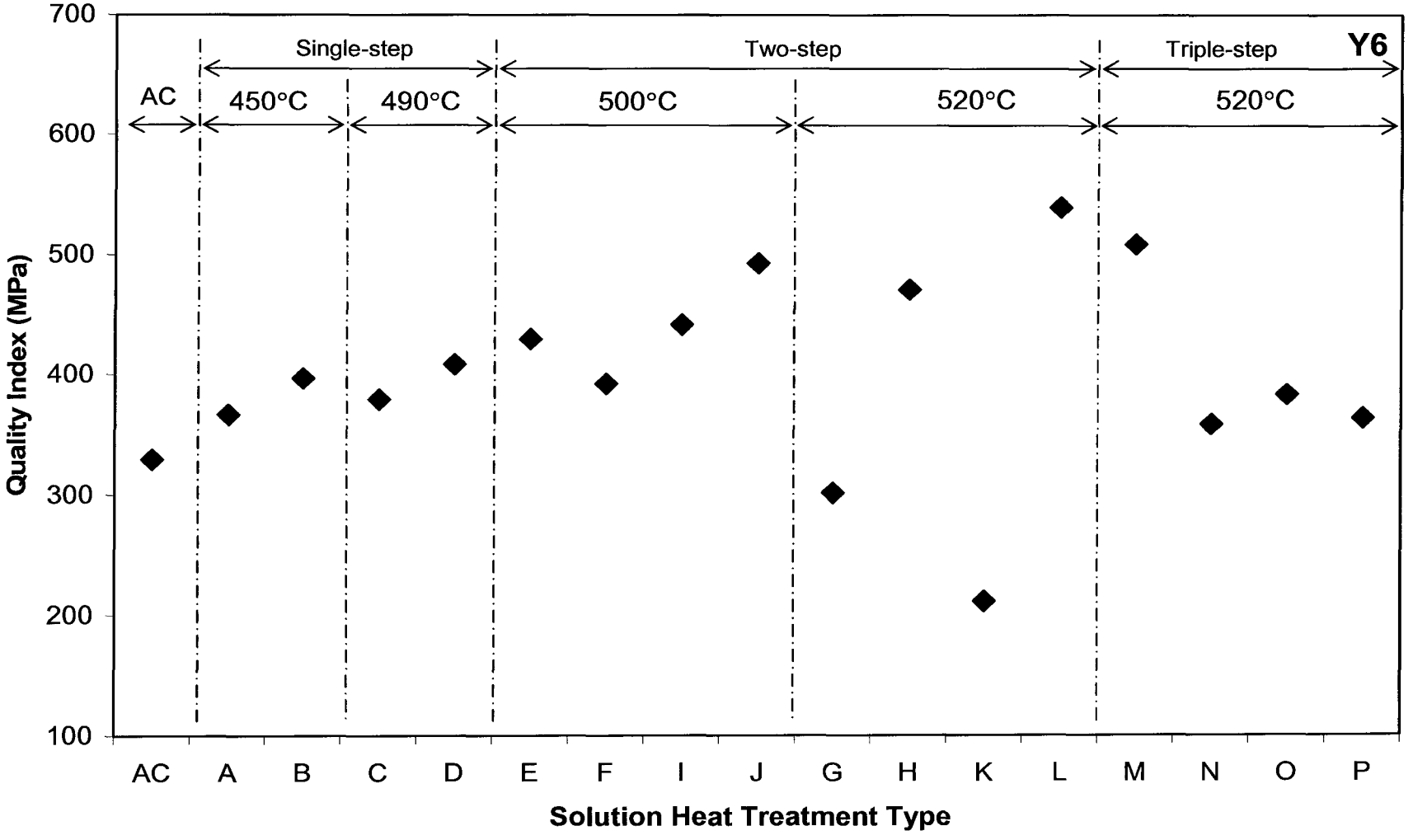

Figure 4.56 Quality index of alloy Y6 as a function of solution heat-treatment type.

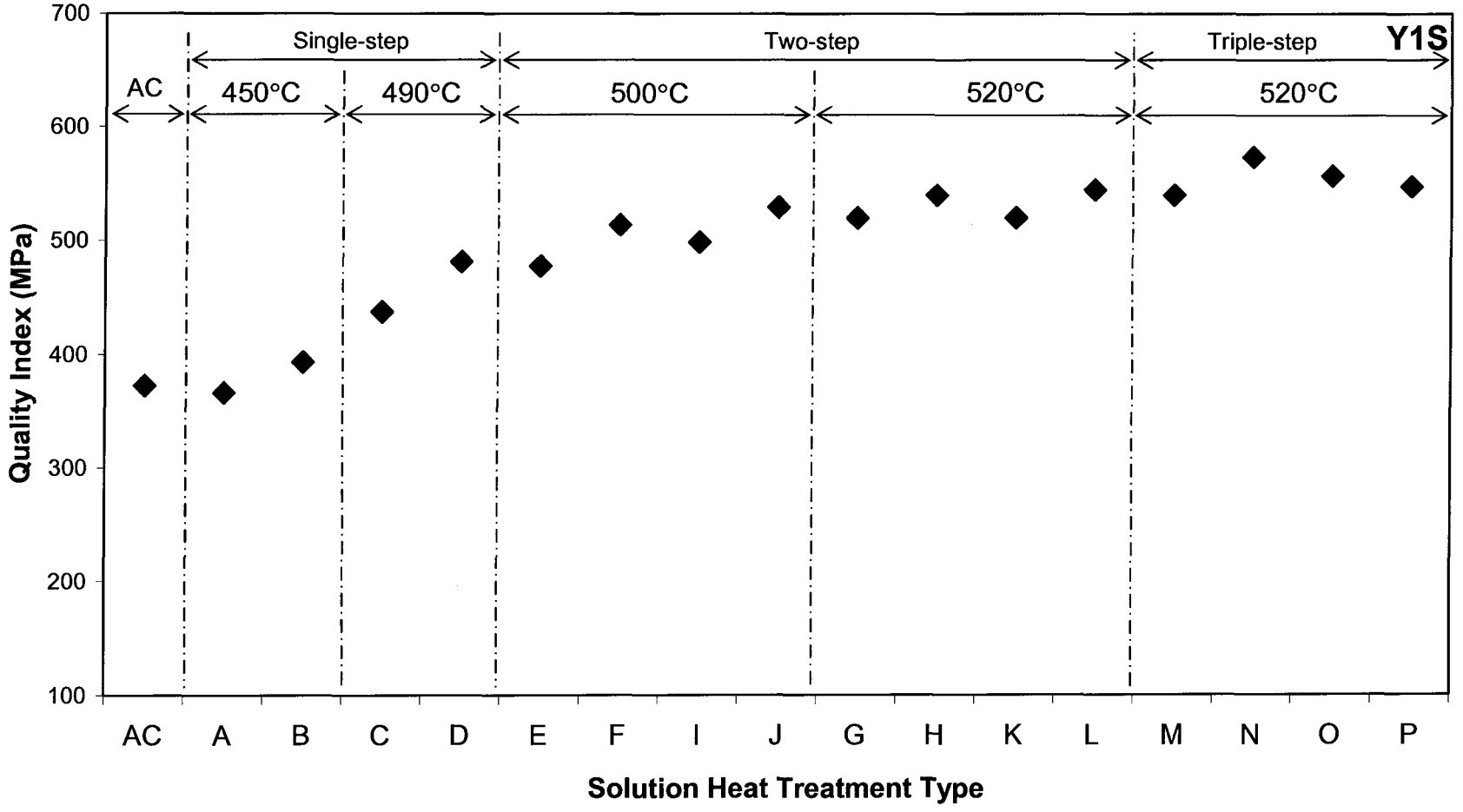

Figure 4.57 Quality index of alloy Y1S as a function of solution heat-treatment type.

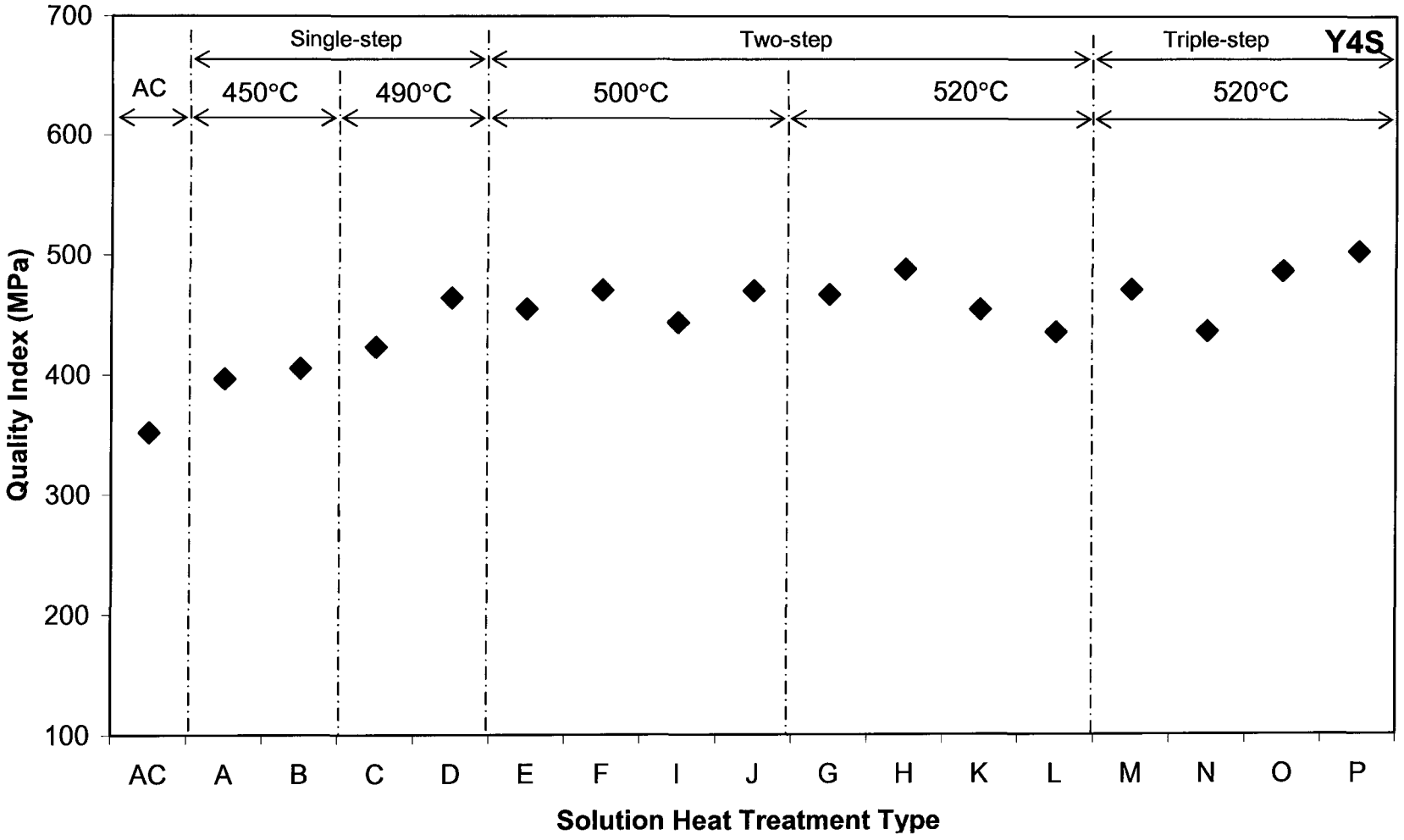

Figure 4.58 Quality index of alloy Y4S as a function of solution heat-treatment type.

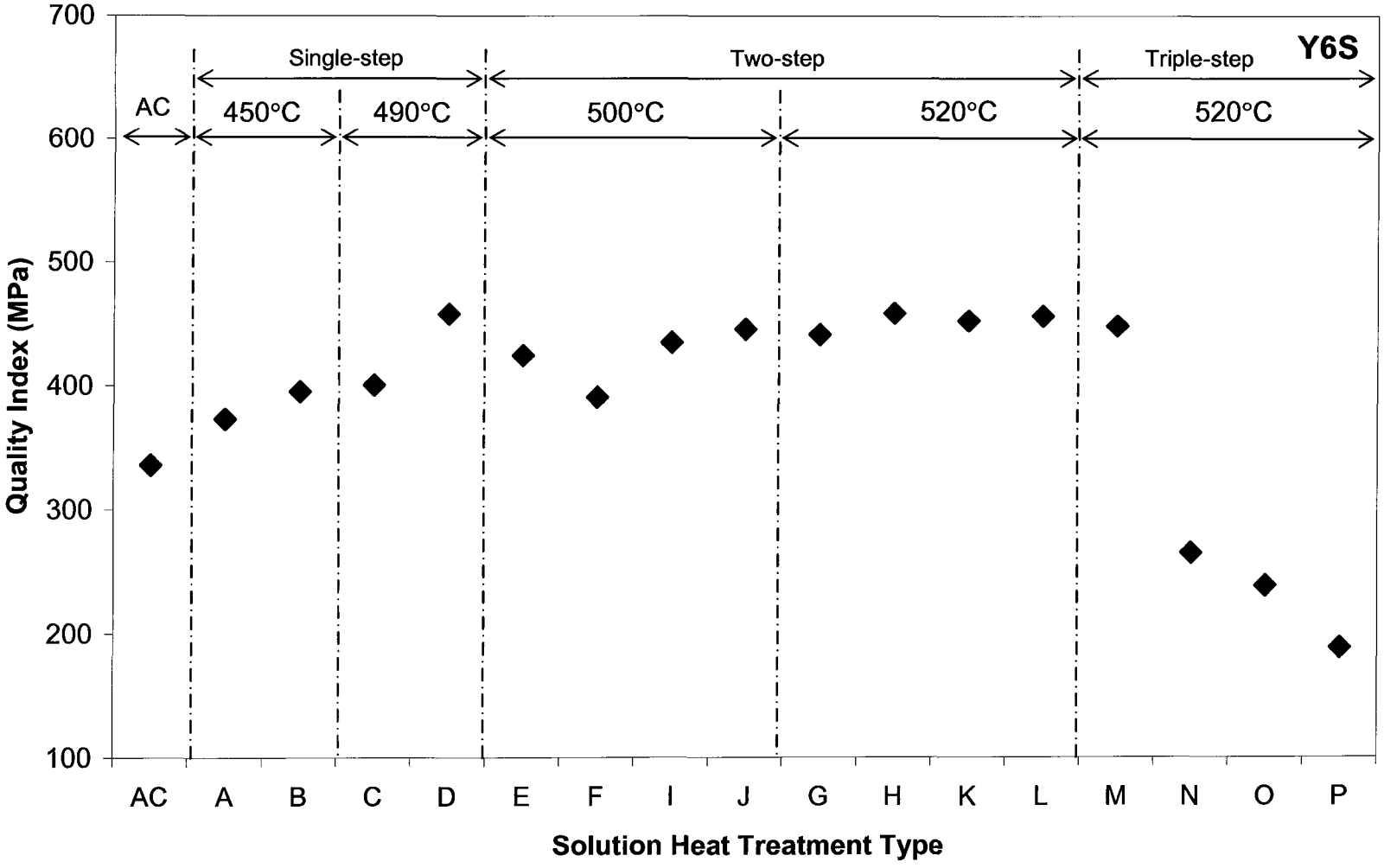

Figure 4.59 Quality index of alloy Y6S as a function of solution heat-treatment type.

4.2.2.2 Industrial alloys

The tensile properties of industrial alloys Y7 and Y8, together with their modified alloys Y7S and Y8S, are illustrated in Figures 4.60 and 4.61, and Figures 4.62 and 4.63, respectively. Yield strength and UTS will be seen to increase after treatment B (450°C/4h); this may be a result of the progressive dissolution of Al_2Cu in the aluminum matrix. Thereafter, both strengths remain more or less the same with further increases in solution temperature and time, up to 490°C/8h+500°C/4h, after which the maximum elongation and the highest Q values are obtained. Treatment G (450°C/4h+520°C/4h) shows noticeably poor tensile properties, which may be attributed to the occurrence of incipient melting and the presence of a high degree of porosity. When the alloy samples are subjected to triple-step heat treatments, tensile properties are also degraded, implying that this type of heat treatment is not suitable for industrial 319 alloys with 0.3 wt% Mg. When 150 ppm Sr is added to alloy Y7, the same results may be observed, but alloy Y7S shows a lower elongation and quality index after the same heat treatment (except for the as-cast condition and treatment G). From Figures 4.61 and 4.65, it will be observed that, for industrial alloy Y8 (containing 0.6 wt% Mg), all the single-step treatments and all the two-step treatments with a final temperature of 500°C lead to an increase in tensile properties. When the solution temperature is raised to 520°C, however, poor tensile properties are obtained, implying that 520°C is too high for 0.6 wt% Mg-containing industrial alloys, since, at this temperature, a considerable amount of incipient melting may occur. The same results are

observed in Sr-modified alloy Y8S, although this alloy shows higher tensile properties than the Y8 alloy after the same solution heat-treatment (except for treatment O).

Compared to experimental alloy Y4 (0.3 wt% Mg), industrial alloy Y7 (0.3 wt% Mg) shows higher YS, UTS and Q values after single-step and two-step treatments ending at 500°C, while if the temperature reaches 520°C, regardless of two-step or triple-step treatments, industrial alloy Y7 shows lower YS, UTS, percent elongation and Q values. The same observations may be made for experimental alloy Y6 (0.6 wt% Mg) and industrial alloy Y8 (0.6 wt% Mg). The only difference between industrial and experimental alloys is the chemical composition and trace elements contained in the industrial alloys; thus, the difference in tensile properties of experimental and industrial alloys should be attributed to the effect of trace elements.

When summarizing all the above results, for Mg-free alloy Y1, it is clear that tensile properties increase with solution treatment time and temperatures, which may be attributed to the dissolution of Al_2Cu and the spheroidization of Si particles. Addition of Sr to the base alloy leads to segregation of Al_2Cu at the dendrite cell boundaries, resulting in block-like, rather than eutectic, Al_2Cu, which is much harder to dissolve in the matrix; thus, in Y1S alloy, higher tensile properties benefit from a longer solution treatment time. When the treatment temperature reaches 520°C, incipient melting of this phase occurs and the Si particles spheroidize at the same time, so that the tensile properties are determined by a balance between these two factors.

When Mg is present in these alloys, the process becomes complicated. On the one hand, the addition of Mg leads to the precipitation of the $Al_5Mg_8Cu_2Si_6$ phase, which has a

low-melting point but is insoluble, thus the solution heat-treatment temperature should be controlled to below its melting point to avoid the occurrence of incipient melting. On the other hand, however, Mg can also lead to the formation of block-like Al_2Cu and an increase in its melting point. In order to cause as much Al_2Cu to dissolve in the matrix as possible, higher temperatures and longer times should be applied, yet this temperature should be lower than its melting point. At the same time, Si particles become finer and rounder at higher temperatures, and if the temperature is close to the eutectic Al-Si temperature, the Si particles will become faceted, which will decrease the tensile properties (especially percent elongation).

Therefore, the tensile properties of Mg-containing alloys are controlled by the combined effects of the dissolution of Al_2Cu, incipient melting of the $Al_5Mg_8Cu_2Si_6$ and Al_2Cu phases and the characteristics of the Si particles. If the Mg-containing alloy is modified with Sr, the process becomes even more complex, because not only does Sr increase the volume fraction of block-like Al_2Cu, modify Si particles and lower the eutectic Al-Si temperature, but it also reacts with Mg to form undesired compounds.

According to the results obtained for the tensile properties, the optimum solution heat-treatment for each alloy investigated in this study was recorded and listed in Table 4.7.

Table 4.7 Optimum solution heat-treatment obtained for 319 alloys investigated in this study.

Alloy	Optimum Solution Heat-Treatment		Tensile Properties			
			YS (MPa)	UTS (MPa)	%El (%)	Q (MPa)
Y1	M	450℃/4h+500℃/4h+520℃/4h	240	385	5.25	493
Y4	M	450℃/4h+500℃/4h+520℃/4h	329	456	4.77	558
Y6	L	490℃/8h+520℃/4h	334	445	4.24	539
Y7	D	490℃/8h	313	415	3.11	489
Y8	J	490℃/8h+500℃/4h	302	416	3.78	503
Y1S	N	450℃/8h+500℃/4h+520℃/4h	275	434	8.52	574
Y4S	P	490℃/8h+500℃/4h+520℃/4h	313	414	3.96	504
Y6S	D	490℃/8h	288	382	3.24	458
Y7S	D	490℃/8h	335	408	2.16	458
Y8S	J	490℃/8h+500℃/4h	323	401	2.14	451

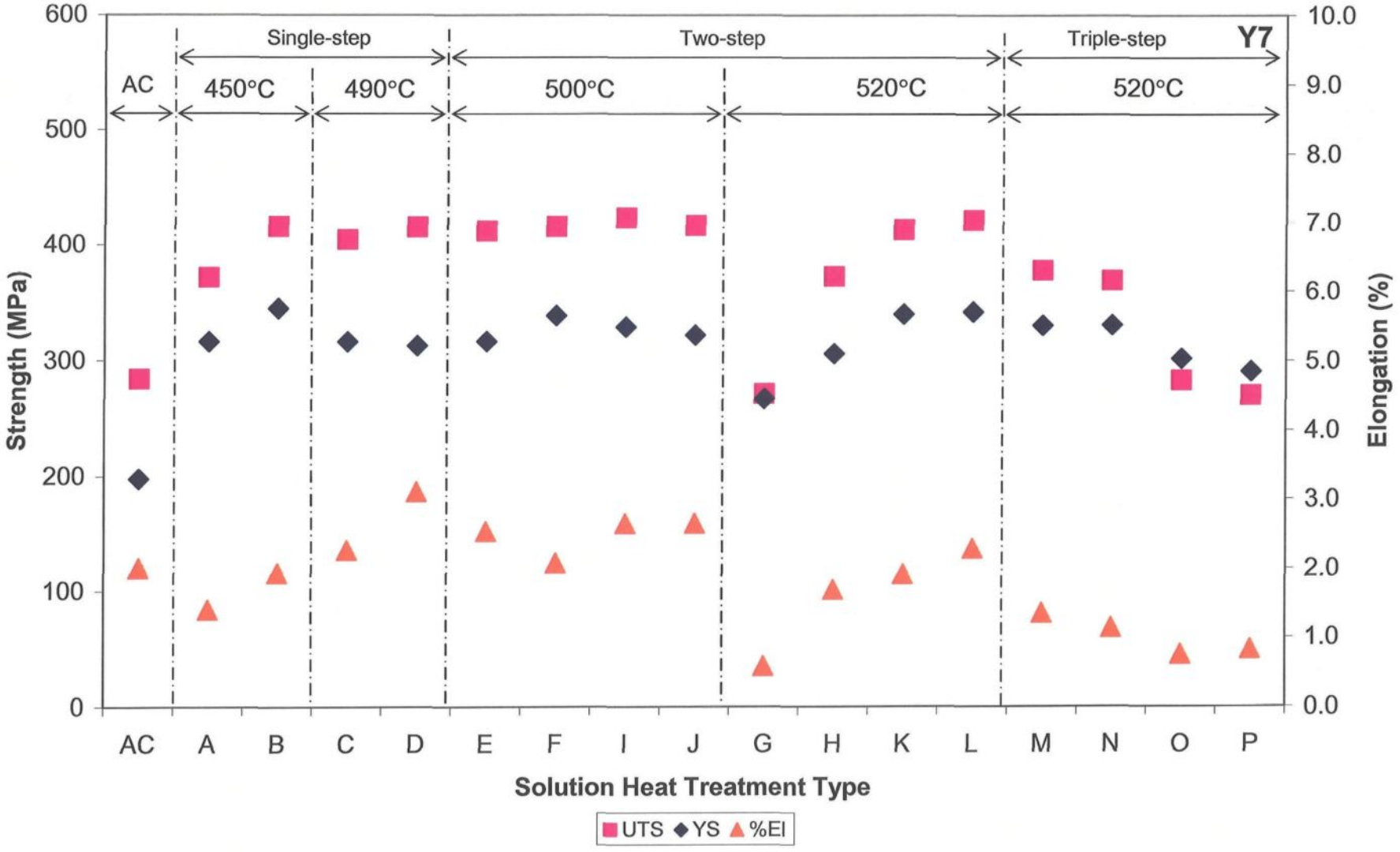

Figure 4.60 Tensile properties of alloy Y7 as a function of solution heat-treatment type.

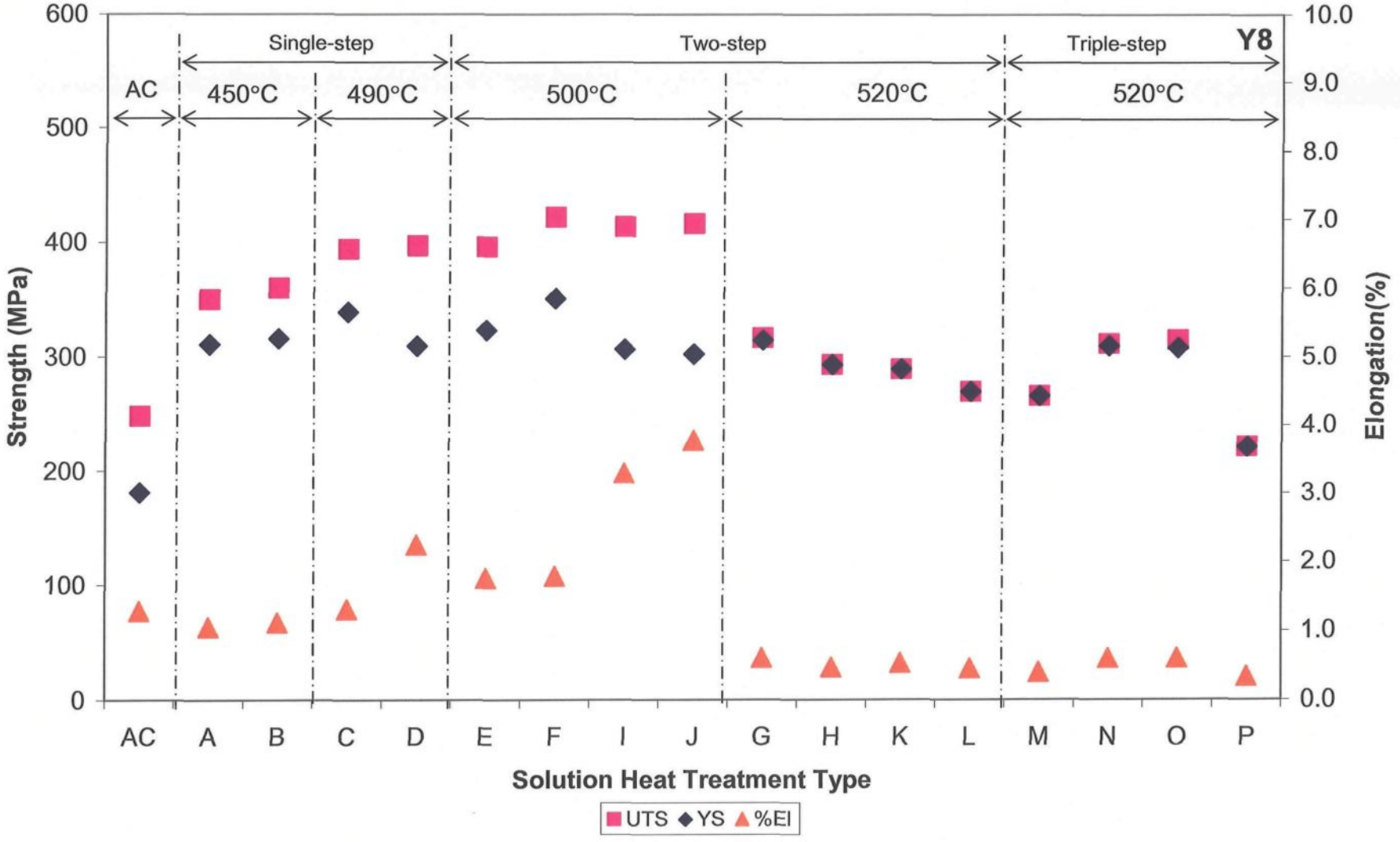

Figure 4.61 Tensile properties of alloy Y8 as a function of solution heat-treatment type.

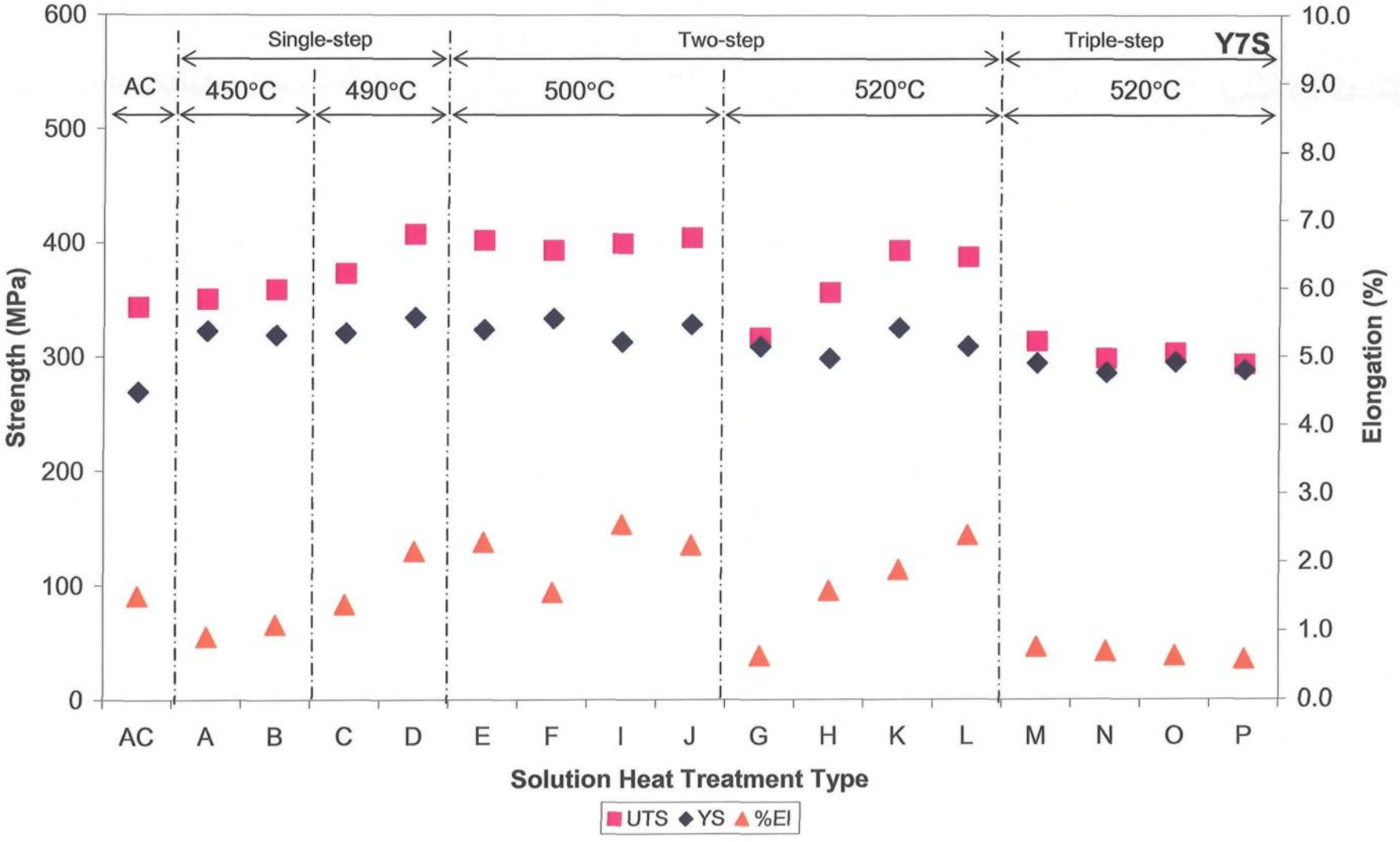

Figure 4.62 Tensile properties of alloy Y7S as a function of solution heat-treatment type.

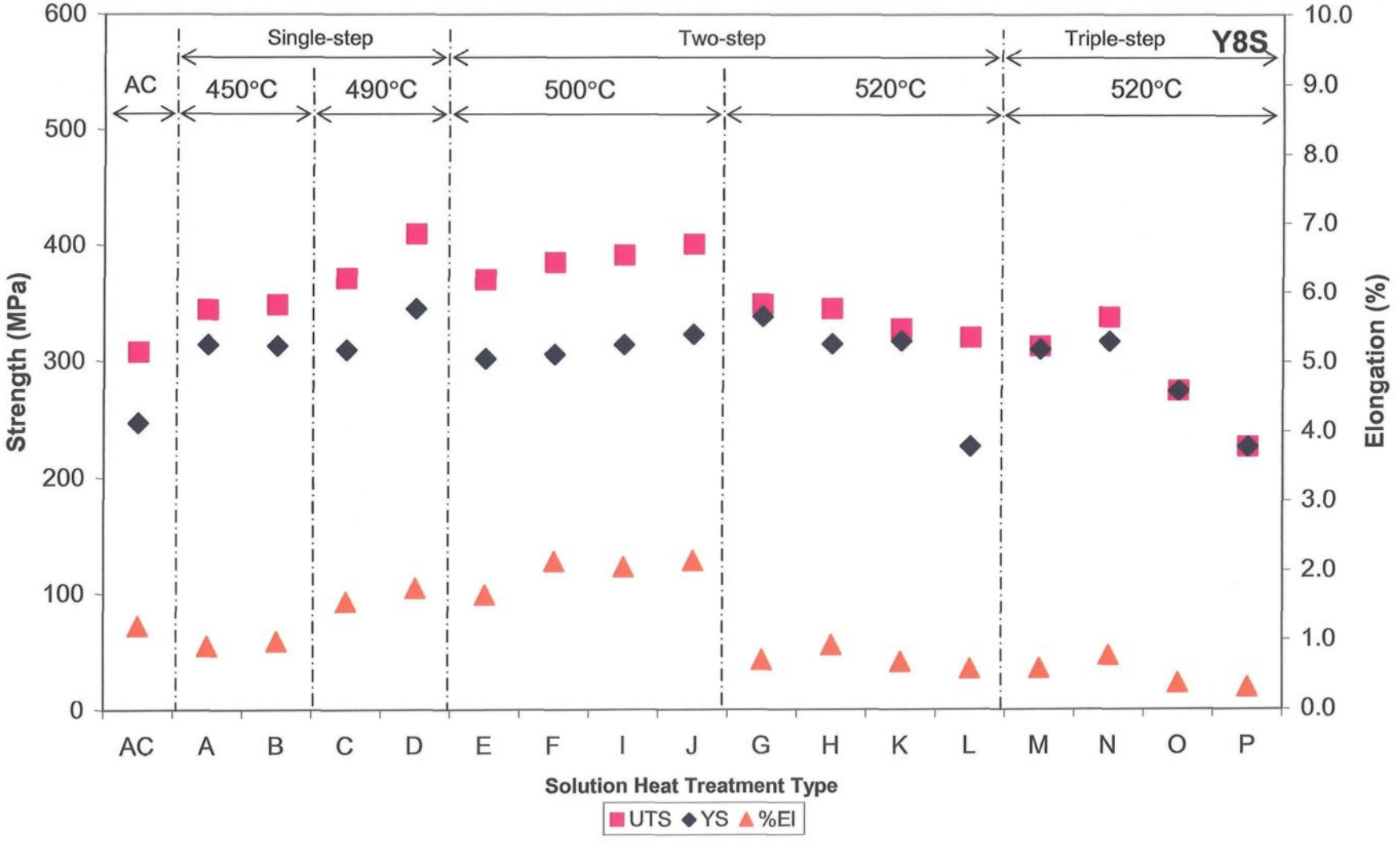

Figure 4.63 Tensile properties of alloy Y8S as a function of solution heat-treatment type.

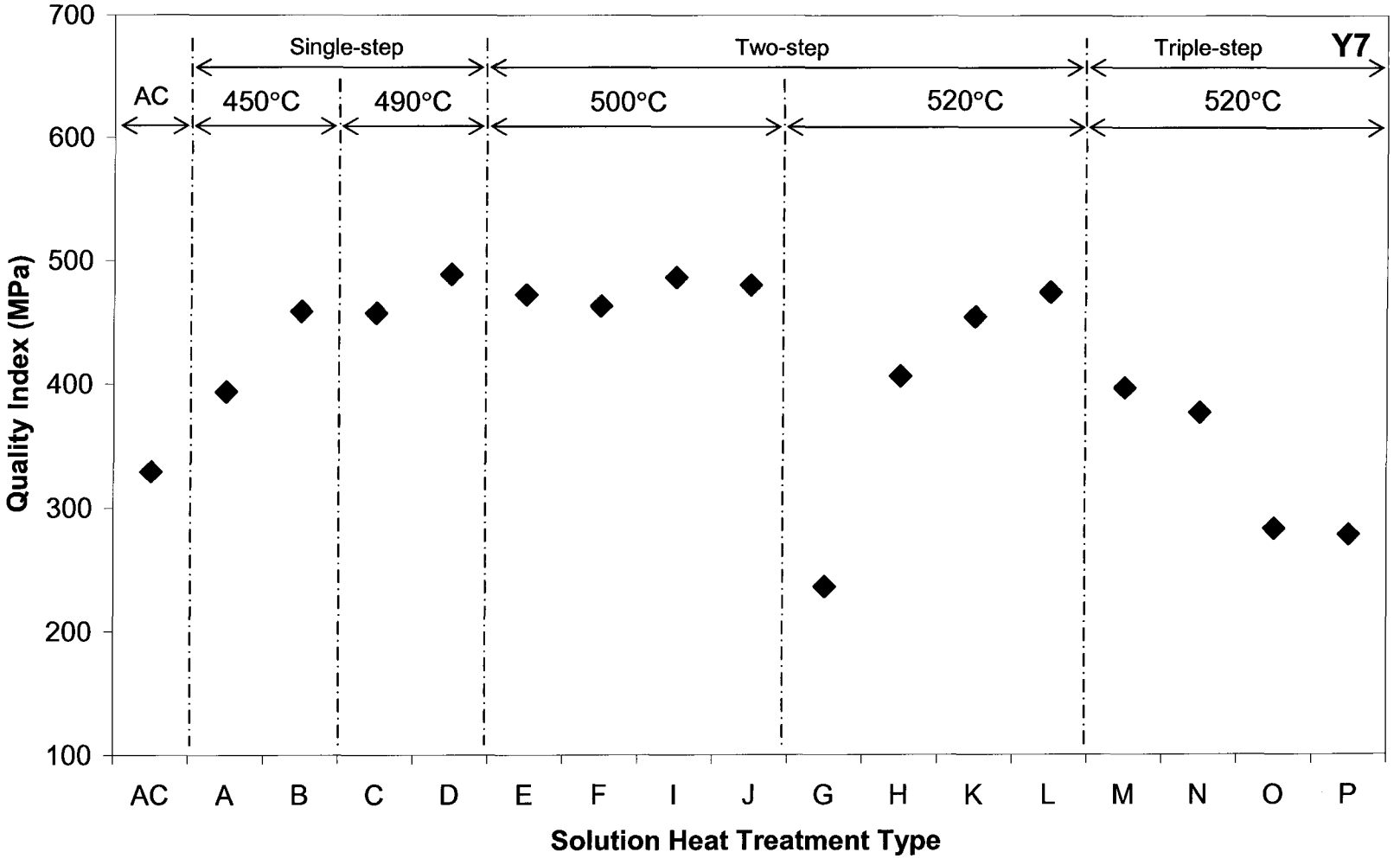

Figure 4.64 Quality index of alloy Y7 as a function of solution heat-treatment type.

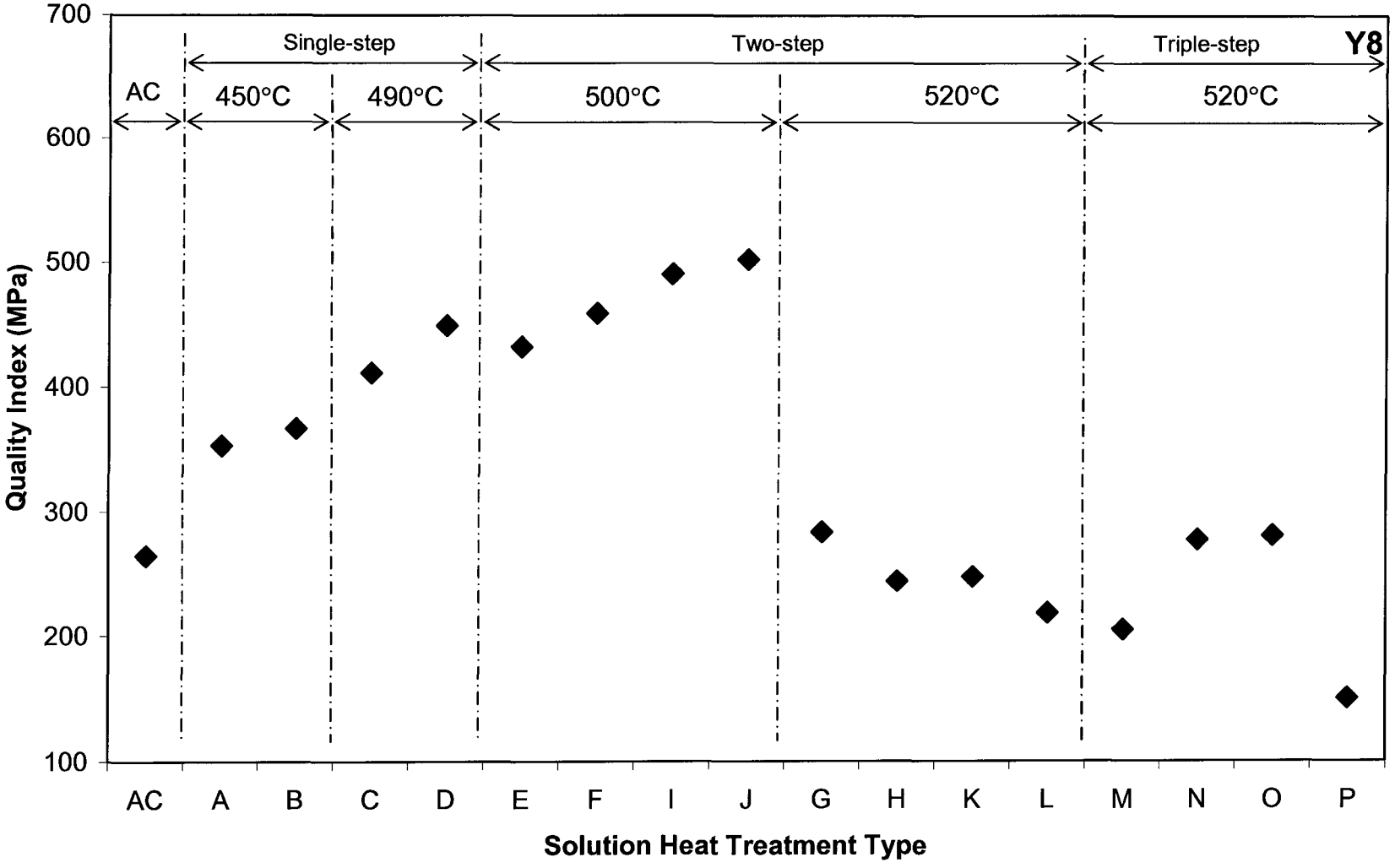

Figure 4.65 Quality index of alloy Y8 as a function of solution heat-treatment type.

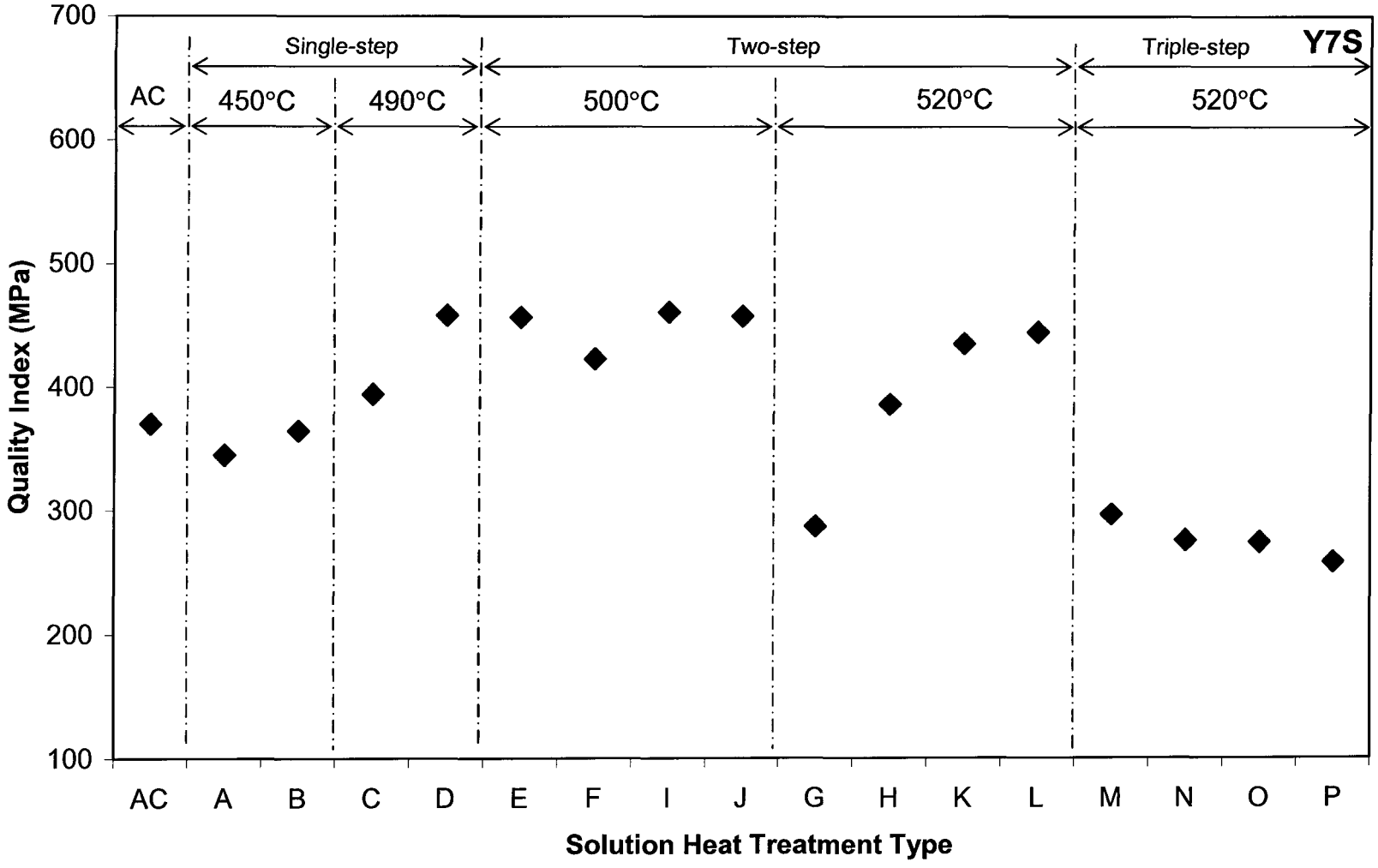

Figure 4.66 Quality index of alloy Y7S as a function of solution heat-treatment type.

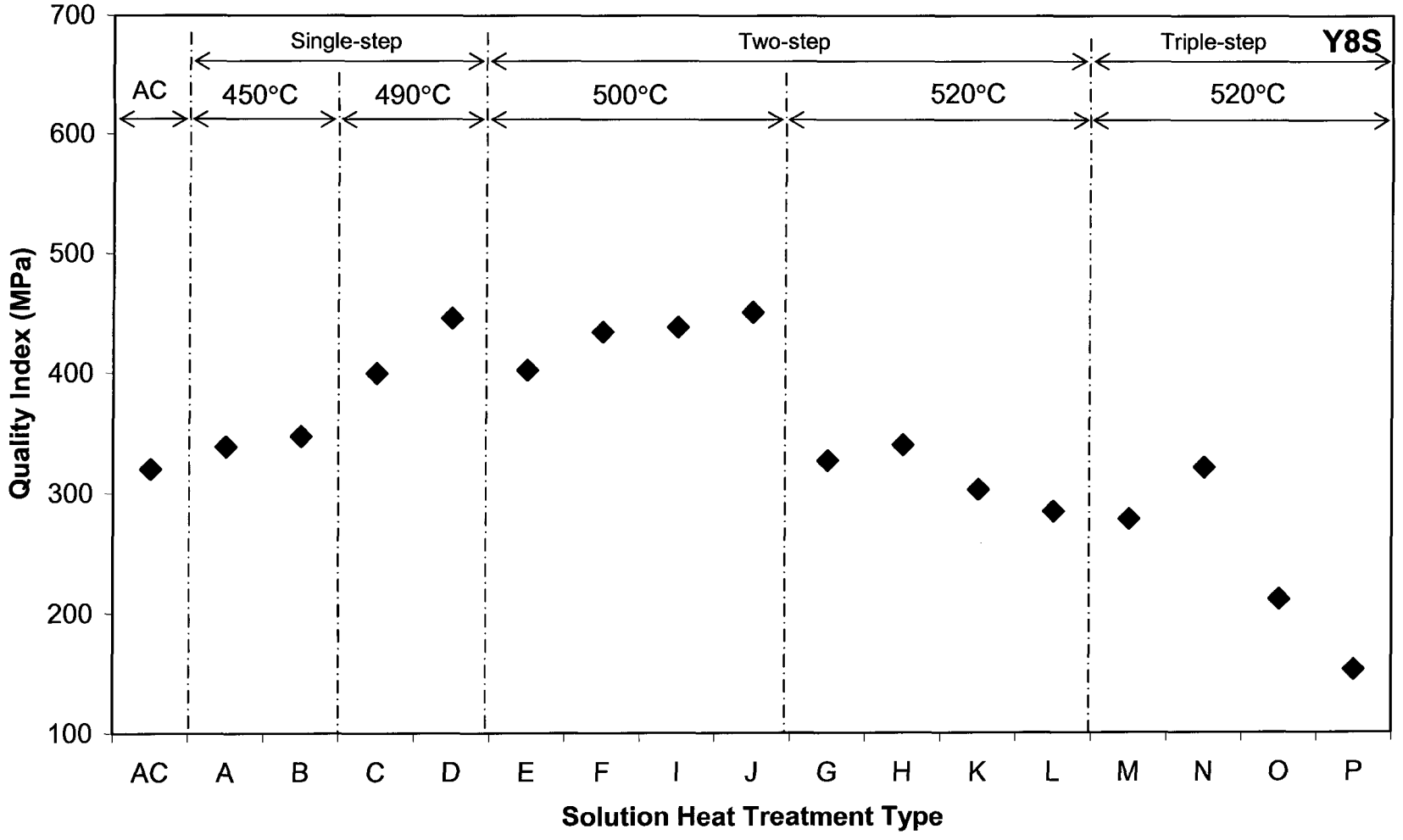

Figure 4.67 Quality index of alloy Y8S as a function of solution heat-treatment type.

CHAPTER 5

CONCLUSIONS

CHAPTER 5

CONCLUSIONS

This study was carried out in order to examine the effects of single and multiple-step solution treatments on the occurrence of incipient melting in non-modified and Sr-modified 319 experimental and industrial alloys containing low and high Mg levels.

Thermal analysis of the alloys investigated was undertaken to determine the reaction temperatures of the eutectic Al-Si, as well as Al_2Cu and other copper-containing phases. The efficiency of a specific solution heat-treatment in dissolving the Al_2Cu phases in the matrix was monitored by measuring the volume fraction of the undissolved portion of the phase in the matrix, and by running line scans across α-Al dendrites to determine the amount of dissolved Cu; melting of the $Al_5Mg_8Cu_2Si_6$ complex phase was also investigated.

To monitor the occurrence of the incipient melting, the porosity was measured in alloy samples corresponding to the various compositions and heat-treatment conditions studied. Eutectic Si particle characteristics were also measured to determine the effects that solution heat-treatment and Mg and Sr additions would have on the Si particles.

The tensile properties of these alloys were investigated in the as-cast and heat-treated conditions and related to the microstructural parameters mentioned above, namely, dissolution of the Al_2Cu phase, porosity caused by the incipient melting of $Al_5Mg_8Cu_2Si_6$

and Al_2Cu phases, and the Si particle characteristics. Based on the results obtained and presented in Chapter 4, the following conclusions may be drawn.

I. Microstructure

(1) Two main Cu-containing phases exist in the Al-Si-Cu-Mg 319 type alloys studied: (a) the Al_2Cu phase, and (b) the complex $Al_5Mg_8Cu_2Si_6$ phase. The Al_2Cu is soluble, whereas the $Al_5Mg_8Cu_2Si_6$ is insoluble. When Mg is added up to 0.6 wt%, the complex phase precipitates before and after the Al_2Cu phase, in pre-eutectic and post-eutectic reactions.

(2) The post-eutectic $Al_5Mg_8Cu_2Si_6$ precipitates at a temperature of 491.3°C, which is 10°C lower than the precipitation temperature of Al_2Cu. During solution heat-treatment and depending on the heat-treatment temperature applied in a specific solution treatment (450°C, 490°C, 500°C, or 520°C), the dissolution or melting of these copper phases will take place.

(3) The mechanism of incipient melting in the presence of Mg commences with the melting of the $Al_5Mg_8Cu_2Si_6$ phase. This phase may usually be observed in the form of spherical entities in the matrix at low Mg levels. During quenching, and as a result of the change in volume fraction from liquid to solid state, shrinkage will occur, leading to porosity formation.

(4) In the case of high-Mg alloys, the melted $Al_5Mg_8Cu_2Si_6$ particles become linked together to form interconnected porosities during solution heat-treatment, a state which is highly detrimental to the properties of the alloy.

(5) Addition of Sr causes the Cu to segregate at the dendrite boundaries, leading to the precipitation of the Al_2Cu phase in the block-like form which is much more difficult to dissolve than the finer eutectic-like form of the phase. After heat treatment, and in the modified alloys, in particular, the copper begins to become evenly distributed across the Al matrix. With increasing solution time and temperatures, the amount of undissolved Al_2Cu decreases and the Cu in the matrix increases, reaching a maximum after the 490°C/8h solution heat-treatment.

(6) The dissolution process of eutectic Al-Al_2Cu is proposed to occur as follows:
(i) necking of the Al-Al_2Cu particles takes place at several sites along the length of the particles, which results in their breaking into small fragments;
(ii) gradual spheroidization of the particles after initial fragmentation; and
(iii) radial diffusion of Cu atoms into the surrounding aluminum matrix.

(7) For the block-like Al_2Cu, because of its massive morphology, the dissolution process goes through the spheroidization and diffusion steps directly, although the dissolution occurs relatively more slowly than in the case of the eutectic Al_2Cu. Thus, a much longer solution time and a higher solution temperature are required to obtain a smaller particle size and for complete dissolution of the phase to occur.

(8) The addition of 0. 3 wt% Mg to the base 319 alloy leads to a decrease in the eutectic Al-Al_2Cu temperature; increasing the Mg level to 0.6 wt% decreases the temperature further.

(9) In Mg-free alloys, solutionizing at 520°C leads to the complete dissolution of the Al_2Cu phase, and hardly any incipient melting of the phase occurs. The Si particles also undergo spheroidization, thus the tensile properties benefit from these two factors.

(10) When Mg is added to 319 alloys, especially up to 0.6 wt%, both area percent porosity and pore lengths increase noticeably. Solutionizing at 500°C leads to incipient melting of the $Al_5Mg_8Cu_2Si_6$ phase, while the Al_2Cu phase does not melt but dissolves. In a multiple-step treatment, if the first-step (at low temperature) solution treatment time is not long enough to allow the Al_2Cu to dissolve, and if the second-step treatment temperature is higher than its melting-point (*i.e.* 450°C/4h + 520°C/4h and 490°C/4h + 520°C/4h), incipient melting of Al_2Cu will occur. In this case, the porosity derives from the incipient melting of the $Al_5Mg_8Cu_2Si_6$ and Al_2Cu phases.

(11) The addition of Sr leads to increases in area percent porosity and pore length, especially when the solution treatment temperature reaches 520°C; at this temperature, the hard-to-dissolve block-like Al_2Cu will melt and result in a significant increase in the area percent porosity.

(12) Coarse and faceted Si particles are observed in the vicinity of both the $Al_5Mg_8Cu_2Si_6$ and Al_2Cu phases, when incipient melting of these phases occurs, and when the last solution temperature (i.e., 520°C) is close to the Al-Si eutectic temperature, of the order of 20°C, for example, 540.9°C in the case of Y8S alloy.

II. Mechanical Properties

(13) The addition of Mg to experimental 319 alloys leads to an increase in yield strength (YS), and ultimate tensile strength (UTS), but to a reduction in percentage elongation (%El). In unmodified alloys, the loss of elongation is compensated by the increase in strength, thus the quality of the alloy increases. It was also found that Mg causes a greater increase in yield strength than it does in ultimate tensile strength.

(14) Compared with experimental alloys of the same Mg content, industrial alloys show higher tensile properties.

(15) In Mg-free alloys, the addition of Sr increases the strength (YS, UTS) and ductility (%El). When Mg is present, in either experimental or industrial alloys, the ductility is reduced.

(16) The optimum combination of Mg and Sr in this study is 0.3 wt% Mg with 150 ppm Sr, viz. for the Y4S alloy. The corresponding tensile properties in the as-cast condition are 260 MPa (YS), 326 MPa (UTS), 1.50% (%El), 352 MPa (Q), compared to 145 MPa (YS), 232 MPa (UTS), 2.4 (%El), 290 MPa(Q) for the base alloy Y1.

(17) In the Mg-free 319 alloys, tensile properties increase with increasing solution treatment time and temperatures. The application of multiple-step solution treatments results in both the dissolution of the Al_2Cu phase and spheroidization of the Si particles. These two factors produce an increase in the mechanical properties, especially in the modified alloys.

(18) For Mg levels up to 0.6 wt%, all modified alloys show higher strength than unmodified alloys after the same solution heat-treatment when the solution

temperature is below 500°C. At 520°C solution temperature, incipient melting of $Al_5Mg_8Cu_2Si_6$ phase and undissolved block-like Al_2Cu takes place. At the same time, the Si particles become rounder. Therefore, the tensile properties of Mg-containing alloys are controlled by the combined effects of dissolution of Al_2Cu, incipient melting of $Al_5Mg_8Cu_2Si_6$ phase and Al_2Cu phase, as well as the Si particle characteristics.

(19) The holding time of the first stage and the solution temperature of the second stage are significant parameters in this context. The optimum solution heat-treatment and corresponding tensile properties of each alloy as determined from this study are summarized as shown below.

Alloy	Optimum Solution Heat-Treatment		Tensile Properties			
			YS (MPa)	UTS (MPa)	%El (%)	Q (MPa)
Y1	N	450℃/8h+500℃/4h+520℃/4h	240	385	5.25	493
Y4	M	450℃/4h+500℃/4h+520℃/4h	329	456	4.77	558
Y6	L	490℃/8h+520℃/4h	334	445	4.24	539
Y7	D	490℃/8h	313	415	3.11	489
Y8	J	490℃/8h+500℃/4h	302	416	3.78	503
Y1S	N	450℃/8h+500℃/4h+520℃/4h	275	434	8.52	574
Y4S	P	490℃/8h+500℃/4h+520℃/4h	313	414	3.96	504
Y6S	D	490℃/8h	288	382	3.24	458
Y7S	D	490℃/8h	335	408	2.16	458
Y8S	J	490℃/8h+500℃/4h	323	401	2.14	451

RECOMMENDATIONS FOR FUTURE WORK

This study concentrated on the occurrence of incipient melting in Al-Si-Cu-Mg alloys. Single and multiple-step solution treatments were carried out to obtain the optimum solution heat-treatment. Factors which control the tensile properties, such as the dissolution of Al_2Cu, porosity characteristics and Si particle characteristics were also investigated. Based on the results obtained in this research, it would be useful to investigate the following concepts further:

(1) The relation between the volume fraction of undissolved $Al_5Mg_8Cu_2Si_6$ (following dissolution of the Al_2Cu phase), measured before and after the incipient melting occurs, and to determine its correlation with the tensile properties.

(2) The relation between the depression of the eutectic Al-Si temperature and the modifying effects of Mg and Sr.

REFERENCES

REFERENCES

1 Jerry H. Sokolowski, Mile B. Djurdjevic, Christopher A. Kierkus and Derek O. Northwood, "Improvement of 319 Aluminum Alloy Casting Durability by High Temperature Solution Treatment", *Journal of Materials Processing Technology*, 2001, Vol. 109, pp. 174-180.

2 Jerry H. Sokolowski, X-C. Sun, G. Byczynski, D.E. Penord, R. Thomas and A. Esseltine, "The Removal of Copper-Phase Segregation and The Subsequent Improvement in Mechanical Properties of Cast 319 Aluminum Alloys by a Two-Stage Solution heat-treatment", *Journal of Materials Processing Technology*, 1995, Vol.53, pp.385-392.

3 I.J. Polmear, *Light Alloys: Metallurgy of the Light Metals*, Third Edition, Elsevier, New York, 1996, pp.174-178.

4 L. Bäckerud, G. Chai and J. Tamminen, *Solidification Characteristics of Aluminum Alloys, Vol. 2: Foundry Alloys*, AFS/Skanaluminium, Des Plaines, IL, 1990, pp. 71-84.

5 John E. Gruzleski and Bernard M. Closset, *The Treatment of Liquid Aluminum-Silicon Alloy*, American Foundrymen's Society, Inc., Des Plaines, IL, 1990, pp. 35-49.

6 J.R. Davis, *ASM Specialty Handbook: Aluminum and Aluminum Alloys*, American Society for Metals, Metals Park, OH, USA, 1993, pp. 23-58.

7 *ASM Handbook, Vol. 3: Alloy Phase Diagrams*, ASM International, Materials Park, OH, 1993, pp. 2-86.

8 F.H. Samuel, A.M. Samuel and H.W. Doty, "Factors Controlling the Type and Morphology of Cu-Containing Phases in 319 Al Alloy" *AFS Transactions*, 1996, Vol. 104, pp. 893-903.

9 A.M. Samuel, J. Gauthier and F.H. Samuel, "Microstructural Aspects of the Dissolution and Melting of Al_2Cu Phase in Al-Si Alloys During Solution Heat-Treatment", *Metallurgical and Material Transactions A*, 1996, Vol. 27A, pp. 1785-1798.

10 Z. Li, A.M. Samuel, F.H. Samuel, C. Ravindran, S. Valtierra and H.W. Doty, "Factors Affecting Dissolution of Al_2Cu Phase in 319 Alloys", *AFS Transactions*, 2003, Vol. 111, Paper 03-100, pp.1-14.

11 A.M. Samuel, H.W. Doty and F.H. Samuel, "Observations on the formation of β-Al_5FeSi phase in 319 type Al-Si alloys", *Journal of Materials Science*, 1996, Vol. 31, No. 20, pp. 5529-5539.

12 Z. Li, "Parameters Controlling the Precipitation and Dissolution of Al_2Cu Phase in 319 Alloys and Their Influence on the Alloy Performance", M. Eng Thesis, Université du Québec à Chicoutimi, Chicoutimi, Canada, 2003.

13 F.H. Samuel, "Incipient melting of $Al_5Mg_8Si_6Cu_2$ and Al_2Cu intermetallics in unmodified and strontium-modified Al-Si-Cu-Mg (319) alloys during solution heat-treatment", *Journal of Materials Science*, 1998, Vol. 33, pp. 2283–2297.

14 D. Apelian, S. Shivkumar and G. Sigworth, "Fundamental Aspects of Heat Treatment of Cast Al-Si-Mg Alloys," *AFS Transactions*, 1989, Vol. 97, pp. 727-741.

15 P.Y. Zhu, Q. Y. Liu and T.X. Hou, "Spheroidization of Eutectic Silicon in Aluminum-Silicon Alloys," *AFS Transactions*, 1985, Vol. 93, pp.609-614.

16 T.J. Shin and D.N. Lee, *J. Korean Inst. Met.& Mater.*, 1955,Vol. 23, pp. 1116-1122.

17 F.A. Calvo, A.J. Criado, J.M. Gomez de Salazar, and F. Molleda, *Rev. Metal. Madrid*, 1985, Vol. 21, pp. 312-316.

18 S. Shivkumar, S. Ricci, Jr., and D. Apelian, "Influence of Solution Parameters and Simplified Supersaturation Treatments on Tensile Properties of A356 alloy," *AFS Transactions*, 1990, Vol. 180, pp. 913-922.

19 F.N. Rhines and M. Aballe, "Growth of Silicon Particles in an Aluminum Matrix", *Metallurgical and Materials Transactions A*, 1986, Vol. 17, pp. 2139-2152.

20 M.M. Tuttle and D.L. MacLellan, "Silicon Particles Characteristics in Al-Si-Mg Castings", MacLellan, *AFS Transactions*, 1982, Vol. 90, pp. 13-23.

21 H. de la Sablonnière and F.H. Samuel, "Solution Heat-Treatment of 319 Aluminum Alloy Containing ~ 0.5 wt% Mg Part 2: Microstructure and Fractography", *International Journal of Cast Metals Research*, 1996, Vol. 9, pp. 151-225.

22 H. Beumler, A. Hammerstad, B. Wieting and R. DasGupta, "Analysis of modified 319 Aluminum Alloy", *AFS Transactions*, 1988, Vol. 96, pp. 1-12.

23 S. Shivkumar, "The Interactive Effects of Sr Modification and Heat Treatment on the Mechanical Properties of Cast Aluminum Alloys", *Heat Treating: Proceedings of the 17th Conference*, Vol. 15-18, 1998 , pp. 265-269.

24 Y. Wang, Z. Zhang, S. Zheng, W. Wang, and X Bian, . "Effect of Sr Addition on the Microstructure of a Rapidly Solidified Al-12wt.% Si Alloy", *Prakt. Metallogr.*, 2005, Vol. 42, pp. 411-421.

25 M. Djurdjevic, T. Stockwell and J. Sokolowski, "The Effect of Strontium on the Microstructure of the Aluminum-Silicon and Aluminum-Copper Eutectics in the 319 Aluminum Alloy", *International Journal of Cast Metals Research*, 1999, Vol. 12, pp. 67-73.

26 G-Q. Wang, X-F. Bian, W-M. Wang and J-Y. Zhang, "Influence of Cu and Minor Elements on the Solution Treatment of Al-Si-Cu-Mg Cast Alloys" *Materials Letters*, 2003, Vol. 57, Issues 24-25,. pp. 4083-4087.

27 L. Heusler and W. Schneider, "Recent Investigations of Influence of P on Na and Sr Modification of Al-Si Alloys", *AFS Transactions*, 1997, Vol. 105, pp. 915-921.

28 H. de la Sablonnière and F.H. Samuel, "Solution heat-treatment of 319 Aluminium Alloy Containing ~0.5wt% Mg Part 1: Solidification and Tensile Properties", *International Journal of Cast Metals Research*, 1996, Vol. 9, pp. 195-211.

29 N. Crowell and S. Shivkumar, "Solution Treatment Effects in Cast Al-Si-Cu Alloys", *AFS Transactions*, 1995, Vol. 103, pp. 721-726.

30 K. Tynelius, J.F. Major and D. Apelian, " A Parametric Study of Microporosity in the A356 Casting Alloy System", *AFS Transactions*, 1993, Vol. 101, pp. 401-413.

31 G. Sigworth, "Theoretical and Practical Aspects of the Modification of Aluminum-Silicon Alloys," *AFS Transactions*, 1983, Vol. 91, pp. 7-16.

32 G.E. Byczynski and D.A. Cusinato, "The Effect of Strontium and Grain Refiner Additions on the Fatigue and Tensile Properties of Industrial Al-Si-Cu-Mg Alloy Castings Produced Using the Ford Motor Company - Cosworth Precision Sand Process ", *International Journal of Cast Metals Research*, 2002, Vol. 14, pp. 315-324.

33 P.C. van Wiggen, P. Huysmans, B.V. KBM Affilips and N. V. Affilips, "Modification by Aluminum-Strontium: Continuous Evolution", *Fonderie d'Aujourd'hui*, 2003, No. 225, pp. 10-19.

34 J.E. Gruzleski, M. Pekguleryuz, and B. Closset, *Proceedings of the Third International Solidification Conference*, Sheffield, Institute of Metals, Sheffield, UK, 1987.

35 M.A. Moustafa, C. Lepage, F.H. Samuel and H.W. Doty, "Metallographic Observations on Phase Precipitation in Strontium-Modified Al-11.7% Si Alloys: Role of Alloying Elements", *International Journal of Cast Metals Research*, 2003, Vol. 15, pp. 609-626.

36 K.R. Van Horn, *Aluminum, Vol. 1: Properties Physical Metallurgy and Phase Diagrams*, American Society for Metals, Metals Park, OH, 1967, Vol.1, pp.235-276.

37 R.W. Bruner, *Metallurgy of Die Casting Alloys*, SDCE Inc., Detroit, MI, 1976, pp. 75-80.

38 A.M. Samuel, P. Ouellet, F.H. Samuel, H.W. Doty, "Microstructural Interpretation of Thermal Analysis of Commercial 319 Al Alloy With Mg and Sr Additions", *AFS Transactions*, 1997, Vol. 105, pp. 951-962.

39 L. Heusler and W. Schneider, "Influence of Alloying Elements on the Thermal Analysis Results of Al–Si Cast Alloys," *Journal of Light Metals*, 2002, Vol. 2, pp. 17-26.

40 P. Ouellet, F.H. Samuel, D. Gloria and S. Valtierra, "Effect of Mg Content on the Dimensional Stability and Tensile Properties of Heat Treated Al-Si-Cu (319) Type Alloys", *International Journal of Cast Metals Research*, 1997, Vol. 105, pp. 67-78.

41 W. Reif , J. Dutkiewicz , R. Ciach, S. Yu, J. Krol, "Effect of aging on the evolution of precipitates in AlSiCuMg alloys", *Materials Science and Engineering*, 1997, Vol. A234-236, pp.165-168.

42 P.R. Dunn and W.Y. Dickert, "Magnesium Effect on the Strength of A380.0 and 383.0 Aluminum Die Casting Alloys," *Die Casting Engineering*, 1975, Vol. 19, pp. 12-17.

43 A.T. Joenoes and J.E. Gruzleski, "Magnesium Effects on the Microstructure of Unmodified and Modified Al-Si Alloys", *Cast Metals*, 1991, Vol. 4, No. 2, pp. 62-71.

44 N. Roy, A.M. Samuel and F.H. Samuel, "Porosity formation in Al-9 wt%Si-3 wt% Cu alloy systems: Metallographic Observations", *Metallurgical and Materials Transactions A*, 1996, Vol. 27, No. 2, pp. 415-429.

45 W. Bonfield and B.K. Dutta, "Precipitation Hardening in Al-Cu-Si-Mg Alloy at 130-220°C," *Journal of Materials Science*, 1976, Vol. 11, pp. 1661-1666.

46 G.Q. Wang, X.F. Bian and J.Y. Zhang, "Gradual Solution Heat-Treatment of AlSiCuMg Cast Alloys", *Rare Metals* (English Version), 2003, Vol. 22, pp. 304-308.

47 S. Shivkumar, S. Ricci, Jr. and D. Apelian, "Influence of Solution Parameters and Simplified Supersaturation Treatments on Tensile Properties of A356 Alloy", *AFS Transactions*, 1990, Vol. 98, pp. 913-922.

48 E.N. Pan, J.F. Hu and C.C. Fan, "Solution Treatment Conditions for Optical Tensile Properties of A357 Alloy," *AFS Transactions*, Vol. 104, 1996, pp. 11-19.

49 J. Gauthier, P.R. Louchez and F.H. Samuel, "Heat Treatment of 319.2 Aluminum Automotive Alloy: Part 1, Solution Heat-Treatment", *Cast Metals*, 1995, Vol. 8, No.2, pp. 91-106.

50 J. Gauthier, P.R. Louchez and F.H. Samuel, "Heat Treatment of 319.2 Aluminum Automotive Alloy: Part 2, Aging Behavior", *Cast Metals*, 1995, Vol. 8, pp. 107-114.

51 D.Y. Yang, "Role of Mg Addition on the Occurrence of Incipient Melting in Experimental and Commercial Al-Si-Cu Alloys and its Influence on the Alloy Microstructure and Tensile Properties", M.Eng. Thesis, UQAC, Chicoutimi, 2006.

52 R. Li, "Solution heat-treatment of 354 and 355 Cast Alloys," *AFS Transactions*, 1996, Vol. 104, pp. 777-783.

53 G. Wang, X. Bian, W. Wang and J. Zhang, "Influence of Cu and Minor Elements on Solution Treatment of Al–Si–Cu–Mg Cast Alloys" *Materials Letters*, 2003, Vol. 57, pp. 4083-4087.

54 E. Cerri, E. Evangelista, S. Spigarelli, P. Cavaliere and F. De Riccardis, "Effects of Thermal Treatments on Microstructure and Mechanical Properties in a Thixocast 319 Aluminum Alloy", *Materials Science and Engineering*, 2000, Vol. A284, pp. 254-260.

55 P. Cavaliere, E. Cerri and P. Leo, "Effect of Heat Treatments on Mechanical Properties and Damage Evolution of Thixoformed Aluminum Alloys", *Materials Characterization*, 2005, Vol. 55, pp. 35-42.

56 L. Lasa and J.M. Rodriguez-Ibabe, "Evaluation of the Main Intermetallic Phases in Al-Si-Cu-Mg Casting Alloys during Solution Treatment", *Journal of Materials Science*, 2004, Vol. 39, pp. 1343-1355.

57 A.I. García-Celis, R. Colás, "Aging in a Heat Treatable Cast Aluminum Alloy", *Proceedings of the First International Automotive Heat Treating Conference*, 1998, Vols 13-15, pp. 372-375.

58 D. Apelian, S. Shivkumar and G. Sigworth, "Fundamental Aspects of Heat Treatment of Cast Al-Si-Mg Alloys", *AFS Transactions*, 1989, Vol. 97, pp. 727-742.

59 J.E. Hatch (ed.), *Aluminum: Properties and Physical Metallurgy*, ASM, Metals Park, OH, 1984, pp. 238-240.

60 J.W. Newkirk, Q. Liu and A. Mohammadi, "Optimizing the Aging Heat Treatment of Cast Aluminum Alloys", *The 2002 Annual Meeting: Automotive Alloys and Aluminum Sheet and Plate Rolling Finishing Technology Symposia*, 2002, pp. 75-82.

61 D. Gloria, F. Hernandez, S. Valtierra and M.A. Cisneros, "Dimentional Changes During Heat Treating of Automotive 319 Alloy", in *Heat Treating: Advances in Surface Engineering: An International Symposium*, 2000, Vols 9-12, pp. 674-679.

62 Guiqing Wang, Xiufang Bian, Xiangfa Liu and Junyan, Zhang, "Effect of Mg on Age Hardening and Precipitation Behavior of AlSiCuMg Cast Alloy", *Journal of Materials Science*, 2004, Vol. 39, pp. 2532-2537.

63 J.M. Boileau, S.J. Weber, R.H. Salzman and J.E. Allison, "The Effect of Porosity Size on the Tensile Properties of a Cast 319-T7 Aluminum Alloy", *AFS Transactions*, 2001, Vol. 109, pp. 419-432.

64 D.E.J. Talbot, "Effect of Hydrogen in Aluminum, Magnesium, Copper and Their Alloys", *International Metallurgical Reviews*, 1975, Vol. 20, pp. 166-184.

65 J. Zou, K. Tynelius, S.Shivkumar, D. Apelian, "Microporosity Formation in A356.2 Castings", *Production, Refining, Fabrication and Recycling of Light Metals*, Pergamon Press, New York, 1990, pp. 323-332.

66 K. Kubo and R.D. Pehlke, "Mathematical Modeling of Porosity Formation in Solidification", *Metallurgical Transactions*, 1985, Vol. 16B, pp. 359-366.

67 J. Campbell, *The Solidification of Metal*s, Iron and Steel Institute, London, Publication 110, 1967, pp. 18-23.

68 S.D. McDonald, K. Nogita, A.K. Dahle, "Eutectic Solidification and Porosity Formation in Al-Si Alloys: Role of Strontium", *AFS Transactions*, 2000, Vol. 108, pp. 463-470.

69 X.F. Bian, Z.H. Zhang and X.F. Liu, "Effect of Strontium Modification on Hydrogen Content and Porosity Shape of Al-Si Alloys", *Materials Science Forum*, 2000, Vol. 331-337, pp. 361-366.

70 G.A. Edwards and G.K. Sigworth, "Microporosity Formation in Al-Si-Cu-Mg Casting Alloys", *AFS Transactions*, 1997, Vol. 105, pp. 809-818.

71 Ph. Meyer, D. Massinon, Ph. Guerin and L. Wang, "Influence of Microstructure on the Static and Thermal Fatigue Properties of 319 Alloys", *International Congress & Exposition,* 1997, Vol. 106, pp. 627-634.

72 "*Special Report on the Mechanical Properties of Permanent Mold Aluminum Test Castings*", Jobbing Foundry Division of the Aluminum Association, Washington, D.C., November, 1990.

73 Glenn E. Byczynski, Witold T. Kierkus, Derek O. Northwood, D. Penrod and Jerry H. Sokolowski, "The Effect of Quench Rate on Mechanical Properties of 319 Aluminum Alloy Castings", *Materials Science Forum*, 1996, Vols 217-222, No. 2, pp. 783-788.

74 Z. Li, A.M. Samuel, F.H. Samuel, C. Ravindran, S. Valtierra and H.W. Doty, "Parameters controlling the performance of AA319-type alloys, Part I: Tensile properties", *Materials Science and Engineering*, 2004, Vol. A367, pp. 96–110.

75 *Metals Handbook, Ninth Edition, Vol. 2: Nonferrous Alloys and Special-Purpose Materials*, ASM, Metals Park, OH, 1985, pp. 152-178.

76 R. DasGupta, C. Brown and S. Marek, "Optimization of Properties in Strontium Modified 319 Alloy Castings," *Proceedings of the 2nd International Conference on Molten Aluminum Processing*, American Foundrymen's Society, Des Plaines, IL,1989, pp. 1-32.

77 M. Drouzy, S. Jacob and M. Richard, "Interpretation of Tensile Results by means of Quality Index and Probable Yield Strength", *AFS International Cast Metals Journal*, 1980, Vol. 5, pp. 43-50.

78 G.K. Sigworth and C.H. Cáceres, "Quality Issues in Aluminum Net Shape Castings", *AFS Transactions*, 2004, Vol. 112, Paper 04-075, pp. 1-15.

79 Adrian S. Sabau and Wallace D. Porter, "Analysis of a Heat-Flux Differential Scanning Calorimetry Instrument", *Metallurgical and Materials Transactions A,* 2007, Vol. 38A, No. 7, pp. 1546-1554.

80 Q.T. Fang and D.A. Granger, "Porosity Formation in Modified and Unmodified A356 Alloy Castings", *AFS Transactions*, 1989, Vol. 97, pp. 989-1000.

81 D. Emadi, J.E. Gruzleski, "Porosity in Modified Aluminium Alloy Castings", *AFS Transactions*, 1988, Vol. 96, pp. 65-74.

82 F. Paray and J.E. Gruzleski, "Microstructure-mechanical property relationship in a 356 alloy. Part 1: Microstructure", *Cast Metals*, 1994, Vol. 7, No. 1, pp. 29-40.

83 S. Shivkumar, S. Ricci, Jr., C. Keller and D. Apelian, "Effect of Solution Treatment Parameters on Tensile Properties of Cast Aluminum Alloys", *Journal of Heat Treating*, 1990, Vol. 8, pp. 63-70.

84 Q.G. Wang and C.H. Cáceres, "Mg Effects on the Eutectic Structure and Tensile Properties of Al-Si-Mg Alloys", *Materials Science Forum*, 1997, Vol. 242, pp. 159-164.

85 G.K. Sigworth, "Quality of Aluminum Castings", Private Communication (2007).